

# Organic carbon fluxes in polar oceans: Subject to changing ice conditions and related secondary effects

Dissertation

zur Erlangung des Doktorgrades der Naturwissenschaften

– Dr. rer. nat. –

im Fachbereich Geowissenschaften der Universität Bremen

vorgelegt von

Ralf Hoffmann

Bremen, 27.04.2018



Begutachtet durch

**Prof. Dr. Antje Boetius**

Alfred-Wegener-Institut, Helmholtz-Zentrum für Polar- und Meeresforschung

Am Handelshafen 12

27570 Bremerhaven

antje.boetius@awi.de

Tel.: +49 471 4831 1100

und

**PD Dr. habil. Stefan Forster**

Universität Rostock, Mathematisch-Naturwissenschaftliche Fakultät,

Institut für Biowissenschaften, Sektion Meeresbiologie

Albert-Einstein-Straße 3

18059 Rostock

stefan.forster@uni-rostock.de

Tel.: +49 381 498 6053

Tag des Promotionskolloquiums: 20.08.2018



*„For me to have questions, first I need to know something.“*

Actor Denzel Washington as Doug Carli in the movie 'Déjà Vu'



## Versicherung an Eides Statt

---

gem. § 5 Abs. 5 der Promotionsordnung vom 15.07.2015

Ich, Ralf Hoffmann, wohnhaft in der Pastor-Moritz-Straße 7 in 14776 Potsdam, immatrikuliert unter der Matrikelnummer 2986112, versichere an Eides Statt durch meine Unterschrift, dass ich die vorliegende Dissertation selbständig und ohne fremde Hilfe angefertigt und alle Stellen, die ich wörtlich dem Sinne nach aus Veröffentlichungen entnommen habe, als solche kenntlich gemacht habe, mich auch keiner anderen als der angegebenen Literatur oder sonstiger Hilfsmittel bedient habe und die zu Prüfungszwecken beigelegte elektronische Version (PDF) der Dissertation mit der abgegebenen gedruckten Version identisch ist.

Ich versichere an Eides Statt, dass ich die vorgenannten Angaben nach bestem Wissen und Gewissen gemacht habe und dass die Angaben der Wahrheit entsprechen und ich nichts verschwiegen habe.

Die Strafbarkeit einer falschen eidesstattlichen Versicherung ist mir bekannt, namentlich die Strafandrohung gemäß § 156 StGB bis zu drei Jahren Freiheitsstrafe oder Geldstrafe bei vorsätzlicher Begehung der Tat bzw. gemäß § 161 Abs. 1 StGB bis zu einem Jahr Freiheitsstrafe oder Geldstrafe bei fahrlässiger Begehung.

Bremen, 27.04.2018

---





## Abstract

---

Primary production and mineralization are key processes and living organisms key components of the biological carbon cycle with an ecosystem. The dynamics of primary production and mineralization as well as organismal parameters such as density, biomass, structure and respiratory activity are controlled by abiotic and biotic factors, which can also be inter-dependently linked with each other. From a global perspective, the carbon cycles of the Southern and Arctic Ocean show quantitatively the largest dynamics on spatial scales. Therefore, this thesis focuses on spatial carbon dynamics in these polar ecosystems.

Changes in the polar cryosphere and related secondary effects, associated with global temperature increase, can have a great impact on processes and components of the biological carbon cycle. For example, nutrients and particles are released into the marine realm by glacial and permafrost soil melt, while thinning, diminishing, retreating and melting sea ice leads to increased light availability but suppresses nutrient upwelling. These secondary effects are known to influence primary productivity, organismal community structures and mineralization rates. The investigation of how changes in polar ice conditions alter primary production, the benthic biota, and benthic mineralization is the overall aim of this thesis and was addressed in three manuscripts.

The methods used in this thesis include the determination of *in situ* and *ex situ* total and diffusive oxygen fluxes to investigate primary production and benthic mineralization. Furthermore, densities, biomasses, and community structures of different size classes of the benthic biota were investigated as well as a set of abiotic and biotic factors. This

allows a descriptive and holistic ecosystem snapshot of the carbon cycle in the investigated polar regions.

Within the first manuscript the impact of glacial melt-related particle release on the primary productivity of benthic microalgae in sediments at 6–9 m water depth in Potter Cove (shallow coastal Southern Ocean) was investigated. The results showed that glacial melt-related particle release led to a suppression of benthic microalgae primary production. Diatoms dominated the benthic microalgae community. Interestingly, the structure of the diatom community was not impacted by glacial melt-related particle release. The suppression of primary production was explained by a higher energy cost for the more frequently happening migration of diatom cells, caused by permanent sedimentation. The impact of increased turbidity, an additional secondary effect of glacial melt-related particle release, was assessed as low, owing to the very good adaption of Antarctic benthic microalgae to low light conditions.

Spatial patterns of benthic mineralization in sediments at 6–9 m water depth in Potter Cove (shallow coastal Southern Ocean) were investigated in the second manuscript. The revealed pattern is impacted by glacial melt-related particle release. The benthic mineralization was mainly mediated by the benthic macrofauna and followed a unimodal correlation with increasing sedimentation. This correlation pattern was explained by physiological reactions of the suspension and deposit feeding community on the disturbance by particles. In addition, this manuscript includes the first holistic ecosystem snapshots of an Antarctic shallow coastal site. It thereby revealed inter-dependent relations between abiotic factors, biotic factors and primary production influencing benthic mineralization.

The third manuscript deals with benthic mineralization in the deep sea Arctic Ocean. The results revealed the spatial pattern of benthic mineralization in sediments at 275–2500 m water depth across the Fram Strait. In the highly sea-ice covered western Fram Strait, benthic mineralization was water depth independent, whereas in the low sea-ice covered eastern Fram Strait it was water depth dependent. This pattern was explained by the suppression of primary production in the western Fram Strait, caused by a lower light availability (sea-ice cover) and lower nutrient supply by the East Greenland current. Nevertheless, the impact of sea-ice cover faded out in water depth >1500 m.

Furthermore, the obtained data were used for a holistic ecosystem snapshot of the Arctic Fram Strait.

The results of the three manuscripts are used to discuss, how changing ice conditions impact primary production, inter-dependent relations between primary production and benthic mineralization, and benthic mineralization in polar regions. In addition, the results are integrated in a discussion on changes in the carbon cycle in a future scenario for the Southern and the Arctic Ocean.

In conclusion, particle release by glacial and permafrost soil melt leads to reduced primary production by the microphytobenthic and macroalgae community within a few hundred meters from the coastline in the shallow coastal regions of the Southern and the Arctic Ocean. In contrast, the release of nutrients, which has the same drivers as the particle release, leads to an enhanced pelagic primary production within tens of kilometers in the same regions. In addition, benthic mineralization in the shallow coastal polar regions can increase or decrease, depending on the intensity of sedimentation rates and supply of organic matter. Increasing light availability in the deep-sea regions of the Southern and the Arctic Ocean only leads to an enhanced primary productivity if these regions also receive an increase in nutrients and iron supply. Deep-sea benthic mineralization between 200 m and >2000 m is impacted by changes in the sea-ice cover (a proxy for a suppressed primary production). Below those depths, the influence of sea-ice cover fades out and the factor water depth (a proxy for loss of organic carbon by pelagic mineralization) becomes dominant.



## Kurzfassung

---

Primärproduktion und Mineralisation sind die wichtigsten Prozesse des biologischen Kohlenstoffkreislaufes und innerhalb eines Ökosystems sind die Organismen die wichtigsten Komponenten. Die Dynamiken von Primärproduktion, Mineralisation und organismischer Parameter wie Individuendichte, Biomasse, Gemeinschaftsstruktur und respiratorische Aktivität werden zudem von abiotischen und biotischen Faktoren kontrolliert. Diese Prozesse, Komponenten und Faktoren können sich auch gegenseitig beeinflussen und ökosysteminterne Abhängigkeiten aufweisen. Aus globaler Sicht zeigen die Kohlenstoffkreisläufe des Antarktischen und Arktischen Ozeans die quantitative größten Dynamiken und stehen deshalb im Fokus dieser Dissertation.

Aufgrund des weltweiten Temperaturanstiegs verändert sich die polare Kryosphäre. Die damit einhergehenden Folgeerscheinungen beeinflussen die Prozesse und Komponenten des biologischen Kohlenstoffkreislaufes im Antarktischen und Arktischen Ozean. Durch das Schmelzen von Gletschereis und Eis in Permafrostböden werden vermehrt Nährstoffe und partikuläres Material in den küstennahen, maritimen Lebensraum transportiert. In den küstenfernen Regionen des Ozeans hingegen nimmt die Meereisdicke und Verbreitung des Meereises ab und verschwindet zum Teil gänzlich, wodurch den dortigen Primärproduzenten mehr Licht zur Verfügung steht. Allerdings verhindert die durch Meereisschmelze verursachte Stratifikation der oberen Meeresschicht den Nachschub von Nährstoffen aus tieferen Meeresschichten. Die Untersuchung, wie stark sich die Folgeerscheinungen der sich verändernden Kryosphäre auf die Primärproduktion, die Lebewesen am Meeresboden und die

benthische Mineralisation in den Polarregionen auswirkt, ist Ziel dieser Dissertation und wurde in drei Manuskripten thematisiert.

Primärproduktion und benthische Mineralisation wurden mittels *in situ* und *ex situ* bestimmten diffusiven und totalen Sauerstoffflüssen ermittelt. Weiterhin wurden Individuendichten, Biomassen und Gemeinschaftsstrukturen von Organismen unterschiedlichster Größenklassen bestimmt und abiotische und biotische Faktoren gemessen. Dies erlaubte zudem die Erstellung eines holistischen Abbildes der Beziehungen und Abhängigkeiten der unterschiedlichsten Parameter innerhalb des ökosystemalen Kohlenstoffkreislaufes in den untersuchten Polarregionen.

Im ersten Manuskript wird der Einfluss partikulären Materials auf die Primärproduktion von benthischen Mikroalgen in 6–9 m Wassertiefe in der Potter Cove (flacher, küstennaher Antarktischer Ozean) behandelt. Das partikuläre Material wird dort durch Gletscherschmelze freigesetzt. Die Untersuchung zeigte, dass die Primärproduktion der benthischen Mikroalgen durch besagtes partikuläres Material verringert bis vollständig unterdrückt wird. Die benthische Mikroalgenegemeinschaft in der Potter Cove ist von Diatomeen dominiert, deren Gemeinschaftsstruktur durch das partikuläre Material jedoch nicht beeinflusst wurde. Die Verringerung der Primärproduktion wird mit einem erhöhten Energieaufwand für die Vertikalbewegung der Diatomeen durch das Sediment erklärt, welche durch die permanente Bedeckung durch neue Partikel ausgelöst wird. Der Einfluss der erhöhten Trübung, eine weitere Folge des Partikeleintrages, wird als gering eingeschätzt, da antarktische, benthische Mikroalgen sehr gut an geringe Lichtverhältnisse angepasst sind.

Das räumliche Verteilungsmuster der benthischen Mineralisation in 6–9 m Wassertiefe in der Potter Cove (flacher, küstennaher Antarktischer Ozean) wurde im zweiten Manuskript untersucht. Das Verteilungsmuster ist dabei durch den gletscherschmelzbedingten Eintrag von partikulärem Material beeinflusst. Der Großteil der benthischen Mineralisation wird durch die benthische Makrofauna umgesetzt und folgt einer unimodalen Korrelation mit zunehmender Sedimentationsintensität des partikulären Materials. Dieses Korrelationsmuster wird durch die physiologische Reaktion der filtrierenden und detritivoren Makrofaunagemeinschaft auf das erhöhte Vorkommen von partikulärem Material erklärt. Des Weiteren beinhaltet das Manuskript

die erste holistische Abbildung der Abhängigkeiten unterschiedlichster Parameter innerhalb des biologischen Kohlenstoffkreislaufes in einem flachen, küstennahen Ökosystem des Antarktischen Ozeans. Dieses Abbild beschreibt, wie Primärproduktion und die davon abhängige benthische Mineralisation miteinander in Verbindung stehen.

Die Ergebnisse des dritten Manuskripts zeigen das räumliche Verteilungsmuster der benthischen Mineralisation in 275–2500 m Wassertiefe in der Fram Straße (arktische Tiefsee). In der hauptsächlich eisbedeckten westlichen Fram Straße war die benthische Mineralisation tiefenunabhängig, während sie in der zumeist eisfreien, östlichen Fram Straße tiefabhängig war. Dieses Muster lässt sich durch die verringerte Primärproduktion in der westlichen Fram Straße erklären, welche durch die verringerte Lichtverfügbarkeit auf Grund der erhöhten Meereisbedeckung und des geringen Nährstoffangebotes verursacht wird. Der Einfluss der Meereisbedeckung auf die benthische Mineralisation wird jedoch ab Wassertiefen von 1500 m durch den Einfluss der geringeren Verfügbarkeit von organischem Kohlenstoff überdeckt, welcher wiederum durch pelagische Mineralisationsprozesse verursacht wird. Zusätzlich wurden die gewonnenen Daten für eine holistische Abbildung der Abhängigkeiten von Primärproduktion und unterschiedlichster abiotischer und biotischer mit der benthischen Mineralisation in der Fram Straße verwendet. Dadurch war es möglich, auch für die Fram Straße die Verbindung zwischen Primärproduktion und der davon abhängigen benthisch Mineralisation erstmals detaillierter zu beschreiben.

Die Ergebnisse der drei Manuskripte wurde genutzt um das grundlegendere Thema zu diskutieren, wie sich Primärproduktion und benthische Mineralisation und deren Beziehungen zueinander durch die sich verändernde Kryosphäre und damit verbundener Folgen in den Polargebieten beeinflusst werden. Weiterhin wurden die Ergebnisse genutzt um Veränderungen im Kohlenstoffkreislauf des Antarktischen und Arktischen Ozeans unter spezifischen Zukunftsszenarien zu diskutieren.

Meine Dissertation zeigt, dass das durch schmelzende Gletscher und tauende Permafrostböden freigesetzte partikuläre Material zu einer immensen Verringerung der Primärproduktion von benthischen Mikro- und Makroalgen in einem Bereich von mehreren hundert Metern in polaren Küstenbereichen führen kann. Die mit der Schmelze einhergehende Freisetzung von Nährstoffen wird im Gegensatz dazu eine

gesteigerte pelagische Primärproduktion in einem Bereich von mehreren Kilometern nach sich ziehen. Die benthische Mineralisation hingegen kann sich in küstennahen, flachen Polarregionen in Abhängigkeit von der Quantität der Sedimentationsraten und der Höhe des Nährstoffeintrages ansteigen oder sich verringern. Eine erhöhte Primärproduktion in den küstenfernen Regionen des Antarktischen und Arktischen Ozeans aufgrund der erhöhten Lichtverfügbarkeit wird jedoch nur erfolgen, wenn gleichzeitig auch das Angebot an primärproduktionslimitierendem Eisen (Antarktischer Ozean) oder stickstoff- und phosphathaltigen Nährstoffen (Arktischer Ozean) ansteigen. Die benthische Mineralisation in der polaren Tiefsee erhöhte sich aufgrund einer sich stark verringernenden Meereisbedeckung nur in dem Tiefspektrum zwischen 200 m bis 1500 m. Unterhalb dieser Tiefe, nimmt der Einfluss von Meereis ab und der Faktor Wassertiefe (stellvertretend für den Verlust von organischem Kohlenstoff durch pelagische Mineralisationsprozesse) dominiert.



# Table of content

---

Versicherung an Eides Statt .....	I
Abstract .....	III
Kurzfassung .....	VII
Table of content.....	XI
List of figures .....	XV
List of tables .....	XVII
1 Introduction .....	1
1.1 The biological carbon cycle .....	1
1.1.1 The importance of carbon in ecology .....	1
1.1.2 The biological carbon cycle in the marine realm .....	4
1.2 Primary production in polar regions.....	6
1.2.1 Spatial and temporal variability of primary production in different habitats of the Southern and Arctic Ocean .....	6
1.2.2 Light availability reduction in polar ecosystems .....	11
1.2.3 Nutrient availability and supply in polar ecosystems .....	13
1.3 Polar benthic mineralization: From shallow coasts to the deep sea.....	14
1.3.1 Pelagic mineralization and vertical flux of organic matter.....	14
1.3.2 Spatial and temporal variability of benthic remineralization across polar coasts, shelves and in the deep sea.....	16
1.4 Climate change associated effects on the carbon cycle in polar environments .....	20
1.4.1 Recent environmental changes in the Southern Ocean .....	20
1.4.2 Recent environmental changes in the Arctic Ocean.....	22
1.5 Objectives and hypotheses .....	25

## Table of content

---

2 Material and methods .....	29
2.1 Study sites .....	29
2.1.1 Potter Cove, Antarctic Peninsula .....	29
2.1.2 Fram Strait, Arctic Ocean .....	31
2.2 Used methods to determine benthic primary production, benthic mineralization, and influencing environmental parameters.....	36
2.2.1 Total and diffusive benthic oxygen fluxes at soft bottom seafloors.....	36
2.2.2 Light suppression, light availability and PAR measurement .....	40
2.2.3 Sediment properties, biogenic sediment compounds and biota .....	41
3 Manuscript I: Implications of glacial melt-related process on the primary production of a microphytobenthic community in Potter Cove (Antarctic).....	45
3.1 Abstract .....	46
3.2 Introduction .....	46
3.3 Material and methods .....	48
3.3.1 Study site and sampling.....	48
3.3.2 Methods .....	50
3.4 Results.....	53
3.4.1 <i>In situ</i> PAR variability.....	53
3.4.1 Diatom community at Potter Cove .....	54
3.4.3 Potential net MPB primary production in Potter Cove .....	55
3.5 Discussion .....	57
3.5.1 The impact of turbidity and sediment accumulation on the microphytobenthic community and their primary production in Potter Cove.....	57
3.5.2 Microphytobenthos as important carbon source in Potter Cove .....	59
3.5.3 Implications of glacial melt-related retreat and particle release on polar benthic communities .....	60
3.6 Supplements.....	61
4 Manuscript II: Spatial variability of biogeochemistry in shallow coastal benthic communities of Potter Cove (Antarctica) and the impact of a melting glacier.....	65
4.1 Abstract .....	66
4.2 Introduction .....	66
4.3 Material and methods .....	69
4.3.1 Study site .....	69
4.3.2 Sediment properties and biogenic sediment compounds.....	71
4.3.3 Benthic community structure .....	72

---

4.3.4 Biogeochemical flux measurements .....	73
4.3.5 Statistical approaches .....	76
4.3.6 Ethics statement.....	77
4.4 Results.....	77
4.4.1 Comparison of abiotic and biogenic parameters .....	77
4.4.2 Comparison of fauna community parameters .....	80
4.4.3 Comparison of biogeochemical fluxes .....	82
4.4.4 Relationships between abiotic and biogenic sediment parameters, the benthic community, and oxygen and nutrient fluxes.....	83
4.5 Discussion .....	84
4.5.1 The influence of glacial melt processes on the Antarctic shallow benthos and benthic mineralization.....	84
4.5.2 Spatial variability of benthic biogeochemical fluxes at shallow coasts of the Western Antarctic Peninsula.....	86
4.5.3 Benthic carbon demand in Potter Cove .....	87
4.6 Supporting information .....	89
5 Manuscript III: Deep-sea benthic communities and oxygen fluxes in the Arctic Fram Strait controlled by sea-ice cover and water depth.....	99
5.1 Abstract .....	100
5.2 Introduction .....	101
5.3 Material and methods .....	103
5.3.1 Study site and field sampling .....	103
5.3.2 Sea ice data .....	105
5.3.3 Sediment compounds and properties .....	106
5.3.4 Benthic community parameters .....	107
5.3.5 Oxygen and bromide fluxes .....	108
5.3.6 Data analyses.....	111
5.4 Results.....	114
5.4.1 Short- and long-term sea ice concentration comparison between the EG and WS area .....	114
5.4.2 Sediment properties and benthic biogenic compounds in the EG and WS area.....	116
5.4.3 Benthic communities and community functions in the EG and WS area .....	121
5.4.4 Benthic remineralization .....	121
5.4.5 Relations of the benthic community, its remineralization activity, and environmental parameters.....	123

## Table of content

---

5.5 Discussion .....	126
5.5.1 Linking contrasting sea-ice conditions with benthic oxygen fluxes .....	126
5.5.2 Primary production and benthic remineralization in the Fram Strait .....	129
5.5.3 A future deep-sea benthic Arctic Ocean scenario .....	132
5.6 Supplements.....	134
6 Authors contribution to manuscripts I–III.....	157
6.1 Contribution to manuscript I .....	157
6.2 Contribution to manuscript II .....	157
6.3 Contribution to manuscript III .....	158
7 Discussion.....	161
7.1 The impact of particle release on the biological carbon cycle in shallow coastal polar regions.....	161
7.1.1 Effects of particle release on primary production in shallow coastal polar regions ...	161
7.1.2 Effects of particle release on benthic mineralization in shallow coastal polar regions .....	164
7.2 The impact of sea ice on polar benthic mineralization .....	167
7.3 Relationships of inter-dependent abiotic and biotic factors with benthic mineralization ..	170
7.4 Potential future developments in polar carbon cycles due to changing ice conditions and related aftereffect.....	174
7.4.1 A two-step scenario for the Southern Ocean .....	174
7.4.2 The sea-ice free Arctic Ocean in summer .....	176
8 Conclusion and outlook .....	179
8.1 Conclusion .....	179
8.2 Outlook .....	181
Acknowledgment .....	185
References.....	XIX
Appendix .....	XLV
Appendix A: List of abbreviations .....	XLV
Appendix B: Data availability.....	XLVII
Appendix C: Oral and poster presentations.....	XLVIII
Appendix D: Expeditions, courses, teaching, outreach and further activities .....	L

## List of figures

---

Figure 1.1 General and simplified carbon cycle .....	2
Figure 1.2 Two examples of biological carbon cycles .....	5
Figure 1.3 Cascade of inter-dependent factors controlling carbon flux quantities.....	6
Figure 1.4 Inter-annual changes of the sea-ice extent in the Southern Ocean and Arctic Ocean.	7
Figure 1.5 Annual pelagic primary production in the Southern Ocean and Arctic Ocean. ....	8
Figure 1.6 Duration of daylight and darkness from 60°N to 90°N.....	11
Figure 1.7 Benthic mineralization in the Southern and Arctic Ocean.....	18
Figure 1.8 Synoptic view on the food bank hypothesis .....	20
Figure 1.9 Global and Arctic atmospheric temperature anomaly.....	23
Figure 2.1 Map of the study site Potter Cove, including investigated locations Faro, Creek and Isla D .....	29
Figure 2.2 Map of the current system in the Arctic Fram Strait .....	32
Figure 2.3 Mean September sea-ice concentration in the Arctic Ocean.....	33
Figure 2.4 Map of the Fram Strait including investigated stations of the LTER HAUSGARTEN.	35
Figure 2.5 Devices used to determine oxygen fluxes across soft bottom seafloors.....	37
Figure 2.6 Example for the decrease in oxygen concentration during an chamber incubation and an oxygen microprofile across the sediment-water interface .....	38
Figure 3.1 Study site Potter Cove .....	49
Figure 3.2 <i>In situ</i> measured photosynthetically active radiation intensities (PAR) on seasonal and daily scale .....	54
Figure 3.3 Carbon fluxes at different PAR intensities.....	56
Figure 3.4 Carbon fluxes normalized by the mean diatom carbon content at different PAR intensities. ....	56
Figure 4.1 Study site Potter Cove .....	70
Figure 4.2 Boxplots of a subset of the measured parameters .....	79

## List of figures

---

Figure 4.3 Mean biomasses of prokaryotes, meio- and macrofauna.....	81
Figure 4.4 PCA results on mean values in the scaling II mode .....	83
Figure S4.1 Sulfate concentration profiles from pore water extractions .....	89
Figure S4.2 Photos of brownish microphytobenthic (MPB) mats at Faro, Creek and Isla D .....	90
Figure 5.1 Location of the sampled stations in the Arctic Fram Strait.....	104
Figure 5.2 Annual mean sea-ice concentrations from 2001 to 2015 of a subset of sampled stations.....	116
Figure 5.3 Boxplots of sediment properties, biogenic compound values, benthic community data and function, and oxygen fluxes, of the East Greenland and West Spitsbergen area.....	117
Figure 5.4 Log-transformed DOU data as a function of water depth at each station and linear regressions in the HSC and LSC categories .....	122
Figure 5.5 Visualization of PCA results on standardized <i>ex situ</i> mean values of abiotic parameters, biogenic compound parameters, benthic community parameters, macrofauna- mediated environmental functions, and oxygen .....	124
Figure 5.6 Sediment oxygen uptakes in different water depths (15 m–4000 m) for HSC and LSC sea-ice categories for the Laptev Sea, Fram Strait, and Pan-Arctic region and related regressions .....	131
Figure S5.1 Oxygen profiles at stations investigated in Fram Strait .....	134
Figure S5.2 Visualization of the comparison between the sampling years 2014 and 2015 using a PCA.....	134
Figure S5.3. Parameters used in PCA displayed as a function of water depth in the HSC and LSC categories .....	135

## List of tables

---

Table 1.1 Mineralization rates at different locations in shallow, shelf, and deep sea locations in the Southern and Arctic Ocean .....	17
Table 2.1 General information about performed measurements at the investigated study sites.	40
Table 3.1 Locations, water depth at sampled locations, and date of sampling .....	49
Table 3.2 P-values of ANOVAs and Games-Howell post-hoc tests regarding sediment core specific slopes of C-fluxes and diatom carbon content-normalized C-fluxes .....	55
Table S3.1 Diatom density of single taxa at the three locations Faro, Creek and Isla D.....	61
Table S3.2 Results of the SIMPER analysis .....	63
Table 4.1 Location, water depth, and date of sampling of the three locations sampled in Potter Cove.....	70
Table S4.1 $R_i$ and $M_i$ according to Queirós et al. [2013] to calculate the bioturbation potential of the macrofauna community in Potter Cove .....	91
Table S4.2 P-values of the Levene's test and t-test, comparing TOUs from black and transparent chamber incubations .....	91
Table S4.3 Result of Pearson correlation .....	92
Table S4.4 Measured mean values $\pm$ SD of sediment, biogenic, benthic community and flux parameters .....	95
Table 5.1 General station information regarding water depth, sampling date, location and station ID in the data archive Pangaea .....	105
Table 5.2 Sea-ice cover and % of days with sea-ice cover on different time scales across the Fram Strait.....	115
Table 5.3 Mean values $\pm$ standard deviation and number of samples in brackets for each measured parameter at each station.....	118
Table S5.1 Number of samples for analyzes of different parameters.....	136
Table S5.2 Results of Pearson correlation.....	137

## List of tables

---

Table S5.3 Annual sea-ice cover values and the annual percentages of days with sea-ice cover from 01/09/2001 until 31/08/2015.....	138
Table S5.4 P-values of the Shapiro-Wilk test, Levene's test, Students t-test, Welch t-test, and Wilcoxon signed rank sum test to identify differences between the EG and WS area ..	143
Table S5.5 Macrofauna density in individuals $m^{-2}$ .....	144
Table S5.6 Macrofauna biomass in mg blotted wet weight $m^{-2}$ .....	146
Table S5.7 Meiofauna density in individuals $10\text{ cm}^{-2}$ .....	149
Table S5.8 Eigenvalue, explained proportion and species score of the PCA to explore if data from 2014 and 2015 differ.....	152
Table S5.9 P-values of Shapiro-Wilk test and p-values of the slope of the linear regression between water depth and a determined parameter within the HSC and LSC categories.....	152
Table S5.10 Results of SIMPER analysis regarding the sea-ice categories HSC and LSC .....	153
Table S5.11 ANOSIM and SIMPER results of the meio- and macrofauna community within water depth categories .....	154
Table S5.12 Results of the two-way crossed PERMANOVA on standardized and fourth roots transformed macrofauna density and macrofauna biomass data based on a Bray Curtis similarity.....	155
Table S5.13 Results of the PERMANOVA pairwise test on standardized and fourth roots transformed macrofauna density and macrofauna biomass data based on a Bray Curtis similarity.....	155
Table 7.1 Recommended list of ecosystem carbon cycle components, controlling factors and proxies or measurable parameters, to create a holistic ecosystem snapshot .....	173



# 1 Introduction

---

## 1.1 The biological carbon cycle

### 1.1.1 The importance of carbon in ecology

Ecology is the study of relationships between structure and function in nature [Odum, 1962]. The term “structure” encompasses the composition of the biological community (species, numbers, biomass, life-history, dispersion, etc.), the quantity and distribution of abiotic materials (nutrients, water, etc.) and the range or gradient of conditions of existence (temperature, light, etc.) [Odum, 1968]. The term “function” encompasses the range of energy flows through the system, the rate of material cycling and the regulation of these processes by the physical environment and by organisms [Odum, 1968]. In addition, energy flow is the sum of production and respiration [Odum, 1968]. Hence, carbon is the ideal study object for ecological studies.

Primary production by photosynthesis and mineralization as a respiration process are important processes within the global carbon cycle (Figure 1.1). Within the carbon cycle, carbon is part of “structure” and part of the “function” [Odum, 1962] and owing to the transfer of organic carbon “through the system” and within the “biological community” [Odum, 1968], carbon fluxes represent matter and energy flux in parallel. Furthermore, primary production and mineralization are mediated by the living biota. Thus, carbon fluxes, which originate from primary production and mineralization processes and involve the transformation from inorganic to organic carbon and vice versa, can be used to determine whether or not an ecosystem is heterotrophic or autotrophic.

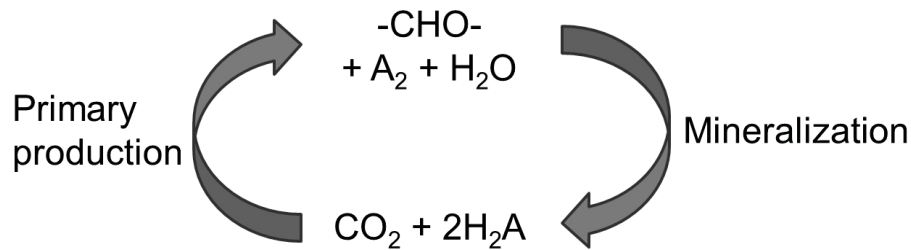


**Figure 1.1.** General and simplified carbon cycle. Primary production and mineralization are processes turning inorganic carbon into organic carbon and vice versa, respectively. The letter “A” represents any molecule, which can be reduced or oxidized, e.g. oxygen or sulfur. The figure is modified after Falkowski and Raven [2007].

Photosynthesis is globally the main process which transforms inorganic carbon into organic carbon, and from which oxygen is produced as a by-product [Field et al., 1998; Raven, 2009; Kirk, 2011]. During the light-independent reaction of photosynthesis, a carbon atom is transferred from inorganic carbon dioxide to organic Ribulose-1,5-bisphosphate via activated Ribulose-1,5-bisphosphate-co-enzyme (RuBisCO) [Falkowski and Raven, 2007; Kirk, 2011]. The energy for the activation of RuBisCO originates from the light-dependent reaction, which precedes the light-independent reaction [Falkowski and Raven, 2007; Kirk, 2011]. Hence, sunlight energy is transferred to and preserved in organic carbon. Carbon is hereby incorporated into the living biota, where it is used as a structural fundament for deoxyribonucleic acid, carbohydrates, proteins and lipids [Bergtrom, 2015]. Therefore, carbon is an irreplaceable element within the “structure of nature” [Odum, 1968; Bergtrom, 2015].

After being incorporated into primary producers, organic carbon is used as an energy resource by heterotrophic consumers. The increase in biomass of heterotrophic consumers is called secondary production. Owing to the prey-predator relationships among the heterotrophic consumers, organic carbon is distributed among the biota present in an ecosystem, forming the ecosystem food web [Pimm, 2002; Knox, 2007; van Oevelen et al., 2011; Marina et al., 2018].

The counterpart of photosynthesis in the global carbon cycle is mineralization (synonym to “respiration”) [Williams and del Giorgio, 2005]. To release the preserved sunlight energy in order to run essential biogeochemical reactions, such as nutrient uptake or muscular contraction, organic carbon is reduced and carbon dioxide is released [Williams, 1984; Canfield et al., 2005; Williams and del Giorgio, 2005]. In

addition, oxygen (= aerobic respiration) or other oxidized molecules (= anaerobic respiration of nitrate or sulfate) are utilized as electron acceptors [Williams and del Giorgio, 2005]. Contrasting to photosynthesis, where only one biochemical pathway turns inorganic carbon into organic carbon, up to 15 different biochemical pathways can be identified for the mineralization of organic carbon [King, 2005; Williams and del Giorgio, 2005]. However, each of these pathways results in the release of inorganic carbon.

To quantify primary production and mineralization, carbon fluxes can be used but this would require the measurement of carbon dioxide concentrations. The measurement of carbon dioxide concentrations in high temporal resolution is mandatory for the reliable calculation of carbon fluxes by sensor-based systems. Though, such carbon dioxide sensors are still at a preliminary stage of development in seawater [Fritzsche et al., 2017; Lochman et al., 2017], due to its complex carbon chemistry which involves the chemical equilibrium between carbon dioxide, carbonic acid, bicarbonate ions, and carbonate ions [Murray, 2004]. However, owing to the close relationship between carbon dioxide and oxygen within the photosynthesis and mineralization processes, oxygen fluxes mirror carbon fluxes. Methods to measure oxygen concentrations in seawater are well established [Winkler, 1888; Revsbech, 1989; Klimant et al., 1995]. Therefore, oxygen fluxes have often been used to quantify primary production and mineralization in the marine realm [Wenzhöfer and Glud, 2002; Glud, 2008; Bourgeois et al., 2017]. Within this thesis, oxygen fluxes (rather than carbon fluxes) have been determined from the environment. For the conversion of oxygen fluxes back to carbon fluxes, the Redfield ratio of 138 O : 106 C was used [Redfield, 1963]. The use of modified Redfield ratios such as 172 O : 140 C [Takahashi et al., 1985] or 170 O : 117 C [Anderson and Sarmiento, 1994] would only lead to minor changes of <10% of the resulting carbon flux [Wenzhöfer and Glud, 2002].

### 1.1.2 The biological carbon cycle in the marine realm

In the marine realm photoautotrophic organisms, organisms which supply their energy demand by photosynthesis, are the main primary producers (>99%) [Raven, 2009]. Chemolithoautotrophic microorganisms, organisms which achieve their energy demand via the chemical oxidation of inorganic molecules such as hydrogen sulfide, elemental sulfur, ammonium and ferrous iron, only contribute substantially to the organic carbon supply in oxygen minimum zones and reduced ecosystems such as deep-sea cold vent and hot seep systems [Raven, 2009; Hügler and Sievert, 2011]. Therefore, the major organic carbon source for the heterotrophic community, basis for the establishment of the great majority of marine food webs, originates from photoautotrophic organisms [Pimm, 2002; Knox, 2007; van Oevelen et al., 2011; Marina et al., 2018].

Nevertheless, primary production in the marine realm via photosynthesis depends on abiotic and biotic factors. In addition to a suitable light availability being available as the energy source, inorganic nutrient supply, wind-induced mixing of the water column and temperature are further important abiotic factors controlling the quantity of primary production [Falkowski and Raven, 2007; Kirk, 2011; Cherkasheva et al., 2014; Fernández-Méndez et al., 2015]. Inorganic nutrients, particularly the concentrations of the key elements of nitrogen and phosphorus, do not control photosynthesis but are essential for primary producers to increase in biomass [Kirk, 2011]. In general, the molar-based Redfield ratio (16 N : 1 P) represents the nutrient demand of primary producers [Redfield, 1934]. Wind-induced vertical mixing of the water column transports pelagic primary producers frequently in and out of the optimal light conditions required by the photosynthetic apparatus for maximum activity [Mahadevan, 2016]. This alters the overall primary production rates of the present primary producer community [Kirk, 2011; Mahadevan, 2016]. Globally, temperature controls the speed of chemical and enzymatic reactions on short time scales [Barry, 1914; Voet et al., 2016]. Though, only in shallow habitats in temperate regions temperature is considered as a limiting factor as only here fast temperature changes occur to which primary producers may not be able to adapt fast enough [Kirk, 2011]. Biotic factors, such as cell internal chlorophyll concentration, the health status of the cell, self-shading, and the phototrophic community

composition also impact primary production rates [Schloss et al., 1998; MacGlathery et al., 2001; Falkowski and Raven, 2007].

Both, phototrophic and heterotrophic organisms mineralize organic carbon (Figure 1.2) [Williams, 1984; Williams and del Giorgio, 2005]. Photoautotrophic primary producers as well as heterotrophic pelagic and benthic meio-, macro- and megafauna solely perform aerobic mineralization (with oxygen as the electron acceptor), while a majority of benthic microorganisms perform anaerobic mineralization (other reducible molecules in the roles as electron acceptors) [Glud, 2008]. Owing to Gibbs energy [Gibbs, 1873] and the laws of thermodynamics, aerobic mineralization provides the highest energy output, whereas the energy output from anaerobic mineralization is less and depends on the electron acceptor molecule [King, 2005]. In turn, the favorable electron acceptor cascade for the mineralization in the marine benthos is oxygen, nitrate, manganese oxide, iron oxide, sulfate and methane (Figure 1.2).

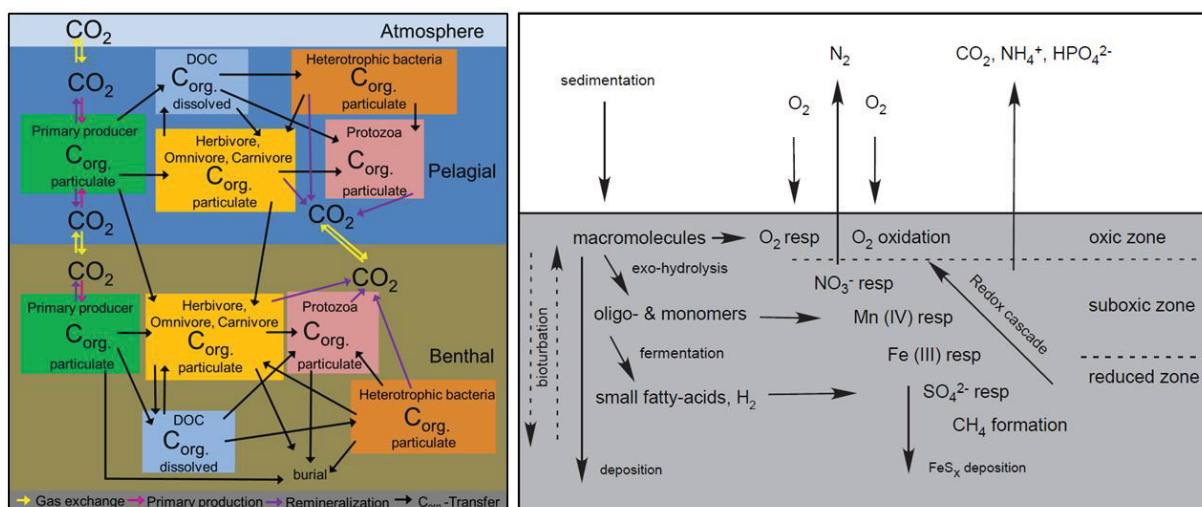


**Figure 1.2.** Two examples of biological carbon cycles. The left-hand example show pathways of organic carbon ( $C_{org}$ ) between different pelagic and benthic organismal groups and includes photosynthesis and mineralization (with a focus on aerobic respiration). The right-hand example from Glud [2008] includes only mineralization and specified the electron acceptor cascade in the benthos.

It should be highlighted that oxygen flux measurements include aerobic and anaerobic mineralization, as products of the anaerobic mineralization will be reoxidized in the oxic zone before they leave the sediment and thereby also consume oxygen, e.g. hydrogen sulfide to sulfate [Williams and del Giorgio, 2005]. Mineralization depends on abiotic factors such as temperature, food supply, and food composition, but also on the

heterotrophic community structure [Williams and del Giorgio, 2005; Brey, 2010]. Consequently, the quantities of carbon fluxes depend on a preceding cascade of inter-dependent factors (Figure 1.3).

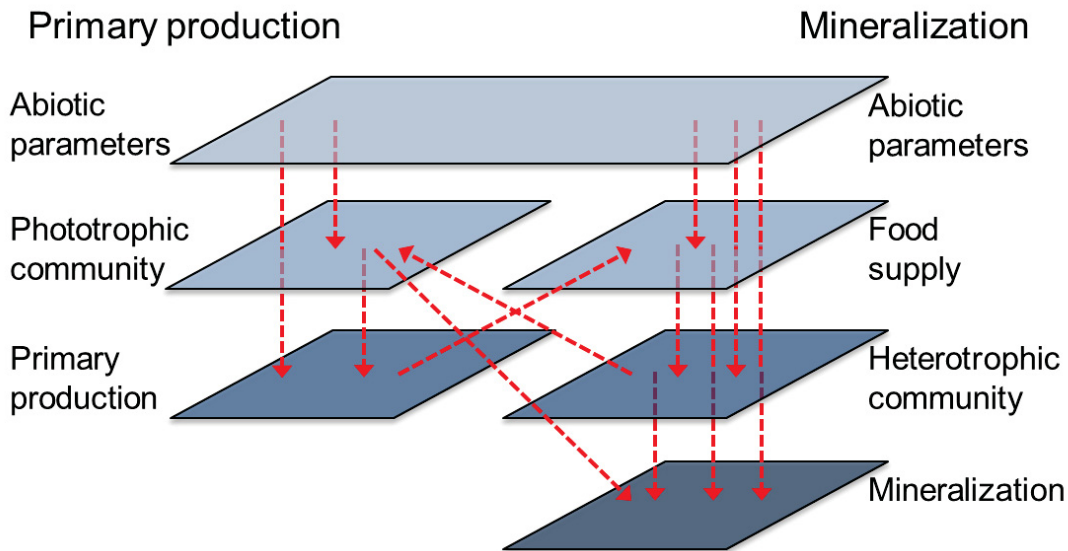


**Figure 1.3.** Cascade of inter-dependent factors controlling carbon flux quantities.

## 1.2 Primary production in polar regions

### 1.2.1 Spatial and temporal variability of primary production in different habitats of the Southern and Arctic Ocean

On spatial and temporal scales, the quantitatively most important regions for worldwide marine organic carbon dynamics are the Southern and the Arctic Ocean [Tjiputra et al., 2013; Heinze et al., 2015], which are characterized by contrasting environmental conditions. The Southern Ocean surrounds the Antarctic continent, has a shelf depth of a maximum of 800 m, and only 2% of the Southern Ocean being shelf [Ainley et al., 2009; Smith, 2010]. Sea ice covers ~19 million km<sup>2</sup> during winter and ~3 million km<sup>2</sup> in summer (mean values 1981–2010, Figure 1.4). Furthermore, 90% of Southern Ocean sea ice is first-year ice and <2 m thick [Horner et al., 1992] and the Southern Ocean does not experience any strong riverine influence [Smith, 2010]. The growth season for primary producers in the Southern Ocean is approximately from October to April [Lizotte, 2001]. In contrast, the Arctic Ocean is an ocean surrounded by

land, with a shelf depth of maximum 200 m and 30–50% of the Arctic Ocean being shelf area [Pabi et al., 2008; Macdonald et al., 2010]. Sea ice covers  $\sim 15$  million  $\text{km}^2$  during winter and  $\sim 6$  million  $\text{km}^2$  in summer (mean values 1981–2010, Figure 1.4). Further, the Arctic Ocean is characterized by 50–90% multi-year sea ice with a thickness of  $>2$  m (depending on season) [Horner et al., 1992; Comiso, 2012] and the Arctic Ocean is strongly influenced by riverine input from the surrounding continents [Smith, 2010]. The growing season for primary producers in the Arctic Ocean is approximately from March to September in the Arctic [McMinn and Hegseth, 2004; Cherkasheva et al., 2014]. Aside from these differences, both polar oceans encompass similar habitats for primary producers: the pelagial, sea ice and glacial ice, and soft and hard bottom seafloor surfaces.

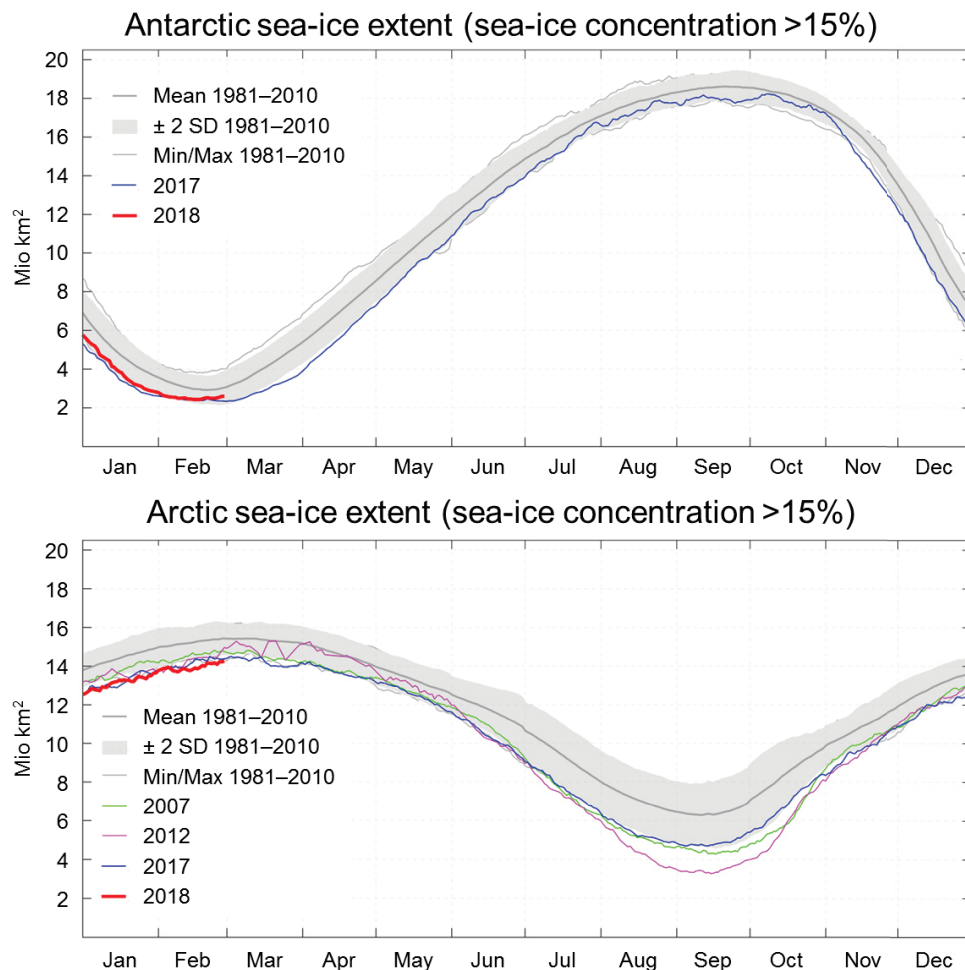


**Figure 1.4.** Inter-annual changes of the sea-ice extent in the Southern Ocean (upper panel) and Arctic Ocean (lower panel). Images provided by [www.seaiceportal.de](http://www.seaiceportal.de).

The pelagic ecosystem of the polar environments can be subdivided into ice-covered regions, the marginal ice zone (MIZ), the open ocean, and shelf regions, with primary producers found in each of these regions [Arrigo et al., 2008a; Pabi et al., 2008]. The area-specific size of these regions undergoes substantial annual change, owing to the seasonal cycle in sea-ice cover (Figure 1.4) and sea-ice extent.

In the Southern Ocean, pelagic primary production contributes up to 90% [Arrigo et al., 1998] to the total primary production, while the MIZ contributes 10–32% [Arrigo et al., 1998; Lizotte, 2001] and the shelf ~2% [Arrigo et al., 1998]. Daily primary production rates vary seasonally between 7–82 mmol C m<sup>-2</sup> d<sup>-1</sup> in the open ocean, 12–141 mmol C m<sup>-2</sup> d<sup>-1</sup> in the MIZ, and 20–328 mmol C m<sup>-2</sup> d<sup>-1</sup> in the shelf regions (Figure 1.5) [Arrigo et al., 1998, 2008a; Schloss et al., 1998]. Prominent pelagic primary producers in the Southern Ocean are Bacillariophyceae species of *Thalassiosira antarctica*, *Corethron criophilum*, *Eucampia antarctica*, *Odonfella weissflogii* [Schloss et al., 1998], the Bacillariophyceae genus *Chaetoceros*, *Fragilariopsis*, and the Coccolithophyceae *Phaeocystis* [Hart, 1942; Arrigo et al., 1998; Esper et al., 2010].

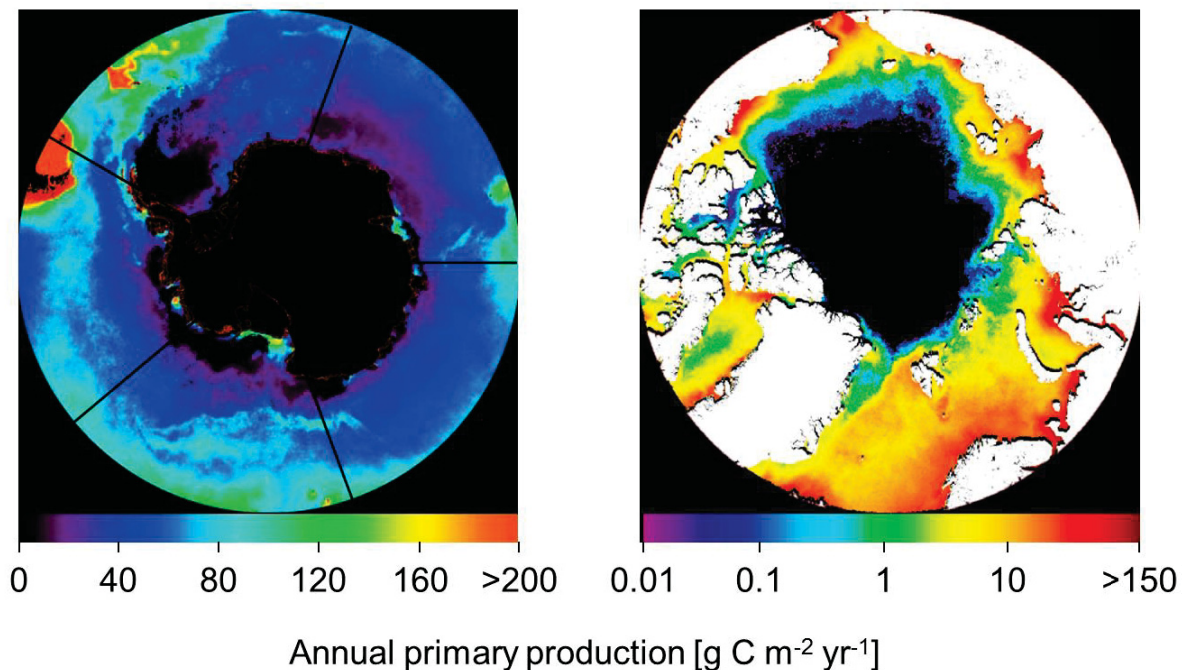


**Figure 1.5.** Annual pelagic primary production in the Southern Ocean (left) and Arctic Ocean (right). Figures modified from Arrigo et al. [2008a] and Pabi et al. [2008], respectively. In black areas, sea-ice cover prevented reliable satellite-based determination of primary production.



In the mostly sea-ice covered central Arctic Ocean 43–98% of the primary production is realized in the pelagial [Gosselin et al., 1997; Fernández-Méndez et al., 2015], which contributes ~24% to the total pelagic Arctic primary production [Pabi et al., 2008; Macdonald et al., 2010]. Annual primary production at the Arctic shelf contributes 16–76% to the total primary production, the MIZ (encompassing shelf and deep sea areas) 37–46% and the open ocean 34–40% (Figure 1.5) [Pabi et al., 2008; Macdonald et al., 2010]. Daily Arctic pelagic primary production varies seasonally, e.g. 2–23 mmol C m<sup>-2</sup> d<sup>-1</sup> in the shelf region of the Kara Sea and 0–60 mmol C m<sup>-2</sup> d<sup>-1</sup> in a Greenland fjord [Sørensen et al., 2015; Demidov et al., 2017]. Important pelagic primary producers in the Arctic are Bacillariophyceae of the genus *Chaetoceros* and *Thalassiosira*, and the Coccolithophyceae *Phaeocystis* [Booth and Horner, 1997].

Sea ice is assumed to be an extreme environment for primary producers, owing to low temperatures, high UV irradiation, low nutrient concentrations and low water availability [Leeuwe et al., 2018]. In addition, the sea-ice habitat undergoes immense spatial changes as it retreats and extends inter-annually (Figure 1.4). However, more than 300 species of diatoms and flagellates are known to inhabit the sea-ice and melt ponds, although some of these are also found within the ocean as phytoplankton [Booth and Horner, 1997]. In the Southern Ocean, sea-ice algae contribute up to 30% to the total primary production [Legendre et al., 1992; Lizotte, 2001]. *Nitzschia stellata*, *Entomoneis kjellmanii*, *Berkeleya adeliensis*, and *Phaeocystis antarctica* and species of the genus *Fragilariopsis* form large blooms under the sea ice in the Southern Ocean [Lizotte, 2001; Trenerry et al., 2002; Armand and Leventer, 2009]. In the central Arctic Ocean, sea-ice algae have been reported to contribute 3–25% to the total primary production [Legendre et al., 1992], although recent studies estimated a higher contribution of up to 57% [Gosselin et al., 1997; Gradinger, 2009; Boetius et al., 2013; Fernández-Méndez et al., 2015]. In the Arctic Ocean, bloom-forming under ice species include *Nitzschia frigida* and *Melosira arctica* [Booth and Horner, 1997; Boetius et al., 2013] with *Phaeocystis pouchetii* dominating the sea-ice surface, brine and infiltration communities [McMinn and Hegseth, 2004]. The existence of sea-ice algae and their substantial contribution to the primary production indicates that sea-ice algae are well

adapted to the above described extreme environmental conditions [Maccario et al., 2015].

Primary producers at the soft bottom seafloor are benthic microalgae, the microphytobenthos (MPB). The MPB mainly occurs in coastal areas of shelf regions and have been estimated to contribute 3–90% of the total coastal primary production [Glud et al., 2009; McMinn et al., 2010]. The daily primary production can range between 0.2–198 mmol C m<sup>-2</sup> d<sup>-1</sup> for both, Arctic and Southern Ocean soft sediments [Dayton et al., 1986; Glud et al., 2009; McMinn et al., 2010; Woelfel et al., 2010; McMinn et al., 2012]. The MPB is a diatom-dominated community [Al-Handal and Wulff, 2008a; Glud et al., 2009] consisting primarily of cosmopolitan species [Hop et al., 2002; Al-Handal and Wulff, 2008a] such as *Gyrosigma fragilis* and *Nitzschia cf. aurariae* [Al-Handal and Wulff, 2008a; Karsten et al., 2012] and species of the genus *Pinnularia*, *Nitzschia*, *Navicula* [Glud et al., 2002].

Hard bottom seafloors in the polar regions (in terms of primary producers) are mainly inhabited by macroalgae and encrusting, coralline red algae. Macroalgae show a strong vertical zonation [Miller and Pearse, 1991; Amsler et al., 1995; Hop et al., 2012]. However, 93% of the polar macroalgae species occur in water depths of maximum 15 m [Kruss et al., 2017]. The primary production of macroalgae may be restricted to shallow environments, but where they are found contributions to total primary production may be high; e.g. 62% to the total primary production reported from a Greenland fjord was in the form of macroalgae [Rysgaard and Nielsen, 2006; McMinn et al., 2012]. Furthermore, macroalgae debris is an important food resource in benthic detrital food chains [Amsler et al., 1995; Quartino et al., 1998; Renaud et al., 2015]. About 700 species are known for the Southern Ocean [Knox, 2007]. The genus *Desmarestia* and *Himantothallus* dominates the macroalgae community and cover up to 72% of the Southern Ocean hard bottom seafloor [Amsler et al., 1995]. Macroalgae of the genus *Enteromorpha*, *Ulothrix*, *Cladophora*, *Leptosarca*, and *Iridea* also contribute substantially to the macroalgae community [Knox, 2007]. Coralline red algae are known to cover 4–60% of the hard bottom seafloor in the Southern Ocean (at shallow water depths) and show a primary production of ~1.3 mmol C m<sup>-2</sup> thallus<sup>-1</sup> d<sup>-1</sup> [Miller and Pearse, 1991; Schwarz et al., 2005]. Dominating species are *Mesophyllum engelhartii*, *Synarthrophyton patena*,

*Lithophyllum aequabile* and *Lithothamnion granuliferum* [Schwarz et al., 2005; Knox, 2007]. In the Arctic Ocean, 55–70 macroalgae species occur which cover up to 39% of the Arctic hard bottom seafloor, depending on the investigated location [Wulff et al., 2009; Kruss et al., 2017]. The macroalgae communities in the Arctic Ocean are dominated by species of *Laminaria digitata*, *Saccharina latissimi*, *Ptilota gunneri*, *Alaria esculenta*, and *Phycodrys rubens* [Hop et al., 2016]. Besides macroalgae, 1–2% of the Arctic hard bottom seafloor is covered by coralline red algae such as *Phymatolithon foecundum* and *Phymatolithon tenue* with a primary production of  $\sim 0.35 \text{ mmol C m}^{-2} \text{ thallus}^{-1} \text{ d}^{-1}$  [Roberts et al., 2002].

### 1.2.2 Light availability reduction in polar ecosystems

Light is the ultimate driving force of primary production [Wassmann et al., 2004; Popova et al., 2010] and the polar environment provides extreme variations and conditions in terms of light for primary producers (Figure 1.6) [Sakshaug, 2004; Serreze and Barry, 2014].

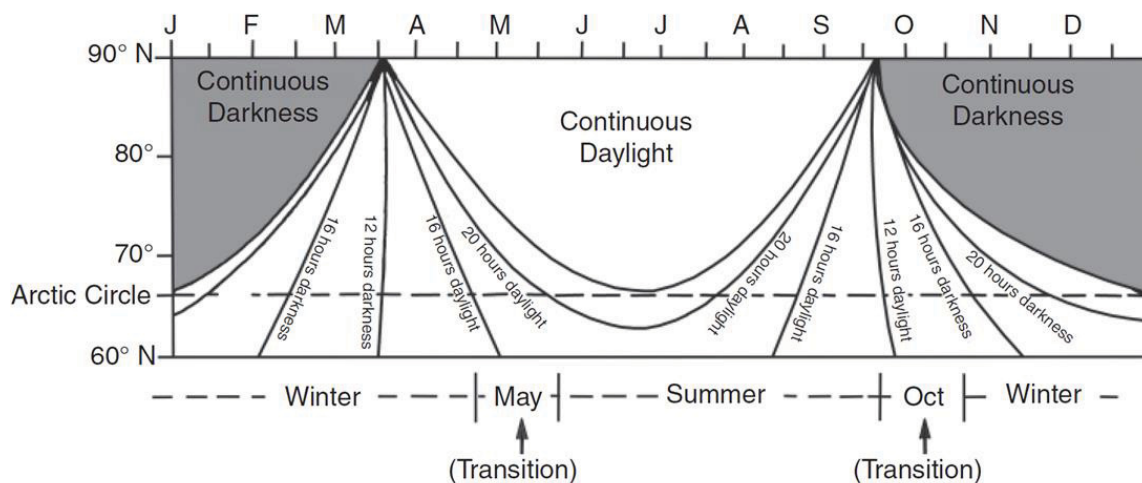


**Figure 1.6.** Duration of daylight and darkness from 60°N to 90°N after Serreze and Barry [2014]. In the Southern Ocean, the light pattern is vice versa.

On an annual basis, the light conditions change from total darkness during polar night to midnight sun during polar day [Serreze and Barry, 2014]. Owing to this seasonal change in day-light availability (Figure 1.6), the primary production season is restricted to only a few months in both the Southern Ocean and Arctic Ocean [Wassmann et al., 2004; Lizotte, 2001]. The photosynthetically active radiation intensity (PAR,

400–700 nm wavelengths) depends on different abiotic factors, phenomena, and events. Owing to the low sun angle, the maximum PAR at the North Pole is  $1200 \mu\text{mol photons m}^{-2} \text{s}^{-1}$  and  $1700 \mu\text{mol photons m}^{-2} \text{s}^{-1}$  at  $60^\circ\text{N}$  [Sakshaug, 2004]. At the Antarctic coast, up to  $2500 \mu\text{mol photons m}^{-2} \text{s}^{-1}$  has been reached [Holm-Hansen et al., 1977]. However, regularly occurring weather phenomena such as fog (typically occurring over sea-ice free areas in summer) and clouds decrease PAR availability at the oceanic surface by 60–70% and 20–90%, respectively [English, 1961; Apollonio, 1980; Bischof et al., 1998; Knox, 2007].

At the oceanic surface of the Southern and Arctic Ocean, ice-covered areas receive only a small portion of available PAR compared to ice-free areas, owing to the light reflecting characteristics of the ice. The albedo (% of reflected light) alters on spatial and temporal scales [Nicolaus et al., 2010; Shao and Ke, 2015]. For example, multi-year sea-ice covered areas have an albedo of 65% and can be 80–90% if snow is topping the multi-year sea-ice [Perovich et al., 2002]. Snow covered one-year sea-ice has an albedo similar to the multi-year sea-ice [Brandt et al., 2005; Perovich and Polashenski, 2012]. However, as soon as melt ponds form, the albedo drops to ~40% [Perovich and Polashenski, 2012]. Furthermore, the albedo of grease sea-ice (slurry of small, plate-like crystals), nilas sea-ice (solidified grease sea-ice with a lot of bubbles and brine inclusions), and young “grey” sea-ice (nilas sea-ice grown to 20 cm thickness) is <30% [Brandt et al., 2005]. In the open ocean and in polynyas the albedo is ~7% [Perovich and Polashenski, 2012]. The main proportion of the spectral PAR that penetrates below sea ice ranges in wavelength between 450–600 nm [Nicolaus et al., 2010]. Thus, by the occurrence of sea-ice, less energy is available for photosynthesis.

Calving and melting of glaciers are also events that influence light availability in polar habitats. Melting glaciers release particles into the water column, directly or via river runoff [Dierssen et al., 2002]. Furthermore, directly at the glacial front chunks of ice drop off, fall into the water, may hit the soft seafloor and thereby resuspend soft sediment seafloor particles [Barnes, 1999; Griffiths, 2010]. In turn, both events lead to an increased turbidity in the water column, a decrease of available PAR for primary producers and an increase in sedimentation rate.

A further reduction of light availability in the water column is caused by storms, which can lead to resuspension in shelf areas [Schloss et al., 1999; Lintern et al., 2013]. In addition, with advancing primary production in spring, the amount of particles in the water column increases, which can reduce the thickness of the euphotic zone (defined as 1% isolume of the surface PAR [Lee et al., 2007]) from 66 m to <3.5 m [Dallokken et al., 1994; Sakshaug, 2004].

### 1.2.3 Nutrient availability and supply in polar ecosystems

The availability of nutrients is also an important factor influencing the primary production [Popova et al., 2010]. In general, the Southern Ocean contains approximately 2–4 times higher nutrient concentrations than the Arctic Ocean [Sakshaug, 2004].

The Southern Ocean is assessed as being the largest high-nutrient-low-chlorophyll region in the global ocean [Pollard et al., 2006; Morrison et al., 2015]. Nitrogen and phosphorus-containing nutrients originate from the upwelling of deep water, which were formed in the north Atlantic, the Pacific and the Indian Ocean [Sakshaug, 2004; Morrison et al., 2015]. However, primary production in the Southern Ocean is limited by the availability of iron [Banse, 1996]. Sources of iron can be upwelling, meltwater runoffs, aeolian dust, release and advection from continental shelf sediments, melting icebergs and recycling of iron within the biological system of the oceanic surface layer [Chester, 1990; Banse, 1996; Lefèvre and Watson, 1999; Walter et al., 2000; Haese, 2006; Monien et al., 2017]. The Arctic Ocean is assumed to be mostly nitrate limited [Sakshaug, 2004; Fernández-Méndez et al., 2015], with the exception of brackish waters with salinities <25 at Arctic estuaries, which are phosphate-limited [Sakshaug et al., 1983]. The Arctic nutrient supply originates mainly from the Bering Sea, the Atlantic Ocean and from riverine input [Rachold et al., 2004; Sakshaug, 2004; Harada, 2015; Tremblay et al., 2015]. However, the riverine input is only relevant for primary production within a few tens of kilometers of the entrance point of river discharge to the marine ecosystem, and therefore mainly associated with the shelf region [Emmerton et al., 2008; Pabi et al., 2008].

Owing to the described nutrient supply, primary production suppressing nutrient limitations are reported for the open ocean areas of the Southern Ocean and the central

Arctic Ocean [Arrigo et al., 1998; Pabi et al., 2008; Popova et al., 2010]. Contrasting to these regions, high primary production rates have been observed at the MIZ and in polynyas (mostly located in shelf areas) [Wassmann et al., 2006]. The MIZ is characterized by stratified conditions of the upper and sea surface waters, in which enhanced primary production takes place until nutrient built up during the winter months has been fully utilized [Tremblay et al., 2015] or new nutrients are supplied by vertical mixing processes [AMAP, 2012], e.g. by storm events. Polynyas receive nutrient supplies by wind-driven upwelling of deep nutrient-rich water masses [Hunt et al., 2016; Park et al., 2017]. Furthermore, wind and ice scouring are two events which can lead to resuspension of soft seafloor particles. Thereby mineralized and stored nutrients can be again made available for primary production [Héquette et al., 1995; Barnes, 1999; Griffiths, 2010; O'Brien et al., 2006]. These events are most commonly occurring in coastal polar regions and therefore the greatest impact of these processes on the primary production occurs with shelf areas [O'Brien et al., 2006].

### 1.3 Polar mineralization: From shallow coasts to the deep sea

#### 1.3.1 Pelagic mineralization and vertical flux of organic matter

In this thesis, I focus on benthic mineralization. As the organic carbon produced at the surface needs to pass the pelagial before it reaches the benthos, a brief introduction to pelagic respiration and vertical carbon fluxes is given in this section.

After carbon uptake by primary producers, organic carbon is distributed among the heterotrophic community of the local food web and mineralized via respiration [Azam et al., 1983; Gontikaki et al., 2011; Marina et al., 2018]. As a result, particulate organic matter (POM) and dissolved organic carbon (DOC) is produced [Pomeroy, 1974; Azam et al., 1983]. POM includes dead phytoplankton, phytodetritus, dead zooplankton, and fecal pellets [Pomeroy, 1974], whereas DOC includes carbohydrates, proteins, and structurally complex carboxyl-rich aliphatic matter [Repeta, 2015]. The DOC will mainly feed the microbial loop in the water column [Pomeroy, 1974; Azam et al., 1983]. As the microbial community is also a food source for pelagic organisms, DOC will be partly recycled into POM [Azam et al., 1983]. After formation, POM and DOC sink towards the

seafloor and may be mineralized in the pelagial to carbon dioxide and other inorganic nutrients. If pelagic mineralization occurs in the euphotic zone, carbon dioxide and nutrients will be recycled by primary producers [Rubin, 2003]. If POM and DOC sink below the euphotic zone, mineralization will continue as the material settles, with carbon dioxide and inorganic nutrients stored in deep ocean water masses or buried in the sediment [Rullkötter, 2006; Morrison et al., 2015].

The relationship between the described vertical carbon flux and water depth follows an exponential regression [Christensen, 2000; Hensen et al., 2000]. Consequently, in shallow coastal shelf areas, a higher portion of carbon produced in the pelagial can reach the seafloor. In addition, benthic primary production by MPB and macroalgae are further carbon sources to supply material for benthic mineralization in shallow coastal regions, besides pelagic and ice algae production. With increasing water depths across shelves and towards the open ocean regions, more POM is mineralized in the pelagial and thus less is available as a food source for the benthic community. For example, approximately 5% of the surface primary production reaches 1000 m water depth [Hensen et al., 2006]. Furthermore, as primary production varies on spatial and temporal scales (see upper paragraph), so do vertical fluxes [Rowe et al., 1994; Hensen et al., 2000; Wassmann et al., 2004; Bauerfeind et al., 2009].

Vertical carbon fluxes in the Southern and Arctic Ocean show a great spatial and seasonal variability. In the Southern Ocean, the annual vertical carbon flux generally decreases with increasing latitude [Schlitzer, 2002]. During spring and summer, vertical carbon fluxes in the Southern Ocean have been observed to range between 0.03–10 mmol C m<sup>-2</sup> d<sup>-1</sup> [Smith et al., 2010; Rigual-Hernández et al., 2015]. However, unexpected high fluxes of up to 50 mmol C m<sup>-2</sup> d<sup>-1</sup> were found in the Atlantic sector of the Southern Ocean [Puigcorb  et al., 2017]. In shallower regions, the vertical carbon flux in summer can be up to 39 mmol C m<sup>-2</sup> d<sup>-1</sup> [Schloss et al., 1999; Smith et al., 2010]. During winter the vertical carbon flux in the open ocean may range between 0–0.2 mmol C m<sup>-2</sup> d<sup>-1</sup> [Rigual-Hernández et al., 2015]. The vertical carbon flux in the Arctic Ocean varies from <0.04 mmol C m<sup>-2</sup> d<sup>-1</sup> in winter to >50 mmol C m<sup>-2</sup> d<sup>-1</sup> in summer [Wassmann et al., 2004]. In the MIZ of the Barents Sea and the Bering Sea, vertical carbon fluxes of 42 mmol C m<sup>-2</sup> d<sup>-1</sup> and 50 mmol C m<sup>-2</sup> d<sup>-1</sup> have been

reported, respectively [Wassmann et al., 2004]. Lower vertical carbon fluxes of  $\leq 42 \text{ mmol C m}^{-2} \text{ d}^{-1}$  were reported for the eastern Arctic Fram Strait [Bauerfeind et al., 2009]. However, on the shelves and across the continental margins the vertical carbon flux can be up to  $108 \text{ mmol C m}^{-2} \text{ d}^{-1}$  [Macdonald et al., 2010]. Therefore, spatial and temporal variations in the vertical carbon flux cover up to three orders of magnitude in the Southern and Arctic Ocean.

### 1.3.2 Spatial and temporal variability of benthic remineralization across polar coasts, shelves and in the deep sea

After organic matter has built up by primary production and subsequently POM and DOC commenced mineralization in the ice or in the pelagial, the remaining organic carbon ultimately reaches the seafloor. Thereby, POM is the largest organic carbon source (>90%) [Hansell et al., 2009]. At the sea floor, if not resuspended, POM supplies the benthic community and will be mineralized. On large scales, benthic mineralization mirrors the surface primary production pattern [Wenzhöfer and Glud, 2002; Sachs et al., 2009; Bourgeois et al., 2017].

At shallow coastal locations ( $\leq 50 \text{ m}$  water depth) in the polar ecosystems, inter- and intra-annual variability of benthic mineralization was reported to range between 0.5–3 times the annual mean [Nedwell et al., 1993] and the spatial variability covers a range of up to two orders of magnitude [Woelfel et al., 2010]. Furthermore, benthic mineralization seems to decrease with increasing water depth at shallow coastal locations [Glud et al., 2002]. However, apart from three studies (Table 1.1), little is known about the benthic mineralization at the sediment-water interface (SWI) in shallow coastal environments of the Southern Ocean. At the Arctic coast, mineralization has been observed to vary between  $0\text{--}62 \text{ mmol C m}^{-2} \text{ d}^{-1}$  at different locations [Grebmeier and Cooper, 1995; Devol et al., 1997; Welch et al., 1997; Glud et al., 2002; Woelfel et al., 2010].

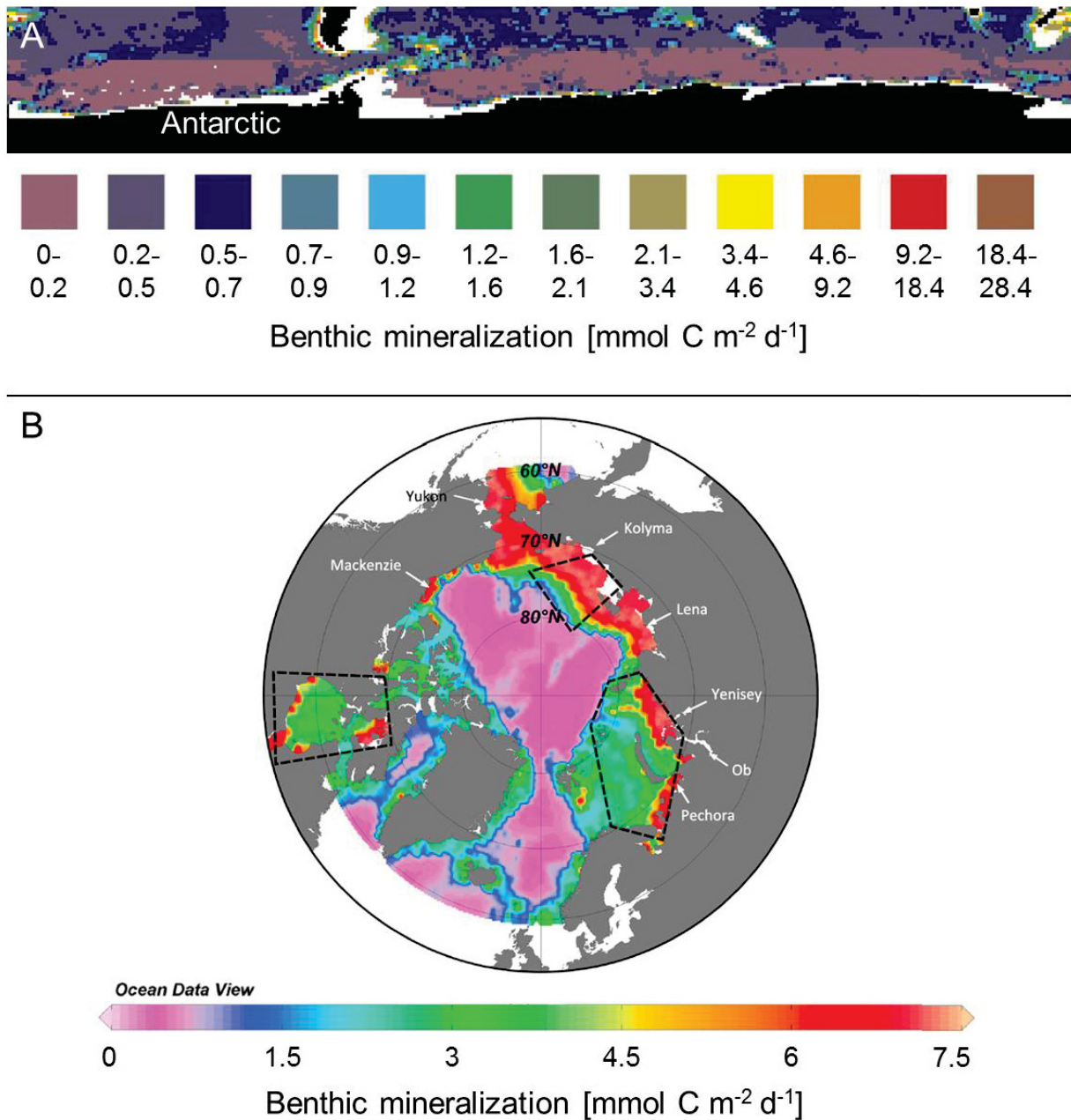
In the Southern Ocean shelf regions ( $>50 \text{ m}$  to  $\leq 800 \text{ m}$  water depth), spatial variability in the benthic mineralization covers up to three orders of magnitude (Table 1.1), while it only varied 2–3.5 times the annual mean [Baldwin and Smith, 2003 (1999–2000); Smith et al., 2006 (1990–1992)]. In Arctic shelf regions ( $>50 \text{ m}$  to  $\leq 200 \text{ m}$ ) benthic



mineralization has been reported to cover two orders of magnitude (Table 1.1, Figure 1.7). However, huge areas of the Lazarev Sea, Cosmonauts Sea, Davis Sea and D'Urville Sea in the Southern Ocean and the Barents Sea, the Kara Sea and the East Siberian Sea in the Arctic Ocean are uninvestigated regarding the benthic mineralization rates [Sachs et al., 2009; Bourgeois et al., 2017].

**Table 1.1.** Mineralization rates at different locations in shallow ( $\leq 50$  m water depth), shelf ( $> 50$  m to  $\leq 800$  m in the Southern Ocean and to  $\leq 200$  m in the Arctic), and deep sea locations ( $> 800$  m in the Southern Ocean and  $> 200$  m in the Arctic Ocean) in the Southern and Arctic Ocean.

Polar region	Location	Mineralization [mmol C m <sup>-2</sup> d <sup>-1</sup> ]	Reference
Antarctic, shallow	Signy Island, South Orkney Islands	15–69	[Nedwell et al., 1993]
Antarctic, shallow	Marian Cove, King Georg Island	9–28	[Shim et al., 2011]
Antarctic, shallow	New Harbour, Ross Sea	0.8–1.1	[Lohrer et al., 2013]
Arctic, shallow	Kongsfjorden (Spitsbergen)	1.5–62	[Woelfel et al., 2010]
Arctic, shallow	Resolute Bay, Canada	5–43	[Welch et al., 1997]
Arctic, shallow	Young Sound, Greenland	0–15	[Glud et al., 2002]
Arctic, shallow	Chukchi Sea	3–14	[Devol et al., 1997]
Arctic, shallow	Bering Sea	5–14	[Grebmeier and Cooper, 1995]
Antarctic, shelf	Weddel Sea and Bellingshausen Sea	0.4–18	[Hulth et al., 1997; Baldwin and Smith, 2003; Smith et al., 2006; Hartnett et al., 2008; Sachs et al., 2009]
Antarctic, shelf	Amundsen Sea	1.2–2.4	[Kim et al., 2016]
Antarctic, shelf	Ross Sea	0–6	[Nelson et al., 1996; Grebmeier et al., 2003]
Arctic, shelf	Eastern Greenland Shelf	0.5–1.3	[Piepenburg et al., 1997; Sauter et al., 2001]
Arctic, shelf	Canadian Archipelago	1.5–16	[Link et al., 2013a, b]
Arctic, shelf	Barents Sea	7–19	[Glud et al., 1998; Renaud et al., 2008]
Arctic, shelf	Laptev Sea	0.5–1.8	[Boetius and Damm, 1998]
Arctic, shelf	Chukchi Sea	3–16	[Clough et al., 2005]
Arctic, shelf	Bering Sea	11–25	[Grebmeier and Cooper, 1995]
Arctic, shelf	Beaufort Sea	2–5	[Renaud et al., 2007]
Antarctic, deep sea	Weddel Sea	0.1–3.8	[Hulth et al., 1997; Sayles et al., 2001; Grebmeier et al., 2003; Sachs et al., 2009]
Antarctic, deep sea	Amundsen Sea	1.3–1.8	[Kim et al., 2016]
Arctic, deep sea	Eastern Fram Strait	0.1–3.2	[Piepenburg et al., 1997; Sauter et al., 2001]
Arctic, deep sea	Western Fram Strait	0.1–1.9	[Cathalot et al., 2015]
Arctic, deep sea	Barents Sea	1.3–29	[Piepenburg et al., 1995; Renaud et al., 2008]
Arctic, deep sea	Laptev Sea	0.1–0.9	[Boetius and Damm, 1998]
Arctic, deep sea	Chukchi Sea	0.3–3.2	[Clough et al., 2005]
Arctic, deep sea	Canadian Archipelago	1.3–5	[Link et al., 2013a, b]
Arctic, deep sea	Beaufort Sea	1.5–8	[Renaud et al., 2007]
Arctic, deep sea	Central Arctic Ocean	0.3–1.1	[Clough et al., 2005; Boetius et al., 2013]



**Figur 1.7.** Benthic mineralization in the Southern and Arctic Ocean. A: Southern Ocean benthic mineralization expressed in water depths >1000 m (modified after Christensen [2000]). B: Benthic mineralization in the Southern Ocean in water depths from 17–4808 m (modified after Bourgeois et al. [2017]). The locations of the main Arctic rivers are indicated in the figure. The dashed black polygons represent areas where no empirical data have been collected.

Benthic mineralization in the Southern Ocean deep sea (>800 m water depth) has been measured to be 0–9  $\text{mmol C m}^{-2} \text{d}^{-1}$  (Figure 1.7) [Christensen, 2000]. At the polar front of the Southern Ocean at ~50°S latitude mineralization ranged between

0.3–2.1 mmol C m<sup>-2</sup> d<sup>-1</sup>, whereas at 60–70°S latitude an average mineralization rate of 3.9 mmol C m<sup>-2</sup> d<sup>-1</sup> was measured, and at 70–80° S latitude 0.5 mmol C m<sup>-2</sup> d<sup>-1</sup> [Wit et al., 1997; Rabouille et al., 1998; Christensen, 2000]. Regional differences in Southern Ocean deep-sea benthic mineralization ranged between 0.1–3.8 mmol C m<sup>-2</sup> d<sup>-1</sup> (Table 1.1) [Hulth et al., 1997; Sayles et al., 2001; Grebmeier et al., 2003; Sachs et al., 2009]. The amount of organic carbon buried in the soft bottom seafloor in the Ross Sea was reported to be <0.5% of POM from the net community production [Catalano et al., 2010]. Arctic deep sea (>200 m water depth) benthic mineralization has been assessed to be <4.2 mmol C m<sup>-2</sup> d<sup>-1</sup> and decreases with increasing water depth (Figure 1.7) [Bourgeois et al., 2017]. However, regional differences in benthic mineralization ranged between 0.1–8 mmol C m<sup>-2</sup> d<sup>-1</sup> (Table 1.1) [Boetius and Damm, 1998; Renaud et al., 2007] and less than 0.1% of the organic carbon reaching the seafloor is assumed to be buried [Cranston, 1997].

In general, benthic mineralization in the Southern Ocean is lower than observed in the Arctic Ocean. This may be explained by the food bank hypothesis, as supported empirically by studies conducted in the Southern Ocean [Mincks et al., 2005; Smith et al., 2006; Smith et al., 2012]. The food bank hypothesis states that a combination of high food input and low temperatures (which prevent fast degradation of organic matter) results in the appearance of benthic food banks which will persist and feed the benthic community throughout an entire year (Figure 1.8) [Smith et al., 2012]. The shelf and deep-sea benthic organisms in the Southern Ocean do not react with increased mineralization activity to large food inputs, as indicated by a lack of seasonal variability in macrofauna densities and bioturbation activity [Glover et al., 2008; McClintic et al., 2008]. Therefore, food is permanently available and is mineralized constantly within an annual cycle. Results of Włodarska-Kowalczyk et al. [2016] indicate that in Arctic fjords the food bank hypothesis may also be applicable. However, such a hypothesis has been rebutted for deep sea Arctic benthos [Boetius et al., 2013].

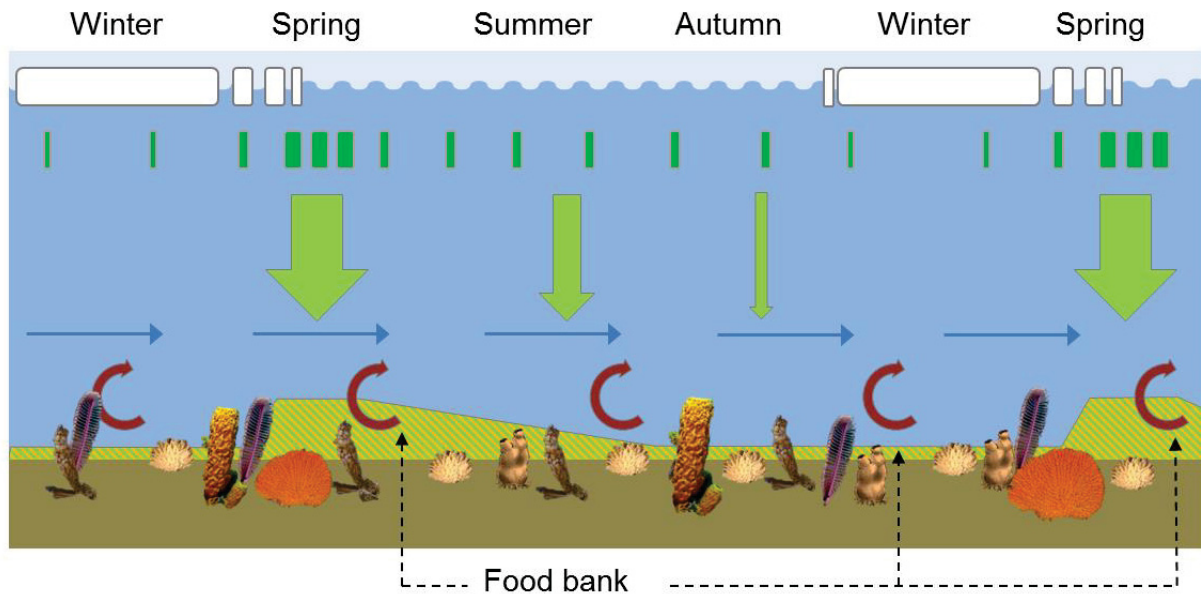


**Figure 1.8.** Synoptic view on food bank hypothesis showing the seasonal vertical flux (light green arrows) of new organic matter (light green bars) originating mainly at the beginning of spring, the seasonal variation of food banks (light green with orange stripes) and the lateral (blue arrows) and resuspension transport just above the seabed (dark red arrows close the bottom). Figure modified after Adams et al. [2009].

## 1.4 Climate change associated effects on the carbon cycle in polar environments

### 1.4.1 Recent environmental changes in the Southern Ocean

An important parameter for assessing climate change is temperature. Increasing near-surface temperature trends were observed in the Antarctic [Vaughan et al., 2001; Turner et al., 2005], which is a result of ozone depletion in the stratosphere [Thompson, 2002], increased heat uptake by the open ocean due to local sea-ice loss [Turner et al., 2013; Parkinson, 2014], enhanced westerly winds [Thompson, 2002; Marshall et al., 2006], and changes in the strength of the Southern Annual Mode [Ding et al., 2011; Clem and Fogt, 2013]. However, these increasing temperature trends were limited to the Western Antarctic and the Antarctic Peninsula [Vaughan et al., 2001; Turner et al., 2005; Chapman and Walsh, 2007; Steig et al., 2009], with a maximum increase of 5°C per decade over the period 1971–2000 [Turner et al., 2005]. Additionally, the sea-surface temperature increased in the entire Southern Ocean by 0.1–0.5°C per

decade over the period 1971–2004 [Zhang, 2007]. However, over the period 1999–2014 temperatures around the Antarctic Peninsula decreased [Turner et al., 2016].

Owing to these increasing temperatures, the sea-ice extent in the Southern Ocean has decreased substantially around the Antarctic Peninsula, in the Bellingshausen Sea, and in the Amundsen Sea over the period 1979–2014 [Stammerjohn et al., 2012; Meehl et al., 2016]. As a consequence, the period of the sea-ice free season increased in the latter areas [Stammerjohn et al., 2015]. However, an increase in the sea-ice concentration over the period 1999–2014 has been reported by for the Antarctic Peninsula [Turner et al., 2016]. Nevertheless, the warming has also contributed to the regional retreat of glaciers [Rückamp et al., 2011; Cook et al., 2016], volume loss of ice shelves [Paolo et al., 2015], and disintegration of floating ice shelves [Vaughan, 1993].

Owing to the melting of sea-ice and glaciers, an increase in the stratification within the upper pelagic zone of the Southern Ocean is predicted [Le Quere et al., 2007]. This would lead to a reduced pelagic primary production, due to a suppressed deep water nutrient supply and a lower ability to remove atmospheric carbon dioxide [Arrigo et al., 2008a]. In contrast, a predicted poleward intensification of the westerly winds [Russell et al., 2006] may counteract the stratification, increase deep water nutrient supply, increase the facility of the ocean for atmospheric carbon dioxide uptake and therefore lead to an increased primary production [Arrigo et al., 2008a]. Taking these factors together into account, the Antarctic sea-ice extent is predicted to decrease by 17–31% [Meehl et al., 2000], with a 25% decrease in the sea-ice extent potentially leading to an increase of >10% in the pelagic primary production [Arrigo and Thomas, 2004; Arrigo et al., 2008a]. In addition, opening shelf ice enables primary production to take place in formerly aphotic areas [Peck et al., 2010] and retreating glaciers offering more space for primary producer colonization [Deregibus et al., 2016]. Again, the situation is complex, as with diminishing of sea ice, also the habitat utilized by sea-ice algae will be removed [Barnes et al., 2009]. Therefore, the contribution of the sea-ice algae primary production to the total primary production will be reduced. Furthermore, particle release by glacial melting lowered light availability in the water column [Schloss et al., 1999; Deregibus et al., 2016], which may suppress primary production.

The ice-melt induced changes to the primary producers also affect the higher levels of the food web. Due to the decline in winter sea ice, there has been a decrease in krill abundances and an increase in salp abundances [Pakhomov et al., 2002; Atkinson et al., 2004]. Krill and salp are key players utilizing the pelagic primary production in the entire Southern [Atkinson et al., 2004; Atkinson et al., 2008; Gleiber et al., 2012]. However, fecal pellets of salps sink faster and contain up to 100 times more carbon than those of krill [Gleiber et al., 2012]. Therefore, implications of climate change may lead to increasing vertical carbon fluxes in the Southern Ocean [Gleiber et al., 2012].

The opening of shelf ice was reported to be accompanied by a rapid increase in benthic macrofauna biomass and retreating glaciers have provided more space for heterotrophic consumers [Fillinger et al., 2013; Lager et al., 2017; Seefeldt et al., 2017]. An increase in biomass may be correlated with an increase in mineralization [Glud et al., 1994; Boetius and Damm, 1998; Moodley et al., 2008; Braeckman et al., 2010; Herrera et al., 2014]. Contrastingly, particle release by glacial melting and permafrost has led to substantial changes in the benthic macrofauna structure in some areas [Schloss et al., 1999; Sahade et al., 2015; Deregibus et al., 2016] with unpredicted implications for the benthic mineralization. In turn, the degree to which climate change-related effects will lead to decreasing or increasing primary production and mineralization in the Southern Ocean is still under debate.

### 1.4.2 Recent environmental changes in the Arctic Ocean

Climate change related increase in temperatures was also observed in the Arctic. The Arctic atmospheric temperature has increased by 3°C since 1880. Due to the polar amplification, this is three times above the global trend of 0.85°C for the same period (Figure 1.9) [Manabe and Stouffer, 1980; Hassol, 2004; IPCC, 2013]. Additionally, sea-surface temperatures globally increased by 0.11°C per decade over the period 1971–2010, while a significant warming in water depths >700 m has not yet been reported [IPCC, 2013].

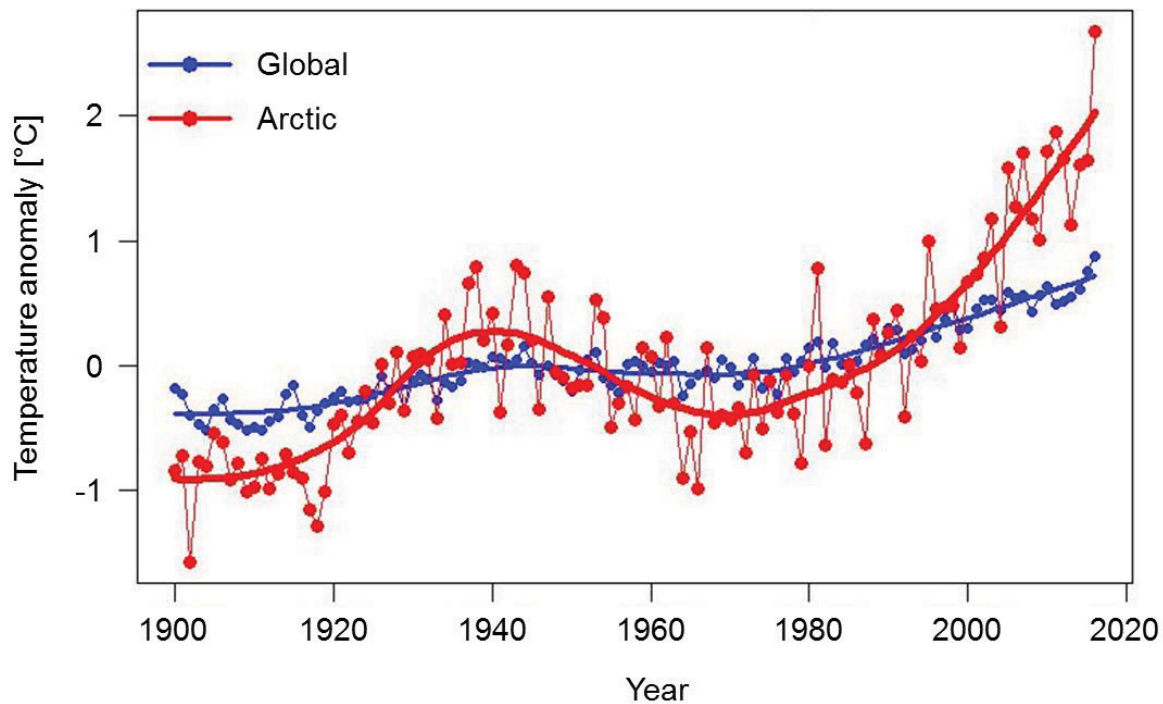


**Figure 1.9.** Global and Arctic atmospheric temperature anomaly. Figure modified after <https://tamino.wordpress.com/2016/12/14/arctic/>.

In the Arctic, the warming trend causes sea-ice thinning, a reduction in sea-ice cover, and a decrease of perennial sea ice [Comiso, 2002; Comiso et al., 2008; Kwok and Rothrock, 2009]. The annual sea-ice extent decreased by 3.7% per decade over the period 1979–2007 with an enhanced negative trend of 10.1% per decade between 1996–2007 [Comiso et al., 2008]. Therefore, the sea-ice edge is progressively moving northwards [Vaughan et al., 2013]. In addition, owing to the low albedo of the dark water surface, the temperature of the upper water column is likely to increase further [Parkinson, 2014]. Consequently, abiotic factors such as light availability, nutrient distribution and surface salinity are predicted to change as a result [Anderson and Kaltin, 2001; Overland et al., 2011; Serreze and Barry, 2011].

These abiotic changes affect the entire marine ecosystem in the Arctic Ocean and may force an alteration of the pelagic primary production [Kahru et al., 2011; Wassmann, 2011; Wassmann et al., 2011]. The likelihood of a general increase in primary production within the Arctic Ocean is still under debate. Some studies have argued that, with increasing melt ponds formation, which allows more light to penetrate into the upper water column, an increasing primary production is likely [Arrigo et al.,

2012; Nicolaus et al., 2012; Boetius et al., 2013]. However, the growth of algae is also limited by the availability of nutrients [Lalande et al., 2014]. An intensified melt season may result in increased freshwater input into the Arctic Ocean, which favors a stratification of the upper water column [Peterson, 2002; Arrigo, 2013]. This would suppress the nutrient supply by deeper water masses and therefore prevent an enhanced primary production [Tremblay et al., 2015]. In addition, the growing season is predicted to be further restricted, due to an earlier and faster spring melt [Arrigo, 2013]. However, increasing wind speeds are predicted for the central Arctic Ocean, which may lead to an enhanced upwelling in some areas [Spren et al., 2011]. In such a situation, the upwelling-related sufficient nutrient supply may support an enhanced primary production. Furthermore, a compositional shift in the spring phytoplankton bloom from diatom-dominated to coccolithophorid or *Phaeocystis* sp. and nanoflagellate-dominated communities is predicted [Bauerfeind et al., 2009; Lalande et al., 2014; Soltwedel et al., 2015]. Such an altered algal composition may reduce zooplankton densities [Caron and Hutchins, 2013] and lead to increased vertical POM fluxes [Wohlers et al., 2009; Wassmann, 2011; Boetius et al., 2013]. However, the labile detritus flux is predicted to decrease [Hop et al., 2006; van Oevelen et al., 2011] and the seasonal patterns of vertical fluxes might also change [Wassmann, 2011]. Consequently, changing sea-ice conditions in the Arctic Ocean may alter the quality and quantity of primary production and the vertical carbon flux to the seafloor, where it can affect benthic deep-sea communities [Jones et al., 2014; Harada, 2015].

If and how these changes may alter the Arctic benthic mineralization is still under discussion and seems to differ strongly on local scales. Shelf and shallow coastal regions may experience an increase in benthic mineralization [Bourgeois et al., 2017], owing to an increased food supply resulting from enhanced primary production [Arrigo and Dijken, 2011]. This is very likely, especially for the Chukchi and the Bering Sea, where a strengthened Pacific inflow can supply additional nutrients for primary production [Findlay et al., 2015; Harada, 2015]. In contrast, a shift towards smaller sized phytoplankton communities might lead to lower sinking rates and an increase in pelagic mineralization [Li et al., 2009; Bourgeois et al., 2017]. Consequently, less food will reach the seafloor and affect the deep-sea benthic mineralization. However, long-term time



series of benthic mineralization rates, which are crucial for predicting future developments, are local and rare [Wassmann et al., 2011].

## 1.5 Objectives and hypotheses

The Southern Ocean and the Arctic Ocean are quantitatively the most important ecosystems for worldwide organic carbon dynamics on spatial and temporal scales [Tjiputra et al., 2013; Heinze et al., 2015]. A key feature of polar ecosystems is the cryosphere, which includes different ice species, e.g. sea ice, ice shelves, glacial ice, and permafrost soil (frozen water-sediment mixture). Changes in the polar cryosphere, e.g. melting glaciers and changing sea-ice cover, may alter the light availability. As introduced, light availability is an important factor for primary production, on which in turn the benthic mineralization relies. Hence, changes in the ice conditions may lead to changes in the organic carbon cycle in the polar oceans.

Glaciers melt and retreat in the Western Antarctic and across Greenland [Straneo and Heimbach, 2013; Paolo et al., 2015; Cook et al., 2016; Hill et al., 2018]. In the same areas and at the Russian, American and Canadian Arctic coasts, permafrost soils melt and the volumes of riverine runoffs are increasing [Peterson, 2002; Hinzman et al., 2005; Gruber, 2012; Vonk et al., 2015; Ramos et al., 2017; Pablo et al., 2018]. The secondary effects of these changes have been observed to include increased release of particles into the marine realm, accompanied by an increased turbidity and sedimentation rate [Schloss et al., 1999; Dierssen et al., 2002; Vonk et al., 2015; Deregibus et al., 2016]. Furthermore, directly at the glacial front chunks of ice drop off, fall into the water, hit the soft seafloor with soft sediment seafloor particles potentially being resuspended, which also can lead to an increased turbidity [Barnes, 1999; Griffiths, 2010]. Thus, glacial and permafrost soil melt likely reduces the light availability in the shallow coastal Southern and Arctic Ocean.

Substantial changes in the sea-ice cover occurred in the Amundsen Sea, Bellingshausen Sea, and Weddel Sea in the Southern Ocean and the central and western Arctic Ocean over time [Turner et al., 2005; Comiso et al., 2008; Adams et al., 2009; Vaughan et al., 2013]. The sea ice in these regions has become thinner, more melt ponds have occurred in the summer seasons, sea ice retreated, sea-ice

concentration decreased, the melting periods have started earlier, and the freezing periods have started later [Comiso, 2002; Turner et al., 2005; Lüthje et al., 2006; Galley et al., 2008; Adams et al., 2009; Vaughan et al., 2013; Gutt et al., 2015]. The secondary effects of these changes include an increased light availability in the polar open oceans.

I investigated if the above-mentioned secondary effects of changes in the cryosphere (turbidity and sediment accumulation, increased light availability) have a substantial impact on primary production and benthic mineralization in shallow and deep-sea polar regions. Other upcoming changes, which may also affect primary production and, owing to its relationship, benthic mineralization in polar ecosystems such as changing nutrient supply or changing wind patterns and speed, are only part of the discussion and are not addressed by any of the included research manuscripts.

The following research questions were identified:

1. To which degree does glacial melt-related particle release affect Southern Ocean MPB primary production in shallow coastal areas?
2. To which degree does glacial melt-related particle release affect Southern Ocean benthic mineralization in shallow, coastal areas?
3. Does the presence of sea-ice impact Arctic deep-sea benthic mineralization patterns?

The following objectives were derived from these questions:

1. Determination of primary production rates of a microphytobenthic community, which was exposed to different intensities of glacial melt-related particle release.
2. Identification of key parameters which influence benthic mineralization in the shallow, coastal Southern Ocean and in the Arctic deep-sea.
3. Investigation of spatial variability of benthic mineralization in the shallow, coastal Southern Ocean and in the Arctic deep-sea.

The following hypotheses are answered within the thesis chapters:

1. Glacial melt-related particle release affects the primary production of Southern Ocean MPB (manuscript I in section 3)
2. Glacial melt-related particle release affect the benthic mineralization in the shallow coastal Southern Ocean (manuscript II in section 4)
3. The presence of sea-ice impacts polar deep-sea benthic mineralization patterns (manuscript II in section 5)

Due to the remoteness and high seasonality of the polar ecosystems, year-round data acquisition is restricted to a limited amount of locations [Takahashi et al., 2009; Wassmann et al., 2011; Sabine et al., 2013; Bourgeois et al., 2017]. In turn, modeled predictions of future carbon flux dynamics need to be assessed carefully. Therefore, results of short-term, observational studies have been used to outline potential future developments regarding primary production and mineralization in the polar ecosystems within this thesis.



## 2 Material and methods

---

### 2.1 Study sites

#### 2.1.1 Potter Cove, Antarctic Peninsula

Potter Cove is a shallow, fjord-like inlet of Maxwell Bay in the southwest of King George Island/Isla 25 de Mayo, an island located at the tip of the Antarctic Peninsula (Figure 2.1).

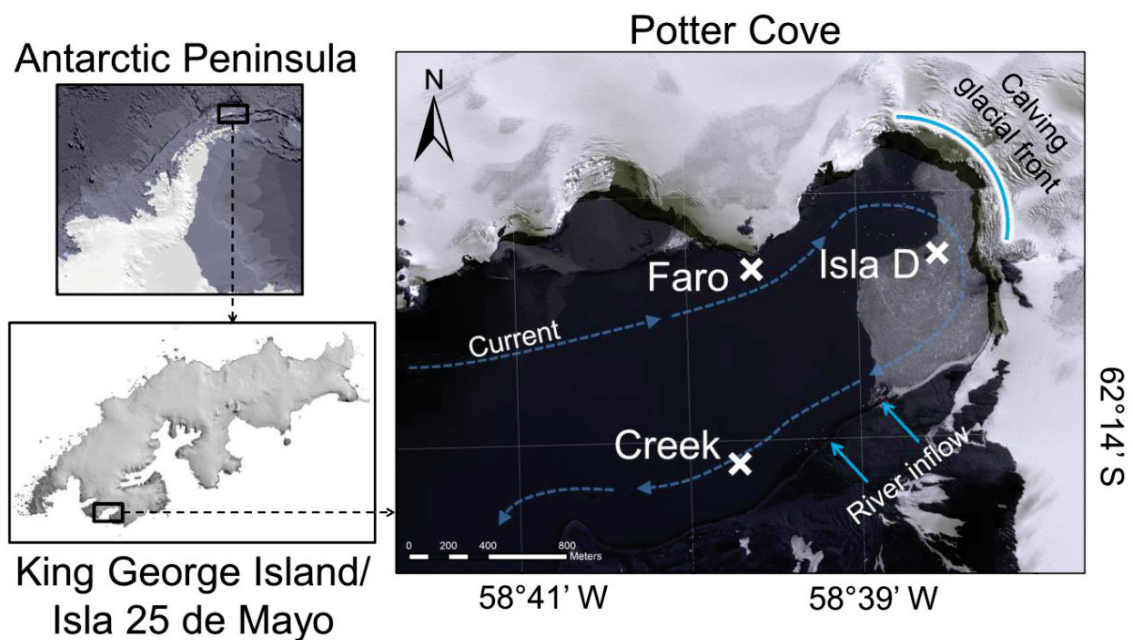


**Figure 2.1.** Map of the study site Potter Cove, including investigated locations Faro, Creek and Isla D.

The cove is approximately 1.2 km wide and 4 km long on the northern and 3 km long on the southern shore site with the mouth located at the western site. At Potter Cove's

mouth, the seafloor lifts from >180 m in an easterly direction to a first sill at ~50 m water depth. After the first sill, water depth remains at ~50 m till a second sill, located roughly one kilometer before the glacial front, where the seafloor lifts to ~20 m water depth.

While the seafloor of the outer cove (before the first sill in <50 m water depth) mainly consists of macroalgae covered hard bottom, the inner part also consists of soft sediment [Quartino and Zaixso, 2008; Wöflf et al., 2014; Pasotti et al., 2015]. The general current moves clock-wise with an average current speed of  $0.03 \text{ m s}^{-1}$  [Lim et al., 2013]. The retreating Fourcade glacier [Rückamp et al., 2011] and seasonal meltwater discharge, a result of permafrost and snow thawing, release a high amount of particles into the cove [Klöser et al., 1993; Schloss et al., 1999]. Consequently, a turbidity gradient occurs across Potter Cove, which starts at the glacial front and decreases along the southern shore site as it follows the general current [Klöser et al., 1993; Sahade et al., 2015; Monien et al., 2017].

Primary producers in Potter Cove are phytoplankton, macroalgae and MPB [Klöser et al., 1993; Schloss et al., 1998; Al-Handal and Wulff, 2008a; Quartino and Zaixso, 2008]. Pelagic primary production in austral spring and summer 1991/1992 ranged between  $8 \text{ mg C m}^{-2} \text{ d}^{-1}$  and  $40 \text{ mmol C m}^{-2} \text{ d}^{-1}$  and remained constant over the period 1991–2009 [Schloss et al., 1998; Schloss et al., 2012]. Monthly species-specific macroalgae primary production was 4–66  $\text{mg dry biomass g}^{-1} \text{ tissue}^{-1} \text{ d}^{-1}$  during the period December 1994 to March 1995, with 15  $\text{mg dry biomass g}^{-1} \text{ tissue}^{-1} \text{ d}^{-1}$  of the most abundant macroalgae species [Quartino and Zaixso, 2008]. MPB communities inhabit the soft bottom of Potter Cove [Al-Handal and Wulff, 2008a; Wulff et al., 2008]. However, benthic carbon demand and an area-specific carbon production by macroalgae and the MPB have not been investigated so far.

Two research campaigns were carried out to Potter Cove (KGI14/15, 15/01/2015–15/03/2015 and KGI16/17, 14/10/2016–31/12/2016). During the campaigns, three stations, namely Faro, Creek and Isla D, were investigated (Figure 2.1), located in water depths between 6 m and 9 m. These stations are glacial ice-free since 1995, the early 1950s, and 2000, respectively [Rückamp et al., 2011], but are covered by sea ice during winter [Schloss et al., 2012]. Furthermore, the three stations experience different intensities of glacial melt-related particle disturbances. The amount of suspended

particulate matter in the water column was intermediate at Faro, lowest at Creek and highest at Isla D [Monien et al., 2013]. The turbidity at Faro and Creek was similar, while Isla D showed a higher turbidity [Deregibus et al., 2016]. The sediment accumulation was lowest at Faro, intermediate at Creek, and highest at Isla D [Pasotti et al., 2015]. The macrofauna biomasses in 15 m water depth were similar at Faro and Creek, while at Isla D the macrofauna biomass was lower [Pasotti et al., 2015]. Meiofauna biomass was highest at Creek and lowest at Isla D and the community composition of both, macro- and meiofauna differed strongly between the three stations [Pasotti et al., 2015].

### 2.1.2 Fram Strait, Arctic Ocean

Fram Strait is an approximately 500 km wide passage between northeast Greenland and the Svalbard archipelago located in the northern Greenland Sea (Figure 2.2). With water depths of up to 5500 m, it is the only exchange route for intermediate and deep Arctic water masses [Soltwedel et al., 2005; Forest et al., 2010]. The inflow volume in the Fram Strait is five times larger than the inflow of Pacific water through the Bering Strait [Coachman and Aagaard, 1988; Roach et al., 1995; Fahrbach et al., 2001]. The East Greenland Current (EGC) and the West Spitsbergen Current (WSC) are the main currents in the Fram Strait and influence the upper 300 m waters column [Manley, 1995]. The EGC is located in the western Fram Strait and transports cold, less saline and nutrient poor ( $1^{\circ}\text{C}$ ,  $<34.4$ ) Arctic waters [Manley, 1995] southward with a flow velocity of  $9\text{ cm s}^{-1}$  [Fahrbach et al., 2001; Hop et al., 2006]. In contrast, the WSC, located in the eastern Fram Strait, transports warmer, nutrient-rich Atlantic waters of higher salinity ( $>3^{\circ}\text{C}$ ,  $>35$ ) [Manley, 1995] with a flow velocity of  $20\text{--}50\text{ cm s}^{-1}$  northward [Hop et al., 2006]. About 22% of the WSC is recirculated as the Return Atlantic Current (RAC). The remaining current bifurcates into the Svalbard Branch (SB; 33%) and the Yermak Branch (YB; 45%), following the Svalbard coast or flowing along the northwest flank of the Yermak Plateau, respectively [Schauer, 2004]. The EGC and WSC are separated by the East Greenland Polar Front [Paquette et al., 1985] and the latter varies between  $5^{\circ}\text{E}$  and  $3^{\circ}\text{W}$  [Hop et al., 2006]. Below the WSC, Norwegian Sea Deep Water enters the Arctic Ocean through the Fram Strait [Jones et al., 1995]. Furthermore, the Spitsbergen Polar Current (SPC) [Helland-Hansen and Nansen, 1909] transports cold and less

saline, Arctic waters masses from the Barents Sea and the Storfjorden along the west coast of Spitsbergen [Nilsen et al., 2016].

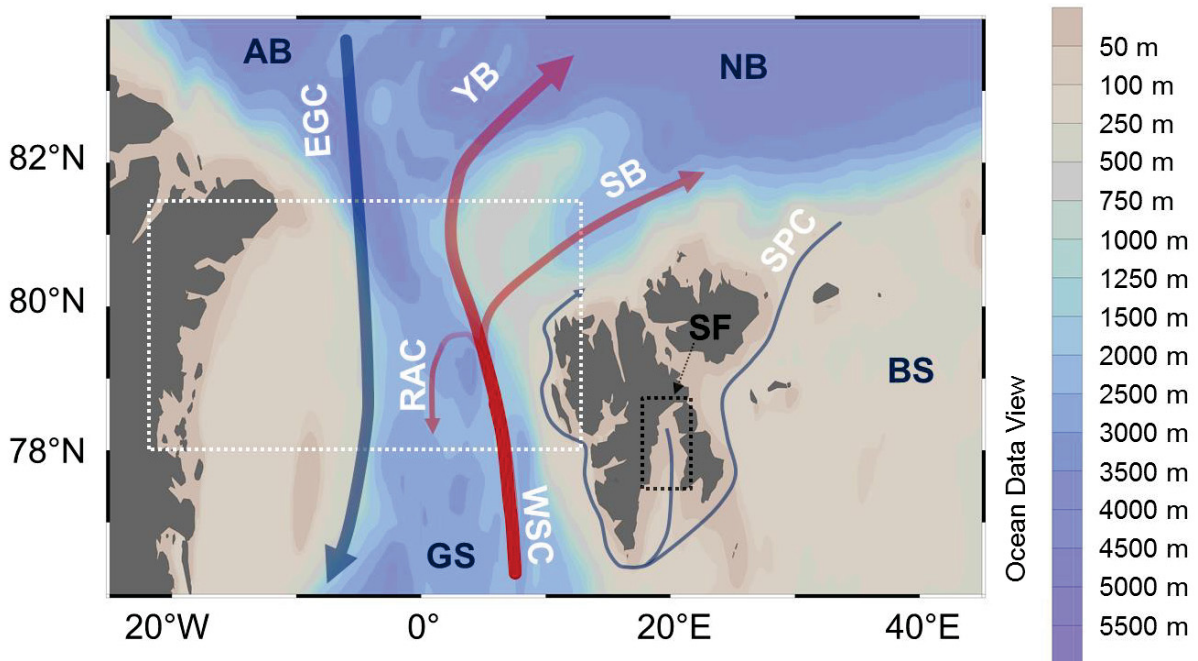


**Figure 2.2.** Map of the current system in the Arctic Fram Strait. White dotted frame = Fram Strait region, Black dotted frame = Storfjorden, Blue = Arctic water, Red = Atlantic water, EGC = East Greenland Current, WSC = West Spitsbergen Current, RAC = Return Atlantic Current, SB = Svalbard Branch, YB = Yermak Branch, SPC = Spitsbergen Polar Current, AB = Amundsen Basin, NB = Nansen Basin, BS = Barents Sea, GS = Greenland Sea.

A high sea-ice cover is reported for the western Fram Strait and a low sea-ice cover for the eastern Fram Strait [Soltwedel et al., 2005; Soltwedel et al., 2015; Spielhagen et al., 2015]. The sea ice in Fram Strait originates from the Laptev Sea and the East Siberian Sea [Hansen et al., 2013]. The sea-ice cover and sea-ice extent in Fram Strait are relatively stable, inter- and intra-annually (Figure 2.3) [Soltwedel et al., 2005; Comiso et al., 2008; NOAA, 2018]. However, the mean sea-ice age becomes younger by 0.6 years per decade [Krumpfen et al., 2016], which is congruent with a decrease in the sea-ice thickness [Hansen et al., 2013; Renner et al., 2014; Krumpfen et al., 2016].

The temporal and spatial distribution of primary production in the Fram Strait is highly variable owing to varying light conditions and nutrient supply [Smith, 1995]. In general, the Fram Strait can be divided into four primary productive regions: i) the coastal region of Spitsbergen, ii) the open ocean in the eastern Fram Strait, iii) the MIZ, and iv) the sea-ice covered western Fram Strait.



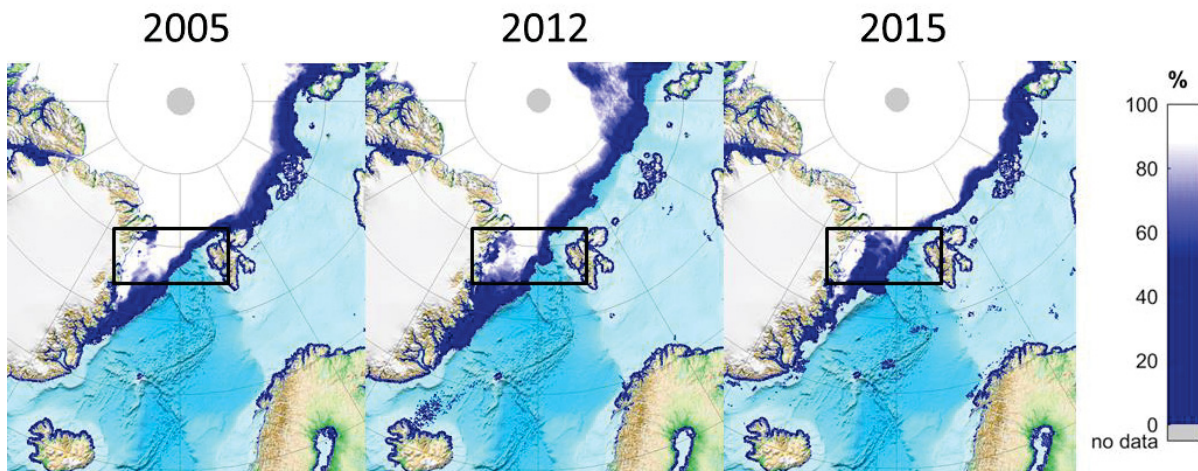


**Figure 2.3.** Mean September sea-ice concentration in the Arctic Ocean in the years 2005, 2012, and 2015. The mean sea-ice concentration in the Fram Strait (black frame) altered annually, but the general sea-ice pattern was stable: A high sea-ice cover occurred in the western Fram Strait and barely any sea ice occurred in the eastern Fram Strait. This general pattern remained also in years with an exceptional low sea-ice extent (2012). Images were provided by [www.meereisportal.de](http://www.meereisportal.de).

The onset of the primary production in the coastal region of Spitsbergen starts earlier than it does in the open ocean, the MIZ, or the western Fram Strait [Cherkasheva et al., 2014]. The annual primary production in the coastal region of Spitsbergen is  $3.3\text{--}5 \text{ mol C m}^{-2} \text{ yr}^{-1}$  [Hill et al., 2013]. In the open water region,  $4.2\text{--}5 \text{ mol C m}^{-2}$  is already produced in the period between May and August [Rey et al., 2011] with the annual primary production reported to be  $6.7\text{--}10 \text{ mmol C m}^{-2} \text{ yr}^{-1}$  [Smith et al., 1987]. A daily primary production of  $142 \text{ mmol C m}^{-2} \text{ d}^{-1}$  is reported for the MIZ in Fram Strait [Niebauer, 1991]. This results in a 2- to 2.5-fold higher annual primary production compared to the open ocean region, assuming a primary production period of 90–120 days [Gradinger, 2009; Cherkasheva et al., 2014]. However, the primary productivity in Fram Straits MIZ is still four times lower than what is observed in the MIZ of the Bering Sea, owing to lower nutrient concentrations [Niebauer, 1991]. Satellite-based annual primary production estimates for the western Fram Strait have ranged between  $2\text{--}20 \text{ g C m}^{-2} \text{ yr}^{-1}$  [Pabi et al., 2008; Hill et al., 2013]. This is similar to on-site measured primary production [Smith, 1995; Pesant et al., 1996]. The lower primary production in the western Fram Strait is a result of the low light availability, owing to a permanent high sea-ice cover, and the low nutrient supply, owing to the predominant Arctic water masses [Manley, 1995; Soltwedel et al., 2005; Krumpfen, 2017]. None of the

mentioned studies includes primary production by ice algae. Their contribution to the total primary production in the Fram Strait has to date been barely investigated. However, ice algae patches, a strong indicator of high ice algae production [Boetius et al., 2013], were not found during a photo surveys of the seafloor in the western Fram Strait (personal comment by James Taylor). Furthermore, it seems that the contribution of ice algae primary production to the total primary production is low in lower latitudes and of more significance in the central Arctic Ocean [Gosselin et al., 1997].

Primary producers are dominated by diatoms, which are responsible for approximately 50% of the biomass that is produced in the northern North Atlantic Ocean [Bauerfeind et al., 1994; Bauerfeind et al., 2009]. However, the composition of the primary production shifts on annual base from the ice algae *Nitzschia frigida* in March [McMinn and Hegseth, 2004] to pelagic algae *Chaetoceros socialis*, *Chaetoceros furcellatus*, *Thalassiosira nordenskiöldii*, *Thalassiosira antarctica*, *Thalassiosira hyaline* and *Fragilariopsis oceanic* during the spring bloom between April and June [McMinn and Hegseth, 2004; Richardson et al., 2005; Cherkasheva et al., 2014]. During the summer months July and August, algal surface communities have been observed to be dominated by the genera of *Chaetoceros* spp., *Nitzschia* spp. and *Thalassiosira* spp. [Spies, 1987; Nöthig et al., 2015].

Approximately 30–45% of the annual primary production leaves the photic zone at the western coast of Spitsbergen, in the open ocean region, and in the MIZ [Sakshaug, 2004; Hop et al., 2006; Bauerfeind et al., 2009]. However, only 2.5–2.7 g C m<sup>-2</sup> yr<sup>-1</sup> reaches the seafloor [Bauerfeind et al., 2009; Lalande et al., 2016]. Thus, 5–9% of the total primary production is available for the deep-sea benthic community as a food and energy resource during the observed years. However, owing to the huge catchment area of particle traps located in the deep sea and the influence of lateral transport processes [Waniek et al., 2000; Lalande et al., 2016], the regions of origin of this settling material (MIZ, open ocean, coast of Spitsbergen) are difficult to assess with certainty. In the western Fram Strait, 2% of the primary production was exported below 1000 m water depth, with 1.2% reaching the seafloor [Schlüter et al., 2001].

The benthic community in the MIZ and the open ocean region mineralizes 0.14–0.84 mmol C m<sup>-2</sup> d<sup>-1</sup> in sediments at water depths between 1000–5500 m [Cathalot

et al., 2015; Donis et al., 2016]. The mineralization in the western Fram Strait ranged between  $0.1\text{--}2.7 \text{ mmol C m}^{-2} \text{ d}^{-1}$  in sediments at water depths between 45–1950 m [Piepenburg et al., 1997; Sauter et al., 2001].

The long-term ecological research (LTER) area HAUSGARTEN, located in the Fram Strait, was established in 1999 to identify key factors controlling deep-sea biodiversity in the Arctic region [Soltwedel et al., 2005]. Currently, the LTER HAUSGARTEN comprises 21 stations located between  $5^{\circ}\text{E}\text{--}11^{\circ}\text{W}$  and  $78.5^{\circ}\text{N}\text{--}80^{\circ}\text{N}$  and cover water depths of 200–5500 m. Two research campaigns were carried out to the LTER HAUSGARTEN with RV Polarstern (PS85, 6/6/2014–3/7/2014 and PS93.2, 22/7/2015–15/8/2015) to obtain relevant parameters for this thesis. During these campaigns, benthic mineralization rates, densities and biomasses of biota, concentrations of biogenic compounds, and abiotic parameters were determined at 12 stations (Figure 2.4). The stations included the coastal region of Spitsbergen, the open ocean in the eastern Fram Strait, the MIZ, and the western Fram Strait and covered water depths of 270–2500 m. For a detailed description of station locations and the conducted measurements, the reader is referred to section 5 and Table 2.1.

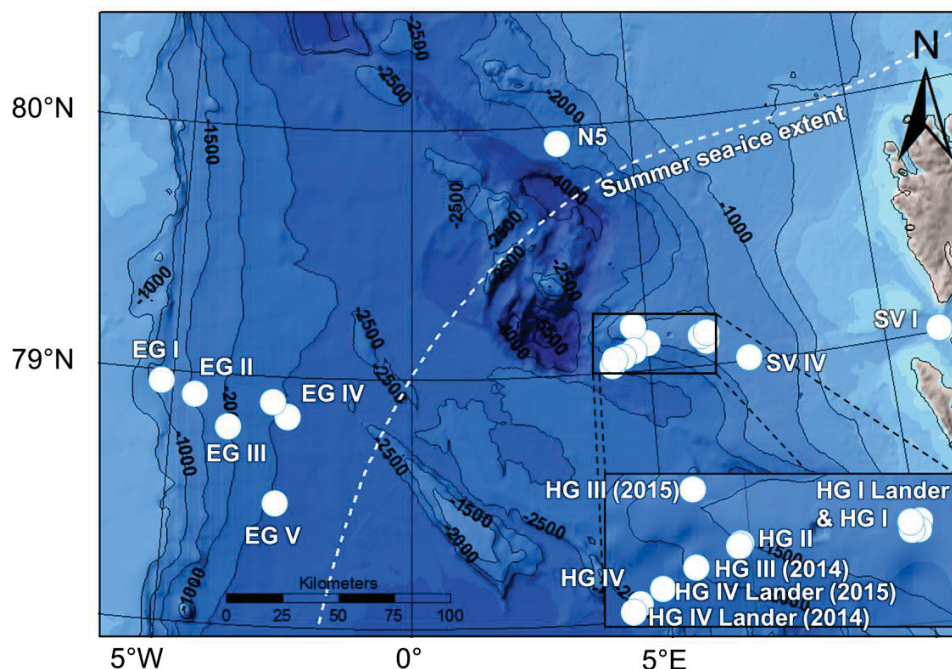


**Figure 2.4.** Map of the Fram Strait including investigated stations of the LTER HAUSGARTEN [Soltwedel et al., 2005]. In case, stations were visited in 2014 and 2015, the sampling year is given in brackets. The term “Lander” refers to stations where an autonomous benthic lander was deployed. The sea-ice extent is the mean sea-ice extent in September for the period 1981-2010 (<http://nsidc.org>).

## 2.2 Used methods to determine benthic primary production, benthic mineralization, and influencing environmental parameters

### 2.2.1 Total and diffusive benthic oxygen fluxes at soft bottom seafloors

Benthic oxygen fluxes at soft bottom seafloors were determined *in situ* and *ex situ* and converted into carbon fluxes, given the close relationship between carbon and oxygen within the carbon cycle [section 1]. Two oxygen flux measures were determined: total oxygen fluxes and diffusive oxygen fluxes [Glud, 2008]. For the determination of total oxygen fluxes, a specific area of the soft bottom seafloor and a specific volume of overlying water were enclosed in a chamber and the oxygen concentration in the overlying water was measured over the incubation period. Diffusive oxygen fluxes were determined by the measurement of oxygen microprofiles across the SWI.

For the *in situ* determination of total oxygen fluxes at Potter Cove, SCUBA diver handled benthic chambers were deployed (Figure 2.5 A). These benthic chambers were carefully pushed into the sediment by hand. The oxygen concentration in the overlying water was measured by taking water samples before and after the incubation through valves attached to the chamber lids using gas-tight glass syringes. Winkler titration [Winkler, 1888] was used to measure the oxygen concentration in the samples. For the *in situ* determination of total oxygen fluxes in the Fram Strait, autonomous benthic landers equipped with benthic chambers were used (Figure 2.5 B) [Reimers, 1987; Glud et al., 1994; Glud, 2008]. After the deployment of an autonomous benthic lander, the benthic chambers were pushed automatically into the sediment. The oxygen concentration in the overlying water was measured continuously with oxygen sensors. At both study sites, the overlying water was kept homogenized during the incubation period by a stirring cross.

For the *ex situ* determinations of total oxygen fluxes at both study sites, Potter Cove and Fram Strait, sediment cores recovered by SCUBA divers or by a multiple corer (MUC) were used. The sediment cores were closed with a lid and incubated. The incubation was performed at *in situ* temperature, which lowers the risk of an artificial bias [Glud, 2008]. During the incubation, the overlying water was kept homogenized with a

magnetic stirring system. The oxygen concentration was measured with optical oxygen sensors.

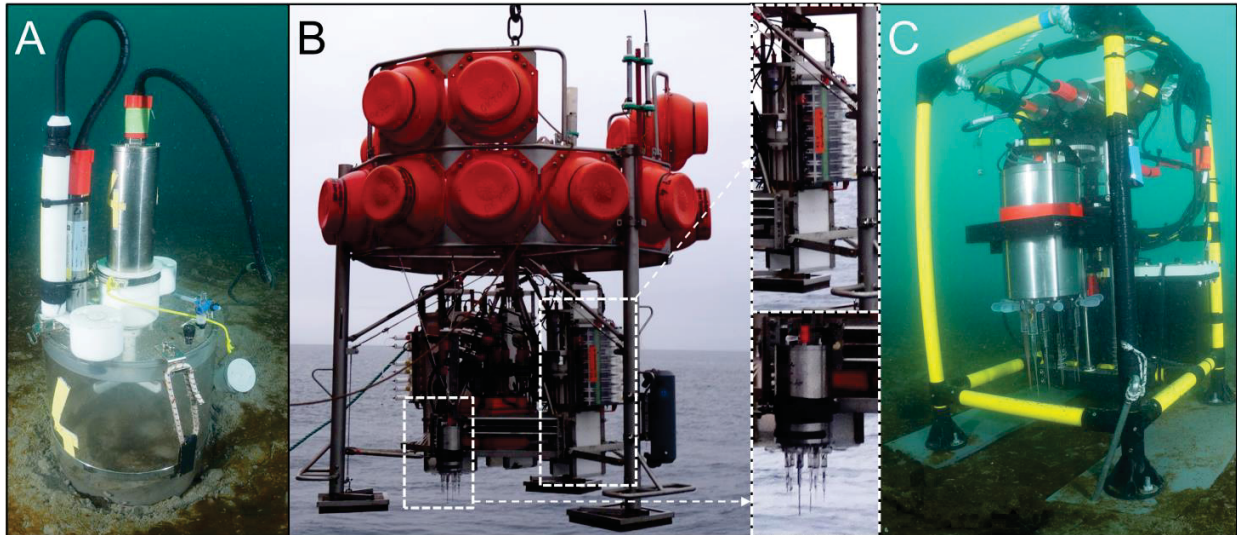


**Figure 2.5.** Devices used to determine oxygen fluxes across soft bottom seafloors. A: Transparent benthic chamber deployed in shallow sediments in Potter Cove, the photo is courtesy of Christopher Brunner; B: Autonomous benthic lander with benthic chamber and microprofiler measurement unit (lower and upper detail of B, respectively) to be deployed in Fram Strait (Arctic deep sea); C: Stand-alone microprofiler deployed on shallow sediments in Potter Cove, the photo is courtesy of Christopher Brunner.

For the *in situ* determination of diffusive oxygen fluxes at Potter Cove, a SCUBA diver handled stand-alone microprofiler was used (Figure 2.5 C) [Wenzhöfer et al., 2000; Lichtschlag et al., 2010]. In the Fram Strait, the autonomous benthic lander was equipped with a microprofiler measurement unit [Reimers, 1987; Glud et al., 1994; Glud, 2008]. At both study sites Potter Cove and Fram Strait, the measurement unit held electrochemical oxygen microsensors [Revsbech, 1989]. The measurement unit and thereby the oxygen microsensors were moved in 100  $\mu\text{m}$  steps towards the soft bottom seafloor and thereby measured the oxygen concentration across the SWI.

For the *ex situ* determination of diffusive oxygen fluxes in the Fram Strait, MUC recovered sediment cores were used. Similar to the *ex situ* total oxygen flux approach, sediment cores were stored at *in situ* temperature and the overlying water was kept homogenous. A micromanipulator was used to take oxygen microprofiles across the SWI in the sediment cores.

Via the change of the oxygen concentration over time (Figure 2.6 A), the total oxygen flux was calculated (Equation 1), in which  $\delta O_2$ ,  $\delta t$ ,  $V$  and  $A$  represent the difference in oxygen concentration, the difference in time, the volume of the overlying water and the enclosed surface area, respectively.

**Equation 1.** 
$$\text{Total oxygen flux} = \frac{\delta O_2 \times V}{\delta t \times A}$$

The calculation is based on the assumption of a linear decrease of the oxygen concentration over time (Figure 2.6 A), discrete sampling of overlying water from the chambers, and that the oxygen concentration does not sink below 10–15% of the initial starting point.

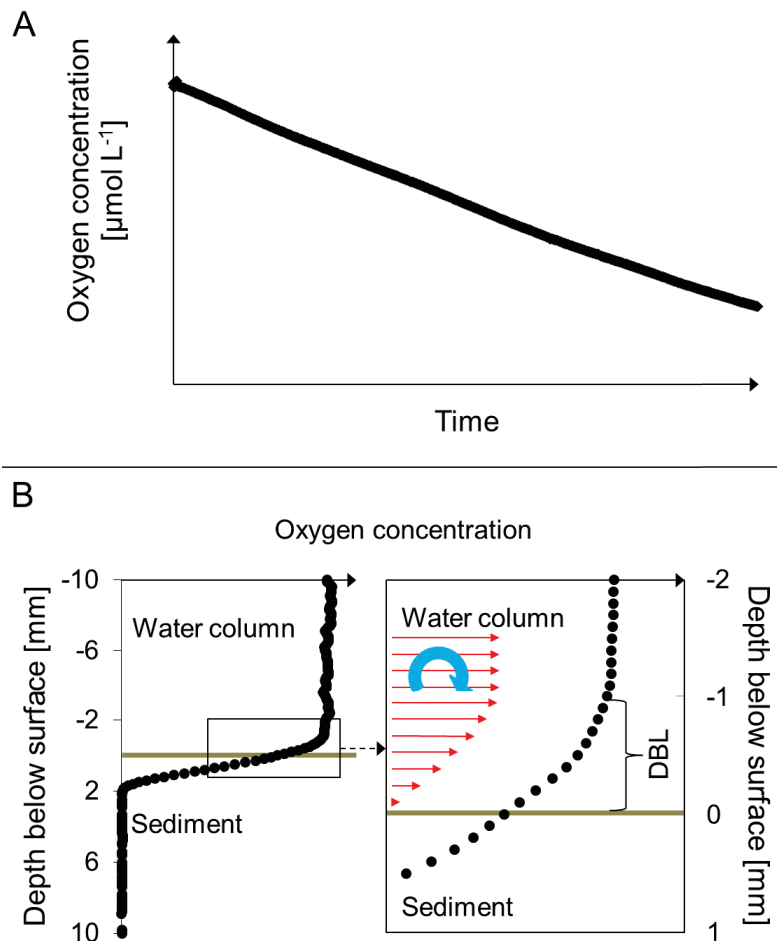


**Figure 2.6.** A: Example of decreasing oxygen concentration during an incubation indicating remineralization, B: Oxygen microprofile across the sediment-water interface. An entire oxygen concentration depth profile is shown on the lefthand side, while on the righthand side the oxygen concentration depth profile shows the oxygen alteration within the diffusive boundary layer (DBL). The DBL is a result of the decreasing bottom current (red arrows) and the change from a turbulent (blue arrow) to a laminar current [Gundersen and Jorgensen, 1990; Glud 2008].

A negative flux was directed towards the seafloor and indicated mineralization, while a positive flux was directed towards the water column and indicated net primary production.

Diffusive oxygen fluxes at soft bottom seafloors were determined by the measurement of the oxygen concentration across the SWI. Via the linear change of the oxygen concentration in the resulting sediment depth oxygen microprofile, diffusive oxygen fluxes were calculated using Fick's first law. In case no primary production takes place, two approaches exist for the calculation of the diffusive oxygen flux. First, via the linear decrease of the oxygen concentration across the entire sediment depth oxygen microprofile (Equation 2, Figure 2.6 B) and second, via the linear decrease across the diffusive boundary layer (DBL, Equation 3, Figure 2.6 B).

**Equation 2.** 
$$\text{Diffusive oxygen flux} = -D_s \times \left[ \frac{\delta O_2}{\delta z} \right]_{z=0}$$

**Equation 3.** 
$$\text{Diffusive oxygen flux} = -D_0 \times \left[ \frac{\delta O_2}{\delta z} \right]_{z=0}$$

Within Equation 2,  $D_s$  is the molecular diffusion coefficient of oxygen in sediments at in situ temperature and salinity and calculated by applying  $D_s = D_0/\theta^2$  [Schulz, 2006], with  $D_0$  as the molecular diffusion coefficient of oxygen in water after [Li and Gregory, 1974], and  $\theta^2 = 1 - \ln(\varphi^2)$  [Boudreau, 1997]. The sediment porosity  $\varphi$  was calculated after Burdige [2006] (Equation 4).

**Equation 4.** 
$$\varphi = \frac{m_w/\rho_w}{m_w/\rho_w + (m_d - (S \times m_w))/\rho_s}$$

Within equation (4),  $m_w$  is the mass of evaporated water,  $\rho_w$  is the density of the evaporated water,  $m_d$  is the mass of dried sediment plus salt,  $S$  is the salinity of the seawater and  $\rho_s$  is the sediment density. In equation 2, the term  $[\delta O_2/\delta z]_{z=0}$  refers to the linear decrease in the oxygen concentration across the entire microprofile, whereas in equation 3 the same term refers only to the linear decrease in the oxygen concentration across the DBL. The latter is assumed to not exceed 1 mm [Gundersen and Jørgensen, 1990; Jørgensen and Marais, 1990]. A detail description of the oxygen flux determinations is given in section 3, 4 and 5. An overview of performed measurements per study site is given in Table 2.1.

**Table 2.1.** General information about performed measurements at the investigated study sites.

	Antarctic		Arctic
Study site	Potter Cove		Fram Strait
Habitat	Shallow coast		Deep Sea
Water depth [m]	6–9	6–9	>200–2500
Investigation	Spatial variability of potential primary production of MPB related to glacial melt disturbances	Spatial variability of biogeochemical fluxes related to glacial melt disturbances	Spatial variability of oxygen fluxes related to sea-ice cover
Aim	Future scenario for Antarctic shallow coastal MPB primary production	Future scenario for Antarctic shallow coastal benthic mineralization	Future scenario for Arctic deep-sea benthic mineralization
Flux type and flux molecule	Total oxygen flux	Total and diffusive oxygen and nutrient fluxes	Total and diffusive oxygen flux
Used approach	<i>Ex situ</i>	<i>In situ</i>	<i>Ex and in situ</i>

### 2.2.1 Light suppression, light availability and PAR measurement

Light is an important factor influencing primary production directly and benthic remineralization indirectly via its influence on the organic matter provision [section 1]. Due to the strong suppression of light by sea ice [Perovich et al., 2002; Nicolaus et al., 2010; Perovich and Polashenski, 2012] and to the relatively low nutrient content of the EGC (this section), sea-ice concentrations were used as a proxy for primary production in the Fram Strait. Daily sea-ice concentrations were calculated based on obtained satellite data (obtained via CERSAT at IFREMER, France) [Ezraty et al., 2007] and using the ARTIST Sea Ice algorithm [Spren et al., 2008]. The sea-ice data cover a spatial resolution of 12.5 x 12.5 km<sup>2</sup> around the investigated stations.

The light availability in Potter Cove was assessed by light sensors. During benthic chamber incubations, HOBO Pendant<sup>®</sup> loggers (Onset, Bourne, USA) recorded the radiation across the wavelength of 150–1200 nm *in situ* close to the benthic chambers and on land. The ratio of *in situ* to land radiation was assessed as light availability at the seafloor. Additionally, *in situ* PAR measurements were performed at three locations in Potter Cove. At Faro and Isla D, a PAR-sensor (Odyssey Photosynthetic Irradiance Recording System, Data Flow Systems, Christchurch, New Zealand) was installed at the seafloor and measured throughout the year 2015. At Creek, a PAR sensor (LI-192, Li-Cor Biosciences, Lincoln, Nebraska, USA) measured for 36 h during the field campaign in 2016.



### 2.2.2 Sediment properties, biogenic sediment compounds, and benthic biota

One objective of this study was the identification of key parameters which might influence benthic remineralization in polar ecosystem besides light availability. Therefore, a set of parameters which characterize sediment properties, biogenic sediment compounds and biota were determined. Required sediments of Potter Cove were sampled by SCUBA divers using acrylic cores or by a Van Veen grab (530 cm<sup>2</sup> surface area) operate from a rubber boat, whereas sediments of Fram Strait were sampled using a MUC or by the benthic chambers of the autonomous benthic lander. Syringes were used to take subsamples from acrylic cores in Potter Cove and MUC cores in Fram Strait in order to measure sediment properties, biogenic sediment compounds, and benthic biota except for macrofauna related parameters. The macrofauna related parameters were measured on sediments from the described sampling devices without taking subsamples. For a detailed description of sediment sampling and storage procedure of the sediment samples, the reader is referred to section 3, 4, and 5.

Sediment properties measured included grain size, water content, and porosity. The grain size partitions were determined with a Malvern Mastersizer 2000G, hydro version 5.40. The Mastersizer utilizes a laser diffraction method and has a measuring range of 0.02–2000  $\mu\text{m}$ . The sediment water content was determined by the difference in weight of the sediment before and after drying. The sediment porosity  $\phi$  was calculated using equation 4 after Burdige [2006].

Biogenic sediment compounds measured included chlorophyll *a* concentration (Chl *a*), phaeopigment concentration (Phaeo), fucoxanthin concentration (Fuco), total carbon, total organic carbon and total nitrogen concentrations (TC, TOC, TN, respectively), phospholipid concentration, protein concentration, proportion of organic matter, and the bacterial enzymatic turnover rate (FDA). Chl *a* and Phaeo of Fram Strait sediment samples were analyzed by extracting them in 90% acetone and were measured with a TURNER fluorometer [Shuman and Lorenzen, 1975]. Chl *a*, Phaeo, and Fuco in sediments of Potter cove were analyzed using high-pressure liquid

chromatography (Gilson) following Wright and Jeffrey [1997]. The bulk of pigments (Chl *a* plus Phaeo) are termed chloroplastic pigment equivalents (CPE) after Thiel [1978]. The ratio of Chl *a* to Phaeo is used as an indicator of the relative age and the ratio of Chl *a* to CPE (% Chl *a*) as a quality indicator of the labile organic matter. TC and TN were measured by combustion using an ELTRA CS2000 with infrared cells. The TOC was measured using the same method after acidifying the sample (3 ml of 10 M hydrogen chloride).

Biota characterizing parameters including prokaryotic, MPB, meiofauna, and macrofauna densities and biomasses were assessed. Furthermore, MPB, meiofauna, and macrofauna taxa were identified. For the microbial density determination, the acridine orange direct count (AODC) method [Hobbie et al., 1977] was used to stain prokaryotes, which were subsequently counted (Axioskop 50 microscope, Zeiss) under ultraviolet light (CQ-HXP-120, LEJ, Germany). Prokaryotic biomass was estimated by the determination of the mean prokaryotic cell volume with a “New Portion” grid (Graticules Ltd, Tonbridge, UK) after Grossmann and Reichardt [1991], converted into biomass using a conversion factor of  $3.0 \times 10^{-13}$  g C  $\mu\text{m}^{-3}$  [Børsheim et al., 1990] and multiplied with the prokaryotic density. The MPB analyzes included the identification and counting of diatoms, which are the major component of MPB in Potter Cove [Al-Handal and Wulff, 2008a]. Diatom valves were cleaned with 30% hydrogen peroxide and mounted in Naphrax after appropriate rinsing with deionized water after Al-Handal and Wulff [2008a]. Identification of taxa was made according to established protocols [Witkowski et al., 2000; Scott and Thomas, 2005; Al-Handal and Wulff, 2008a, 2008b]. Enumeration of diatom valves on the slides was made by counting intact valves on the whole slide using Zeiss Axio Image 2 compound microscope equipped with differential interference contrast under 400 -fold magnification. Length and width of pennate valves and the diameter of centric valves were measured using a micrometer during the identification of taxa. The average length and width of at least 30 valves per taxon and the assumed height of 1  $\mu\text{m}$  [Edler, 1979] were used to calculate the biovolume of diatom cells after Hillebrand et al. [1999] and Sun and Liu [2003]. The diatom cell biovolumes were converted into carbon units using a conversion factor of 0.089 pg C  $\mu\text{m}^{-3}$  cell volume [Sundbäck et al., 1996]. For meiofauna analyzes, samples were sieved over a 1000  $\mu\text{m}$  and 32  $\mu\text{m}$  mesh.

Both fractions were centrifuged three times in a colloidal silica solution (Ludox TM-50, density =  $1.18 \text{ g cm}^{-3}$ ) and stained with Rose Bengal [Heip et al., 1985]. Afterwards, the taxa were identified and counted. The meiofauna biomass in terms of carbon was determined by the combustion of single taxa. Foraminifera were not considered, as the extraction efficiency of Ludox for different groups of foraminifera is insufficient for a quantitative assessment of the group. Therefore, only metazoan meiofauna taxa were recorded and hereinafter the use of the term meiofauna refers only to metazoan meiofauna organisms. For macrofauna analyses, recovered sediments of Potter Cove were sieved over a  $1000 \mu\text{m}$  mesh, while sediments of Fram Strait were sieved over a  $500 \mu\text{m}$  mesh. In both cases, sediment samples were stored in seawater buffered 4% formaldehyde and stained with Rose Bengal [Heip et al., 1985]. Afterwards, macrofauna taxa were identified to the lowest possible taxonomic level (at least family level), counted and weighted (blotted wet weight). Ash-free dry weight (AFDW) of macrofauna taxa was determined by subtracting the ash weight (after combustion at  $500^\circ\text{C}$ ) from the dry weight (dried for 48 h at  $60^\circ\text{C}$ ). AFDW was converted into carbon by assuming that 50% of the AFDW is carbon [Wijsman et al., 1999]. From the macrofauna density ( $A_i$ ) and biomass ( $B_i$ ), together with a mobility score ( $M_i$ ) and sediment reworking score ( $R_i$ ) of each taxon, the community bioturbation potential (BPC) was calculated following Queirós et al. [2013].

In addition, a photo survey of Potter Coves sediments was conducted with a Nikon D750 (rectilinear Nikon 16–35 mm lens, Nauticam underwater housing, two Inon Z-240 strobes). The photos were used to count siphons of the dominant Antarctic bivalve *Laternula elliptica* [Urban and Mercuri, 1998; Philipp et al., 2011; Harper et al., 2012]. Since this large bivalve retracts quickly into deeper sediments upon disturbance, Van Veen grab sampling is not adequate enough to estimate densities of *L. elliptica*. Therefore, the photos were used to determine the density of *L. elliptica* and to measure the siphon width (maximum distance between outer edges of the two siphons of one individual). Assuming a linear relationship between siphon width and AFDW, siphon width was converted into biomass of *L. elliptica*.



### 3 Manuscript I: Implications of glacial melt-related process on the primary production of a microphytobenthic community in Potter Cove (Antarctic)

---

Ralf Hoffmann<sup>1</sup>, Adil Yousif Al-Handal<sup>2</sup>, Angela Wulff<sup>2</sup>, Dolores Deregibus<sup>3</sup>, Ulrike Braeckman<sup>4</sup>, María Liliana Quartino<sup>3</sup>, Frank Wenzhöfer<sup>1,5</sup>

<sup>1</sup> Alfred Wegener Institut, Helmholtz Zentrum für Polar- und Meeresforschung, Am Handelshafen 12, 27570 Bremerhaven, Germany

<sup>2</sup> University of Gothenburg, Department of Biological and Environmental Sciences, Box 461, SE-405 30, Gothenburg, Sweden

<sup>3</sup> Instituto Antártico Argentino, 25 de mayo 1143, San Martín, Provincia de Buenos Aires, Argentina

<sup>4</sup> Ghent University, Marine Biology Research Group, Krijgslaan 281, S8, 9000 Gent, Belgium

<sup>5</sup> Max Planck Institute for Marine Microbiology, Celsiusstraße 1, 28359 Bremen, Germany

*In preparation to be submitted to the journal 'Frontiers in Marine Science'*

### 3.1 Abstract

The Antarctic Peninsula experiences a fast retreat of glaciers, which correlates with an increased release of particles and related increased sedimentation and shading of the benthic community. We investigated how changes in the general sedimentation and shading patterns affect the primary production by benthic microalgae, the microphytobenthos. In order to determine potential net primary production and respiration of the microphytobenthic community, sediment cores from locations exposed to different sedimentation rates and shading were exposed to photosynthetic active radiation (PAR, 400–700 nm) of 0–70  $\mu\text{mol photons m}^{-2} \text{s}^{-1}$ . Total oxygen fluxes and microphytobenthic diatom structure, density, and biomass were determined. Our study revealed that the net primary production of the microphytobenthos decreased with increasing sedimentation and shading, while the microphytobenthic diatom density and composition remained similar. By comparing our experimental results with *in situ* measured PAR intensities, we furthermore assessed the microphytobenthic primary production as an important carbon source within Potter Cove's benthic ecosystem. We propose that the microphytobenthic contribution to the total primary production may drop drastically due to Antarctic glacial retreat and correlated sedimentation and shading, with yet unknown consequences for the benthic heterotrophic community, its structure, and diversity.

### 3.2 Introduction

The Antarctic Peninsula is one of the fastest warming areas on Earth [Ducklow et al., 2007]. As a result, glaciers in the West Antarctic [Paolo et al., 2015] and especially at the Western Antarctic Peninsula [Rückamp et al., 2011; Cook et al., 2016] are melting and retreating. As a consequence, vast amounts of particles are released into the water column with the start of the melting season in spring, which leads to an increased turbidity [Dierssen et al., 2002] and sedimentation [Schloss et al., 1999; Pasotti et al., 2015]. Furthermore, ice scouring events, which are also related to glacial melt, lead to resuspension of particles from soft bottom seafloor and therefore, to an additional increase in the turbidity [Barnes, 1999; Griffiths, 2010].

Consequently, the photosynthetic active radiation intensity (PAR, 400–700 nm wavelengths) for primary production can be reduced in areas influenced by glacial melt. This might affect especially the primary production of benthic microalgae, the microphytobenthos (MPB) [Dayton et al., 1986; Skowronski et al., 2009], since they are already dependent on the water depth-related light attenuation. The MPB are important primary producers, as they contribute substantially to the total primary production in the coastal Antarctic marine realm. For example, McMinn et al. [2010] reported that the MPB primary production could be responsible for up to 90% of the total primary production during the sea-ice free season. Diatoms dominate the Antarctic MPB community [Palmisano et al., 1985; Al-Handal and Wulff, 2008a] and are known to be well adapted to low light conditions [Palmisano et al., 1985; Rivkin and Putt, 1987; Longhi et al., 2003; Gómez et al., 2009], often associated with ice cover. However, the glacial melt-related particle release and correlated intensive shading and covering of MPB communities might be a new threat influencing MPB primary production.

Owing to the retreating Fourcade Glacier [Rückamp et al., 2011] and the general current system [Lim et al., 2013], the benthos in Potter Cove (King George Island/Isla 25 de Mayo) experiences different intensities of turbidity and sedimentation [Schloss et al., 1999; Pasotti et al., 2015; Deregibus et al., 2016]. In this study, we exposed sediment cores from different locations to increasing PAR and measured the resulting total oxygen flux. Further, we determined the diatom density, which dominates the MPB community [Al-Handal and Wulff, 2008a], and identified the diatom community structure at each location to assess small-scale differences and estimated the diatom biomass. We conducted this study to investigate if glacial melt-related particle release and correlated shading and sedimentation were able to influence the primary production of an Antarctic MPB assemblage. To address this question, we tested the following null-hypotheses:

1. The diatom community structure and density is comparable among areas experiencing different shading and sedimentation.
2. MPB community primary production is similar among areas experiencing different intensities of sedimentation and shading.

In addition, it was hypothesized that the MPB are important primary producers in Potter Cove, which are able to provide substantial amounts of organic carbon for the benthic

carbon demand [Hoffmann et al., section 4], however, without knowing the MPB primary production in Potter Cove. By comparing our results with *in situ* PAR data, measured over a period of one year, we discuss the hypothesis of Hoffmann et al. [section 4].

### 3.3 Material and methods

#### 3.3.1 Study site and sampling

The study was conducted at the Dallmann Laboratory annex of the Carlini research location, located at the roughly 3 km long and 1.2 km wide Potter Cove. The cove is a shallow, fjord-like inlet of Maxwell Bay on King George Island/Isla 25 de Mayo (South Shetland Islands, Western Antarctic Peninsula). The general current is clock-wise with an average current speed of  $0.03 \text{ m s}^{-1}$  [Lim et al., 2013]. Potter Cove is regularly covered by sea ice during winter [Schloss et al., 2012] and experienced a fast retreat of the Fourcade glacier within the last decades [Rückamp et al., 2011]. The melting and retreating glacier and also seasonal meltwater discharge, a consequence of permafrost and snow thawing, release a high amount of particles into the cove [Klöser et al., 1993; Schloss et al., 1999]. As a consequence, a turbidity gradient was created within the cove [Klöser et al., 1993; Sahade et al., 2015]. Therefore, our sampled locations within Potter Cove, namely Faro, Creek, and Isla D, which were located in 6–9 m water depth and in a radius of less than 1 km distance to each other (Figure 3.1, Table 3.1), experience different intensities of sedimentation and shading [Pasotti et al., 2015; Deregibus et al., 2015; Monien et al., 2017].

For MPB community analyses, triplicates of small sediment cores (10 cm length, 3.6 cm diameter) were taken at each location by SCUBA divers during a field campaign in November and December 2016 (Table 3.1). Additionally, for primary production estimates, five larger sediment cores (50 cm length, 10 cm diameter) were also collected by SCUBA divers (Table 3.1). One sediment core was subsampled for an additional MPB community sample as described above, while the four remaining sediment cores were used for primary production estimates. During recovery and transport to the laboratory, the sediment cores were kept vertical and special care was taken to leave



the sediment surface undisturbed. All samples were processed within 1.5 h after recovery.

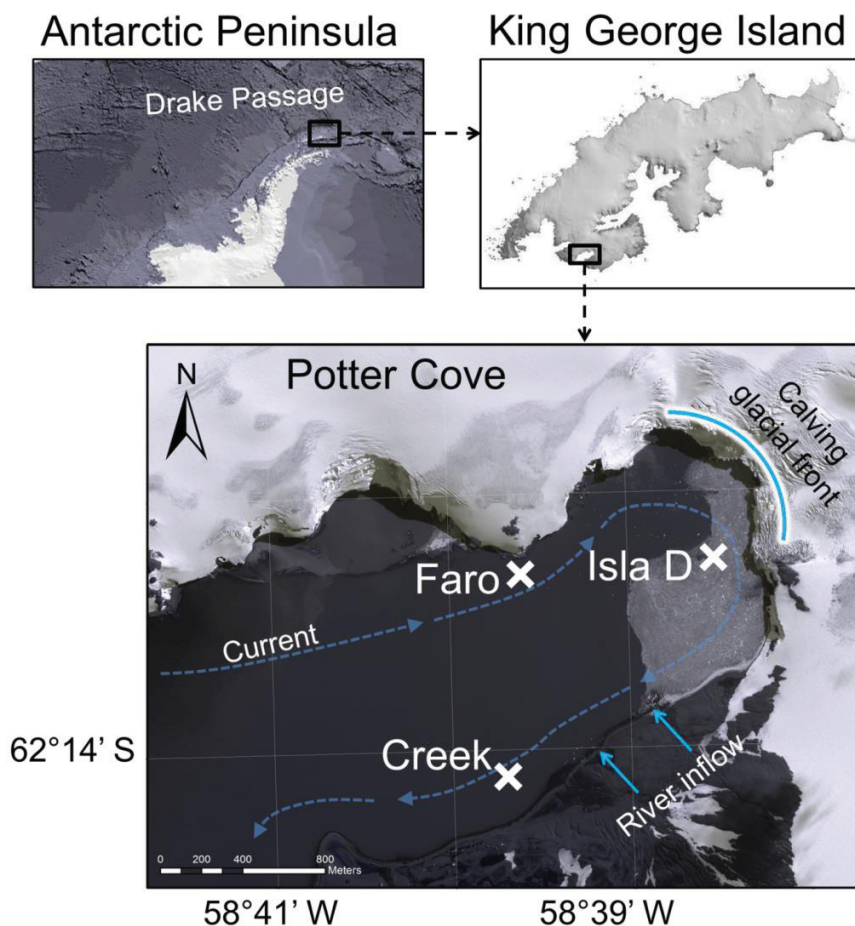


**Figure 3.1.** Study site Potter Cove. At Faro, Creek, and Isla D sediment cores for microphytobenthic analyses and primary production estimates were recovered by SCUBA divers. The position of sampled locations is marked with a cross. The curved, bright blue line marks the front of the Fourcade glacier. The bright blue arrows indicate river run-offs supplied mainly by glacier, permafrost and snowmelt water. The dashed blue arrows indicate the direction of the main current in Potter Cove. More detailed information about the locations is given in Table 3.1.

**Table 3.1.** Locations, water depth at sampled locations, and date of sampling.

	Faro	Creek	Isla D
Latitude S	62° 13.31'	62° 14.8'	62° 13.30'
Longitude W	58° 39.37'	58° 39.43'	58° 38.30'
Depth [m]	8–9	8–9	6–7
Microphytobenthic sampling [Date]	05/11/2016	11/11/2016	09/11/2016
Sediment core sampling for primary production estimates Date]	22/11/2016	03/12/2016	11/12/2016

### 3.3.2 Methods

#### *In situ PAR measurement*

To assess whether the underwater light regime at the three locations allowed MPB primary production, *in situ* PAR measurements were conducted. Close to Faro (62° 13.35' S, 58° 40.47' W) and at Isla D (62° 13.31' S, 58° 38.30' W) PAR-sensors (Odyssey Photosynthetic Irradiance Recording System, Data Flow Systems, Christchurch, New Zealand) were installed approximately 0.5 m above the seafloor in 2015. Data from Isla D only encompass the period 11/02–04/04 and 16/11–31/12, as the sensor was damaged probably by passing chunks of ice. The PAR-sensors were calibrated according to Deregibus et al. [2015] and measured with a temporal resolution of 30 minutes. At Creek (62° 14.08' S, 58° 39.43" W) a PAR sensor (LI-192, Li-Cor Biosciences, Lincoln, Nebraska, USA) measured for 36 h during the field campaign in 2016.

#### *Microphytobenthic density, biomass and community structure*

The upper 0.5 cm sediment layer of an MPB sediment core was transferred into a scintillation vial and 5 mL GF/F filtered seawater (Whatman, UK) and 1 mL of 25% glutaraldehyde was added. The vial was wrapped in parafilm (Bemis Company, USA) and stored at 4°C until further analyses.

For the identification and counting of diatoms, which are the major components of microphytobenthos in the study area [Al-Handal and Wulff, 2008a], diatom valves were cleaned with 30% hydrogen peroxides and mounted in Naphrax after proper rinsing with deionized water [Al-Handal and Wulff, 2008a]. Identification of taxa was made following established protocols [Witkowski et al., 2000; Scott and Thomas, 2005; Al-Handal and Wulff, 2008a, 2008b]. Enumeration of diatom valves on the slides was made by counting intact valves on the whole slide using Zeiss Axio Image 2 compound microscope equipped with differential interference contrast under 400-fold magnification. In addition, this procedure ensures that only living cells were taken into account of the adjacent analyses. During the identification of taxa, the length and width of pennate valves and the diameter of centric valves were measured using a micrometer. The average length and width of at least 30 valves per taxon and the assumed height of 1 µm [Edler, 1979]

were used to calculate the biovolume of diatom cells following Hillebrand et al. [1999] and Sun and Liu [2003]. The diatom cell biovolumes were converted into diatom carbon contents using a conversion factor of  $0.089 \text{ pg C } \mu\text{m}^{-3} \text{ cell}^{-1} \text{ biovolume}^{-1}$  [Sundbäck et al., 1996]. The Shannon-Wiener diversity index  $H'$  was calculated using Primer v6.

#### *Carbon normalized potential primary production and light compensation point*

Four sediment cores were stored in a water bath at *in situ* temperature of  $0.5^\circ\text{C}$ . A magnetic stirrer was inserted into the core and the overlying water was permanently aerated. Thereby, the overlying water was kept homogeneous and oxygen saturated. Cold-light lamps (Osram Lumilux Cool Daylight L36W/865, Osram, Munich, Germany) were installed above the sediment cores and the emitted PAR was permanently controlled with a spherical PAR-sensor (US-SQS/L and ULM-500, Walz, Germany). The spherical PAR-sensor was placed in the water bath, adjusted to the lowest height of the sediment surface of the sediment cores and covered with sea-water.

Sediment cores from Faro and Creek were exposed to PAR intensities of 0, 5, 10, 15, 20, 25, 47 and  $70 \mu\text{mol photons m}^{-2} \text{ s}^{-1}$ , starting with lowest PAR. Sediment cores from Isla D were additionally exposed to  $35 \mu\text{mol photons m}^{-2} \text{ s}^{-1}$ . In order to enable the MPB to adjust to the experimental light conditions, the sediment cores were pre-incubated for 4 h at a certain PAR. Afterwards, the cores were closed airtight with no air bubbles in the overlying water and the volume of the overlying water was determined. An optical oxygen microsensor (Pyroscience, Aachen, Germany) with a tip size diameter of  $50 \mu\text{m}$  was installed in the lid, which allowed a continuous measurement of the oxygen concentration in the overlying water. On beforehand, the microsensor was calibrated at *in situ* temperature with a two-point calibration using air saturated and anoxic waters (by adding sodium dithionite).

The sediment cores were incubated at a certain PAR for  $\geq 3$  h and a 2 s temporal measurement resolution, while the overlying water was kept homogeneous by rotating magnets. After the incubation, the sediment core was exposed to the next higher PAR by adjusting the height of the cold-light lamps and the procedure for total oxygen flux measurement was repeated. The spare sediment core was treated similar to the other cores but without installing the oxygen microsensor. The PAR sensor was also covered

with a lid during the incubations. To avoid an oxygen oversaturation at the highest PAR, the overlying water of the sediment cores was aerated with helium until an oxygen concentration of  $240 \mu\text{mol O}_2 \text{ L}^{-1}$  was reached (70% oxygen saturation, controlled by above-mentioned oxygen microsensors).

The total oxygen flux over the period of each PAR exposure was calculated using the formula:

$$\text{Total oxygen flux} = -\frac{\delta O_2 \times V}{\delta t \times A}$$

in which  $\delta O_2$ ,  $\delta t$ ,  $V$  and  $A$  represent the difference in oxygen concentration, the difference in time, the volume of the overlying water and the enclosed surface area, respectively. Total oxygen fluxes were converted to carbon equivalents (C-flux) by applying the Redfield ratio of C : O = 106:138 [Redfield, 1934, 1963]. A negative flux is directed towards the sediment, while a positive is directed towards the water column. C-fluxes were plotted against PAR to create a PI-curve from which the light compensation point and the light-dependent primary production performance were derived. C-fluxes of each location were normalized to the mean diatom carbon content, assuming that  $1 \text{ mg C cm}^{-3} \text{ sediment}^{-1}$  equals  $1 \text{ mg C cm}^{-2} \text{ sediment}^{-1}$ . The normalized C-fluxes were also plotted against the used PAR incidence intensities. The oxygen and carbon fluxes represent benthic community net fluxes, as microbial and faunal mineralization processes are included. Consequently and owing to the experimental conditions, the calculated primary production needs to be assessed as potential net primary production.

### *Statistical analyses*

To test whether MPB densities,  $H'$  and the slopes of C-fluxes and diatom carbon content-normalized C-fluxes differed among locations, a one-way ANOVA (type III SS) and a Tukey post hoc test was performed. A Shapiro-Wilk test was performed to test data normality, whereas a Levene's test was used to test homoscedasticity. In case data were not homoscedastic, an adjusted ony-way ANOVA and a non-parametric Games-Howell post-hoc test [Games and Howell, 1976] was performed to identify locations showing significant differences. The tests were performed using R Statistical Software

(version 3.4.0, R Core Team, 2017) and the packages “CAR” [Fox and Weisberg, 2011] and “Userfriendlyscience” [Peters, 2007].

Analyses of the multivariate MPB community structure were based on square root transformed density data of sediment core replicates. Non-metric multidimensional scaling (MDS, [Kruskal, 1964]) and hierarchical cluster analysis with group average clustering were used to present the multivariate similarities between samples based on Bray–Curtis similarity. Significance of multivariate differences between locations within the MPB community data were tested by the ANOSIM procedure (ANalysis Of SIMilarity) based on Clarke’s R statistic [Clarke and Warwick, 1994] with 5775 permutations (number of all possible permutations). The SIMPER (SIMilarity PERcentage) routine was applied to determine the contribution of certain MPB taxa towards the discrimination between the locations. The tests regarding the MPB community were conducted using Primer v6. Results are expressed as mean values  $\pm$  standard deviation.

## 3.4 Results

### 3.4.1 *In situ* PAR variability

The *in situ* PAR was investigated on seasonal and daily temporal scales and as well as on spatial scales (Figure 3.2). The average PAR at Faro (Figure 3.2 A) in spring (Oct.–Nov.), summer (Dec.–Mar.), autumn (Apr.–May) and winter (June–Sept.) over the available period was  $37 \pm 43$ ,  $16 \pm 19$ ,  $5 \pm 6$ , and  $3 \pm 13$   $\mu\text{mol photons m}^{-2} \text{s}^{-1}$ , respectively. At Isla D (Figure 3.2 B), the average PAR within the spring period (Nov.) was  $13 \pm 18$   $\mu\text{mol photons m}^{-2} \text{s}^{-1}$  and within the summer period (Dec. and Feb.–Mar.) average PAR was  $5 \pm 11$   $\mu\text{mol photons m}^{-2} \text{s}^{-1}$ . The PAR measurement on a daily scale at Creek (10–11/11/2016, Figure 3.2 C) revealed an average PAR of  $84 \pm 117$   $\mu\text{mol photons m}^{-2} \text{s}^{-1}$  and a maximum PAR value of  $>550$   $\mu\text{mol photons m}^{-2} \text{s}^{-1}$ . The PAR results indicate that in Potter Cove effects of sedimentation and shading differ strongly among the study locations on temporal and spatial scales.

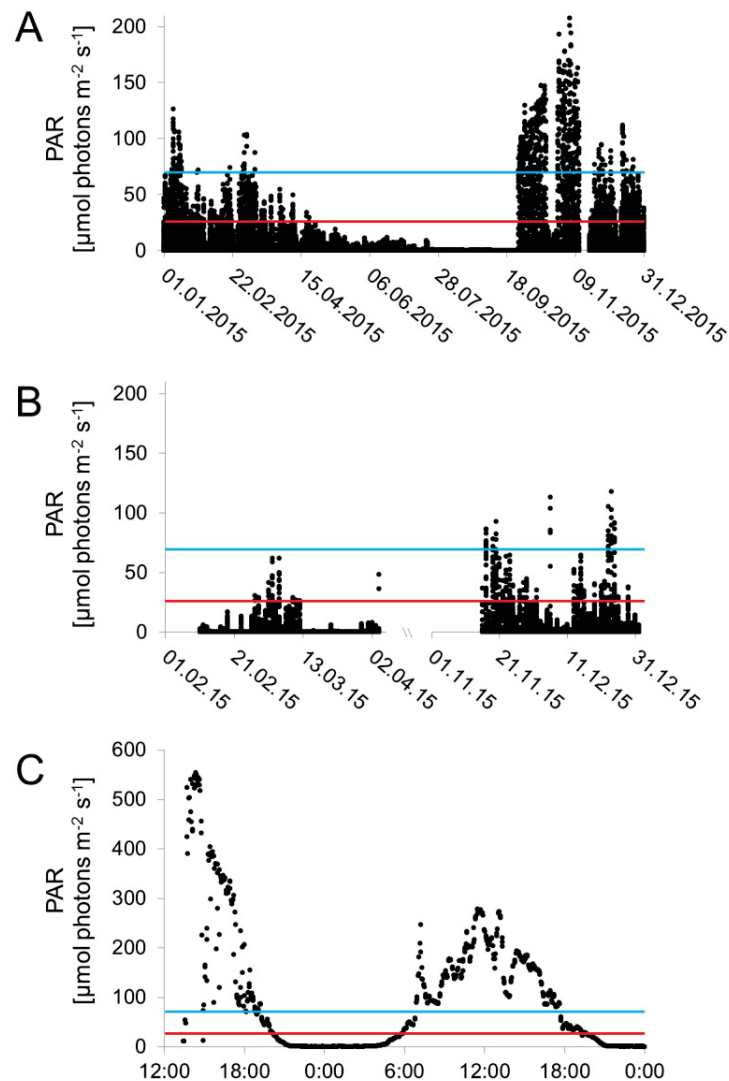


**Figure 3.2.** *In situ* measured photosynthetically active radiation intensities (PAR) on a seasonal scale at A: Faro (entire year 2015), B: and Isla D (11/02/2015–04/04/2015 and 16/11/2015–31/12/2015), and on a daily scale at C: Creek (10/11/2016–11/11/2016). The red line marks the light compensation point of  $26 \mu\text{mol photons m}^{-2} \text{s}^{-1}$  and the bright blue line the maximum PAR used in the experiment.

### 3.4.2 Diatom community at Potter Cove

Overall 48 diatoms species were found in the upper 0.5 cm sediment layer (Table S3.1) with *Gyrosigma fasciola* as dominant species at all three locations ( $30 \pm 15\%$  at Faro,  $40 \pm 20\%$  at Creek,  $44 \pm 18\%$  at Isla D). Ten pelagic species were found in the samples, which made up 11%, 25%, and 14% of the MPB density at Faro, Creek, and Isla D, respectively (Table S3.1, indicated with an asterisk). The mean MPB density was  $4895 \pm 1237 \text{ cells cm}^{-3}$ ,  $18321 \pm 8727 \text{ cells cm}^{-3}$ ,  $8332 \pm 6565 \text{ cells cm}^{-3}$

and  $H'$  was  $3.25 \pm 0.24$ ,  $2.43 \pm 0.28$ ,  $2.93 \pm 0.82$  at Faro, Creek and Isla D, respectively. Both, MPB densities and  $H'$  did not differ between the locations ( $p_{\text{density}} = 0.07$ ,  $p_{H'} = 0.21$ ). The ANOSIM results (Global  $R = 0.236$ ,  $p\text{-value} = 0.058$ ) indicated no differences in the MPB community structure among the three locations, which was confirmed by the SIMPER with similarities within groups of  $>50\%$  (Table S3.2).

### 3.4.3 Potential net MPB primary production in Potter Cove

At each location, the C-flux increased with increasing PAR. Faro and Creek showed similar slopes, whereas the slope at Isla D was significantly lower (Figure 3.3, Table 3.2). The community mineralization (C-flux in darkness) at Faro, Creek, and Isla D was  $-18 \pm 1 \text{ mmol C m}^{-2} \text{ d}^{-1}$ ,  $-21 \pm 2 \text{ mmol C m}^{-2} \text{ d}^{-1}$ , and  $-14 \pm 2 \text{ mmol C m}^{-2} \text{ d}^{-1}$ , respectively. The light compensation point for the MPB community was reached at  $26 \mu\text{mol photons m}^{-2} \text{ s}^{-1}$  at Faro and Creek, whereas no light compensation point was reached at Isla D. The maximum net primary production at Faro was at  $70 \mu\text{mol photons m}^{-2} \text{ s}^{-1}$  ( $47 \pm 16 \text{ mmol C m}^{-2} \text{ d}^{-1}$ ) and at Creek at  $47 \mu\text{mol photons m}^{-2} \text{ s}^{-1}$  ( $41 \pm 10 \text{ mmol C m}^{-2} \text{ d}^{-1}$ ). At Isla D, no net primary production was observed.

**Table 3.2.** P-values of ANOVAs and Games-Howell post-hoc tests regarding sediment core specific slopes of C-fluxes (Figure 3.3) and diatom carbon content-normalized C-fluxes (Figure 3.4), both plotted against PAR.

Flux	ANOVA (p-value)	Grouped locations	Games-Howell post-hoc test (p-value)
C-flux	<0.001	Faro-Creek	0.876
		Faro-Isla D	0.010
		Creek-Isla D	0.009
Diatom carbon content-normalized C-fluxes	<0.001	Faro-Creek	0.017
		Faro-Isla D	0.009
		Creek-Isla D	0.011

The diatom carbon content-normalized C-fluxes also increased with increasing PAR, and showed significant differences regarding their slopes (Figure 3.4, Table 3.2). The slope steepness was highest at Faro, intermediate at Creek and lowest at Isla D, indicating different net primary production performances by the MPB community at the three locations.

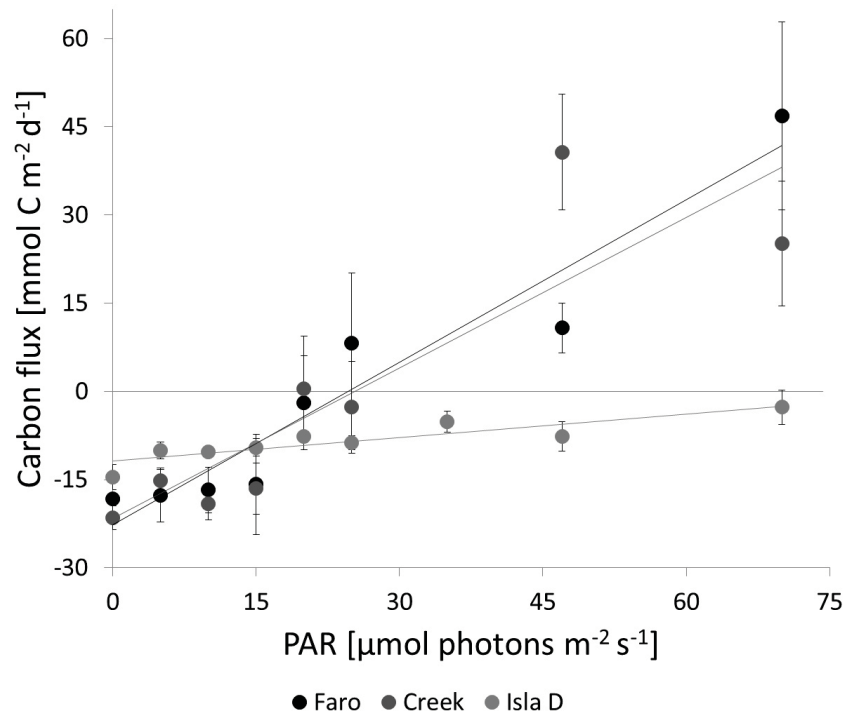


**Figure 3.3.** Carbon fluxes at different PAR intensities. Negative fluxes are net respiration and positive fluxes net primary production of the benthic community. The linear regression for Faro, Creek and Isla D is  $y = 0.9221x - 22.72$  ( $r^2 = 0.925$ ),  $y = 0.8536x - 21.59$  ( $r^2 = 0.781$ ), and  $y = 0.1327x - 11.83$  ( $r^2 = 0.779$ ), respectively.

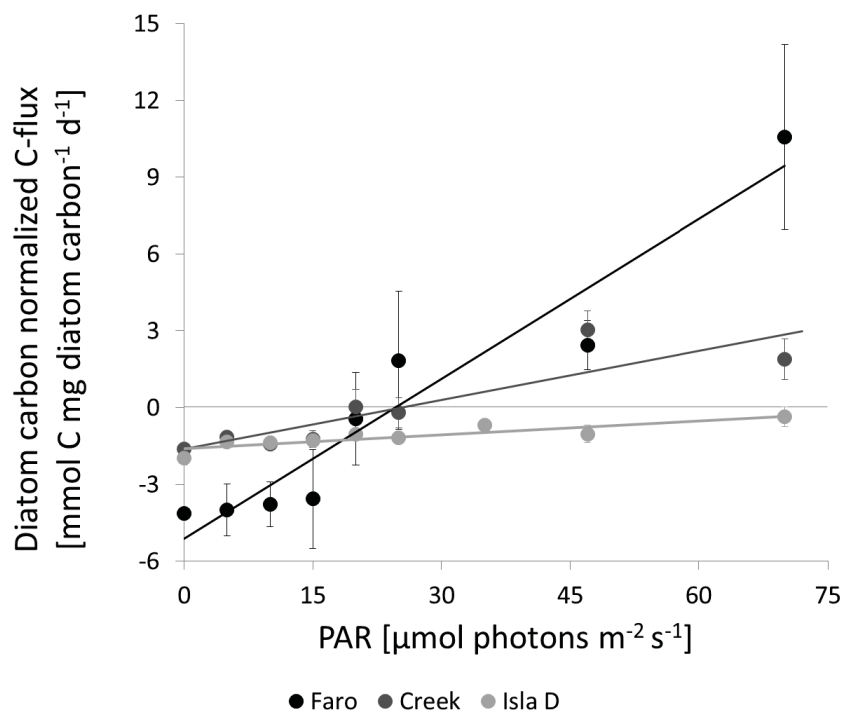


**Figure 3.4.** Carbon fluxes normalized by the mean diatom carbon content at different PAR intensities. The linear regression for Faro, Creek and Isla D is  $y = 0.208 - 5.126$ ,  $y = 0.064 - 1.618$ , and  $y = 0.0178 - 1.591$ , respectively.  $R^2$  is similar to the regressions in Figure 3.3.



## 3.5 Discussion

### 3.5.1 The impact of turbidity and sediment accumulation on the microphytobenthic community and their primary production in Potter Cove

The melting Fourcade glacier releases particles into Potter Cove, both directly and indirectly via river run-offs [Sahade et al., 2015; Monien et al., 2017]. Owing to their location and the current system in Potter Cove, the investigated locations were permanently and naturally exposed to contrasting intensities of turbidity and sediment accumulation [Pasotti et al., 2015; Deregibus et al., 2016], which we define as “disturbance”. Thus, the MPB at Faro was less disturbed, at Creek intermediately disturbed and at Isla D highly disturbed. We observed that the primary production performance of the MBP decreased with increasing disturbance while the community structure remained unaffected. A positive net primary production was even completely suppressed at Isla D. However, large brownish mats were visible at Isla D during summer [Hoffmann et al., section 4]. This indicates that the energy demand for growth and reproduction of the MPB community at Isla D seems to be covered by the photosynthetic apparatus throughout the sea-ice free season, even under permanent glacial melt-related disturbance. Thus, we assess the found primary production pattern is a result of the sedimentation accumulation process rather than due to the low PAR.

Antarctic MPB is known for its exceptional adaption to low light conditions [Gómez et al., 2009]. The median light saturation of an MPB community at Casey station was reached at  $66 \mu\text{mol photons m}^{-2} \text{s}^{-1}$  and  $6\text{--}20 \mu\text{mol photons m}^{-2} \text{s}^{-1}$  were reported for an MPB community in the McMurdo Sound [Rivkin and Putt, 1987; McMinn et al., 2012]. The data presented in our study does not allow an estimation of the light saturation value. However, the estimated light compensation point of Potter Coves MPB community was reached at  $26 \mu\text{mol photons m}^{-2} \text{s}^{-1}$ , which is frequently exceeded at Faro and Creek and rarely at Isla D. Therefore, it is unlikely that the low PAR is responsible for the revealed primary production pattern.

MPB primary production might also depend on the MPB community structure, which can be influenced by turbidity. Longhi et al. [2003] revealed differences in the low light

adaption of *Gyrosigma subsalinum* var. *antarctica* and *Odontella litigiosa*, both species occurred in Potter Cove [Al-Handal and Wulff, 2008a]. Consequently, we would expect that low light adapted species were dominant at Isla D and thereby change the MPB structure. We also found *Gyrosigma* species and *Odontella litigiosa* in our samples, but a difference in the MPB structure between our three study locations was not observed.

It is known that diatoms are able to migrate vertically through the sediment as a reaction on tides, light and endogenous factors (e.g. phototaxy, aerotaxy, geotaxy), as most important factors and disturbances, carbon dioxide and nutrient limitations as less important factors [Consalvey et al., 2004, and references therein]. The glacial melt-related sediment accumulation steadily covers the MBP community. As a consequence, the diatoms have to migrate over longer distances and migrate more often to locate themselves to the best available light conditions. In turn, the MPB community in high sedimentation areas needs more energy for migration, which lowers the overall net primary production. This is relevant for epipelagic diatoms with raphe, which are highly motile [Round, 1979]. Episammic diatoms are only able to move very slowly [Round, 1979] and therefore would be completely covered by sediments for a longer period. A full recovery in terms of their primary production performance will take more than two weeks [Wulff et al., 1997], and only if sediment accumulation cease to cover the MPB community. Therefore, we assess the sediment accumulation as responsible factor for the observed primary production pattern.

Our used approach might be biased as three of four MPB samples, which were used for the normalization of the C-fluxes, were recovered one month before the sediment cores for the primary production assessment. One additional sample was recovered parallel to the experimental sediment cores, however, differing from the other MPB samples in terms of diatom density and diatom carbon content. Whether this was due to temporal or spatial variability is hard to assess. Nevertheless, the diatom carbon content was observed to vary 3-fold and the diatom density 5.5-fold between the locations. The latter is within the 2- to 15-fold range of spatial variability observed in other Antarctic MPB communities [Dayton et al., 1986; McMinn et al., 2012]. However, in terms of chlorophyll concentrations and depending on water depths, temporal variability was observed to vary 3- to 11-fold [Dayton et al., 1986; Gilbert, 1991a]. Consequently, as

spatial and temporal variability of MPB densities strongly overlap, an assessment whether the revealed differences among the MPB samples were due to temporal or spatial variability was impossible. Nevertheless, as we merged MPB samples from two different samplings dates, our results cover both spatial and temporal variability in the MPB community.

### 3.5.2 Microphytobenthos as important carbon source in Potter Cove

Our study gives a first insight into the MPB primary production in Potter Cove. The MPB community at the locations Faro and Creek is potentially able to fully supply and even exceed the benthic carbon demand of 11–33 mmol C m<sup>-2</sup> d<sup>-1</sup> in 6–9 m water depth [Hoffmann et al., section 4]. This indicates the MPB community can be an important carbon source for the benthic community, which might be able to partly supply also benthic fauna in deeper water depths. Although, the carbon supply by MPB primary production seems to be spatially limited and undergo substantial temporal changes, as the average PAR exceeded the light compensation point of 26 μmol photons m<sup>-2</sup> s<sup>-1</sup> only in spring and only at Faro. However, in combination with pelagic primary production data [Schloss et al., 1998; Schloss et al., 2012], the benthic carbon demand might be fully supplied in the spring. This would indicate that Potter Cove is an autotrophic ecosystem in spring, whereas it is heterotrophic in summer months [Hoffmann et al., section 4].

We assess the obtained *ex situ* measured net MPB primary production values as reliable and transferable to *in situ* conditions. The observed primary production by Potter Cove's MPB community under different PAR intensities was in a similar range as *in situ* measured primary production of MBP communities from McMurdo Sound [Dayton et al., 1986], Signey Island [Gilbert, 1991b] and at Casey Station [McMinn et al., 2010; McMinn et al., 2012]. Furthermore, the community mineralization (oxygen flux under darkness) was within the same range as *in situ* measure mineralization rates of the benthic community in Potter Cove [Hoffmann et al., section 4].

The *in situ* measured PAR exceeds the maximum of 70 μmol photons m<sup>-2</sup> s<sup>-1</sup> used in our experiment and thus, we cannot assess at which PAR the light saturation would be reached and when photoinhibition might start. *G. subsalinum* and *O. litigiosa*, for example, showed maximum growth rates at 25 μmol photons m<sup>-2</sup> s<sup>-1</sup> and

100  $\mu\text{mol photons m}^{-2} \text{ s}^{-1}$ , respectively [Longhi et al., 2003], which was also the start value for photoinhibition. Comparing these results with the *in situ* PAR conditions in Potter Cove indicates that the MPB might experience photoinhibition. However, McMinn et al. [2012] reported that photoinhibition only became evident at actinic light levels above 413  $\mu\text{mol photons m}^{-2} \text{ s}^{-1}$ . This only occurred shortly at Creek, but in general *in situ* measured PAR in Potter Cove was below that value. In addition, results of Wulff et al. [2008] did not reveal any photoinhibition in Antarctic marine microalgae when exposed to 600  $\mu\text{mol photons m}^{-2} \text{ s}^{-1}$ . Therefore, photoinhibition might have affected a few microalgae species, but the gross of the MPB likely grew under either ideal or low light conditions.

### 3.5.3 Implications of glacial melt-related retreat and particle release on polar benthic communities

The ongoing melt of Antarctic glaciers [Rückamp et al., 2011; Paolo et al., 2015; Cook et al., 2016] might lay free new settling ground for macroalgae [Deregibus et al., 2016; Lager et al., 2017], benthic macrofauna [Lager et al., 2017], and also MPB. Nevertheless, the melting of glaciers is related with the release of particles and as such lead to increased sediment accumulation [Pasotti et al., 2015; Monien et al., 2017]. Sediment accumulation in turn, is known to trigger changes in the macrofauna community [Torre et al., 2012; Sahade et al., 2015; Torre et al., 2017], changes in benthic mineralization [Hoffmann et al., section 4] and reduce MPB primary production [this section]. MPB might survive increasing sedimentation rates [Wulff et al., 1997] but their contribution to the overall primary production as a food resource for the heterotrophic benthic fauna is likely to decline strongly.

The effect of sediment accumulation seemed to affect also MPB communities in the Arctic Ocean. In the Arctic Kongsfjorden, the MPB primary production was reduced at locations close to glacial fronts and riverine inflows (where high sedimentation rates are likely) compared to less disturbed locations [Woelfel et al., 2010]. In addition, the MPB primary production is an important carbon source in shallow coastal areas of the Arctic Ocean by exceeding pelagic productivity by a factor of 1.5 for water depths down to 30 m [Glud et al., 2009; Attard et al., 2014]. Consequently, the reduction of the MPB

primary production is likely to increase the food competition of the benthic heterotrophic community in both the Southern and the Arctic Ocean, with unpredictable consequences in biomass, density, structure and diversity for the benthic community.

### 3.6 Supplements

**Table S3.1.** Diatom density [cells cm<sup>-3</sup>] of single taxa at the three locations Faro, Creek and Isla D. The asterisk refers to pelagic species. Location specific replicates were recovered in parallel roughly one month before the sediment cores for the "Extra" sample was recovered (Table 3.1).

Species	Location											
	Faro				Creek				Isla D			
	Replicate 1	Replicate 2	Replicate 3	Extra	Replicate 1	Replicate 2	Replicate 3	Extra	Replicate 1	Replicate 2	Replicate 3	Extra
<i>Achnanthes bongrainii</i> (M. Peragallo), A. Mann	80	48	57	NA	109	2	29	81	48	26	10	32
<i>Actinocyclus actinochilus</i> (Ehrenberg), Simonsen *	211	94	147	1	NA	81	113	162	145	194	169	82
<i>Amphora gourdonii</i> , M. Peragallo	1	2	NA	NA	NA	NA	NA	NA	NA	NA	NA	1
<i>Amphora holsatica</i> , Hustedt	83	0	96	178	0	NA	NA	14	NA	NA	NA	2
<i>Amphora marina</i> , W. Smith	2	17	NA	44	226	5	NA	9	11	NA	31	5
<i>Amphora</i> sp.	NA	2	30	30	21	27	NA	195	NA	0	27	NA
<i>Asteromphalus parvulus</i> , Karsten *	NA	0	NA	NA	NA	NA	NA	NA	NA	NA	NA	0
<i>Biremis</i> sp.	15	NA	27	40	390	109	23	341	NA	NA	NA	2
<i>Cocconeis costata</i> , Gregory	70	136	1	NA	NA	NA	NA	NA	0	2	NA	1
<i>Cocconeis imperatrix</i> , A. Schmidt	824	649	759	80	576	519	226	584	926	225	391	308
<i>Cocconeis matsii</i> , Al-Handal, Riaux-Gobin and Wulff	NA	5	11	NA	NA	NA	NA	NA	NA	NA	2	NA
<i>Cocconeis orbicularis</i> , Frenguelli & Orlando	127	49	17	NA	2	146	NA	96	60	NA	39	6
<i>Cocconeis pottercovei</i> , Al-Handal, Riaux-Gobin and Wulff	NA	NA	2	NA	NA	NA	NA	NA	NA	NA	NA	NA
<i>Cocconeis schuettii</i> , van Heurck	158	39	90	2	126	161	NA	32	175	7	6	NA

**Table S3.1** (continued)

<i>Corethron pennatum</i> (Grunow), Ostenfield	2	NA	7	NA	129	74	62	259	30	2	71	276
<i>Diploneis smithii</i> (Bre'bisson), Cleve	NA	NA	NA	NA	NA	NA	NA	NA	NA	NA	0	3
<i>Entomoneis gigantea</i> , Grunow	37	87	0	160	2	63	287	48	81	NA	323	82
<i>Entomoneis paludosa</i> (W. Smith), Reimer	NA	NA	NA	NA	106	NA	NA	106	43	194	NA	NA
<i>Entomoneis kjellmanii</i> (Cleve), Poulin et Cardinal	NA	NA	7	NA	NA	NA	NA	44	NA	NA	3	159
<i>Entopyla ocellata</i> (Arnott), Grunow	NA	NA	1	NA	NA	NA	NA	NA	NA	NA	NA	NA
<i>Fragilariopsis cylindrus</i> (Grunow ex Cleve), Helmcke and Krieger	NA	14	NA	NA	NA	NA	NA	NA	NA	NA	NA	NA
<i>Gyrosigma arcuatum</i> *	NA	NA	NA	NA	7353	NA	NA	NA	NA	NA	2	NA
<i>Gyrosigma fasciola</i> (Ehrenberg), Griffith et Henfrey	2126	2619	276	1479	2185	11403	3058	20970	10037	4799	715	274
<i>Gyrosigma obscurum</i> (W. Smith), Griffith & Henfrey	374	161	4	227	2	2358	565	357	3709	601	293	225
<i>Licmophora antarctica</i> , Carlson	66	91	68	NA	NA	104	90	113	NA	5	3	32
<i>Licmophora decora</i> , Heiden	37	30	5	8	NA	NA	NA	NA	NA	6	29	0
<i>Lyrella abrupta</i> (Gregory), D.G.Mann	NA	1	NA	NA	NA	NA	NA	NA	NA	NA	NA	NA
<i>Navicula cancellata</i> , Donkin	54	145	NA	2	292	128	NA	991	NA	NA	NA	1
<i>Navicula directa</i> (W. Smith), Ralfs	814	552	128	260	323	357	52	340	71	28	130	57
<i>Navicula perminuta</i> , Grunow	NA	78	585	178	NA	130	NA	843	NA	NA	56	113
<i>Nitzschia angularis</i> (M. Peragallo), A. Mann	38	2	NA	NA	16	1	2	NA	NA	25	NA	29
<i>Nitzschia hybrida</i> , Grunow	53	94	28	256	64	2	31	697	64	NA	80	60
<i>Odontella litigiosa</i> (Van Heurck), Hoban *	177	227	211	15	618	702	82	439	1090	30	126	4
<i>Parlibellus delognei</i> (Van Heurck), Cox	0	0	36	NA	161	66	NA	NA	8	1	10	47
<i>Petroneis plagiostoma</i> (Grunow), D.G. Mann	95	0	0	31	184	211	37	9	125	NA	5	NA

**Table S3.1** (continued)

<i>Petronis</i> sp.	176	NA	NA	0	NA	NA	NA	0	NA	NA	30	NA
<i>Pinnularia quadratarea</i> (A. Schmidt), Cleve	130	274	1	1466	161	256	9	150	1	12	48	2
<i>Pleurosigma strigosum</i> , W. Smith	97	57	9	384	3481	2223	257	3481	2409	228	109	56
<i>Porosira glacialis</i> (Grunow), Jørgensen *	NA	53	53	NA	95	28	1228	43	NA	1329	1072	307
<i>Pseudogomphonema kamtschaticum</i> (Grunow), Medlin	81	66	13	NA	97	NA	0	130	NA	19	1	6
<i>Rhabdonema arcuatum</i> (Lyngbye), Kützing	NA	NA	7	NA	NA	NA	NA	NA	11	NA	NA	NA
<i>Surirella</i> sp.	1	0	0	NA	NA	NA	NA	NA	NA	NA	NA	NA
<i>Synedropsis fragilis</i> (Manguin), Hasle, Syvertsen et Medlin *	NA	NA	5	NA	NA	NA	NA	NA	NA	NA	NA	51
<i>Thalassiosira gravida</i> , Cleve *	32	10	NA	NA	NA	47	NA	66	2	NA	NA	NA
<i>Thalassiosira maculata</i> , Fryxell et Johansen *	2	32	1	NA	NA	NA	NA	1	NA	NA	1	48
<i>Thalassiosira tumida</i> (Janisch), Hasle *	NA	NA	2	NA	NA	3	4	NA	32	18	6	39
<i>Thalassiosira</i> sp. *	32	146	189	NA	96	97	48	145	NA	115	NA	145
<i>Trachyneis aspera</i> (Ehrenberg), Cleve	NA	141	4	NA	396	6	45	NA	396	6	45	NA

**Table S3.2.** Results of the SIMPER analysis

Location	Faro	Creek	Isla D
Similarity within group [%]	57	57	53
Location groups	Faro-Creek	Faro-Isla D	Creek-Isla D
Dissimilarity between groups [%]	48	49	47

## Acknowledgement

We would like to acknowledge the immense support of the staff and especially of the military divers at Carlini Station, which was essential for the success of our campaign. In addition, we like to thank Christopher Brunner and Elisa Merz for support during the campaign and Moritz Holtappels for providing the PAR data from Creek. Furthermore, we like to thank Christiane Hasemann for statistical support.

Our research was funded by the European Union FP7 Project SenseOCEAN Marine Sensors for the 21st century (Grant agreement no° 614141, [www.senseocean.eu](http://www.senseocean.eu)), by European Union FP7 Project IMCONet (Grant agreement no° 319718), by the Flemish Research Fund, and by institutional funds of the Alfred-Wegener-Institut Helmholtz-Zentrum für Polar- und Meeresforschung, of the Max-Planck Institute for Marine Microbiology, and of the University of Gothenburg. UB is a postdoctoral fellow at the Research Foundation Flanders (FWO; grant no° 1201716N).



## 4 Manuscript II: Spatial variability of biogeochemistry in shallow coastal benthic communities of Potter Cove (Antarctica) and the impact of a melting glacier

---

Ralf Hoffmann<sup>1</sup>, Francesca Pasotti<sup>2</sup>, Susana Vázquez<sup>3</sup>, Nene Lefaible<sup>2</sup>, Anders Torstensson<sup>4,#a</sup>, Walter MacCormack<sup>3,5</sup>, Frank Wenzhöfer<sup>1,6</sup>, Ulrike Braeckman<sup>2,6</sup>

<sup>1</sup> HGF MPG Join Research Group for Deep-Sea Ecology and Technology, Alfred-Wegener-Institut, Helmholtz Zentrum für Polar- und Meeresforschung, Bremerhaven, Bremen, Germany

<sup>2</sup> Marine Biology Research Group, Ghent University, Ghent, Belgium

<sup>3</sup> Cátedra de Biotecnología, Facultad de Farmacia y Bioquímica, Universidad de Buenos Aires; Nanobiotec UBA-Conicet, Buenos Aires, Argentina

<sup>4</sup> Department of Biological and Environmental Sciences, University of Gothenburg, Gothenburg, Sweden

<sup>5</sup> Instituto Antártico Argentino, San Martín, Provincia de Buenos Aires, Argentina

<sup>6</sup> HGF MPG Join Research Group for Deep-Sea Ecology and Technology, Max Planck Institute for Marine Microbiology, Bremen, Bremen, Germany

<sup>#a</sup> Current address: School of Oceanography, University of Washington, Seattle, Washington, USA

*Submitted to the journal 'PLoS One'*

## 4.1 Abstract

Measurements of biogeochemical fluxes at the sediment-water interface are essential to investigate organic matter mineralization processes but are rarely performed in shallow coastal areas of the Antarctic. We investigated biogeochemical fluxes across the sediment-water interface in Potter Cove (King George Island/Isla 25 de Mayo) at water depths between 6–9 m. Total fluxes of oxygen and inorganic nutrients were quantified *in situ*. Diffusive oxygen fluxes were also quantified *in situ*, while diffusive inorganic nutrient fluxes were calculated from pore water profiles. Biogenic sediment compounds (concentration of pigments, total organic and inorganic carbon and total nitrogen), and benthic prokaryotic, meio-, and macrofauna density and biomass were determined alongside abiotic parameters (sediment granulometry and porosity). The measurements were performed at three locations in Potter Cove, which differ in terms of glacial melt disturbance intensity. This study aims to assess the implications of glacial melt-related disturbances such as ice scouring and particle release on the benthic community and the biogeochemical cycles they mediate. Further, we discuss small-scale spatial variability of biogeochemical fluxes and assess the carbon demand of Potter Cove's shallow benthic communities. Our results showed that an intermediate glacial melt-related disturbance can lead to an enhanced mineralization in soft sediments, while a high disturbance can reduce mineralization. The benthic macrofauna assemblage was the major benthic carbon stock (>87% of total benthic biomass) and the main responsible fauna for the benthic mineralization. However, the biomass of the dominant Antarctic bivalve *Laternula elliptica*, contributing 39–69% to the total macrofauna biomass, increased with enhanced glacial melt disturbance. This is contrary to the pattern of the remaining macrofauna. Our results further indicated that pelagic and microphytobenthic primary production does not fully supply Potter Cove's benthic carbon demand. Therefore, Potter Cove is a heterotrophic ecosystem in the summer season.

## 4.2 Introduction

Continental shelves comprise only 8% of the global marine realm but are an important component of the marine carbon cycle [Walsh, 1991; Fennel, 2010]. Approximately 50%

of global benthic mineralization takes place at continental shelves [Middelburg et al., 1998]. In shelf areas, benthic mineralization is mainly mediated by the benthic macrofauna community and therefore depends on their biomass, density, structure and functional traits [Kristensen et al. 1992; Braeckman et al. 2010], which in turn are influenced by food supply from primary producers and abiotic factors like sediment structure and water temperature [Vanreusel et al., 1995; Piepenburg et al., 1997; Wenzhöfer and Glud, 2002].

The Antarctic continental shelf contributes 1–6% to the entire area of the Southern Ocean [Arrigo et al., 2008a; Griffiths, 2010; Smith, 2010]. However, pelagic primary production at the continental shelf is approximately three times higher than at the open ocean and can reach up to  $1600 \text{ mg C m}^{-2} \text{ d}^{-1}$  during austral summer [Arrigo et al., 2008a]. The high amount of provided organic matter may explain the high benthic faunal biomass found at the Antarctic continental shelf [Smith et al., 2006]. At shallow, coastal sites at both Signy Island (South Orkney Islands) and Marian Cove (King George Island, Western Antarctic Peninsula), benthic mineralization measured as oxygen fluxes were  $12\text{--}90 \text{ mmol O}_2 \text{ m}^{-2} \text{ d}^{-1}$  and therefore similar to those of temperate regions [Nedwell et al., 1993; Shim et al. 2011]. However, apart from these two studies, little is known about the benthic mineralization of primary produced organic matter at the sediment-water interface (SWI) in shallow coastal environments of the Antarctic.

The Antarctic summer sea-ice extent and the sea-ice concentration are decreasing at unprecedented rates [Haumann et al., 2014; Turner et al., 2016]. Furthermore, glaciers in the West Antarctic and especially at the Western Antarctic Peninsula are melting and retreating [Rückamp et al., 2011; Paolo et al., 2015; Cook et al., 2016]. These environmental changes can alter physicochemical conditions and benthic communities. A calving-related increase in the ice scouring frequency, for example, can cause higher faunal mortality on a local scale [Conlan et al., 1998; Barnes and Souster, 2011]. Furthermore, during an ice scouring event, the sediment surface is dug over [Conlan et al., 1998; Barnes and Souster, 2011] and thereby the seafloor topography is altered [Woodworth-Lynas et al., 1991]. As juveniles or mobile organisms repopulate these areas, ice scouring can result in a patchy but diverse benthic community [Barnes, 1999], which experiences a permanent rejuvenation [Brown et al., 2004]. In addition, melting

glaciers and melting permafrost soils release mainly inorganic particles into marine waters [Khim et al., 2007], directly or via river runoffs, and therefore increase the turbidity of the water column [Dierssen et al., 2002]. Resuspension events by ice scouring also increase water column turbidity [Barnes, 1999; Griffiths, 2010]. As a consequence, less light is available for primary producers, which may result in a limited primary production, a decreased food supply, and ultimately in a lower benthic mineralization. Furthermore, particle sedimentation is an important stressor for filter feeders [Trush et al., 2004] such as common Antarctic ascidians [Torre et al., 2012] or bivalves [Philipp et al., 2011], which can lead to changes in the benthic community structure [Philipp et al., 2011; Torre et al., 2012]. However, when tidewater glaciers calve and retreat, they lay free new settling grounds. Colonization of these newly glacial free areas can increase the local organic carbon supply by primary producers [Deregibus et al., 2016] and the local biomass by heterotrophic consumers [Lagger et al., 2017; Seefeldt et al., 2017].

At Potter Cove, King George Island/Isla 25 de Mayo, benthic communities have been studied in relation to glacial melt [Philipp et al., 2011; Pasotti et al., 2015; Deregibus et al., 2016; Lagger et al., 2017; Seefeldt et al., 2017]. Directly in front of the glacier, the soft bottom meio- and macrofauna community biomass was reduced, while at other locations less influenced by glacial melt-related disturbances, an enriched biomass and a more diverse macrofauna community was found [Pasotti et al., 2015]. In the present study, we investigate the influence of glacial-melt related alterations in benthic communities and mediated benthic carbon and nutrient mineralization as important ecosystem services. We determined biogeochemical fluxes, the macro-, meio- and prokaryotic community, food supply, and sediment characteristics at three different locations, each influenced by a different intensity of glacial-melt related disturbance. We tested the following null-hypotheses within this study:

1. Benthic community structure and function are similar among areas experiencing different intensities of melting glacier disturbance.
2. Organic matter mineralization is similar among areas experiencing different intensities of melting glacier disturbance.

Additionally, our study aimed to assess small-scale spatial variability of mineralization at the Antarctic shallow coast. Further, we addressed the discrepancy in food supply to the benthic community by comparing primary production and benthic carbon demand.

## 4.3 Material and methods

### 4.3.1 Study site

Potter Cove is a roughly 3 km long and 1.2 km wide, shallow, fjord-like bay in the southwest of King George Island/Isla 25 de Mayo, an island located at the tip of the Antarctic Peninsula. The cove receives freshwater input from the Foucade glacier [Rückamp et al., 2011] and from seasonal meltwater discharge as a consequence of permafrost and snow melt. The water current moves generally clock-wise around Potter Cove, with an average current speed of  $0.03 \text{ m s}^{-1}$  [Lim et al., 2013]. The three locations included in the present study (6–9 m water depth, Figure 4.1, Table 4.1) are located in the inner part of the cove and are mainly characterized by soft sediment [Wölfl et al., 2014; Pasotti et al., 2015]. The locations, namely Faro, Creek and Isla D, became glacial ice-free between 1988 and 1995, before the 1950s, and before 2003, respectively [Rückamp et al., 2011], but are regularly covered by sea ice during winter [Schloss et al., 2012]. The three locations experienced different intensities of glacial melt-related disturbances. The amount of suspended particulate matter in the water column was highest at Isla D, intermediate at Faro and lowest at Creek [Monien et al., 2017]. The turbidity at Faro and Creek was similar, while Isla D showed a higher turbidity (based on interpolation of data from Deregibus et al. [2016]). The sediment accumulation was lowest at Faro, intermediate at Creek, and highest at Isla D [Pasotti et al., 2015]. At 15 m water depth, the youngest ice-free aged and most disturbed site (Isla D) is characterized by the lowest macro- and meiofauna biomass, compared to the older ice-free aged and less disturbed sites Faro and Creek [Pasotti et al., 2015]. The community composition of both macro- and meiofauna differed strongly between the three locations, with the highest trophic diversity found at Faro [Pasotti et al., 2015]. We measured biogeochemical fluxes at the sediment-water interface and sampled benthic communities and environmental

parameters during a field campaign in February and March 2015 (Table 4.1) at the Argentinean-German Dallmann Laboratory at the Argentinean Carlini research station.

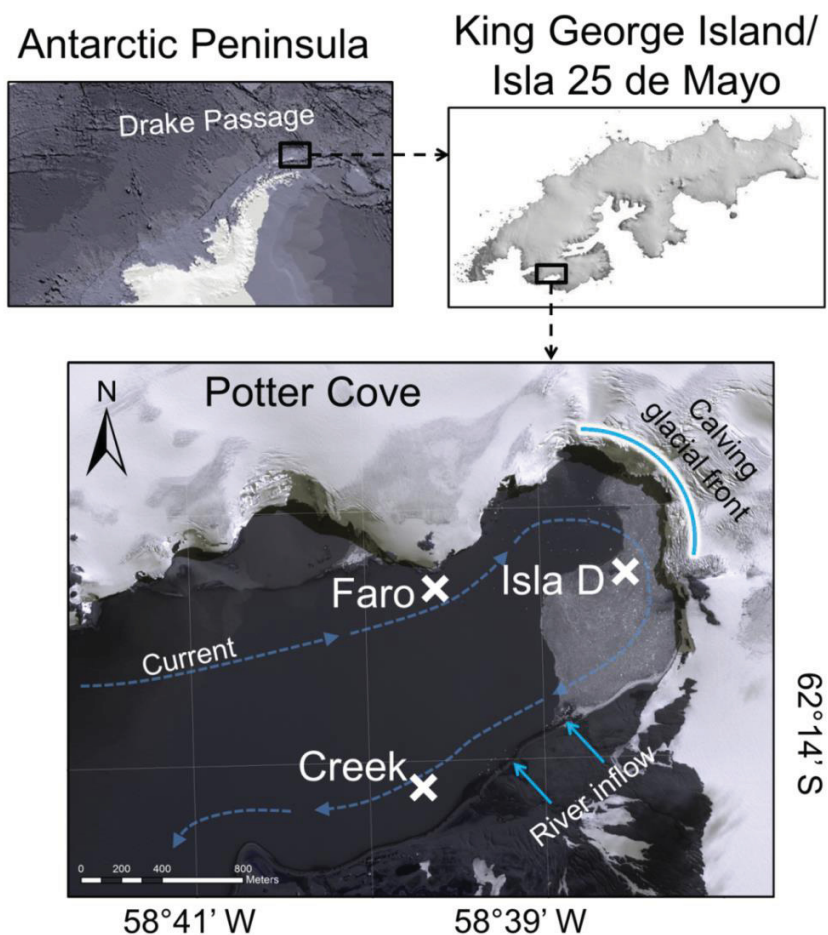


**Figure 4.1.** Study site Potter Cove. At Faro, Creek, and Isla D *in situ* measurements and sediment sampling were conducted. The position of locations is marked with a cross. The curved, bright blue line marks the front of the Fourcade glacier. The bright blue arrows indicate river run-offs supplied mainly by glacier, permafrost and snow melt. The dashed blue arrows indicate the direction of the main current.

**Table 4.1.** Location, water depth, and date of sampling of the three locations sampled in Potter Cove.

Location	Faro	Creek	Isla D
Latitude	62° 13.31' S	62° 14.08' S	62° 13.30' S
Longitude	58° 39.36' W	58° 39.43' W	58° 38.30' W
Depth [m]	8–9	8–9	6–7
<i>In situ</i> measurements and sampling for biogenic compounds [Dates]	10/02/2015–12/03/2015	28/02/2015–01/03/2015	18/02/2015–19/02/2015
Pore water sampling dates and number of sediment cores sampled	09/02/2015: 4 cores	26/02/2015: 2 cores 01/03/2015: 2 cores	18/02/2015: 2 cores 19/02/2015: 2 cores

### 4.3.2 Sediment properties and biogenic sediment compounds

For the determination of sediment properties and biogenic sediment compounds, sediment was sampled with 3.6 cm diameter cores in five replicates by SCUBA divers. Sediment subsamples were taken with cut-off syringes (cross-sectional area = 1.65 cm<sup>2</sup>) and sliced in 1 cm intervals down to 5 cm sediment depth. Each interval was analyzed for various parameters including median grain size, porosity, photosynthetic pigments, total carbon, total organic carbon and total nitrogen. Sediment samples for photosynthetic pigments were stored at -80°C. Sediment samples of other parameters were stored at -20°C until analyses at the home laboratory.

The median grain size was determined with a Malvern Mastersizer 2000G, hydro version 5.40. The Mastersizer used a laser diffraction method and had a measuring range of 0.02–2000 µm. Sediment porosity was determined after drying sediment samples over a period of at least two days at 105°C. The sediment porosity  $\phi$  was calculated with the following formula of Burdige [2006]:

$$\phi = \frac{m_w/\rho_w}{m_w/\rho_w + (m_d - (S \times m_w))/\rho_s}$$

In this equation,  $m_w$  is the mass of evaporated water,  $\rho_w$  is the density of the evaporated water,  $m_d$  is the mass of dried sediment plus salt,  $S$  is the salinity of the overlying water and  $\rho_s$  is the sediment density (2.66 g cm<sup>-3</sup> [Burdige, 2006]). To calculate  $m_w$ ,  $\rho_w$ ,  $m_d$  the weight loss of wet sediment samples that were dried at 105°C was measured. Chlorophyll *a* (Chl *a*), phaeophytin (Phaeo) and fucoxanthin (Fuco) pigment concentrations were determined by HPLC (Gilson) [Wright and Jeffrey, 1997]. The bulk of pigments (Chl *a* plus Phaeo) was termed chloroplastic pigment equivalents (CPE) [Thiel, 1978]. The ratio of Chl *a* to Phaeo served as an indicator for the relative age of the material. The total carbon (TC) and total nitrogen (TN) were measured by combustion using an ELTRA CS2000 with infrared cells. The total organic carbon (TOC) was measured using the same method after acidifying the sample (3 ml of 10 M HCl). Total inorganic carbon (TIC) was calculated by subtracting TOC from TC.

### 4.3.3 Benthic community structure

For prokaryotic density determination, the same sampling and sub-sampling approach was used as for the sediment properties. Each sediment interval was fixed in a 2% formaldehyde/seawater filtered solution and stored at 4°C. The acridine-orange-direct-count method [Hobbie et al., 1977] was used to stain prokaryotes in the sub-samples and subsequently counted with a microscope (Axioskop 50, Zeiss) under UV-light (CQ-HXP-120, LEJ, Germany). For each sample, single cells were counted on two replicate filters and for 30 random grids per filter (dilution factor 4000). Prokaryotic biomass was estimated by the determination of the mean prokaryotic cell volume in the first two centimetres with a “New Portion” grid (Graticules Ltd, Tonbridge, UK) [Grossmann and Reichardt, 1991], converted into biomass using a conversion factor of  $3.0 \times 10^{-13} \text{ g C pm}^{-3}$  [Børsheim et al., 1990] and multiplied with the prokaryotic density. Thereby, each mean prokaryotic cell volume represents the mean of 100 counted grids.

For the determination of meiofauna density, biomass and identification of meiofauna taxa, five sediment samples were taken with small sediment cores ( $\varnothing$  3.6 cm). Sediment samples of the first five centimeters were stored in filtered seawater buffered 4% formaldehyde solution at 4°C until extraction at the home laboratory. The samples were sieved over a 1 mm and 32  $\mu\text{m}$  mesh, centrifuged three times in a colloidal silica solution (Ludox TM-50) with a density of  $1.18 \text{ g cm}^{-3}$ , and stained with Rose Bengal [Heip et al., 1985]. Afterwards, benthic meiofauna was identified on higher taxon level and counted. In order to determine the meiofauna biomass, the total organic carbon content of single taxa was measured with a FLASH 2000 NC Elemental Analyzer (Thermo Fischer Scientific, Waltham, USA). Calcifying organisms were acidified prior to the analysis.

The benthic macrofauna was sampled with a Van Veen grab (530  $\text{cm}^2$  surface area). At each location, four recovered sediment samples were sieved over a 1 mm mesh and stored in seawater buffered 4% formaldehyde. In the laboratory, the taxa were identified to the lowest possible taxonomic level (at least family level), counted, weighted, and the Shannon-Wiener diversity index ( $H'$ ) was calculated in Primer v6.0. Ash-free dry weight (AFDW) was determined by subtracting the ash weight (after combustion at 500°C) from the dry weight (dried for 48 h at 60°C). AFDW was converted into carbon by assuming



that 50% of the AFDW was carbon [Wijsman et al., 1999]. The Van Veen grab sampling results in a strong underestimation of the density of the Antarctic bivalve *Laternula elliptica*. Therefore, two transects of eight grids (45 cm x 45 cm) were randomly placed on the seafloor by scuba divers and photos were taken (Nikon D750, rectilinear Nikon 16–35 mm lens, Nauticam underwater housing, two Inon Z-240 strobes). The photos were used to count siphons of *L. elliptica* to determine their density and to measure the siphon width (maximum distance between outer edges of the two siphons of one individual) at the three locations. Assuming a linear relationship between siphon width and AFDW, a conversion factor was used to calculate an estimated biomass of *L. elliptica*. The calculation of the conversion relationship of the siphon width to AFDW was performed on data from the same *L. elliptica* population. From the macrofauna abundance ( $A_i$ ) and biomass ( $B_i$ ), together with a mobility score ( $M_i$ , score between 1–4) and sediment reworking score ( $R_i$ , score between 1–5) of each taxon (Table S4.1), the community bioturbation potential ( $BP_c$ ) was calculated with the following formula [Queirós et al., 2013]:

$$BP_c = \sum_{i=1}^n \sqrt{B_i/A_i} \times A_i \times M_i \times R_i$$

in which  $i$  displays the specific taxon in the sample.

#### 4.3.4 Biogeochemical flux measurements

To quantify the *in situ* benthic organic matter mineralization, three transparent and three black chambers (inner diameter 19 cm, height 33 cm) were carefully pushed into the sediment at each location by SCUBA divers, who took special care to not disturb the sediment surface during the procedure. About 15 cm of sediment and 18 cm of overlying water was enclosed. Cross-shaped stirrers powered by a 12 V lead-acid battery kept the overlying water homogenous. The incubation lasted 20–22 h and included light and dark periods. Owing to dive security regulations, we could not perform measurements after sunset to distinguish between day-time and night-time oxygen fluxes. Therefore, the resulting fluxes are net fluxes. HOBO Pendant® loggers (Onset, Bourne, USA) were placed both *in situ* and on land to record the amount of radiation (150–1200 nm) during the incubation with a temporal resolution of 5 minutes. The transmission of radiation to

the seafloor was calculated based on the readings on land and *in situ*. The enclosed overlying water in the chambers was sampled through valves in the chamber lids at the start and end of the chamber incubation, using gas-tight glass syringes. The water samples were kept at *in situ* temperature and in darkness until further processing, which took place within 1.5 h after the samples were taken.

Subsamples were taken to determine the oxygen concentration, the concentration of dissolved inorganic carbon (DIC) and the concentrations of phosphate, ammonium, nitrite, nitrate, and sulfate. Winkler titration was used to determine the oxygen concentration in the water sample in technical duplicates on site. For DIC analyses technical triplicates were poisoned with mercury-di-chloride and stored at 4°C until measurement after 6 months at the home laboratory. DIC samples were analyzed using an autosampler (Techlab, Spark Basic Marathon) with a digital conductivity measuring cell (VWR, digital conductivity meter, Germany) [Hall and Aller, 1992; Lustwerk and Burdige, 1995]. For nutrient analyses technical triplicates were filtered through a GF/F filter (Whatman, Maidstone, U.K.) and stored at -20°C until analysis. The samples were analyzed with an autosampler (CFA SAN-plus, Skalar Analytical B.V., Netherlands) for ammonium, phosphate, nitrite and [nitrate + nitrite] concentrations [Grasshoff et al., 1999]. The nitrate concentration was determined by subtracting the nitrite concentration from the [nitrate + nitrite] concentration.

The total oxygen uptake (TOU) by the benthic community during the incubation was calculated using the formula:

$$\text{TOU} = \frac{\delta O_2 \times V}{\delta t \times A}$$

in which  $\delta O_2$ ,  $V$ ,  $\delta t$  and  $A$  represent the difference in oxygen concentration, the volume of the overlying water, the difference in time and the surface area, respectively. The volume of the overlying water was calculated by using the average height between the seafloor and the chamber lid, measured at five locations of each chamber. The TOU was converted to carbon equivalents (C-TOU) by applying the Redfield ratio of C : O = 106:138 [Redfield, 1934]. The same formula as for calculating the TOU was used to calculate total DIC and total flux of specific nutrients, with  $\delta_{\text{DIC}}$  and  $\delta_{\text{Nutrient}}$

instead of  $\delta O_2$ , respectively. Several total DIC flux values were omitted as the difference between t0 and t1 was lower than the method's detection limit of 0.05  $\mu\text{M}$ .

High resolution *in situ* oxygen profiles were measured using a microprofiler [Wenzhöfer et al., 2000; Lichtschlag et al., 2010]. The microsensors were driven from the water phase into the sediment with a spatial resolution of 100  $\mu\text{m}$  and a temporal resolution of 30 seconds. On the profiler electronic unit, three custom-made electrochemical oxygen microsensors [Revsbech, 1989] were mounted and calibrated before deployment, as previously described [Wenzhöfer et al., 2000; Beer et al., 2006]. The microprofiler was programmed, so microsensors penetrated the SWI around noon at the same or the following day after the deployment. Running average smoothed profiles [Hoffmann et al., 2018] were used to calculate the diffusive oxygen uptake (DOU) over the SWI using Fick's first law:

$$\text{DOU} = -D_s \times \left[ \frac{\delta O_2}{\delta z} \right]_{z=0}$$

in which  $D_s$  is the molecular diffusion coefficient of oxygen in sediments at *in situ* temperature and salinity, and  $[\delta O_2/\delta z]_{z=0}$  is the oxygen gradient at the SWI calculated by linear regression from the first alteration in the oxygen concentration profile over a maximum depth of 1 mm.  $D_s = D/\theta_2$  [Schulz, 2006], with  $D$  as the molecular diffusion coefficient of oxygen in water [Li and Gregory, 1974], and  $\theta^2 = 1 - \ln(\phi_2)$  [Boudreau, 1997]. Due to hidden dropstones or hard-shelled organisms, a few microsensors broke at a very early stage of the profiling, which resulted in a reduced number of calculated diffusive fluxes per location.

For the calculation of the diffusive flux of sulfate, DIC, and nutrients, sediment was sampled with cores (10 cm diameter) with pre-drilled holes at 1 cm intervals that were sealed with diffusion-tight tape. The pore water was extracted using Rhizons (type: core solution sampler, Rhizosphere Research Products, filter pore diameter of 0.1 mm) connected to 10 mL Luer lock syringes. The Rhizons were horizontally inserted into the sediment and by creating a permanent vacuum in the syringes, pore water was extracted. The first drops were used to rinse the syringe and then discarded. The extracted pore water was split for sulfate analyses (sample fixed in 5% ZnAc, stored at 4°C), DIC analyses (sample fixed in mercury-di-chloride, stored at 4°C) and nutrient

analyses (frozen at  $-20^{\circ}\text{C}$ ). DIC and nutrients were analyzed as described above. Sulfate was analyzed by using non-suppressed ion chromatography with the Methrom 761 Compact IC equipped with a Metrosep A SUPP 5 column (Methrom, Herisau, Switzerland). From the resulting depth profiles, diffusive fluxes were calculated using the same formula as for the DOU calculation, but with  $D_s$  of the specific molecule [Schulz, 2006].

#### 4.3.5 Statistical approaches

Fluxes were calculated for each chamber using the slope of concentration over time (incubations; total flux) or depth (vertical profile; diffusive flux). Whenever possible, we tested the significance of the slopes and only significant regressions over time or sediment depth were used in this study. In case only two data points were available for the slope calculation, we assumed significant increase or decrease by considering the detection limits of each measurement method.

To test whether the light or dark treatment had an influence on the total fluxes, Students t-tests were performed on the fluxes of black and transparent chambers. In case of heteroscedasticity, tested with a Levene's test, a Welch two sample t-test was carried out. The Gaussian distribution of the data was assumed. Since all t-tests indicated that light had no effect on the total fluxes (Table S4.2), the data of the different chambers were pooled in all further analyses.

To test whether single parameters differed between locations, a one-way ANOVA with type III SS was performed. A Shapiro-Wilk test was performed to test data normality, whereas a Levene's test was used to test homoscedasticity. To identify the locations showing significant differences, a parametric Tukey or, in case data were normally distributed but not homoscedastic, a Games-Howell post-hoc test [Games and Howell, 1976] was performed. When data were not normally distributed, absolute values of data were square root transformed and the Shapiro-Wilk test was repeated. In case transformed data did still not met the assumptions for parametric tests, a non-parametric Kruskal-Wallis test and a post-hoc Bonferroni test [Dunn, 1964] were performed to identify significant differences between the locations.

To visualize the variables responsible for the small-scale variability among Faro, Creek and Isla D, a principal component analyses (PCA) was performed on standardized mean values of turbidity [Deregibus et al., 2016], median grain size, Chl *a*, TC, macrofauna biomass (excluding *L. elliptica*), *L. elliptica* biomass, TOU, diffusive phosphate efflux, and diffusive nitrate flux. All other parameters were excluded from the PCA as they correlated strongly with one of the mentioned parameters (correlation >0.8, Pearson correlation, Table S4.3) used within the PCA. This procedure results in a more resilient outcome of the PCA.

All mentioned tests were performed using R Statistical Software (version 3.4.0, R Core Team, 2017) and the packages “vegan” [Oksanen et al., 2017], “CAR” [Fox and Weisberg, 2011], “Userfriendlyscience” [Peters, 2007] and “PMCMR” [Pohlert, 2014]. Where replicates were available, results are expressed as mean value  $\pm$  standard deviation.

#### 4.3.6 Ethics statement

In advance of the field campaign, the Environmental and Tourism Antarctic Management Program of the National Direction of the Antarctic (Dirección Nacional del Antártico) in the Republic of Argentina, permitted the conducted research to the Specially Protected Area N° 132 “Peninsula Potter” (under art. 7, Annex V of the Madrid Protocol, Law 25260). This permission properly followed the regulations in force. None of the protected species were sampled.

## 4.4 Results

### 4.4.1 Comparison of abiotic and biogenic parameters

During the incubations, the seafloor at the locations Faro, Creek, and Isla D experienced 13.5 hr, 14.5 hr, and 13.5 hr of light incidence, respectively. The light transmission to the seafloor (= light incidence at the seafloor/light incidence at land) during daytime was  $0.5 \pm 0.3\%$ ,  $4.4 \pm 1.8\%$ , and  $0.7 \pm 0.5\%$  at Faro, Creek and Isla D, respectively.

The median grain size and porosity at Faro was  $116 \pm 27 \mu\text{m}$  and  $0.56 \pm 0.08$  over the first 5 cm sediment depth (Figure 4.2 A), respectively, with a sand fraction of  $61 \pm 5\%$  (Table S4.4). Creek displayed a similar median grain size and porosity ( $120 \pm 9 \mu\text{m}$  and  $0.51 \pm 0.05$ , respectively, Figure 4.2 A), but a higher sand fraction of  $72 \pm 4\%$  (Table S4.4). The sediment at Isla D was finer (median grain size:  $20 \pm 30 \mu\text{m}$ , sand fraction:  $17 \pm 12\%$ ) and displayed a higher porosity ( $0.76 \pm 0.12$ ) over the first 5 cm sediment depth (Figure 4.2 A).

TC, TIC, TOC, and TN contents over the first 5 cm sediment depth at Faro were  $7.2 \pm 1.4 \mu\text{g C mg}^{-1} \text{ sediment}^{-1}$ ,  $4.8 \pm 0.8 \mu\text{g C mg}^{-1} \text{ sediment}^{-1}$ ,  $2.3 \pm 0.9 \mu\text{g C mg}^{-1} \text{ sediment}^{-1}$  and  $0.5 \pm 0.2 \mu\text{g N mg}^{-1} \text{ sediment}^{-1}$  (Figure 4.2 B, Table S4.4), respectively, and the organic carbon portion (TOC/TC) was  $32 \pm 8\%$  (Table S4.4). TC, TIC, and TN contents were significantly lower at Creek ( $2.6 \pm 0.5 \mu\text{g C mg}^{-1} \text{ sediment}^{-1}$ ,  $0.6 \pm 0.3 \mu\text{g C mg}^{-1} \text{ sediment}^{-1}$  and  $0.4 \pm 0.1 \mu\text{g N mg}^{-1} \text{ sediment}^{-1}$ , respectively) compared to Faro, while TOC content ( $2.0 \pm 0.4 \mu\text{g C mg}^{-1} \text{ sediment}^{-1}$ ) was similar (Figure 4.2 B, Table S4.4). Therefore, the TOC/TC ratio was twice as high at Creek ( $78 \pm 11\%$ ) compared to Faro (Table S4.4). TC ( $5.5 \pm 0.9 \mu\text{g C mg}^{-1} \text{ sediment}^{-1}$ ), TIC ( $3.3 \pm 0.4 \mu\text{g C mg}^{-1} \text{ sediment}^{-1}$ ), TN content ( $0.5 \pm 0.2 \mu\text{g N mg}^{-1} \text{ sediment}^{-1}$ ) and the TOC/TC ratio ( $39 \pm 10\%$ ) at Isla D had intermediate values between Faro and Creek, while the TOC content ( $2.2 \pm 0.8 \mu\text{g C mg}^{-1} \text{ sediment}^{-1}$ ) was in a similar range (Figure 4.2 B, Table S4.4).

The Chl *a* concentration at Faro was  $6.3 \pm 4.6 \mu\text{g g}^{-1} \text{ sediment}^{-1}$  and the Fuco and Phaeo concentrations were  $3.1 \pm 2.6 \mu\text{g g}^{-1} \text{ sediment}^{-1}$  and  $2.4 \pm 0.8 \mu\text{g g}^{-1} \text{ sediment}^{-1}$ , respectively. The relative age of the biodegradable organic matter, represented by the chlorophyll *a* to phaeophytin ratio (Chl *a*/Phaeo), was 2.6. At Creek, Chl *a* and Fuco concentrations were higher ( $11.3 \pm 9.3 \mu\text{g g}^{-1} \text{ sediment}^{-1}$ ,  $6.6 \pm 5.7 \mu\text{g g}^{-1} \text{ sediment}^{-1}$ , respectively), while Phaeo concentrations were lower ( $1.8 \pm 1.0 \mu\text{g g}^{-1} \text{ sediment}^{-1}$ , Figure 4.2 B, Table S4.4) compared to Faro. Consequently, organic matter at Creek had a higher Chl *a*/Phaeo ratio of 6.3. Chl *a* and Fuco concentrations, and the Chl *a*/Phaeo ratio over the first five centimeter sediment depth at Isla D were similar to Faro ( $3.0 \pm 1.4 \mu\text{g g}^{-1} \text{ sediment}^{-1}$ ,  $1.3 \pm 0.9 \mu\text{g g}^{-1} \text{ sediment}^{-1}$ , and 1.6, respectively),

while Phaeo concentrations ( $1.9 \pm 0.7 \mu\text{g g}^{-1} \text{ sediment}^{-1}$ ) were similarly low as in Creek (Table S4.4).

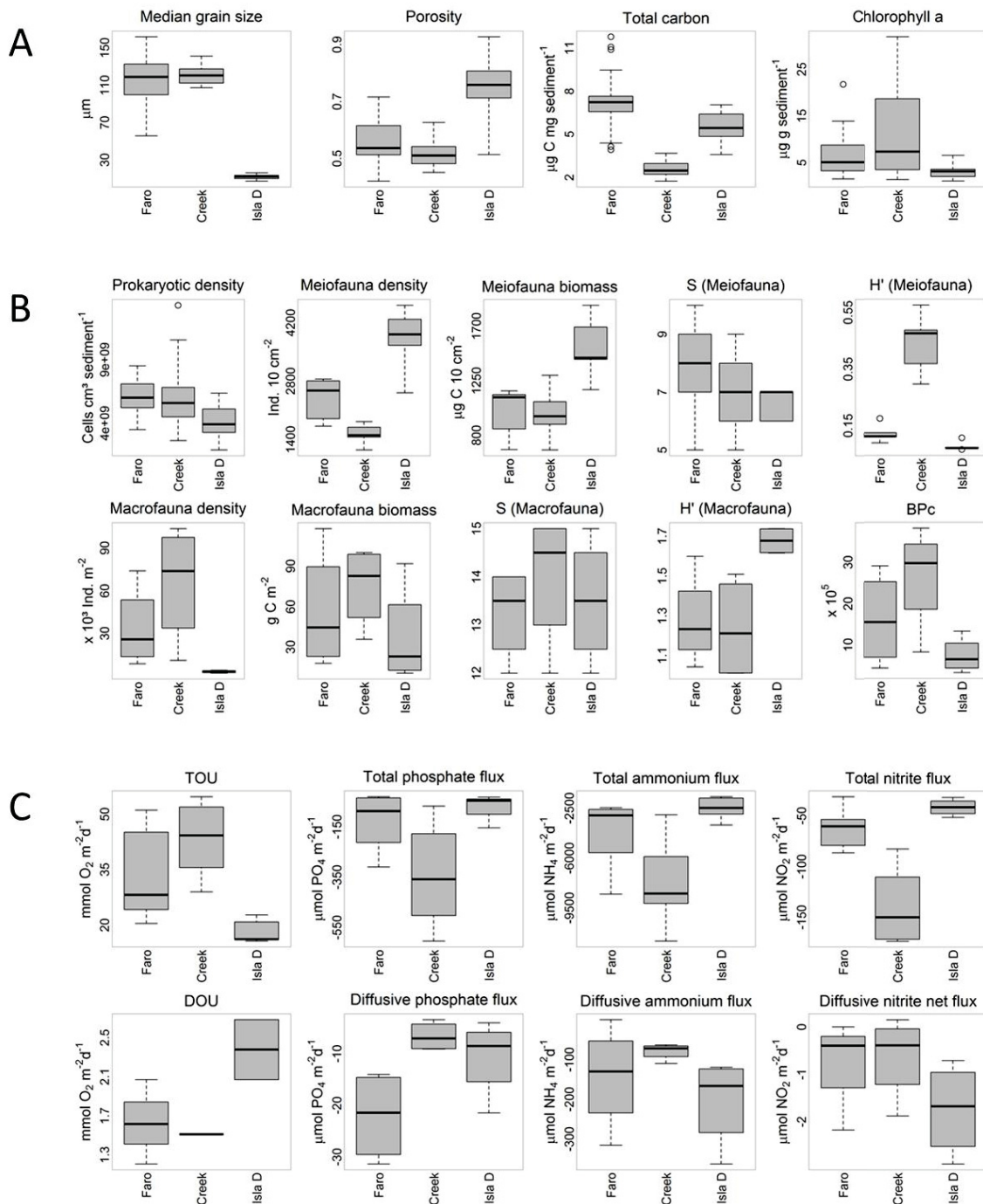


**Figure 4.2.** Boxplots of a subset of the measured parameters. Panel A refers to sediment properties and biogenic sediment compounds, panel B refers to fauna community parameters and diversity indices, and panel C refers to total fluxes and diffusive fluxes. Macrofauna density and biomass do not include results of the photo survey of *Laternula elliptica*, due to the use of different determination approaches.

Median grain size increased with sediment depth at Faro, while no vertical change was determined for the other locations. The porosity and TC, TOC, TN, Chl a, Fuco, and Phaeo concentrations decreased with sediment depth at the three locations, while TIC concentration did not change over sediment depth. The sulfate concentration in the pore water also did not change over sediment depth and was  $\sim 27 \text{ mmol SO}_4^{2-} \text{ L}^{-1}$  at the three locations (Figure S4.1).

#### 4.4.2 Comparison of fauna community parameters

At Faro, the prokaryotic density was  $6.1 \pm 1.2 \times 10^{09} \text{ cells cm}^{-3}$  of sediment and the prokaryotic biomass was  $0.29 \pm 0.44 \text{ mg C cm}^{-3}$  of sediment (Table S4.4). The meiofauna density and the meiofauna biomass was  $2368 \pm 471 \text{ ind. } 10 \text{ cm}^{-2}$  and  $990 \pm 190 \mu\text{g C } 10 \text{ cm}^{-2}$ , while the macrofauna density and macrofauna biomass (excluding *L. elliptica*) were  $33574 \pm 24902 \text{ ind. m}^{-2}$  and  $56 \pm 39 \text{ g C m}^{-2}$ , respectively (Table S4.4). The photo survey revealed an estimated *L. elliptica* density of  $93 \pm 26 \text{ ind. m}^{-2}$ , a *L. elliptica* biomass of  $36 \pm 9 \text{ g C m}^{-2}$  and an *L. elliptica* individual biomass of  $0.39 \pm 0.16 \text{ g C ind.}^{-1}$  (Table S4.4).

At Creek, the prokaryotic density, prokaryotic biomass, meiofauna density, meiofauna biomass, macrofauna density (excluding *L. elliptica*), and macrofauna biomass (excluding *L. elliptica*) were similar compared those reported at Faro (Figure 4.2 B, Table S4.4). However, values of estimated *L. elliptica* density and *L. elliptica* biomass ( $157 \pm 44 \text{ ind. m}^{-2}$ ,  $54 \pm 16 \text{ g C m}^{-2}$ , respectively) were significantly higher at Creek compared to those at Faro, whereas the *L. elliptica* individual biomass ( $0.34 \pm 0.14 \text{ g C ind.}^{-1}$ ) was significantly lower (Table S4.4).

At Isla D, prokaryotic biomass, meiofauna biomass, and macrofauna biomass (latter excluding *L. elliptica*;  $0.19 \pm 0.12 \text{ mg C cm}^{-3}$  sediment,  $1522 \pm 240 \mu\text{g C } 10 \text{ cm}^{-2}$ ,  $37 \pm 33 \text{ g C m}^{-2}$ , respectively) were similar to those reported at Faro and Creek (Figure 4.2 B, Table S4.4). The macrofauna density (excluding *L. elliptica*,  $3074 \pm 815 \text{ ind. M}^{-2}$ ) at Isla D was similar to Faro, but significantly lower compared to Creek (Figure 4.2 B, Table S4.4). Furthermore, prokaryotic density, *L. elliptica* density, and *L. elliptica* individual biomass ( $4.2 \pm 1.2 \times 10^{09} \text{ cells cm}^{-3}$  sediment,  $276 \pm 50 \text{ ind. m}^{-2}$ ,  $0.29 \pm 0.10 \text{ g C ind.}^{-1}$ , respectively) were significantly lower compared to Faro and



Creek, whereas meiofauna density and *L. elliptica* biomass ( $3799 \pm 719$  ind.  $10 \text{ cm}^{-2}$ ,  $81 \pm 15 \text{ g C m}^{-2}$ , respectively) were significantly higher (Figure 4.2 B, Table S4.4). The macrofauna community carbon stock made up >90% of the entire community carbon stock at each location and *L. elliptica* contributed with 39%, 42% and 69% to the total macrofauna biomass at Faro, Creek and Isla D, respectively (Figure 4.3).

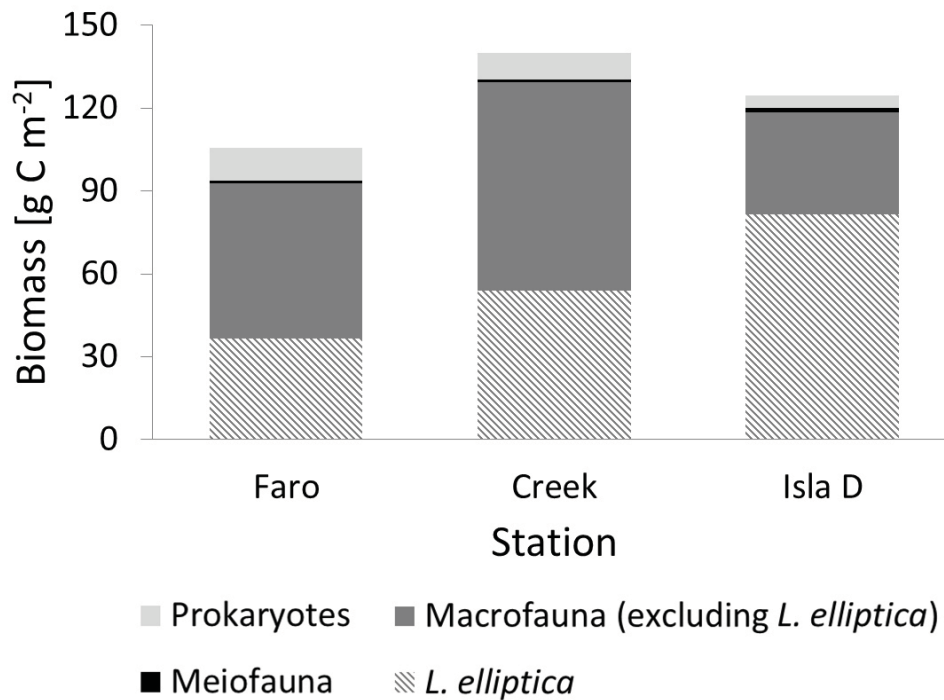


**Figure 4.3.** Mean biomasses of prokaryotes, meio- and macrofauna. Macrofauna is the major standing carbon stock in Potter Cove and the bivalve *L. elliptica* contributes a large portion to the total macrofauna biomass. Prokaryotic biomass refers to the sum of the first 5 cm sediment and in order to compare it with the biomass of the other biota size classes, the prokaryotic biomass is expressed as densities per surface.

Meiofauna density was dominated by nematodes (98%, 87%, and 99% at Faro, Creek, and Isla D, respectively). Further, macrofauna density at Faro was dominated by the cumacean family *Leuconidae sp.*, at Creek by the bivalve *Mysella sp.*, and at Isla D by the burrowing bivalve *Aequiyoldia eightsii*, while macrofauna biomass was dominated by *Aequiyoldia eightsii* at each location (87%, 81%, 74% at Faro, Creek, and Isla D, respectively), *L. elliptica* biomass not included. The meiofauna taxon and macrofauna species richness did not differ between locations, while the Shannon-Wiener diversity index was highest at Creek and differed significantly from Isla D for both meio- and macrofauna (Figure 4.2 B, Table S4.4). The bioturbation potential of the macrofauna community (BPc) did not differ among the three locations (Figure 4.2 B, Table S4.4).

#### 4.4.3 Comparison of biogeochemical fluxes

Total fluxes, determined by *in situ* chamber incubations, showed no differences between transparent and black chambers. Therefore, fluxes from transparent and black chambers at each location were pooled. In general, only benthic oxygen influxes were measured in Potter Cove (from the water column to the seafloor). The TOU at Creek ( $43 \pm 9 \text{ mmol O}_2 \text{ m}^{-2} \text{ d}^{-1}$ ) exceeded Isla D's TOU ( $18 \pm 3 \text{ mmol O}_2 \text{ m}^{-2} \text{ d}^{-1}$ ) significantly, while at Faro the TOU ( $33 \pm 11 \text{ mmol O}_2 \text{ m}^{-2} \text{ d}^{-1}$ ) did not differ significantly from the TOU of Creek and Isla D (Figure 4.2 C, Table S4.4). *In situ* measured oxygen profiles revealed an oxygen penetration depth of 3–8 mm and a DOU that ranged between 1.5–2.4  $\text{mmol O}_2 \text{ m}^{-2} \text{ d}^{-1}$  (Figure 4.2 C, Table S4.4). The DOU made up 4.0% of the TOU at Faro, 1.3% at Creek and 9.4% at Isla D. The C-TOU was  $25 \pm 9$ ,  $33 \pm 7$ , and  $11 \pm 6 \text{ mmol C m}^{-2} \text{ d}^{-1}$  at Faro, Creek, and Isla D, respectively.

The total DIC efflux was 12–23  $\text{mmol DIC m}^{-2} \text{ d}^{-1}$  and the diffusive DIC efflux was 0.1–0.7  $\text{mmol DIC m}^{-2} \text{ d}^{-1}$ . Both DIC fluxes, total and diffusive, did not differ between the locations (Table S4.4). The sediment respiration quotient (RQ = total DIC/TOU) was 0.55, 0.53, and 0.65 for Faro, Creek, and Isla D, respectively.

Phosphate, ammonium, and nitrite were released from the sediment to the water column (efflux), whereas the nitrate flux was directed into the sediment (influx). Furthermore, the total nutrient fluxes exceeded their diffusive equivalents at least 5.4 times (phosphate flux at Creek). For each nutrient, the highest total flux was measured at Creek and the lowest at Isla D, differing significantly from each other (Figure 4.2 C, Table S4.4). Total nutrient fluxes at Faro were either similar to both locations (total phosphate efflux and total ammonium efflux) or only similar to Isla D and differed significantly from Creek (total nitrite efflux and nitrate influx (Figure 4.2 C, Table S4.4). The diffusive ammonium efflux and the diffusive nitrite net efflux were similar at the three locations. However, the diffusive phosphate efflux was highest at Faro and differed significantly from Creek and the diffusive nitrate uptake was significantly lower at Creek, compared to Faro and Isla D (Figure 4.2 C, Table S4.4).

#### 4.4.4. Relationships between abiotic and biogenic sediment parameters, the benthic community, and oxygen and nutrient fluxes

The results of the PCA revealed that Faro, Creek and Isla D represented different habitats within the Potter Cove ecosystem (Figure 4.4). The turbidity was positively correlated with *L. elliptica* biomass and both parameters were negatively correlated with median grain size, TOU, macrofauna biomass (excluding *L. elliptica* biomass), and Chl *a*. The TC was independent of the above-mentioned parameters, but positively correlated with Phaeo and the diffusive nitrate flux, and negatively correlated with the diffusive phosphate flux (Figure 4.4). The first dimension is mainly represented by TOU, macrofauna biomass, and Chl *a* (Eigenvalues: -0.669, 0.667, -0.657, respectively) and distinguishes Creek from Isla D. The second dimension is mainly represented by Phaeo, the diffusive phosphate flux and TC (Eigenvalues: 0.668, -0.658, -0.549, respectively) and sets Faro aside from the other two locations. It needs to be mentioned that each parameter also represents other correlated parameters (S4.3 Table).

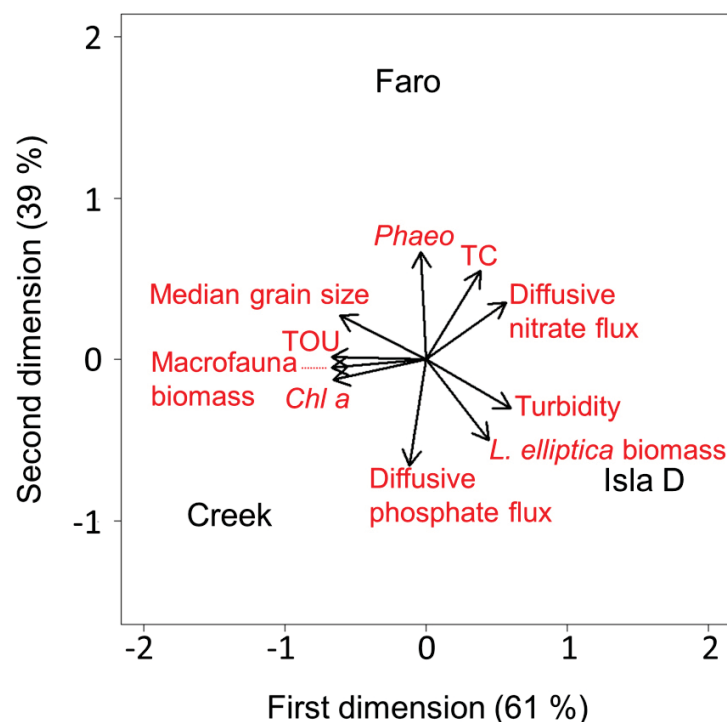


**Figure 4.4.:** PCA results on mean values in the scaling II mode. Each parameter represents several measured and strongly correlated parameters ( $r = 0.8$ , Table S4.3). The angles between the arrows of two parameters represent relations ranging between total dependence ( $0^\circ$  angle) and total independence ( $90^\circ$  angle). Faro, Creek and Isla D display different habitats within the Potter Cove ecosystem. The macrofauna biomass is represented with exclusion of *L. elliptica* biomass.

## 4.5 Discussion

### 4.5.1 The influence of glacial melt processes on the Antarctic shallow benthos and benthic mineralization

Glacial melting effects include sediment release and resuspension of the sedimentary seafloor by ice scouring events [Woodworth-Lynas et al., 1991; Dierssen et al., 2002; Brown et al., 2004; Smith, 2010; Barnes and Souster, 2011]. Based on patterns in suspended particulate matter [Monien et al., 2017], turbidity [Deregibus et al., 2016] and sediment accumulation [Pasotti et al., 2015] in combination with our findings on the median grain size and porosity (Figure 4.2), we suggest a categorization of the locations in less disturbed (Faro), intermediately disturbed (Creek) and highly disturbed (Isla D). The highly disturbed site Isla D was characterized by the lowest densities in prokaryotes and macrofauna (excluding *L. elliptica*), the highest meiofauna and *L. elliptica* densities and biomass, and the highest macrofauna diversity (Figure 4.2 B, Table S4.4). At the intermediately disturbed location Creek, the highest macrofauna densities and the highest meiofauna taxon diversity were determined (Figure 4.2 B, Table S4.4). Therefore, we can reject our null-hypothesis that the benthic community structure and functions are similar among areas experiencing different intensities of glacial melt-related disturbance. The differences in time since the investigated locations were ice-free might have an additional influence on the benthic community structure [Pasotti et al., 2015]. It should be noted that the BPC might increase when *L. elliptica* density and biomass would be included in the BPC calculation.

We can also reject our second null-hypothesis that organic matter mineralization is similar among areas experiencing different intensities of implications of a melting glacier. The TOU at Isla D is significantly lower than at Faro and Creek. In general, total fluxes of all investigated molecules were highest at the intermediately disturbed location Creek and lowest at the highly disturbed location Isla D. Therefore, our results indicate that an intermediate disturbance leads to an increased mineralization, while a high disturbance leads to a strong drop in the mineralization. This pattern is supported by a lower bioturbation potential and the smallest individuals of *L. elliptica* found at Isla D (Table S4.4), suggesting that the sediment is mixed over smaller distances [Zaklan and

Ydenberg, 1997; Queirós et al., 2015]. This limits the oxygenation of the sediment, indicated by shallower oxygen penetration depth (Table S4.4), which in the end suppresses the mineralization process.

The strong relation between food supply and organic matter, macrofauna biomass and mineralization [Kristensen et al., 1992; Glud et al., 1994; Braeckman et al., 2010] and the negative impact of sedimentation (indicated by turbidity in Figure 4.4) on macrofauna respiration have been observed before [Philipp et al., 2011; Torre et al., 2012]. The increased mineralization at Creek and the drastic decrease at Isla D might be a result of a stress reaction of the benthic community. An increase in metabolic rates at intermediate suspended sediment concentrations in the water column is known for the filter feeding ascidians *Ascidia challengerii* and *Cnemidocarpa verrucosa*, both common in Potter Cove [Torre et al., 2012]. Further, *A. challengerii* showed a decrease in its metabolic rate at higher sediment concentrations [Torre et al., 2012]. In addition, reduced metabolic rates under strong sedimentation were also reported for *L. elliptica* [Philipp et al., 2011].

Surprisingly, the highest abundances and biomass of *L. elliptica* were found at the most disturbed location, which is in contrast to the patterns in the remaining macrofauna biomass and in the overall mineralization. However, at Isla D *L. elliptica* contributed the most to the macrofauna biomass (Figure 4.3). Thus, *L. elliptica* seems to be better adapted to the strong sedimentation at this location compared to other macrofauna species, which is a similar finding to that of Philipp et al [2011]. This indicates that, in terms of spatial competition, more individuals are able to inhabit this location. With a food supply similar to Faro, the Isla D *L. elliptica* population accumulates a high biomass, despite reduced metabolic rates and potentially frequent ice scouring injuries [Philipp et al., 2011]. The negative correlation of *L. elliptica* biomass with TOU can be a result of the reworking capacity by smaller *L. elliptica* found at Isla D. The resulting lower oxygen penetration depth probably leads to more anaerobic bacterial respiration and consequently a reduction of the total oxygen flux. Furthermore, the individual respiration of *L. elliptica* could decrease as well, due to impairment of ciliary activity by the silt film covering the gill surface [Stevens, 1987; Summers et al., 1996].

The limited number of investigated locations did not allow us to perform a broad scale test to verify whether glacial melt-related disturbances are the most influential factor shaping the small-scale spatial variability of biogeochemical fluxes in Potter Cove. Nonetheless, our study shows that glacial melt-related disturbances such as increased sediment accumulation and decreased light availability can locally impact the benthic community and the mineralization processes they mediate [Philipp et al., 2011; Lager et al., 2017; this study].

#### 4.5.2 Spatial variability of benthic biogeochemical fluxes at shallow coasts of the Western Antarctic Peninsula

The TOU measured in this study was of the same order of magnitude as TOU values found at Signy Island at 8–9 m depth in austral summer ( $20\text{--}90 \text{ mmol O}_2 \text{ m}^{-2} \text{ d}^{-1}$ ) [Nedwell et al., 1993] and Marian Cove at 30 m depth ( $12\text{--}36 \text{ mmol O}_2 \text{ m}^{-2} \text{ d}^{-1}$ ) [Shim et al., 2011]. However, the oxygen penetration depth was up to four times deeper than the reported 2–3 mm for the Signy Island [Nedwell et al., 1993]. This difference could also be related to temporal variability, since the inter-annual differences between benthic oxygen fluxes can be large, e.g.  $25 \text{ mmol O}_2 \text{ m}^{-2} \text{ d}^{-1}$  in February 1991 and  $60 \text{ mmol O}_2 \text{ m}^{-2} \text{ d}^{-1}$  in February 1992; even if the organic matter supply was similar [Nedwell et al., 1993]. However, the studies of Nedwell et al. [1993] and Shim et al. [2011] investigated the benthic oxygen flux at only one location. Our study provides a first insight into the small-scale spatial variability of benthic oxygen fluxes in shallow coastal Antarctic sediments. Within a radius of less than a kilometer, total and diffusive benthic oxygen fluxes can vary 2- to 3-fold, which is similar to seasonal variations [Nedwell et al., 1993]. This might be a result of the heterogeneous distribution of different habitats (Figure 4.4) in Potter Cove [Pasotti et al., 2015].

The RQ of Potter Cove's benthic community of less than 0.7 is unusually low. It would mean that much more oxygen is consumed than DIC released. This might be caused by less reliable DIC analysis compared to the oxygen analysis. Despite this, such low RQs were also reported in the temperate Boston Harbor region [Giblin et al., 1997] and for an Arctic fjord [Sørensen et al., 2015]. The low RQs in these studies are explained by high faunal abundances and low values of near-surface sulfide concentrations [Giblin et al.,

1997], which were also found in Potter Cove [Monien et al., 2014; Pasotti et al., 2015]. However, the low RQs were reported for the winter season [Sørensen et al., 2015], which is vice versa to our findings in Potter Cove.

Our nutrient fluxes were in a similar range as those measured in the neighboring Marian Cove at 30 m water depth [Shim et al., 2011], except for 3–4 times higher ammonium fluxes at Creek than those measured in Marian Cove [Shim et al., 2011]. This indicates that nutrient fluxes of Antarctic coastal sediments from 30 m and 8 m water depth and from December and February can be in the same range, except for increased ammonium fluxes at Creek in our study. Further, sulfate concentration in pore water profiles is constant in the first 10 cm (Figure S4.1) indicating the absence of sulfide in this sediment depth and a deep aerobic and suboxic sediment layer in Potter Cove. This is similar to findings of Monien et al. [2014] in Potter Cove.

#### 4.5.3 Benthic carbon demand in Potter Cove

Schloss et al. [1998] suggested that the water column production in Potter Cove would probably not be sufficient to nourish the benthic community. The total pelagic primary production between October 1991 and February 1992 ranged between 236–259 mg C m<sup>-2</sup> d<sup>-1</sup> (= 19.7–21.6 mmol C m<sup>-2</sup> d<sup>-1</sup>) [Schloss et al., 1998] and seems to remain constant over the period 1991–2009 [Schloss et al., 2012]. This is indeed lower than our total benthic carbon uptake at Faro and Creek, but it exceeded the carbon uptake at Isla D. This discrepancy might be partly related to interannual variability in the magnitude of the phytoplankton bloom, which depends on the timing of the sea ice break up. Furthermore, the calculations of Schloss et al. [1998] on pelagic primary production are based on measurements at two stations, located in the inner and outer Potter Cove, while our study resolves spatial variability only in the inner part at three locations. In any case, the pelagic primary production seems to be able to partly feed the benthic carbon demand. However, we assume that this only holds true close to the glacial front of Potter Cove. Other carbon sources such as microorganisms, macroalgae debris and microphytobenthos (MPB) may supply the benthic carbon demand in Potter Cove [Schloss et al., 1998].

A diverse and abundant MPB community is known in Potter Cove [Al-Handal and Wulff, 2008a] and large, brownish MPB mats were reported and documented by SCUBA divers for Faro, Creek and Isla D (Figure S4.2). Further, the relatively high values for Fuco indicate that diatoms constituted most of the biomass of these mats (Table S4.4) with the majority of live diatom species found in the sediment being benthic taxa [Al-Handal and Wulff, 2008a]. Unfortunately, no MPB production estimates exist for Potter Cove so far. Nevertheless, the TOU values presented in this study are net fluxes. As there was no difference in the TOU between transparent and black chambers (Table S4.1), the included MPB community seems also not able to cover the benthic carbon demand during our measurements. This might be the result of high turbidity in summer [Deregibus et al., 2016], limiting microphytobenthic production. Therefore, we assume that Potter Cove was a mainly net heterotrophic ecosystem during our campaign in austral summer. In other shallow Antarctic areas, MPB primary production can be highly variable on spatial scales and frequently exceeds the benthic carbon demand of Potter Cove [Dayton et al., 1986; Gilbert, 1991b; McMinn et al., 2010, 2012]. So possibly, owing to seasonal changes in the turbidity [Deregibus et al., 2016], MPB at Faro and Creek might be able to supply the benthic carbon demand in spring and autumn.

In coastal areas, the spatial variability of the benthic carbon demand is closely related to the benthic carbon supply by primary production [Glud, 2008]. The latter, however, is influenced by light in terms of turbidity [Schloss et al., 1998] and thus by glacial melt-related disturbances. Our findings suggest that with ongoing melting of many Antarctic glaciers [Paolo et al., 2015], vast shallow coastal areas will eventually face alterations in benthic mineralization, owing to the succession processes of assemblages of newly ice-free areas [Pasotti et al., 2015; Deregibus et al., 2016; Lagger et al., 2017; Seefeldt et al., 2017], changes to the benthic community structure [Philipp et al., 2011; Torre et al., 2012; Deregibus et al., 2016; Lagger et al., 2017; Seefeldt et al., 2017] and their metabolic adaptive response to sedimentation [Philipp et al., 2011; Torre et al., 2012]. Nevertheless, alterations of the benthic mineralization will ultimately depend on the pace of predicted climatic changes [Gutt et al., 2015] and the related intensity of the glacial melting processes developing in the affected areas.



## 4.6 Supporting information

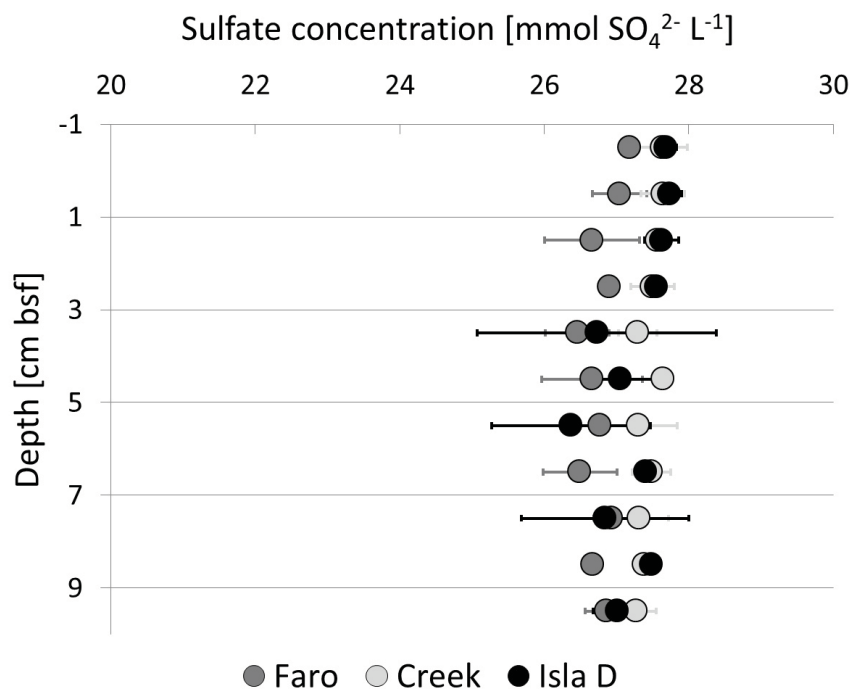


**Figure S4.1.** Sulfate concentration profiles from pore water extractions. The term “bsf” abbreviates “below seafloor”.

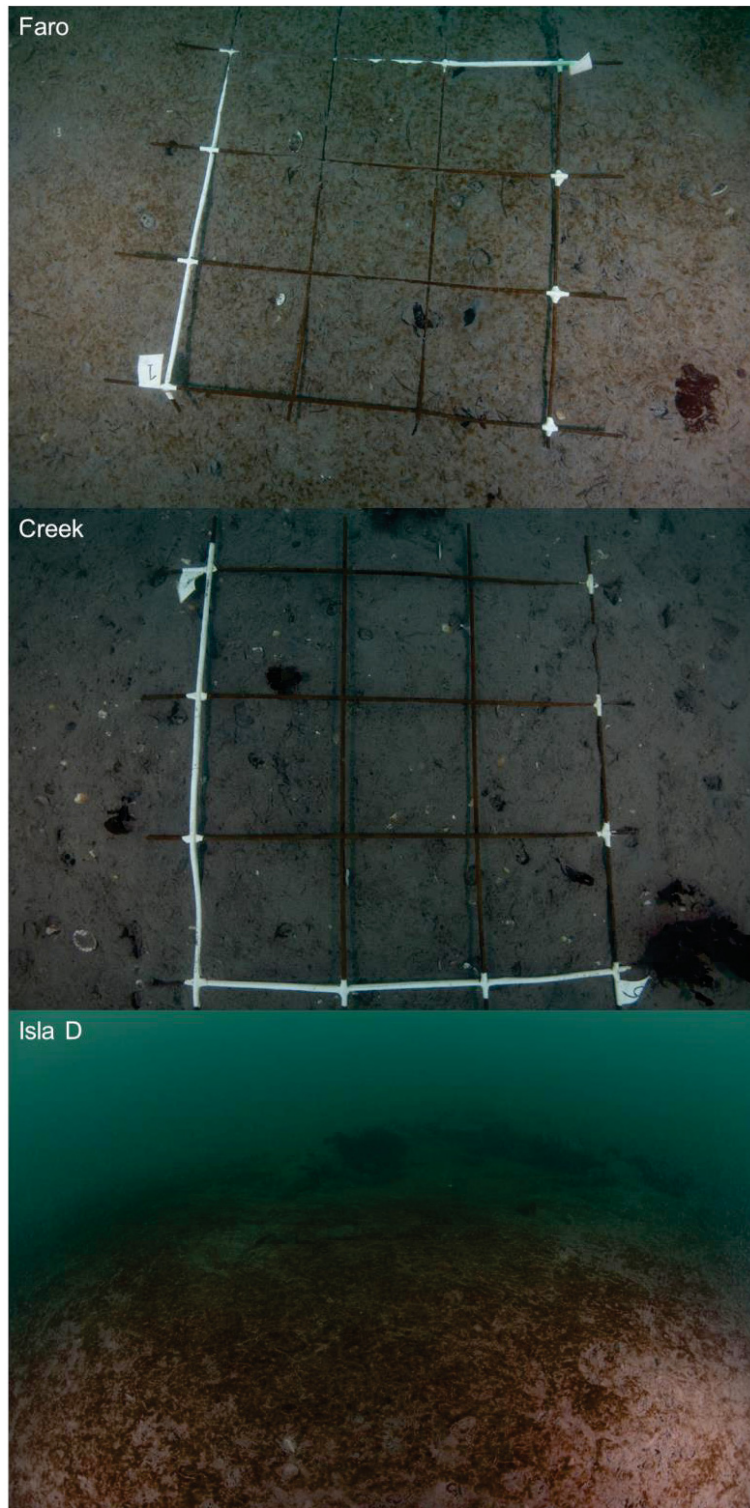


**Figure S4.2.** Photos of brownish microphytobenthic (MPB) mats at Faro, Creek and Isla D. The photos prove the occurrence of MPB in Potter Cove and underpin the patchiness and spatial variability of the MPB community.

**Table S4.1.**  $R_i$  and  $M_i$  according to Queirós et al. [2013] to calculate the bioturbation potential ( $BPC$ ) of the macrofauna community in Potter Cove.

Taxon	$R_i$	$M_i$
<i>Amphipoda</i>	2	3
<i>Bodotriidae</i>	2	3
<i>Cirratulidae</i>	2	2
<i>Gastropoda</i>	2	3
<i>Isopoda</i>	2	3
<i>Leuconidae</i>	2	3
<i>Maldanidae</i>	3	2
<i>Mysella sp.</i>	2	2
<i>Nannastacidae</i>	2	3
<i>Nephtyidae</i>	4	3
<i>Nucula sp.</i>	2	3
<i>Ophelina sp.</i>	4	3
<i>Orbinidae</i>	4	3
<i>Ostracoda</i>	2	3
<i>Pennatularia</i>	2	2
<i>Polynoidae</i>	4	3
<i>Priapulidae</i>	4	2
<i>Spionidae</i>	3	2
<i>Tanaidacea</i>	2	2
<i>Terebellidae</i>	3	1
<i>Thyasiridae</i>	3	2
<i>Travisia</i>	4	3
<i>Aequiyoldia</i>	2	3

**Table S4.2.** P-values of the Levene's test and t-test, comparing TOUs from black and transparent chamber incubations.

	Location	Levene's test	t-test
TOU	Faro	0.73	0.79
	Creek	0.65	0.92
	Isla D	0.36	0.21
Total DIC efflux	Faro	not enough observations	
	Creek	<0.05	not enough observations
	Isla D	<0.05	not enough observations
Total phosphate efflux	Faro	1.00	0.87
	Creek	0.60	0.78
	Isla D	<0.05	0.46
Total ammonium efflux	Faro	0.66	0.67
	Creek	0.36	0.95
	Isla D	0.61	0.74
Total nitrite efflux	Faro	0.22	0.83
	Creek	0.91	0.48
	Isla D	<0.05	0.48
Total nitrate uptake	Faro	0.48	0.79
	Creek	0.78	0.57
	Isla D	0.30	0.40

**Table S4.3.** Result of Pearson correlation.

	CPE	Phaeo	Fuco	Chl <i>a</i>	Silt fraction < 63 μm	Sand fraction > 63μm	Water content	Porosity	Median grain size	Sediment accumulation	Turbidity	SPM
CPE	1.000											
Phaeo	-0.048	1.000										
Fuco	0.989	-0.195	1.000									
Chl <i>a</i>	0.996	-0.129	0.997	1.000								
Silt fraction < 63 μm	-0.929	-0.323	-0.865	-0.896	1.000							
Sand fraction > 63μm	0.929	0.323	0.865	0.896	-1.000	1.000						
Water content	-0.916	-0.355	-0.847	-0.880	0.999	-0.999	1.000					
Porosity	-0.926	-0.330	-0.860	-0.892	0.999	-0.999	0.999	1.000				
Median grain size	0.865	0.457	0.782	0.821	-0.989	0.989	-0.993	-0.990	1.000			
Sediment accumulation	-0.644	-0.732	-0.524	-0.579	0.880	-0.880	0.896	0.884	-0.940	1.000		
Turbidity	-0.838	-0.502	-0.749	-0.791	0.980	-0.980	0.986	0.982	-0.998	0.956	1.000	
SPM	-0.993	-0.068	-0.965	-0.980	0.966	-0.966	0.956	0.964	-0.918	0.729	0.896	1.000





**Table S4.4.** Measured mean values  $\pm$  standard deviation of sediment, biogenic, benthic community and flux parameters. For the sediment parameters, the uppermost 5 cm were considered. The letters a, b, c indicate significant differences (ANOVA,  $p < 0.05$ ) of a parameter between the locations, while NS indicate no significant differences.

	Faro	Creek	Isla D	Sqrt-Transformation	Test	Post-hoc Test
Median grain size [ $\mu\text{m}$ ]	116 $\pm$ 27 <sup>a</sup>	120 $\pm$ 9 <sup>a</sup>	20 $\pm$ 30 <sup>b</sup>	-	ANOVA	Games-Howell
Portion of silt and mud [%]	39 $\pm$ 5 <sup>a</sup>	28 $\pm$ 4 <sup>b</sup>	83 $\pm$ 12 <sup>c</sup>	-	Kruskal-Wallis	Bonferroni
Portion of sand [%]	61 $\pm$ 5 <sup>a</sup>	72 $\pm$ 4 <sup>b</sup>	17 $\pm$ 12 <sup>c</sup>	-	Kruskal-Wallis	Bonferroni
Porosity	0.56 $\pm$ 0.08 <sup>a</sup>	0.51 $\pm$ 0.05 <sup>a</sup>	0.76 $\pm$ 0.12 <sup>b</sup>	-	ANOVA	Games-Howell
TC [ $\mu\text{g C mg}^{-1}$ sediment <sup>-1</sup> ]	7.3 $\pm$ 1.4 <sup>a</sup>	2.6 $\pm$ 0.5 <sup>b</sup>	5.5 $\pm$ 0.9 <sup>c</sup>	-	Kruskal-Wallis	Bonferroni
TIC [ $\mu\text{g C mg}^{-1}$ sediment <sup>-1</sup> ]	4.8 $\pm$ 0.8 <sup>a</sup>	0.6 $\pm$ 0.3 <sup>b</sup>	3.3 $\pm$ 0.4 <sup>c</sup>	-	Kruskal-Wallis	Bonferroni
TOC [ $\mu\text{g C}_{\text{org}} \text{mg}^{-1}$ sediment <sup>-1</sup> ]	2.3 $\pm$ 0.9 <sup>NS</sup>	2.0 $\pm$ 0.4 <sup>NS</sup>	2.2 $\pm$ 0.8 <sup>NS</sup>	-	Kruskal-Wallis	-
TN [ $\mu\text{g N mg}^{-1}$ sediment <sup>-1</sup> ]	0.51 $\pm$ 0.24 <sup>a</sup>	0.37 $\pm$ 0.08 <sup>b</sup>	0.45 $\pm$ 0.16 <sup>ab</sup>	-	Kruskal-Wallis	Bonferroni
TOC/TC [%]	32 $\pm$ 8 <sup>a</sup>	78 $\pm$ 11 <sup>b</sup>	39 $\pm$ 10 <sup>c</sup>	-	Kruskal-Wallis	Bonferroni
Chl <i>a</i> [ $\mu\text{g g}^{-1}$ sediment <sup>-1</sup> ]	6.3 $\pm$ 4.6 <sup>a</sup>	11.3 $\pm$ 9.3 <sup>b</sup>	3.0 $\pm$ 1.4 <sup>a</sup>	X	ANOVA	Games-Howell
Fuco [ $\mu\text{g g}^{-1}$ sediment <sup>-1</sup> ]	3.1 $\pm$ 2.6 <sup>a</sup>	6.6 $\pm$ 5.7 <sup>b</sup>	1.3 $\pm$ 0.9 <sup>a</sup>	X	ANOVA	Games-Howell
Phaeo [ $\mu\text{g g}^{-1}$ sediment <sup>-1</sup> ]	2.4 $\pm$ 0.8 <sup>a</sup>	1.8 $\pm$ 1.0 <sup>b</sup>	1.9 $\pm$ 0.7 <sup>b</sup>	-	Kruskal-Wallis	Bonferroni
Prokaryotic density [ $10^9$ cells $\text{cm}^{-3}$ sediment <sup>-1</sup> ]	6.1 $\pm$ 1.2 <sup>a</sup>	6.0 $\pm$ 2.1 <sup>a</sup>	4.2 $\pm$ 1.2 <sup>b</sup>	X	ANOVA	Tukey
Prokaryotic biomass [ $\text{mg C cm}^{-3}$ sediment <sup>-1</sup> ]	0.29 $\pm$ 0.44 <sup>NS</sup>	0.25 $\pm$ 0.21 <sup>NS</sup>	0.19 $\pm$ 0.12 <sup>NS</sup>	-	Kruskal-Wallis	-
Meiofauna density [Ind. $10 \text{ cm}^{-2}$ ]	2368 $\pm$ 471 <sup>a</sup>	1524 $\pm$ 231 <sup>a</sup>	3799 $\pm$ 719 <sup>b</sup>	-	ANOVA	Tukey
Meiofauna biomass [ $\mu\text{g C } 10 \text{ cm}^{-2}$ ]	990 $\pm$ 190 <sup>NS</sup>	980 $\pm$ 204 <sup>NS</sup>	1522 $\pm$ 240 <sup>NS</sup>	-	ANOVA	Tukey
Macrofauna density without <i>L. elliptica</i> [Ind. $\text{m}^{-2}$ ]	33574 $\pm$ 24902 <sup>ab</sup>	65612 $\pm$ 35948 <sup>a</sup>	3074 $\pm$ 815 <sup>b</sup>	-	ANOVA	Tukey
Macrofauna biomass without <i>L. elliptica</i> [ $\text{g C m}^{-2}$ ]	56 $\pm$ 39 <sup>NS</sup>	75 $\pm$ 26 <sup>NS</sup>	37 $\pm$ 32 <sup>NS</sup>	-	ANOVA	-
<i>L. elliptica</i> density [Ind. $\text{m}^{-2}$ ]	93 $\pm$ 26 <sup>a</sup>	157 $\pm$ 44 <sup>b</sup>	276 $\pm$ 50 <sup>c</sup>	-	ANOVA	Tukey
<i>L. elliptica</i> biomass [ $\text{g C m}^{-2}$ ]	36 $\pm$ 9 <sup>a</sup>	54 $\pm$ 16 <sup>b</sup>	81 $\pm$ 15 <sup>c</sup>	X	ANOVA	Tukey

**Table S4.4** (continued)

Individual <i>L. elliptica</i> biomass [g C ind. <sup>-1</sup> ]	0.39 ± 0.16 <sup>a</sup>	0.34 ± 0.14 <sup>b</sup>	0.29 ± 0.10 <sup>c</sup>	-	Kruskal-Wallis	Bonferroni
S Meiofauna	7.8 ± 1.7 <sup>NS</sup>	7 ± 1.4 <sup>NS</sup>	6.6 ± 0.5 <sup>NS</sup>	-	ANOVA	-
H <sup>+</sup> Meiofauna	0.12 ± 0.03 <sup>ab</sup>	0.44 ± 0.10 <sup>a</sup>	0.08 ± 0.01 <sup>b</sup>	-	Kruskal-Wallis	Bonferroni
S Macrofauna	13.3 ± 0.8 <sup>NS</sup>	14 ± 1.2 <sup>NS</sup>	13.5 ± 1.1 <sup>NS</sup>	-	ANOVA	-
H <sup>+</sup> Macrofauna	1.3 ± 0.2 <sup>ab</sup>	1.2 ± 0.2 <sup>a</sup>	1.7 ± 0.1 <sup>b</sup>	-	Kruskal-Wallis	Bonferroni
BPc	160205 ± 97300 <sup>NS</sup>	264121 ± 111263 <sup>NS</sup>	72678 ± 37278 <sup>NS</sup>	-	ANOVA	Tukey
Oxygen penetration depth [mm]	4.5-6	8	3.5-4	-	-	-
TOU [mmol O <sub>2</sub> m <sup>-2</sup> d <sup>-1</sup> ]	33 ± 11 <sup>ab</sup>	43 ± 9 <sup>a</sup>	18 ± 3 <sup>b</sup>	-	ANOVA	Tukey
Total DIC efflux [mmol DIC m <sup>-2</sup> d <sup>-1</sup> ]	18 ± 3 <sup>NS</sup>	23 ± 8 <sup>NS</sup>	12 ± 5 <sup>NS</sup>	-	ANOVA	-
Total phosphate efflux [μmol PO <sub>4</sub> m <sup>-2</sup> d <sup>-1</sup> ]	119 ± 106 <sup>ab</sup>	345 ± 187 <sup>a</sup>	64 ± 46 <sup>b</sup>	-	Kruskal-Wallis	Bonferroni
Total ammonium efflux [mmol NH <sub>4</sub> m <sup>-2</sup> d <sup>-1</sup> ]	4.2 ± 3 <sup>ab</sup>	7.8 ± 2.7 <sup>a</sup>	2.5 ± 0.7 <sup>b</sup>	X	ANOVA	Tukey
Total nitrite efflux [μmol NO <sub>2</sub> m <sup>-2</sup> d <sup>-1</sup> ]	62 ± 18 <sup>a</sup>	140 ± 33 <sup>b</sup>	36 ± 12 <sup>a</sup>	-	ANOVA	Tukey
Total nitrate uptake [mmol NO <sub>3</sub> m <sup>-2</sup> d <sup>-1</sup> ]	0.7 ± 0.2 <sup>a</sup>	1.2 ± 0.2 <sup>b</sup>	0.5 ± 0.3 <sup>a</sup>	-	ANOVA	Tukey
DOU [mmol O <sub>2</sub> m <sup>-2</sup> d <sup>-1</sup> ]	1.6 ± 0.4 <sup>NS</sup>	1.5 <sup>NS</sup>	2.4 ± 0.3 <sup>NS</sup>	-	ANOVA	-
Diffusive DIC efflux [mmol DIC m <sup>-2</sup> d <sup>-1</sup> ]	0.4 ± 0.2 <sup>NS</sup>	0.1 ± 0.08 <sup>NS</sup>	0.7 ± 0.3 <sup>NS</sup>	-	ANOVA	-
Diffusive phosphate efflux [μmol PO <sub>4</sub> m <sup>-2</sup> d <sup>-1</sup> ]	22.1 ± 7.6 <sup>a</sup>	6.6 ± 2.5 <sup>b</sup>	10.6 ± 6.6 <sup>ab</sup>	-	ANOVA	Tukey
Diffusive ammonium efflux [mmol NH <sub>4</sub> m <sup>-2</sup> d <sup>-1</sup> ]	388 ± 227 <sup>NS</sup>	80 ± 18 <sup>NS</sup>	204 ± 98 <sup>NS</sup>	-	ANOVA	-
Diffusive nitrite net efflux [μmol NO <sub>2</sub> m <sup>-2</sup> d <sup>-1</sup> ]	1.3 ± 0.9 <sup>NS</sup>	0.6 ± 0.8 <sup>NS</sup>	1.7 ± 0.8 <sup>NS</sup>	-	ANOVA	-
Diffusive nitrate uptake [mmol NO <sub>3</sub> m <sup>-2</sup> d <sup>-1</sup> ]	0.073 ± 0.02 <sup>a</sup>	0.041 ± 0.009 <sup>b</sup>	0.075 ± 0.012 <sup>a</sup>	-	ANOVA	Tukey



## Acknowledgments

We acknowledge the immense support of the staff and especially of the military divers at Carlini research Station, which was crucial for the success of the campaign. Further, we like to thank Volker Asendorf, Axel Nordhausen, Fabian Schramm, Volker Meyer and Paul Färber for preparing the benthic chambers and the microprofiler and support during deployment, Cäcilia Wiegand and Ines Schröder for the production of the Clark-type oxygen sensors, Martina Alisch for carbon and nitrogen analysis of the sediments, Bart Beuselinck for granulometric and pigment analyses, and Kerstin Jerosch and Frauke Scharf for interpolation of turbidity data (using ArcGIS).



## 5 Manuscript III: Deep-sea benthic communities and oxygen fluxes in the Arctic Fram Strait controlled by sea-ice cover and water depth

---

Ralf Hoffmann<sup>1</sup>, Ulrike Braeckman<sup>2,3</sup>, Christiane Hasemann<sup>1</sup>, Frank Wenzhöfer<sup>1,3</sup>

<sup>1</sup> Alfred Wegener Institut, Helmholtz Zentrum für Polar- und Meeresforschung, Am Handelshafen 12, 27570 Bremerhaven, Germany

<sup>2</sup> Ghent University, Marine Biology Research Group, Krijgslaan 281, S8, 9000 Gent, Belgium

<sup>3</sup> Max Planck Institute for Marine Microbiology, Celsiusstraße 1, 28359 Bremen, Germany

*Invited to second review round at the journal 'Biogeosciences'*

## 5.1 Abstract

Arctic Ocean surface sea-ice conditions are linked with the deep-sea benthic oxygen fluxes via a cascade of dependencies across ecosystem components like primary production, food supply, the activity of the benthic community, and their functions. Additionally, each of the ecosystem components is influenced by abiotic factors such as light availability, temperature, water depth or grain size structure. In this study, we investigated the coupling between surface sea-ice conditions and deep-sea benthic remineralization processes through a cascade of dependencies in Fram Strait. We measured sea-ice concentrations, a set of different sediment compounds, benthic community parameters, and oxygen fluxes at 12 stations in the HAUSGARTEN area of Fram Strait in water depth between 275–2500 m. Our investigations reveal that the Fram Strait is bisected in a permanently and highly sea-ice covered area and a seasonally and low sea-ice covered area, which both are long-lasting and stable. Within the Fram Strait ecosystem, sea-ice concentration and water depth are two independent abiotic factors, controlling the deep-sea benthos. Sea-ice concentration correlates well with the available food, water depth with the oxygen flux, and both abiotic factors correlate with the macrofauna biomass. However, in water depths >1500 m the influence of the surface sea-ice cover fades out and the water depth effect becomes more dominant. Remineralization across the Fram Strait is  $\sim 1 \text{ mmol C m}^{-2} \text{ d}^{-1}$ . Our data indicate that the portion of newly produced carbon that is remineralized by the benthos is  $\sim 2.6\%$  in the seasonally low sea-ice covered Fram Strait but can be  $>15\%$  in the permanently high sea-ice covered Fram Strait. Furthermore, by comparing a permanently sea-ice covered area with a seasonally sea-ice covered area, we discuss a potential scenario for the deep-sea benthic ecosystem in the future Arctic Ocean, in which an increased surface primary production can lead to increasing benthic remineralization in water depths <1500 m.

## 5.2 Introduction

Benthic deep-sea remineralization depends on primary production and is as such closely linked with primary production patterns, known as pelagic-benthic coupling [Graf, 1989]. The relationship, however, includes many and partly inter-dependent factors. Benthic deep-sea remineralization is positively correlated with surface primary production [Graf et al., 1995; Wenzhöfer and Glud, 2002], which is on its turn controlled by light availability and nutrient supply [Kirk, 2011; Cherkasheva et al., 2014; Fernández-Méndez et al., 2015]. Though, only the annual new production leaves the euphotic zone [Piatt et al., 1989] and can supply the benthos with organic carbon. Benthic remineralization is negatively correlated to water depth [Wenzhöfer and Glud, 2002], as it represents a loss of organic carbon by pelagic remineralization [Rullkötter, 2006; Belcher et al., 2016] and thereby a loss of benthic food. After organic carbon reached the seafloor, it is ingested and remineralized by the benthic community. Benthic community parameters, e.g. biomass, density, structure, and functions of different fauna size classes, are controlled by food supply (and thus by primary production) and water depth [Piepenburg et al., 1997; Flach et al., 2002; Smith et al., 2008] but also by sediment properties [Wheatcroft, 1992; Vanreusel et al., 1995]. Benthic remineralization rates also depend on benthic community biomass [Glud et al., 1994]. Furthermore, benthic remineralization is enhanced if the benthic community intensifies oxygenation of the seafloor [Glud, 2008] and thus also depends on the benthic community structure. Therefore, the ecosystem processes primary production, pelagic remineralization and benthic remineralization, as well as the components benthic community biomass, density, and structure are controlled by abiotic and biotic factors and additionally create a cascade of dependencies from the ocean's surface zone of primary production to and within the deep-sea benthos.

In the Arctic Ocean, pelagic-benthic coupling is assumed to be stronger relative to temperate and tropical waters [Ambrose and Renaud, 1995; Graf et al., 1995; Grebmeier and Barry, 2007]. A pan-arctic benthic remineralization model showed a better fit when water depth and benthic chlorophyll data (representing food supply from primary production) were taken into account, compared to a model using only water depth as controlling factor [Bourgeois et al., 2017]. This indicates that surface primary

production patterns and water depth are both relevant factors controlling benthic remineralization in the Arctic Ocean. The occurrence of sea ice in the Arctic Ocean, however, ultimately reduces the light availability and thereby suppresses primary production [Arrigo et al., 2008b; Bourgeois et al., 2017]. As a consequence, climate change-induced alterations in the sea-ice cover influence biogeochemical cycles in the Chukchi and Beaufort Sea [Harada, 2015]. Boetius and Damm [1998] also found a good correlation between sea-ice cover, benthic chlorophyll and benthic carbon remineralization in the Laptev Sea. However, the principal factor controlling microbial activity in their study was most likely the supply of labile organic matter such as chloroplastic pigment equivalents (CPE) [Thiel, 1978], proteins and dissolved free amino acids. Therefore, the strength of the relationship between sea-ice cover (controlling primary production) and benthic remineralization, even if assumed as direct and strong, needs to be considered more carefully [Renaud et al., 2008].

We were interested in the question, if we can link contrasting sea-ice conditions between the eastern and western Arctic Fram Strait [Soltwedel et al., 2005; Soltwedel et al., 2015; Spielhagen et al., 2015] with the deep-sea benthic oxygen fluxes over the cascade of dependencies. Benthic oxygen fluxes thereby represent benthic remineralization of carbon [Thamdrup and Canfield, 2000; Wenzhöfer and Glud, 2002; Smith et al., 2013]. Our study provides sea-ice concentrations, sediment properties, biogenic sediment compounds, benthic community parameters, and benthic oxygen fluxes from 12 stations across the Arctic Fram Strait in water depths from 275 m to 2500 m. We hypothesize that the contrasting sea-ice conditions in the eastern and western Fram Strait lead to differences between parameters representing the cascade of dependencies and result in contrasting benthic oxygen fluxes. Furthermore, our results allow us to estimate the portion of newly produced carbon that is remineralized by the benthic ecosystem. Furthermore, by comparing a permanently sea-ice covered area with a seasonally sea-ice covered area (western and eastern Fram Strait, respectively), we discuss a potential scenario for the deep-sea benthic ecosystem in the future Arctic Ocean.

## 5.3 Material and methods

### 5.3.1 Study area and field sampling

The Fram Strait is located in the northern Greenland Sea and forms a large passage (ca. 500 km wide) between northeast Greenland and the Svalbard archipelago (Figure 5.1). It provides the only exchange route of intermediate and deep water masses between the Arctic and the Atlantic Ocean [Soltwedel et al., 2005; Forest et al., 2010]. Two main currents influence the upper 300 m of Fram Strait waters [Manley, 1995]: the East Greenland Current (EGC) and the West Spitsbergen Current (WSC). The EGC is located in the western Fram Strait and transports cold, less saline and nutrient poor ( $1^{\circ}\text{C}$ ,  $\leq 34$ ) Arctic waters southward [Manley, 1995; Mauritzen et al., 2011; Graeve and Ludwichowski, 2017a, b]. In contrast, the WSC, located in the eastern Fram Strait, transports warmer, nutrient-rich Atlantic waters of higher salinity ( $>3^{\circ}\text{C}$ ,  $>34$ ) northward [Manley, 1995; Mauritzen et al., 2011; Graeve and Ludwichowski, 2017a, b]. About 22% of the WSC is recirculated as the Return Atlantic Current (RAC). The remaining current bifurcates into the Svalbard Branch (SB; 33%) and the Yermak Branch (YB; 45%) following the Svalbard islands or flowing along the north-west flanks of the Yermak Plateau, respectively [Schauer, 2004]. A high sea-ice cover is reported for the western Fram Strait and a low sea-ice cover for the eastern Fram Strait [Soltwedel et al., 2005; Soltwedel et al., 2015; Spielhagen et al., 2015]. The sea-ice cover is relatively stable within the Fram Strait, even in the summer [Comiso et al., 2008; Soltwedel et al., 2015, NOAA, 2018]. However, the sea-ice age becomes younger by 0.6 years per decade (2001–2012) [Krumpfen et al., 2016], which goes along with a decrease in the sea-ice thickness [Renner et al., 2014; Krumpfen et al., 2016]. The onset of the spring bloom usually starts in Mai [Cherkasheva et al., 2014].

Two sampling campaigns were carried out at the long-term ecology research observatory HAUSGARTEN [Soltwedel et al., 2005] in the Fram Strait with RV Polarstern, expedition “PS85” from 6/6–3/7/2014 and expedition “PS93.2” from 22/7–15/8/2015. Samples were taken at five stations at the East Greenland continental slope (EG area) and at seven stations at the West Spitsbergen continental slope (WS area) in water depths between 275–2500 m (Figure 5.1, Table 5.1). Thereby the stations in the

EG area (namely EG I, EG II, EG III, EG IV and EG V) and in the HG area (namely SV I, HG I, SV IV, HG II, HG III, HG IV, and N5) form a bathymetric transect with a similar bottom slope of  $\sim 11.2^\circ$ . The station EG IV includes two sites which are located  $< 2$  km from each other (Table 5.1) and the stations HG I, HG II, HG III, and HG IV were sampled during both sampling years, 2014 and 2015.

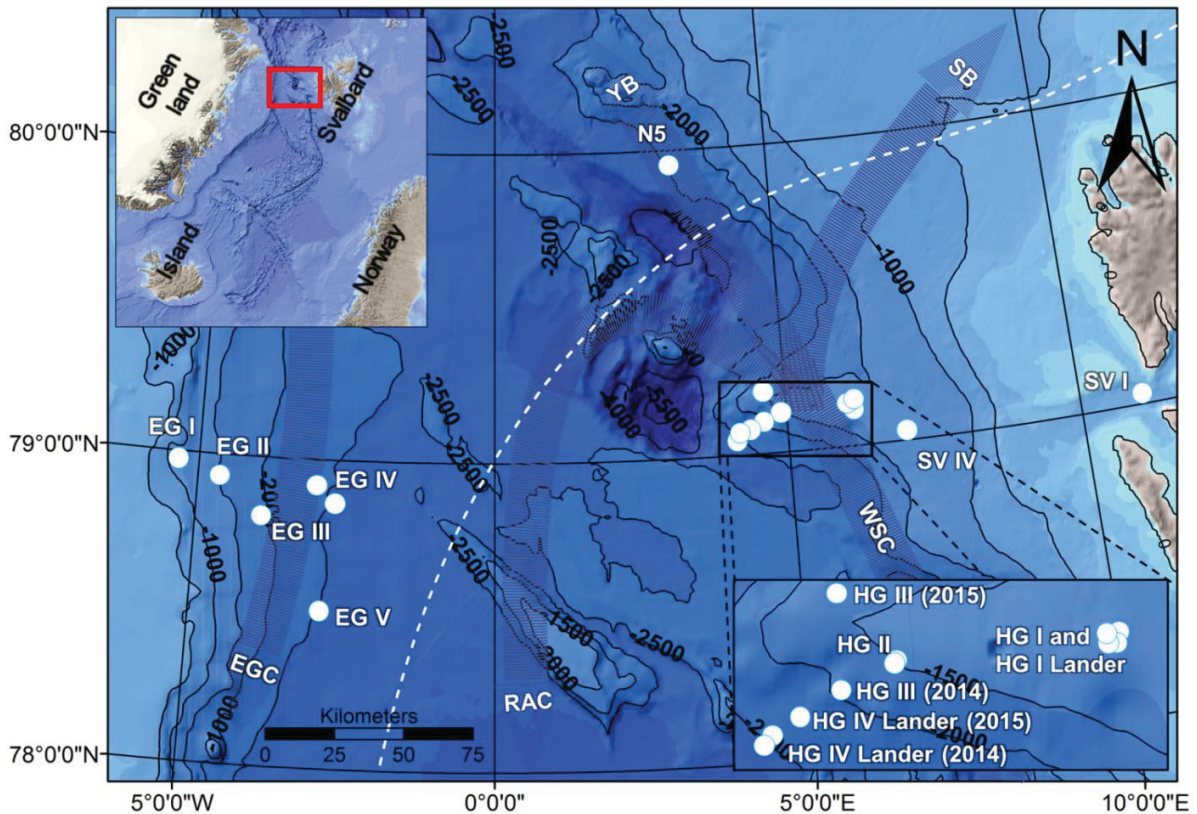


**Figure 5.1.** Location of the sampled stations in the Arctic Fram Strait. White dashed line = mean summer sea-ice extent in September (1981–2010, <http://nsidc.org>). Grey arrows = general current system. EGC = East Greenland Current, WSC = West Spitsbergen Current, SB = Svalbard branch, YB = Yermak branch, RAC = Return Atlantic current. White dots = stations with station names. More station-specific details are given in Table 5.1.

Sediment sampling was performed by using a multiple corer (MUC) with eight tubes and autonomous benthic lander systems [Reimers, 1987; Glud et al., 1994] equipped with three benthic chambers and a sediment profiler with oxygen sensors. A detailed list of the number of used samples per station for the determination of different parameters is given in Table S5.1.



**Table 5.1.** General station information regarding water depth, sampling date, location and station ID in the data archive Pangaea. Order of stations for each area follows the water depth gradient.

Area	Station name	Water depth [m]	Sampling date	Latitude [dd.ddd °N]	Longitude [d.ddd °E]	Pangaea Station ID
EG	EG I	1056.3	17/06/2014	78.973	-5.290	PS85/0436-1
	EG II	1499.7	18/06/2014	78.933	-4.650	PS85/0441-1
	EG III	1943.8	19/06/2014	78.803	-3.875	PS85/0445-1
	EG IV	2592	31/07/2015	78.862	-2.710	PS93/0058-12
		2518.5		78.914	-2.961	PS93/0058-17
EG V	2557.7	20/06/2014	78.505	-2.817	PS85/0454-3	
WS	SV I	275	06/08/2015	79.028	11.087	PS93/0066-2
	HG I	1244.2	24/06/2014	79.133	6.1065	PS85/0470-3
		1287.7	10/08/2015	79.138	6.0835	PS93/0080-9
	HG I Lander	1257.6	26/06/2014	79.142	6.124	PS85/0476-1
		1282.2	10/08/2015	79.134	6.092	PS93/0080-8
	SV IV	1304	08/08/2015	79.029	6.999	PS93/0074-3
	HG II	1492.3	24/06/2014	79.132	4.906	PS85/0469-2
		1550.2	09/08/2015	79.130	4.902	PS93/0078-2
	HG III	1904.8	24/06/2014	79.106	4.585	PS85/0468-1
		1916	08/08/2015	79.208	4.600	PS93/0077-2
	HG IV	2402.6	22/06/2014	79.065	4.183	PS85/0460-4
		2465.2	27/07/2015	79.065	4.179	PS93/0050-19
	HG IV Lander	2492.6	24/06/2014	79.052	4.138	PS85/0466-1
2277.5		27/07/2015	79.083	4.337	PS93/0050-18	
N5	2548.2	03/08/2015	79.938	3.193	PS93/0060-10	

### 5.3.2 Sea ice data

Daily sea ice concentrations for each of the analyzed stations were obtained from the Center for Satellite Exploitation and Research (CERSAT) at the Institut Français de Recherche pour l'Exploitation de la Mer (IFREMER), France [Ezraty et al., 2007] and were previously published [Krumpen, 2017], except for station EG V. Sea-ice concentration was calculated based on the ARTIST Sea Ice algorithm developed at the University of Bremen, Germany [Spreen et al., 2008]. The data used in this study cover the period from 01/09/2001 till 31/08/2015 (long-term data) with a 12.5 x 12.5 km<sup>2</sup> spatial resolution around the station. Mismeasurements, which were <0.5% of the long-term data and were indicated by an algorithm output value of “128”, were omitted. Three subsets for short-term examinations were extracted: the period a year before sampling, the period since the first of May till sampling, and one month before sampling. The period a year before sampling was 01/07/2013–30/06/2014 for stations sampled in 2014 and 01/08/2014–31/07/2015 for stations sampled in 2015. From each dataset (long-term and short-term) the sea-ice cover and the percentage of days with sea-ice cover were extracted.

### 5.3.3 Sediment compounds and properties

Various biogenic sediment compounds including grain size, water content, chlorophyll *a* (Chl *a*) and phaeopigment concentrations (Phaeo), portion of total organic carbon (TOC), phospholipids concentrations, protein concentrations, portion of organic matter, and the bacterial enzymatic turnover rate (FDA) as bacterial activity proxy were determined from the sediments sampled by the MUC and chambers of the autonomous benthic lander system. Generally, three pseudo-replicates from each MUC (sampled from different sediment cores, inner MUC tube diameter = 9.5 cm) were taken. Sediment samples of the 0–5 cm layer were taken by means of syringes with cut-off ends (1.17 / 3.14 cm<sup>2</sup> cross-sectional area). Samples for FDA, Chl *a*, and Phaeo were immediately analyzed on board. All other samples were shock frozen at -80°C and stored at -20°C until they were analyzed at the home laboratory. Sediment samples, taken by the benthic chambers of the autonomous lander system, were treated similarly.

The grain size partitions were determined with a Malvern Mastersizer 2000G, hydro version 5.40. The Mastersizer utilizes a laser diffraction method and has a measuring range of 0.02–2000 µm. The water content of the sediment was determined by the difference in weight of the sediment before and after drying at 105°C. The bioavailability of phytodetritus at the seafloor was assessed by analyzing sediment-bound Chl *a* and Phaeopigments. Chloroplastic pigments were extracted in 90% acetone and measured with a TURNER fluorometer [Shuman and Lorenzen, 1975]. The bulk of pigments (Chl *a* plus Phaeo) are termed chloroplastic pigment equivalents (CPE) after Thiel [1978]. Additionally, the ratios of Chl *a* to Phaeo, as an indicator of the relative age of the food, and the Chl *a* to CPE (%Chl *a*), a quality indicator of the labile organic matter, was calculated. The percentage of the TOC was measured by combustion using an ELTRA CS2000 with infrared cells. To indicate the quantity of cell wall material, phospholipids were measured following Findlay et al. [1989] with modifications after Boetius and Lochte [1994]. Particulate proteins, defined as  $\gamma$ -globulin equivalents [Greiser and Faubel, 1988], were measured to differentiate between living organisms and detrital organic matter in the sediments. Hereafter, particulate proteins will be referred to only as proteins. The organic matter was determined as ash-free dry weight after combustion (2 h, 500°C). Bacterial enzymatic turnover rates were calculated using the fluorogenic

substrate fluorescein-di-acetate (FDA) as an indicator of the potential hydrolytic activity of bacteria [Köster et al., 1991].

#### 5.3.4 Benthic community parameters

For the bacterial density determination, sediment subsamples were taken with modified syringes (1.17 cm<sup>2</sup> cross-sectional area) from MUC recovered sediment cores after oxygen flux measurements were performed and from benthic chambers. The first centimeter of each sample, generally holding the highest bacterial density [Quéric et al., 2004], was stored in a 2% filtered formalin solution at 4°C. The acridine orange direct count (AODC) method [Hobbie et al., 1977] was used to stain bacteria in the subsamples and subsequently bacteria were counted with a microscope (Axioskop 50, Zeiss) under UV-light (CQ-HXP-120, LEj, Germany).

For the determination of the meiofauna density and identification of meiofauna taxa, sediment subsamples were taken with modified syringes (3.14 cm<sup>2</sup> cross-sectional area) from MUC recovered sediment cores after oxygen flux measurements were performed and from benthic chambers. The first centimeter of each sample, usually holding the highest meiofauna density [Górska et al., 2014], was stored in borax buffered 4% formaldehyde solution at 4°C. The samples were sieved over a 1000 µm and 32 µm mesh. Both fractions were centrifuged three times in a colloidal silica solution (Ludox TM-50) with a density of 1.18 g cm<sup>-3</sup> and stained with Rose Bengal [Heip et al., 1985]. Afterwards, the taxa were identified and counted at order level. Foraminifera were not considered, as the extraction efficiency of Ludox for different groups of foraminifera is insufficient for a quantitative assessment of the group. Therefore, only metazoan meiofauna is recorded and hereinafter the use of the term meiofauna refers only to metazoan meiofauna organisms.

After taking subsamples for bacteria and meiofauna densities, the remaining sediment from MUC recovered sediment cores and from the benthic chambers was used for macrofauna taxonomical identification, and density and biomass determination. For these macrofauna analyzes, only the 0–5 cm layer from MUC sediment cores and the entire remaining sediment from the benthic chambers was used, sieved over a 500 µm mesh and stored in borax buffered 4% formaldehyde and stained with Rose

Bengal [Heip et al., 1985]. Afterward, macrofauna taxa were identified to the highest taxonomic level (at least class level), counted and weighted (blotted wet weight).

From the macrofauna density ( $A_i$ ) and biomass ( $B_i$ ), together with a mobility score ( $M_i$ ) and sediment reworking score ( $R_i$ ) of each taxon, the community bioturbation potential (BP<sub>c</sub>) was calculated following Queirós et al. [2013]:

$$BP_c = \sum_{i=1}^n \sqrt{B_i/A_i} \times A_i \times M_i \times R_i$$

in which  $i$  displays the specific taxon in the sample. This index represents the bioturbation potential of the benthic macrofauna community.

### 5.3.5 Oxygen and bromide fluxes

Immediately after the retrieval of sediment cores by the MUC, a part of the overlying water was removed and stored separately. At least 10 cm overlying water remained in the cores. The sediment of each core was carefully pushed upwards without disturbing the surface sediment layer until the sediment-water interface (SWI) was at a distance of around 10 cm from the upper edge of the core. A magnetic stirrer was added to the overlying water. In this position, the sediment cores were stored in a water bath at *in situ* temperature (-0.75°C) until the start of the oxygen flux measurements.

For the determination of the *ex situ* diffusive oxygen uptake (DOU) at least two oxygen microprofiles per sediment core were measured simultaneously within 2 h after sampling with a vertical resolution of 100 µm. The profiling was performed by oxygen optical microsensors (OXR50, Pyroscience, Aachen, Germany) with a tip size of 50 µm in diameter, a response time of <2 s and an accuracy of ±0.02%, calibrated with a two-point calibration using air saturated and anoxic waters (by adding sodium dithionite). The overlying water in the MUC cores was magnetically stirred and the water surface was gently streamed with a soft air stream during the profiling. The maximum penetration depth of the sensors during *ex situ* profiling was 42 mm. For *in situ* DOU determination autonomous landers were used [Reimers, 1987; Glud et al., 1994; Glud, 2008]. The profiling unit was equipped with electrochemical oxygen microsensors (custom made after Revsbech [1989]) and calibrated with a two-point calibration. As the first calibration

point, the bottom water oxygen concentration (water sample were taken by Niskin bottle), estimated by Winkler titration [Winkler, 1888], was used. As the second calibration point, the sensor signal in the anoxic zone of the sediment (when reached) or the sensor signal in an anoxic solution of sodium dithionite was used. The measurements started three hours after the deployment of the autonomous lander, allowing resuspended sediment to settle on beforehand. Profiling was performed with a depth resolution of 100  $\mu\text{m}$ . The maximum penetration depth of the sensors during *in situ* profiling was 180 mm. Running average smoothed oxygen profiles from *ex situ* and *in situ* approaches were used to calculate the DOU rates across the SWI using Fick's first law:

$$DOU = -D_s \times \left[ \frac{\delta O_2}{\delta z} \right]_{z=0}$$

in which  $D_s$  is the molecular diffusion coefficient of oxygen in sediments at *in situ* temperature and salinity, and  $\left[ \frac{\delta O_2}{\delta z} \right]_{z=0}$  is the oxygen gradient at the SWI calculated by linear regression from the first alteration in the oxygen concentration profile across a maximum depth of 1 mm.  $D_s$  was calculated following Schulz [2006] as  $D/\theta^2$ , with  $D$  as the molecular diffusion coefficient of oxygen in water after Li and Gregory [1974], and  $\theta^2$  as  $1-\ln(\phi^2)$  [Boudreau, 1997]. The sediment porosity  $\phi$  was calculated following the equation of Burdige [2006]:

$$\phi = \frac{m_w/\rho_w}{m_w/\rho_w + (m_d - (S \times m_w))/\rho_s}$$

In this equation,  $m_w$  is the mass of evaporated water,  $\rho_w$  is the density of the evaporated water,  $m_d$  is the mass of dried sediment plus salt,  $S$  is the salinity of the overlying water and  $\rho_s$  is the density of deep-sea sediment ( $2.66 \text{ g cm}^{-3}$ , after Burdige, [2006]). To calculate  $m_w$ ,  $\rho_w$ , and  $m_d$ , the weight loss of wet sediment samples was measured by weighing wet samples, drying them overnight at 70 °C, weigh them again, dry the sample for 1 h at 70 °C and weigh them a second time. This procedure was repeated until the weights of the two dried samples differ not more than 0.05%. Over all samples,  $4.5 \pm 1.9\%$  of the sediment mass was attributed to salt. Non-local mixing was observed in some microprofiles and therefore the reported DOUs for those cases are underestimations. However, only at eight out of 81 *ex situ* obtained oxygen microprofiles

at various stations and at one out of 34 *in situ* obtained oxygen microprofiles signs of non-local mixing were observed.

For *ex situ* total oxygen uptake (TOU) measurements, sediment cores were used after oxygen microprofiling (see upper paragraph in this section). The sediment cores were closed airtight with no air bubbles in the overlying water. The distance between the SWI and the edge of the lid was measured for volume calculations of the overlying water. An optical oxygen microsensors (Pyroscience, Aachen, Germany) with a tip size diameter of 50  $\mu\text{m}$  was installed in the lid, allowing a continuous measurement of the oxygen concentration in the overlying water. The sediment cores were incubated in darkness for >40 h and the overlying water was kept homogenized by rotating magnets over that period. For *in situ* TOU measurements, benthic chambers (K/MT 110, KUM, Kiel, Germany) with an inner dimension of 20x20 cm were used. These chambers were pushed into the sediment and thereby enclosed a sediment volume of approximately 8 L and an overlying water volume of approximately 2–3 L. The oxygen concentration was measured in the overlying water continuously with an Aanderaa optode (4330, Aanderaa Instruments, Norway, two-point calibrated as described in the upper section) over an incubation period of 20–48 h. During the measurement, the overlying water was kept homogenized by a stirring cross at the inner top of the chamber. TOU from both *ex situ* sediment core and *in situ* benthic chamber incubations were calculated using:

$$TOU = \frac{\delta O_2 \times V}{\delta t \times A}$$

in which  $\delta O_2$ ,  $\delta t$ ,  $V$  and  $A$  represent the difference in oxygen concentration, the difference in time, the volume of the overlying water and the enclosed surface area, respectively.

The oxygen fluxes were converted to carbon equivalents (C-DOU and C-TOU) by applying the Redfield ratio (C : O = 106:138; Redfield [1934]) in order to compare them to the carbon fixed by primary production. Modifications, as suggested by Takahashi et al. [1985] and Anderson and Sarmiento [1994], would result only in minor changes of <10% in the benthic carbon flux.

To assess the exchange of solutes across the SWI, which results from molecular diffusion, physical advection, and faunal ventilation activities, sodium bromide (NaBr)

was added to the removed overlying water of the sediment cores to create a NaBr-solution of similar density as seawater ( $1028 \text{ g L}^{-1}$ ). The NaBr-solution was added to the sediment cores before the TOU incubation started. Three subsamples of water were taken during the incubation at three different times ( $t_0$ ,  $t_1$ ,  $t_2$ ) and stored at  $4^\circ\text{C}$ . Removed water volume of the subsampling at  $t_1$  was replaced with the NaBr–seawater solution. The bromide concentrations were measured using ion chromatography. The dilution of the  $t_2$ -sample, due to the sampling procedure, was corrected by the known bromide concentration in the removed and the added water. The bromide exchange is represented by the bromide flux, calculated using:

$$\text{Bromide flux} = \left( \frac{\delta \text{Bromide concentration} \times V}{\delta t \times A} \right)$$

in which  $\delta \text{Bromide concentration}$ ,  $\delta t$ ,  $V$  and  $A$  represent the difference in bromide concentration, the difference in time, the volume of the overlying water and the enclosed surface area, respectively.

### 5.3.6 Data analyzes

The analyzed data were obtained during two consecutive years (Table 5.1). To test whether there is a significant offset between sampling years, a principal component analysis (PCA) was performed on standardized ( $x$  to zero mean and unit variance) abiotic parameters (year, water depth, sea ice cover, percentage of days with sea ice cover, the portion of grain size  $>63 \mu\text{m}$ , median grain size) and all sediment compounds and property parameters from the 0–1cm sediment horizon, as it was the most complete dataset. Additionally, a non-parametric Wilcoxon signed rank sum test was performed on station specific mean values of both years on water content, TOC, organic matter, Chl *a*, Phaeo, protein, phospholipids, FDA, DOU and TOU following Cathalot et al. [2015]. Both tests were performed only on data of stations that were sampled in both 2014 and 2015.

To reveal significant differences in measured parameters between the EG and the WS area, Students t-tests were performed. If t-test assumption of Gaussian distribution of the data (tested with a Shapiro-Wilk test) was not met, a non-parametric Wilcoxon signed rank sum test was performed. In case of heteroscedasticity (tested with a

Levene's test) a Welch two sample t-test was carried out. The values from station SV I were excluded from the tests, due to its exceptional low water depth.

To identify the most important parameters influencing the benthic Fram Strait ecosystem, a second PCA was performed in the scaling II mode on standardized (x to zero mean and unit variance) *ex situ* mean values of abiotic parameters (water depth, short-term sea-ice cover (year before sampling), the portion of grain size >63  $\mu\text{m}$ , water content), biogenic compound parameters (Chl *a*, TOC, organic matter), oxygen fluxes (DOU, TOU), the benthic community (bacterial density, macrofauna biomass), and the BPc. All other parameters were excluded from the PCA as they correlated strongly (correlation >0.74, Pearson correlation, Table S5.2) with one of the mentioned parameters used for the PCA. This procedure results in a more resilient outcome of the PCA. Owing to its exceptional low water depth, the values from station SV I were also excluded from the PCA. For further insights and descriptions of the usage and interpretation of a PCA, the reader is referred to Buttigieg and Ramette [2014].

Water depth and sea ice have a profound impact on benthic oxygen fluxes [Wenzhöfer and Glud, 2002; Harada, 2015]. To investigate the influence of water depth and sea ice in our data, the stations were merged into two sea-ice cover categories. First, a "high sea-ice concentration" area (HSC), which include stations with a short-term (a year before sampling) mean sea-ice concentrations of  $\geq 30\%$ . Second, a "low sea-ice concentration" area (LSC), which include stations with a short-term (a year before sampling) mean sea-ice concentrations of  $<30\%$ . Regression analysis was used to test the water depth dependence of sediment compounds and property parameters, the benthic community parameters, the oxygen fluxes, and parameters of the macrofauna mediated environmental functions within the HSC and LSC categories. If the residuals over the slope did not follow the Gaussian distribution (tested with a Shapiro-Wilk test), values were transformed, either by square root or logarithmic transformation. Individual values that failed due to technical failure or mismeasurements were removed before statistical analyzes. For all above mentioned statistical treatments, R Statistical Software (version 3.4.0) was used.

Analyzes of the multivariate meio- and macrofauna community structure were based on square root transformed density and biomass data of sediment core replicates. Non–



metric multidimensional scaling (MDS, [Kruskal, 1964]) and hierarchical cluster analysis with group average clustering were used to present the multivariate similarities between samples based on Bray–Curtis similarity. Significant multivariate differences between pre-defined group structures within the meio- and macrofaunal data were tested by the ANOSIM procedure (ANalysis Of SIMilarity) based on Clarke’s R statistic [Clarke and Warwick, 1994] with 9999 permutations. The SIMPER (SIMilarity PERcentage) routine was applied to determine the contribution of certain meio- and macrofauna taxa towards the discrimination between sea-ice cover categories and water depth categories. Differences ( $p < 0.05$ ) between HSC, LSC and water depth regarding macrofauna density and macrofauna biomass were examined using a two-way crossed PERMANOVA (PERMANOVA+ for PRIMER) [Anderson, 2005; Anderson et al., 2007] analysis with “site” (levels “HSC” and “LSC”) or “water depth” (levels: 1000, 1500, 2000, 2500 m) as fixed factors. The significance level was set at 0.05. Significant main PERMANOVA tests were followed by pairwise PERMANOVA tests. Permutational P-values (PPERM) were interpreted when the number of unique permutations was  $>100$ ; alternatively, Monte Carlo p-values (PMC) were considered. Bray-Curtis similarity was used to construct resemblance matrices. Data were standardized and fourth-root transformed (to down-weight the importance of the most dominant taxa) prior to the construction of resemblance matrices. The station SV I and the *in situ* stations HG I Lander and HG IV Lander were excluded from these test, owing to its shallow location (SV I) and different sampling device (benthic chambers instead of MUC). All analyzes of multivariate community structure were performed using the routines implemented in PRIMER vers. 6.1.15 [Clarke and Gorley, 2006; Anderson et al., 2007]. Results are expressed as means  $\pm$  standard deviation.

## 5.4 Results

### 5.4.1 Short- and long-term sea ice concentration comparison between the EG and WS area

Short-term and long-term data of the mean sea-ice concentrations and the percentage of sea-ice covered days were in a similar range (Table 5.2). Both parameters decreased from west to east with a sharp drop between N5 and HG IV in each short and in the long-term dataset (Table 5.2). Therefore, the categorization into a high sea-ice covered area (HSC) and a low sea-ice covered area (LSC) was introduced. The HSC includes all East Greenland stations (EG I–V) and the most northern West Spitzbergen station N5, while the LSC includes the remaining West Spitzbergen stations (HG I–IV, SV I, and SV IV).

As expected, the east Greenland stations showed the highest sea ice concentration due to the influence of the East Greenland current. The short-term sea-ice concentration in the EG area one year before sampling was highest at EG I with  $82 \pm 20\%$  ( $n=364$ ) and lowest at EG V with  $56 \pm 34\%$  ( $n=364$ ). In the WS area, sea-ice concentration was highest at N5 with  $40 \pm 31\%$  ( $n=365$ ) and lowest at SV IV with  $0.1 \pm 2\%$  ( $n=365$ ). The percentage of days, which showed sea-ice cover, during the short-term period in the EG area was highest at EG I, EG II and EG III (each with 100%) and lowest at EG V (93%). In the WS area the percentage of days, which showed sea-ice cover, during the short-term period was highest at N5 (82%) and lowest at SV IV ( $>0.1\%$ , Table 5.2). This pattern also occurred in the other short-term datasets and in the long-term dataset. The latter indicated that this pattern was stable across the Fram Strait the last 15 years (Figure 5.2, Table S5.3).

**Table 5.2.** Sea-ice cover (%) and % of days with sea-ice cover on different time scales across the Fram Strait. The values are given in mean values  $\pm$  standard deviation and the number of samples is given in brackets. Sea-ice data a year before sampling are mean values for the period 01/07/2013–30/06/2014 for stations only sampled in 2014 and 01/08/2014–31/07/2015 for stations only sampled in 2015. For stations sampled in both years, data of both periods were combined. The date of sampling is given in Table 5.1.

Month before sampling		Since 01.05. till sampling		Year before sampling		2001–2015		Station name
Days with sea-ice coverage within a year before sampling <small>(n)</small>	Sea-ice coverage [%] <small>(n)</small>	Days with sea-ice coverage within a year before sampling <small>(n)</small>	Sea-ice coverage [%] <small>(n)</small>	Days with sea-ice coverage within a year before sampling <small>(n)</small>	Sea-ice coverage [%] <small>(n)</small>	Days with sea-ice coverage within a year before sampling <small>(n)</small>	Sea-ice coverage [%] <small>(n)</small>	Para-meter
100	76 $\pm$ 16 (31)	100	79 $\pm$ 15 (48)	100	82 $\pm$ 20 (364)	97	80 $\pm$ 24 (5101)	EG I
100	73 $\pm$ 17 (31)	100	77 $\pm$ 16 (49)	100	80 $\pm$ 21 (364)	97	79 $\pm$ 24 (5101)	EG II
100	84 $\pm$ 10 (31)	100	81 $\pm$ 13 (50)	100	75 $\pm$ 27 (364)	95	74 $\pm$ 26 (5102)	EG III
100	57 $\pm$ 22 (31)	99	56 $\pm$ 24 (90)	98	72 $\pm$ 24 (365)	92	64 $\pm$ 31 (5102)	EG IV
100	74 $\pm$ 19 (31)	100	67 $\pm$ 22 (51)	93	56 $\pm$ 34 (364)	84	47 $\pm$ 33 (5102)	EG V
7	1 $\pm$ 4 (30)	10	1 $\pm$ 4 (96)	6	1 $\pm$ 5 (365)	15	5 $\pm$ 16 (5102)	SV I
28	9 $\pm$ 11 (31)	18	5 $\pm$ 9 (77)	4	1 $\pm$ 7 (729)	4	1 $\pm$ 6 (5101)	HG I
24	8 $\pm$ 11 (31)	17	15 $\pm$ 9 (78)	4	1 $\pm$ 7 (729)	4	1 $\pm$ 6 (5101)	HG I Lander
0	0 (30)	0	0 (98)	0	0.1 $\pm$ 2 (365)	2	0 $\pm$ 4 (5101)	SV IV
41	16 $\pm$ 12 (31)	32	10 $\pm$ 12 (77)	13	4 $\pm$ 12 (729)	8	2 $\pm$ 3 (5101)	HG II
41	15 $\pm$ 12 (31)	34	10 $\pm$ 12 (77)	16	5 $\pm$ 14 (729)	11	4 $\pm$ 13 (5102)	HG III
52	22 $\pm$ 17 (31)	45	19 $\pm$ 15 (71)	25	10 $\pm$ 21 (729)	18	7 $\pm$ 18 (5102)	HG IV
52	23 $\pm$ 18 (31)	45	19 $\pm$ 16 (71)	24	9 $\pm$ 19 (729)	17	6 $\pm$ 17 (5102)	HG IV Lander
74	25 $\pm$ 21 (31)	89	35 $\pm$ 23 (94)	82	40 $\pm$ 31 (365)	66	32 $\pm$ 33 (5102)	N5

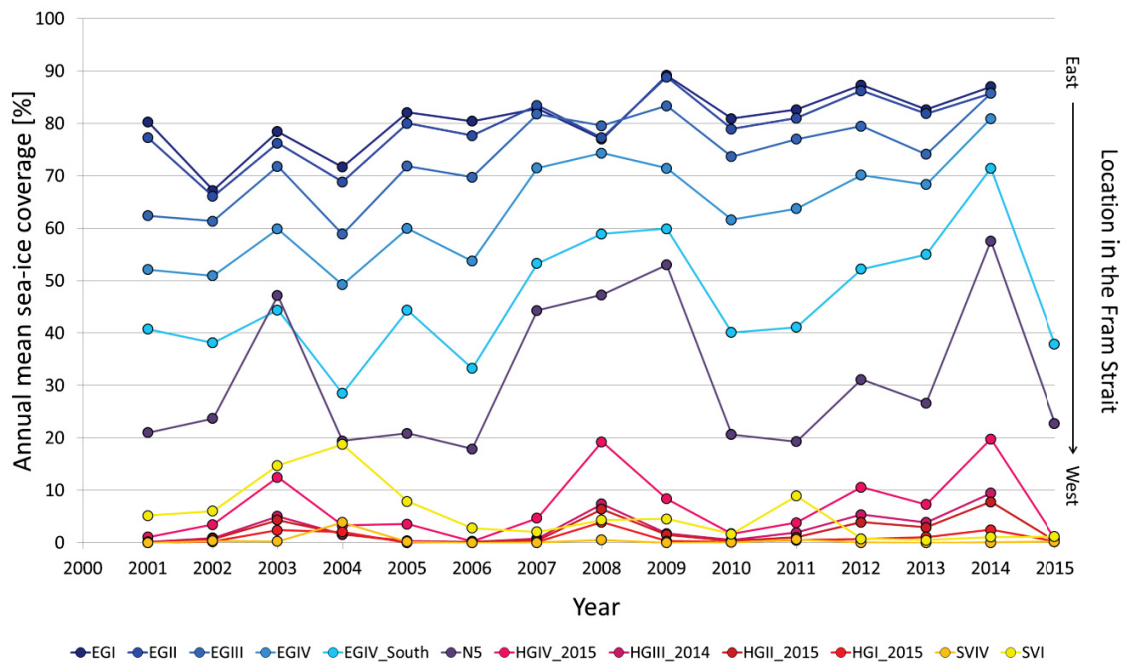


**Figure 5.2.** Annual mean sea-ice concentrations from 2001 to 2015 of a subset of sampled stations. The sampling year at the HG stations is given, as HG stations were sampled in 2014 and 2015 and therefore, the given sampling year refers to the exact position from which the sea ice data were obtained.

#### 5.4.2 Sediment properties and benthic biogenic compounds in the EG and WS area

Sediment properties and biogenic compound values at the deeper stations (>1500 m) in the EG and WS area were in the same range. In contrast, shallow stations ( $\leq 1500$  m) of the WS area showed higher values compared to shallow stations of the EG area (Table 5.3). This led to a higher variability in the WS area for most of the determined parameters (Figure 5.3).

The median grain size in the EG area ranged between  $13 \pm 1 \mu\text{m}$  ( $n = 15$ ) at EG I and  $74 \pm 30 \mu\text{m}$  ( $n = 15$ ) at EG V and in the WS area between  $10 \pm 3 \mu\text{m}$  ( $n = 15$ ) at N5 and  $24 \pm 5 \mu\text{m}$  ( $n = 30$ ) at HG IV. The portion of sediment grain size  $>63 \mu\text{m}$  in the EG area ranged between  $4 \pm 2\%$  ( $n = 15$ ) at EG I and  $52 \pm 7\%$  ( $n = 15$ ) at EG V and in the WS area between  $11 \pm 6\%$  ( $n = 30$ ) at HG I and  $25 \pm 5\%$  ( $n = 30$ ) at HG IV. The water content in the EG area ranged between  $42 \pm 6\%$  ( $n = 15$ ) at EG V and  $51 \pm 7\%$  ( $n = 15$ ) at EG I and in the WS area it ranged between  $51 \pm 14\%$  ( $n = 15$ ) at SV I and  $66 \pm 5\%$  ( $n = 30$ ) at HG I.

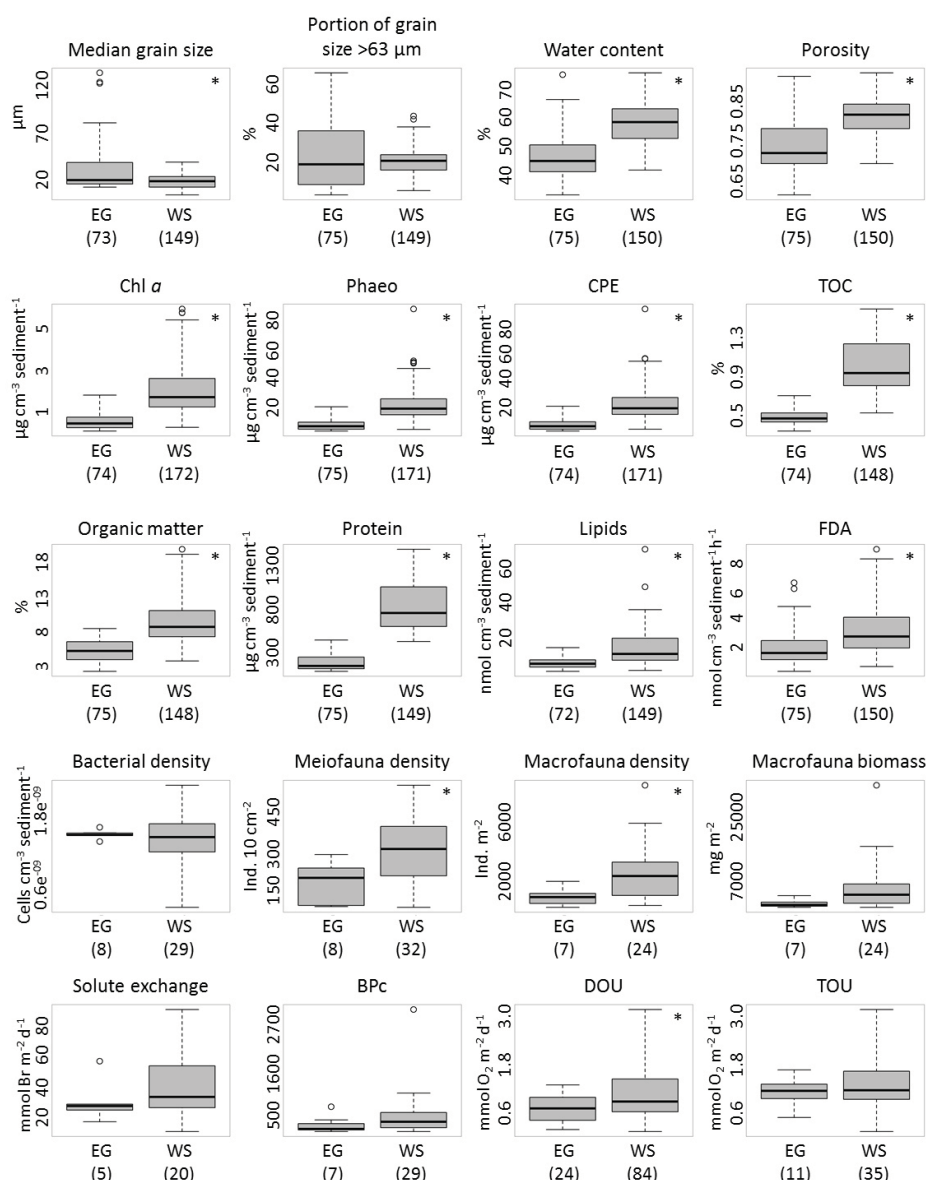


**Figure 5.3.** Boxplots of sediment properties, biogenic compound values (Chl *a* = chlorophyll *a*, Phaeo = phaeophytin, CPE = chloroplastical pigment equivalents, TOC = total organic carbon, FDA = bacterial enzymatic turnover rates calculated using the fluorogenic substrate fluorescein-di-acetate), benthic community data and function (BPc = bioturbation potential), and oxygen fluxes (DOU = diffusive oxygen flux, TOU = total oxygen flux), of the East Greenland (EG) and West Spitsbergen (WS) area. For a detailed description of which stations were included at which site, the reader is referred to section 5.3.1. The number of observations is given in brackets below the area. Parameters showing significant differences between areas are marked with an asterisk. For comparability, the WS site does not contain values from SV I station.

The porosity in the EG area ranged between  $0.77 \pm 0.06$  ( $n = 15$ ) at EG I and  $0.69 \pm 0.06\%$  ( $n = 15$ ) at EG V and in the WS area it ranged between  $0.88 \pm 0.04\%$  ( $n = 30$ ) at HG II and  $0.77 \pm 0.06\%$  ( $n = 30$ ) at HG I. Results of all stations are listed in Table 5.3.

Median grain size, water content and porosity differed significantly between the WS and EG area, while the portion of sediment grain size >63  $\mu\text{m}$  was similar (Table S5.4).

The sediment-bound Chl *a* concentration ranged between  $0.4 \pm 0.3 \mu\text{g ml}^{-1} \text{ sediment}^{-1}$  ( $n = 15$ ) at EG III and  $12.7 \pm 3.1 \mu\text{g ml}^{-1} \text{ sediment}^{-1}$  ( $n = 15$ ) at SV I (Table 5.3) and differed significantly between the EG and WS area (Figure 5.3, Table S5.4). A similar pattern was found for sediment-bound Phaeo concentrations and CPE concentration with over 4 times higher median values in the WS area compared to the EG area (Figure 5.3). The Chl *a*/CPE and Chl *a*/Phaeo ratios did not differ between the EG and WS area (Table S5.4), which indicates that the benthic community in both areas fed on a similar food quality and received the spring bloom food supply at the same time, respectively. Sediment-bound TOC ranged between  $0.44 \pm 0.04\%$  ( $n = 15$ ) at EG II and  $1.58 \pm 0.27\%$  ( $n = 15$ ) at SV I and differed between the EG and WS area, similar to organic matter, which ranged between  $3.45 \pm 0.6\%$  ( $n = 15$ ) at EG II and  $12.0 \pm 4.2\%$  ( $n = 30$ ) at HG III (Table 5.3, Figure 5.3, Table S5.4). Proteins, lipids, and FDA also differed between the EG and WS area with 5.6 times, 2.3 times, and 1.8 times higher median values in the WS area, respectively (Figure 5.3, Table S5.4).

**Table 5.3.** Mean values  $\pm$  standard deviation and number of samples in brackets for each measured parameter at each station. The CPE is the chloroplastic pigment equivalent and the sum of Chl *a* and Phaeo. Chl *a* –CPE ratio indicates the available labile carbon source, while the Chl *a* –Phaeo ratio indicates the relative age of the carbon source. No value could be calculated for solute exchange across the sea-water-interface at EG II.

Parameter category	Parameter	Station													
		EG I	EG II	EG III	EG IV	EG V	SV I	HG I	HG I Lander	SV IV	HG II	HG III	HG IV	HG IV Lander	N5
Sediment property	Median grain size [ $\mu\text{m}$ ]	13.4 $\pm$ 1.2 (15)	15.1 $\pm$ 1.7 (15)	20.3 $\pm$ 3.9 (15)	31.6 $\pm$ 7.3 (15)	74.2 $\pm$ 29.3 (13)	12.3 $\pm$ 2.7 (15)	12.7 $\pm$ 6.0 (30)	NA	20.4 $\pm$ 6.4 (15)	12.7 $\pm$ 5.8 (30)	19.3 $\pm$ 5.3 (29)	23.8 $\pm$ 5.3 (30)	NA	10.4 $\pm$ 2.9 (15)
	Portion of grain size >63 $\mu\text{m}$ [%]	3.5 $\pm$ 1.5 (15)	8.6 $\pm$ 2.9 (15)	18.6 $\pm$ 6.0 (15)	29.5 $\pm$ 6.8 (15)	52.2 $\pm$ 6.7 (15)	17.7 $\pm$ 2.2 (15)	11.4 $\pm$ 5.7 (30)	NA	24.4 $\pm$ 5.6 (15)	12.6 $\pm$ 6.0 (30)	20.1 $\pm$ 4.2 (29)	24.5 $\pm$ 5.3 (30)	NA	20.7 $\pm$ 2.6 (15)
	Water content (%)	51 $\pm$ 7 (15)	48 $\pm$ 7 (15)	46 $\pm$ 9 (15)	48 $\pm$ 10 (15)	42 $\pm$ 6 (15)	51 $\pm$ 14 (15)	66 $\pm$ 5 (30)	NA	55 $\pm$ 5 (15)	62 $\pm$ 4 (30)	55 $\pm$ 5 (30)	51 $\pm$ 8 (30)	NA	60 $\pm$ 5 (15)
	Porosity	0.76 $\pm$ 0.06 (15)	0.73 $\pm$ 0.06 (15)	0.71 $\pm$ 0.08 (15)	0.73 $\pm$ 0.08 (15)	0.68 $\pm$ 0.06 (15)	0.75 $\pm$ 0.14 (15)	0.88 $\pm$ 0.03 (30)	NA	0.80 $\pm$ 0.04 (15)	0.85 $\pm$ 0.03 (30)	0.80 $\pm$ 0.04 (30)	0.77 $\pm$ 0.06 (30)	NA	0.84 $\pm$ 0.03 (15)

Table 5.3 (continued)

Other biogenic compounds						Food availability				
FDA [nmol ml <sup>-1</sup> sediment <sup>-1</sup> h <sup>-1</sup> ]	Lipids [nmol ml <sup>-1</sup> sediment <sup>-1</sup> ]	Lipids [nmol ml <sup>-1</sup> sediment <sup>-1</sup> ]	Proteins [µg ml <sup>-1</sup> sediment <sup>-1</sup> ]	Organic matter [%]	TOC [%]	Chl a- Phaeo ratio	Chl a- CPE ratio	CPE [µg ml <sup>-1</sup> sediment <sup>-1</sup> ]	Phaeo µg ml <sup>-1</sup> sediment <sup>-1</sup> ]	Chl a [µg ml <sup>-1</sup> sediment <sup>-1</sup> ]
1.9 ± 0.7 (15)	2.9 ± 1.1 (15)	100 ± 20 (15)	7.1 ± 1.0 (15)	0.55 ± 0.05 (14)	0.11 ± 0.03 (15)	0.10 ± 0.02 (15)	4.7 ± 2.6 (15)	4.2 ± 2.2 (15)	0.5 ± 0.4 (15)	
1.1 ± 0.8 (15)	5.2 ± 2.1 (14)	122 ± 22 (15)	3.5 ± 0.6 (15)	0.44 ± 0.04 (15)	0.13 ± 0.02 (15)	0.11 ± 0.02 (15)	4.2 ± 2.7 (15)	3.7 ± 2.4 (15)	0.5 ± 0.3 (15)	
1.3 ± 0.8 (15)	4.2 ± 2.4 (14)	120 ± 22 (15)	3.5 ± 0.6 (15)	0.45 ± 0.04 (15)	0.11 ± 0.03 (15)	0.10 ± 0.02 (15)	3.4 ± 2.5 (15)	3.0 ± 2.2 (15)	0.4 ± 0.3 (15)	
2.6 ± 2.1 (15)	5.3 ± 2.2 (14)	337 ± 80 (15)	6.6 ± 0.7 (15)	0.51 ± 0.11 (15)	0.08 ± 0.02 (14)	0.08 ± 0.01 (14)	7.8 ± 6.1 (15)	7.2 ± 5.6 (15)	0.6 ± 0.5 (15)	
2.1 ± 1.1 (15)	8.4 ± 2.8 (15)	259 ± 43 (15)	5.0 ± 0.9 (15)	0.53 ± 0.09 (15)	0.10 ± 0.02 (15)	0.09 ± 0.02 (15)	7.4 ± 4.2 (15)	6.7 ± 3.6 (15)	0.63 ± 0.4 (14)	
31.3 ± 12.2 (15)	49.7 ± 21.0 (15)	3253 ± 475 (15)	8.0 ± 2.2 (15)	1.58 ± 0.27 (15)	0.19 ± 0.03 (15)	0.16 ± 0.02 (15)	80.0 ± 13.1 (15)	67.3 ± 10.8 (15)	12.7 ± 3 (15)	
4.7 ± 1.5 (30)	10.4 ± 7.1 (30)	998 ± 314 (30)	9.1 ± 2.9 (30)	1.37 ± 0.08 (28)	0.10 ± 0.03 (30)	0.09 ± 0.02 (30)	34.0 ± 9.7 (30)	30.9 ± 8.8 (30)	3 ± 1 (29)	
NA	NA	NA	NA	NA	0.16 ± 0.04 (10)	0.13 ± 0.03 (10)	18.9 ± 9.9 (10)	16.4 ± 8.6 (10)	2.5 ± 1.5 (10)	
1.7 ± 0.6 (15)	22.3 ± 10.9 (15)	686 ± 85 (14)	8.0 ± 1.0 (15)	0.98 ± 0.13 (15)	0.10 ± 0.02 (15)	0.09 ± 0.01 (15)	26.7 ± 21.3 (14)	24.4 ± 20 (14)	2.2 ± 1.1 (14)	
3.3 ± 2.1 (30)	16.4 ± 8.5 (30)	1053 ± 95 (30)	10.6 ± 1.3 (29)	1.05 ± 0.19 (30)	0.10 ± 0.02 (30)	0.09 ± 0.02 (30)	20.4 ± 9.6 (29)	18.5 ± 8.6 (29)	2.0 ± 1.2 (30)	
3.0 ± 1.3 (30)	13.7 ± 5.5 (29)	1004 ± 313 (30)	11.4 ± 3.8 (28)	0.92 ± 0.11 (30)	0.11 ± 0.03 (30)	0.10 ± 0.02 (30)	22.1 ± 6.7 (30)	20.0 ± 6.2 (30)	2.1 ± 0.8 (30)	
2.8 ± 1.7 (30)	16.6 ± 16.3 (30)	530 ± 64 (30)	6.5 ± 0.9 (29)	0.69 ± 0.07 (30)	0.11 ± 0.02 (30)	0.10 ± 0.02 (30)	13.6 ± 6.7 (30)	12.4 ± 6.2 (30)	1.3 ± 0.6 (30)	
NA	NA	NA	NA	NA	0.12 ± 0.03 (15)	0.10 ± 0.02 (15)	10.7 ± 6.2 (15)	9.8 ± 5.7 (15)	1.1 ± 0.6 (15)	
2.2 ± 0.6 (15)	8.5 ± 3.4 (15)	748 ± 76 (15)	8.4 ± 0.4 (15)	0.88 ± 0.03 (15)	0.08 ± 0.02 (15)	0.07 ± 0.02 (15)	16.0 ± 4.2 (13)	14.8 ± 3.8 (13)	1.2 ± 0.4 (14)	

Table 5.3 (continued)

Carbon flux equivalent		Oxygen flux			Community functions		Benthic community			
C-TOU [mmol C m <sup>-2</sup> d <sup>-1</sup> ]	C-DOU [mmol C m <sup>-2</sup> d <sup>-1</sup> ]	DOU/ TOU	TOU [mmol O <sub>2</sub> m <sup>-2</sup> d <sup>-1</sup> ]	DOU [mmol O <sub>2</sub> m <sup>-2</sup> d <sup>-1</sup> ]	BPC	Solute exchange [mmol Br m <sup>-2</sup> d <sup>-1</sup> ]	Macrofauna density [ind. m <sup>-2</sup> ]	Macrofauna biomass [mg m <sup>-2</sup> ]	Meiofauna density [ind. 10cm <sup>-2</sup> ]	Bacteria density [cells x10 <sup>09</sup> ml <sup>-1</sup> sediment <sup>-1</sup> ]
0.7 ± 0.3 (2)	0.7 ± 0.2 (4)	1.00	0.9 ± 0.3 (2)	0.9 ± 0.2 (4)	644 (1)	29.3 (1)	1414 (1)	3524 (1)	229 (1)	1.60 (1)
1.3 (1)	0.7 ± 0.2 (2)	0.63	1.6 (1)	1.0 ± 0.1 (2)	318 (1)	NA	991 (1)	1971 (1)	83 (1)	1.57 (1)
1.1 ± 0.1 (2)	0.5 ± 0.3 (4)	0.40	1.5 ± 0.1 (2)	0.6 ± 0.4 (4)	93 (1)	57.7 (1)	284 (1)	1301 (1)	86 (1)	1.55 (1)
0.8 ± 0.1 (4)	0.6 ± 0.2 (10)	0.73	1.1 ± 0.1 (2)	0.8 ± 0.3 (4)	55 ± 25 (3)	17.7 (1)	1058 ± 722 (3)	433 ± 287 (3)	192 ± 79 (4)	1.57 ± 0.09 (4)
1.0 ± 0.2 (2)	0.4 ± 0.1 (4)	0.40	1.0 ± 0.2 (4)	0.4 ± 0.1 (10)	132 (1)	28.1 (1)	1064 (1)	450 (1)	245 (1)	1.56 (1)
3.9 ± 0.2 (3)	2.3 ± 1.3 (6)	0.59	5.1 ± 0.2 (3)	3.0 ± 1.7 (6)	1586 ± 1042 (3)	38.8 ± 1.8 (3)	4945 ± 6286 (3)	45370 ± 25609 (3)	1150 ± 159 (3)	NA
1.5 ± 0.5 (5)	1.0 ± 0.5 (12)	0.63	1.9 ± 0.6 (5)	1.2 ± 0.6 (12)	556 ± 266 (4)	51.3 ± 14.1 (4)	2860 ± 1206 (4)	12196 ± 13652 (4)	333 ± 134 (3)	1.79 ± 0.13 (4)
1.0 ± 0.1 (4)	0.9 ± 0.3 (15)	0.92	1.3 ± 0.2 (4)	1.2 ± 0.3 (15)	397 (1)	NA	942 (1)	6929 (1)	357 ± 151 (5)	1.14 ± 0.20 (3)
1.4 ± 0.2 (3)	1.6 ± 0.4 (8)	1.17	1.8 ± 0.2 (3)	2.1 ± 0.6 (8)	909 ± 852 (8)	39.9 ± 6.3 (3)	4143 ± 2817 (3)	8733 ± 1671 (3)	402 ± 123 (3)	1.83 ± 0.43 (3)
0.8 ± 0.2 (5)	1.1 ± 0.7 (8)	1.00	1.1 ± 0.2 (5)	1.1 ± 0.6 (8)	199 ± 51 (4)	38.9 ± 13.0 (5)	2471 ± 612 (4)	1325 ± 479 (4)	277 ± 75 (4)	1.81 ± 0.08 (4)
0.8 ± 0.2 (5)	0.7 ± 0.2 (7)	0.90	1.0 ± 0.2 (5)	0.9 ± 0.3 (7)	391 ± 90 (4)	53.2 ± 27.3 (3)	4343 ± 2818 (4)	6186 ± 6137 (4)	273 ± 83 (4)	1.29 ± 0.19 (4)
1.1 ± 0.4 (5)	0.4 ± 0.1 (8)	0.33	1.5 ± 0.5 (5)	0.5 ± 0.2 (8)	74 ± 40 (4)	50.8 ± 39.3 (2)	1148 ± 542 (4)	2784 ± 1578 (4)	352 ± 141 (4)	1.49 ± 0.07 (4)
0.4 ± 0.2 (5)	0.5 ± 0.3 (18)	1.40	0.5 ± 0.2 (5)	0.7 ± 0.4 (18)	70 (1)	NA	417 (1)	836 (1)	293 ± 202 (6)	9.28 ± 0.35 (4)
1.0 ± 0.2 (3)	0.9 ± 0.5 (8)	1.00	1.2 ± 0.3 (3)	1.2 ± 0.6 (8)	106 ± 39 (3)	15.0 ± 3.1 (3)	2023 ± 409 (3)	8166 ± 7364 (3)	268 ± 98 (3)	1.54 ± 0.04 (3)



### 5.4.3 Benthic communities and community functions in the EG and WS area

Overall, 17 meiofauna taxa and 18 macrofauna taxa were identified (Tables S5.5, S5.6, S5.7). The meiofauna density was dominated by nematodes (86%), the only taxon present at each station. Crustaceans were the second most dominant group with 4.5% nauplii and 3.5% Copepoda. The macrofauna density was dominated by polychaetes (40%), followed by Copepoda (26%), and Nematoda (12%). Polychaetes (57%) also dominated the macrofauna biomass, followed by Bivalvia (16%) and Porifera (14%). The mean values of the benthic faunal community parameters meiofauna density, macrofauna density and macrofauna biomass were 1.5 times, 4.6 times and 2.5 times higher in the WS area than in the EG area (Table S5.2), respectively, and differed significantly from each other (Table S5.4). Contrasting, the bacterial density was similar between the EG and WS area but showed a greater variability in the WS area (Figure 5.3, Table S5.4).

The solute exchange across the SWI, represented by the bromide flux, did not differ between the EG and WS area (Table S5.4). The lack of difference might have methodological reasons. Bromide flux incubations were performed on 40 sediment cores but measurements from 13 sediment cores were omitted (seven from EG area, six from WS area), as either the calculations revealed a positive flux or the residuals were not homogeneously distributed across the decreasing slope of the bromide concentration over time or slopes were not significantly different from zero. The community bioturbation potential, represented by the BPc, was also similar between the EG and WS area (Table S5.4) but the median BPc at the WS area was 2.9 times higher than in the EG area (Figure 5.3). This indicates that the benthic macrofauna community in the WS area is potentially able to rework the sediment stronger than the benthic macrofauna community in the EG area.

### 5.4.4 Benthic remineralization

All oxygen microprofiles showed decreasing oxygen concentrations across the SWI (Figure S5.1) and steepness of oxygen gradients varied among microprofiles and across



$1.9 \pm 0.6 \text{ mmol O}_2 \text{ m}^{-2} \text{ d}^{-1}$  ( $n = 5$ ) at HG I. At the shallow SV I station TOU reached  $5.1 \pm 0.3 \text{ mmol O}_2 \text{ m}^{-2} \text{ d}^{-1}$  ( $n = 3$ , Table 5.3). DOU differed significantly between the WS and EG area, while TOU was similar (Figure 5.3, Table S5.4).

The mean DOU/TOU ratio, which describes the fraction of the total community mediated oxygen flux (TOU) covered by the microbial-mediated oxygen flux (DOU) [Glud, 2008] across the entire Fram Strait was  $0.79 \pm 0.30$ , with  $0.63 \pm 0.22$  in the EG area and  $0.92 \pm 0.30$  in the WS area, indicating that the total oxygen uptake is mainly microbially mediated. In the EG area, DOU values showed no correlation with water depth, while in the WS area the correlation of DOU with water depth was significant (Figure 5.4) and showed greater variability (Figure 5.3). In contrast, TOU values in the EG and in the WS areas showed no correlation with water depth (Figure S5.3), but again, the variability of TOU values was higher in the WS area (Figure 5.3). C-DOU and C-TOU followed the same trends as DOU and TOU, respectively, and are listed in Table 5.3.

#### 5.4.5 Relations of the benthic community, its remineralization activity, and environmental parameters

The PCA, which includes only abiotic parameters (year, water depth, sea ice cover, the percentage of days with sea ice cover, portion of grain size  $>63 \mu\text{m}$ , and median grain size) and biogenic compounds of the first sediment centimeter (Chl *a*, Phaeo, CPE, TOC, organic matter, lipids, and proteins), revealed differences between the sampling years 2014 and 2015 (Figure S5.2). The difference occurred only in the second dimension, which explained 15.4% of the variability and is mostly influenced by the parameters Phaeo and CPE (Table S5.8). The non-parametric Wilcoxon signed rank sum test of the station specific mean values revealed no differences ( $p > 0.05$ ) for any of the parameters between the sampling years. Furthermore, Henson et al. [2016] showed that it takes at least 15 years of continuous data to prove temporal trends in ocean biogeochemistry; and even longer in high latitudinal areas. Therefore, it is more likely that statistically revealed differences between sampling years reflect spatial variability rather than time-related differences. In turn, the data from stations sampled in 2014 and 2015 were merged and thus this study focuses solely on spatial patterns.

The PCA on station specific, *ex situ* obtained mean values (Figure 5.5) revealed that water depth was positively correlated with median grain size and negatively correlated with the DOU, the TOU, bacterial density, and the BPc. Sea-ice concentration was negatively correlated with the porosity, Chl *a*, TOC, organic matter, and solute exchange. Similarly, macrofauna biomass was negatively correlated with, water depth, sea-ice concentration, and the median grain size. Additionally, stations of the EG area were strongly influenced by the sea-ice cover. The two dimensions of the plot explained 72% of the total variability of the data. The eigenvalues indicated that ‘Chl *a*’, ‘TOC’, and ‘Macrofauna biomass’ (-0.89, -0.88, -0.83, respectively) were responsible for the gradient along the x-axis and ‘Bacterial density’, ‘water depth’, organic matter’ and ‘sea-ice concentration’ (0.59, -0.57, -0.54, respectively) for the gradient along the y-axis.

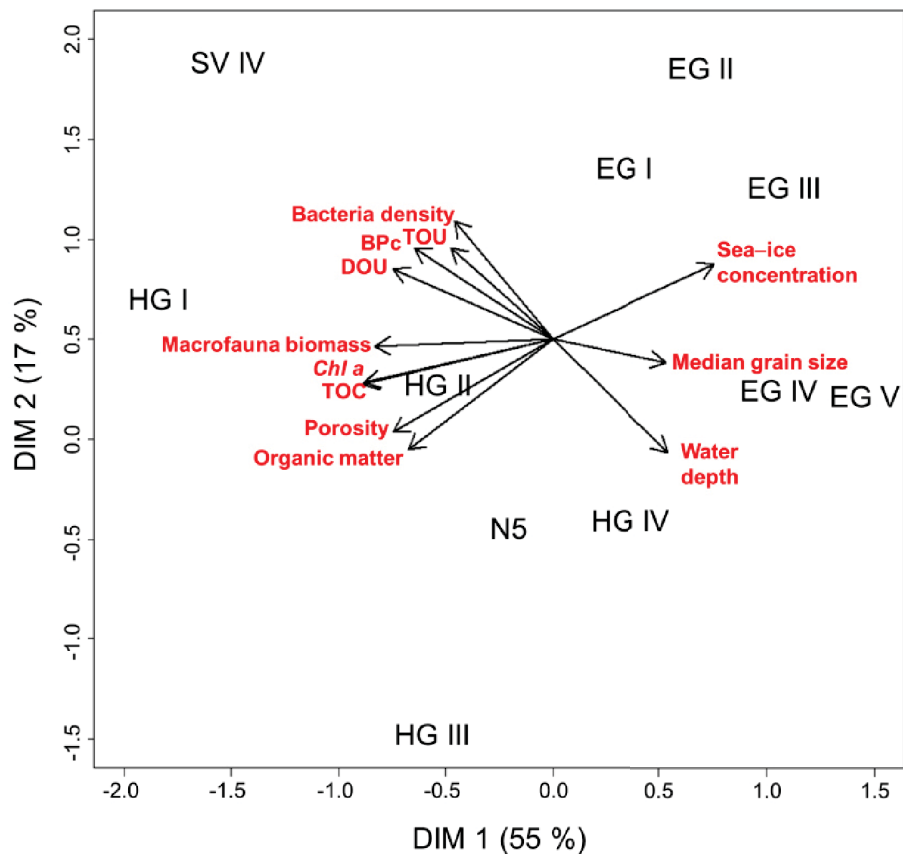


**Figure 5.5.** Visualization of PCA results on standardized *ex situ* mean values of abiotic parameters (water depth, sea-ice concentration, median grain size, porosity), biogenic compound parameters (Chl *a*, TOC, organic matter), benthic community parameters (bacterial density, macrofauna biomass), bioturbation potential (BPc), and oxygen fluxes (DOU, TOU). All other parameters were excluded from the PCA as they correlated strongly with one of the mentioned parameters (correlation >0.74, Pearson correlation, Table S5.2). For comparability, Station SV I was excluded from the PCA. Therefore, the figure reflects relations of different parameters in the Fram Strait in water depths of 1000–2500 m.

Across the HSC area, DOU and TOU were not linearly dependent on water depth (Figure 5.4, Figure S5.3, Table S5.9). The same was found for the water content, FDA, meiofauna and macrofauna densities, macrofauna biomass, and the solute exchange across the SWI. Otherwise, the fraction of sand in the sediment (% of grain size  $>63 \mu\text{m}$ ), Phaeo, CPE, the Chl *a*-Phaeo ratio, the Chl *a*-CPE ratio, and lipids were positively linearly dependent on water depth across the HSC area and the BPC was negatively linearly dependent on water depth. Across the LSC area, the DOU was negatively linearly dependent on water depth, as well as sediment water content, Chl *a*, Phaeo, CPE, FDA, bacteria density and bioturbation potential. Contrastingly, TOU, Chl *a*-Phaeo ratio, protein, meio- and macrofauna densities, macrofauna biomass, and the solute exchange were not water depth dependent in the LSC area. Within both sea-ice categories HSC and LSC, no linear water depth dependencies were found for median grain size, TOC, and organic matter as the residuals over the slopes did not follow the Gaussian distribution. This also applied for Chl *a*, protein, and bacteria density across the HSC area and for the portion of grain size  $>63 \mu\text{m}$ , the Chl *a*-CPE ratio, and lipids across the LSC area (Table S5.9).

The ANOSIM (Global  $R = 0.122$ ,  $p = 0.063$ ) and SIMPER (33% dissimilarity) routine revealed no differences between the HSC and LSC area regarding the meiofauna community based on density. Regarding macrofauna communities based on density (Global  $R = 0.257$ ,  $p = 0.007$ ) and biomass (Global  $R = 0.238$ ,  $p = 0.003$ ), the ANOSIM revealed significant but weak differences between the HSC and LSC area. SIMPER routine results indicated dissimilarities of 56% for the macrofauna density and 76% for the macrofauna biomass between the HSC and LSC areas. The taxa which contributed most to the average similarity within and to the average dissimilarity between the HSC and LSC area are given in Table S5.10. The ANOSIM results for water depth groups showed that bathymetry could at least explain the dissimilarity in meiofauna communities based on density (Global  $R = 0.219$ ;  $p = 0.01$ ), even if the difference was weak. The SIMPER analysis, however, showed that the observed differences in meiofauna density regarding water depth were mainly due to the marked difference between the shallowest station (SV I at 275 m) and all other stations deeper than 1000 m (dissimilarity  $>50\%$ , Table S5.11). ANOSIM results for macrofauna communities

based on density (Global  $R = 0.2$ ,  $p = 0.008$ ) and biomass (Global  $R = 0.346$ ,  $p = 0.0001$ ) revealed significant but also weak differences between water depth categories with >50% dissimilarity between all water depth categories for macrofauna density (except between 1000 m and 1500 m) and macrofauna biomass (SIMPER, Supplement Table S11). Further, the two-way crossed PERMANOVA revealed that the sea-ice coverage (LSC and HSC) explains a significant ( $p = 0.008$ ) portion of the macrofauna density variability, while the portion explained by water depth ( $p = 0.06$ ) and by the interaction of sea-ice cover and water depth ( $p = 0.09$ ) was not significant (Table S5.12). However, the results of the pairwise test showed that only the neighboring water depth classes 1000 m and 1500 m showed no significant differences ( $p = 0.45$ ) while all other pairwise comparisons showed significant differences between water depths (Table S5.13). For macrofauna biomass, the two-way crossed PERMANOVA revealed that the interaction of sea-ice cover and water depth explains a significant ( $p = 0.034$ ) portion of the macrofauna biomass variability, while the portion explained by the sea-ice cover categories ( $p = 0.051$ ) and by water depth ( $p = 0.058$ ) was not significant (Table S5.12). The results of the pairwise test showed that only the water depth classes 1000 m and 2500 m showed significant differences ( $p = 0.0187$ ), while all other pairwise comparisons showed no significant differences between water depths (Table S5.13).

## 5.5 Discussion

### 5.5.1 Linking contrasting sea-ice conditions with benthic oxygen fluxes

The main aim of this study was to link sea-ice conditions within the Arctic Fram with the deep-sea benthic oxygen fluxes over a cascade of dependencies. Our results documented two contrasting sea-ice concentration regimes in the Fram Strait with a high sea-ice concentration in the western Fram Strait and a low sea-ice concentration in the eastern Fram Strait (Table 5.2, Figure 5.2). This is similar to sea-ice concentration snapshot observations by Schewe and Soltwedel [2003] and satellite observations of Krumpfen et al. [2016]. The observed pattern can be explained by the two major current systems present in the Fram Strait [Schauer, 2004], the EGC transporting cold, nutrient-poor water and sea ice from the central Arctic Ocean southwards into the EG area and the WSC transporting warmer, nutrient richer and sea-ice free water from the Atlantic

Ocean northwards into the WS area [Manley, 1995; Mauritzen et al., 2011; Graeve and Ludwichowski, 2017a, b]. If there were a strong link between sea-ice conditions and deep-sea benthic oxygen fluxes, we would expect contrasting primary production, benthic food supply, benthic community parameters and benthic oxygen fluxes between the EG and the WS area.

The results of Pabi et al. [2008] showed that in the Fram Strait the annual primary production pattern followed the general sea-ice concentration pattern and that the annual primary production was up to 10 times larger in the WS area compared to the EG area. Thus, the sea-ice concentration represents the general primary production pattern in the Fram Strait. Thus, the sea-ice concentration represents the general primary production pattern in the Fram Strait. As the sampling was performed in Mid/End of June 2014 and July/August 2015, it is very likely that the spring bloom, which usually starts in May [Cherkasheva et al., 2014], had finished. This is indicated by lower nutrient concentrations in water depth  $\leq 50$  m compared to the nutrient concentrations between  $>50$ – $300$  m water depths [Graeve and Ludwichowski, 2017a, b]. The N : P ratio in the upper 50 m during the expeditions was six and seven in the EG and WG area, respectively [Graeve and Ludwichowski, 2017a, b], indicating that primary production was nitrate limited, similar to the permanently sea-ice covered central Arctic Ocean [Tremblay et al., 2012; Fernández-Méndez et al., 2015]. Furthermore, the timing of our sampling suggests that the increased carbon supply by the spring bloom had already reached the seafloor and enhanced the benthic remineralization [Graf, 1989] in both areas. The pattern of contrasts between the EG and WS area continued in the benthic food supply, which was also found by Boetius and Damm [1998] for areas with contrasting sea-ice cover at the continental margin of the Laptev Sea.

Continuing the cascade of dependencies, benthic community parameters should follow the same pattern as the sea ice at the surface and the benthic food supply parameters. Indeed, there were differences between the EG and WS area regarding meiofauna density and macrofauna density but not in the macrofauna biomass. In addition, also the macrofauna community structure differed between areas with high and low sea-ice cover. However, only when taking sea ice and water depth into account. The performed PERMANOVA confirmed the influence of water depth on the macrofauna

community and indicated that water depth is a considerable factor besides sea-ice cover. Consequently, in the low sea-ice covered WS area macrofauna is mainly influenced by the abiotic factor water depth [Soltwedel et al., 2015], while in the highly sea-ice covered EG area the abiotic factor sea-ice cover co-acts or even replaces water depth as the most influencing abiotic factor.

Benthic remineralization across the Fram Strait, represented by the oxygen flux, was not correlated with sea-ice concentrations or benthic food supply, only with water depth (Figure 5.5). This is in contrast to our expectations and to findings of Boetius and Damm [1998]. However, a PCA only shows correlations, which does not necessarily prove causal relationships and does not test for the significance of these relationships. Therefore, we tested the significance of the correlation of water depth with DOU within the sea-ice concentration categories HSC and LSC, which reveals a slightly different pattern. The regression of the DOU on water depth is only significant in the LSC category, but not in the HSC (Figure 5.4). Therefore, the bacterial benthic remineralization, which makes up ~80% of the TOU, depends on water depth in low sea-ice covered areas, but not in the highly sea-ice covered EG area. A test, if this pattern is also true for the macro- and meiofauna activity, represented by the fauna mediated oxygen uptake (= TOU minus DOU), was assessed as not reliable owing a lower reproducibility of TOU values.

A PCA displays an ecosystem snapshot of factors which likely respond on different time scales. For example, benthic faunal biomass, density, and structure will respond in a more seasonally to decadal fashion, while benthic remineralization responds on short time scales such as days to weeks [Graf, 1989; Renaud et al., 2008]. To acknowledge this, we decided to use the short-term dataset 'year before sampling' in the PCA. Additionally, the origin of the primary production responsible for the benthic food supply is difficult to assess and can be located >3000 km from the Fram Strait [Lalande et al., 2016]. In turn, the complexity of advective and vertical pelagic food input influencing processes in the Fram Strait is not considered in the ecosystem snapshot.

To summarize, sea-ice cover in the Fram Strait is a proxy for light availability and nutrient supply and therefore represents primary production in Fram Strait. In addition, water depth represents a proceeding degradation state of settling organic material



towards the sea floor [Belcher et al., 2016]. Both processes are responsible for the food supply to the benthos. Therefore, the independent factors 'sea-ice cover' and 'water depth' were the most important abiotic factors in the Fram Strait as they controlled the benthic food supply. This fits earlier findings, that labile organic matter is the most important factor determining Arctic deep-sea benthic communities [Grebmeier et al., 1988; Boetius and Damm; 1998; Klages et al., 2004]. Regarding benthic remineralization, the Fram Strait is bisectonal: water depth independent in the highly sea-ice covered western Fram Strait and water depth dependent in the low sea-ice covered eastern Fram Strait. However, the impact of sea-ice on the benthic remineralization cannot be distinguished from the impact of water depth in water depth >1500 m.

### 5.5.2 Primary production and benthic remineralization in the Fram Strait

The reported oxygen fluxes within the HSC and LSC categories are comparable to earlier findings within the Fram Strait [Sauter et al., 2001; Cathalot et al., 2015] and the continental margin of the Laptev Sea [Boetius and Damm, 1998], but are slightly lower than the modelled results for the pan-Arctic region (Figure 5.6) [Bourgeois et al., 2017]. In general, the total benthic carbon remineralization across the entire Fram Strait is  $\sim 1 \text{ mmol C m}^{-1} \text{ d}^{-1}$ .

The new primary production, the part of the total production which can fuel the benthos [Piatt et al., 1989], is  $55 \text{ g C m}^{-2} \text{ yr}^{-1}$  [Sakshaug, 2004, and references therein] in the West Spitsbergen area. This is equal to  $38 \text{ mmol C m}^{-1} \text{ d}^{-1}$ , assuming a production period of 120 days [Gradinger, 2009]. Codispoti et al. [2013] reported net community production from nutrient depletion for the WS area of  $27\text{--}32 \text{ g C m}^{-2}$ . These values reflect the annual new production and thus can be converted to  $19\text{--}22 \text{ mmol C m}^{-1} \text{ d}^{-1}$  (under the same assumption of 120 days of production). This indicates that approximately 2.6–5.2% of the new primary production in the WS area would be remineralized by the benthos. However, Lalande et al. [2016] reported that only  $2.7 \text{ g C m}^{-2} \text{ yr}^{-1}$  ( $= 1.9 \text{ mmol C m}^{-1} \text{ d}^{-1}$  under the same assumption of 120 days of production, particle trap study at HG IV) and therefore 5–14% of the primary production reaches the seafloor. Taking these export fluxes into account, this indicates that only

40% of the organic material reaching the seafloor is remineralized by the benthos in the West Spitzbergen area in the eastern Fram Strait.

The net primary production in the mainly sea-ice covered western Fram Strait is approximately  $8 \text{ g C m}^{-2} \text{ yr}^{-1}$  [Codispoti et al., 2013], which is  $5.6 \text{ mmol C m}^{-1} \text{ d}^{-1}$  (under the same assumption of 120 days of production). This is similar to the similarly sea-ice covered central Arctic Ocean [Codispoti et al., 2013; Fernández-Méndez et al. 2015]. Thus, 18% of the new primary production in the EG area would be remineralized by the benthos. Annual POC flux values of  $1\text{--}2.7 \text{ g C m}^{-2} \text{ yr}^{-1}$  ( $= 0.7\text{--}1.9 \text{ mmol C m}^{-1} \text{ d}^{-1}$ , under the same assumption of 120 days of production) were reported for the ice-covered regions at the Greenland shelf at  $80^\circ\text{N}$  [Bauerfeind et al., 1997] and  $1.6 \text{ g C m}^{-2} \text{ yr}^{-1}$  ( $= 1.1 \text{ mmol C m}^{-1} \text{ d}^{-1}$ , under the same assumption of 120 days of production) at the Greenland shelf at  $74^\circ\text{N}$  (Bauerfeind et al., 2005). These values indicate that 13–34% of the primary production reaches the seafloor, which is comparable to Arctic shallow shelf regions [Grebmeier et al., 1988; Renaud et al., 2007]. It further suggests that 50% to >100% of the organic material, that reaches the seafloor, is remineralized by the benthic organisms at the East Greenland continental margin and that this area has to be supplied by organic carbon from other areas.

However, these numbers have to be interpreted with caution, as a more reliable calculation of the primary production across the entire Fram Strait still remains difficult. Satellite-based chlorophyll measurements are only available in ice-free areas when there are no clouds or fog [Cherkasheva et al., 2014]. Additionally, satellites only measure chlorophyll a in the upper water column. Therefore, to calculate the primary production, additional information about the mixed water depth, photosynthetically active radiation, water temperature, salinity, nutrient availability, the chlorophyll a to carbon ratio, growth rates of the different occurring algae [Sakshaug, 2004] and further parameters needed to be measured during the bloom period, which can be exclusively obtained by ship-based expeditions. The approach of Codispoti [2013] is preferable when primary production and benthic remineralization are compared. However, it relies on a good spatial resolution of nutrient profiles in the water column. Furthermore, the measurements of the benthic oxygen flux, crucial to evaluate the pelagic-benthic-coupling, remain only snapshots of remineralization. The question, if the Arctic deep-sea

benthic oxygen fluxes follow seasonal changes, has only been sparsely evaluated [Bourgeois et al., 2017]. A full annual cycle of benthic remineralization is still missing and as such, a more reliable discussion of the pelagic-benthic-coupling and the carbon cycle remains difficult.

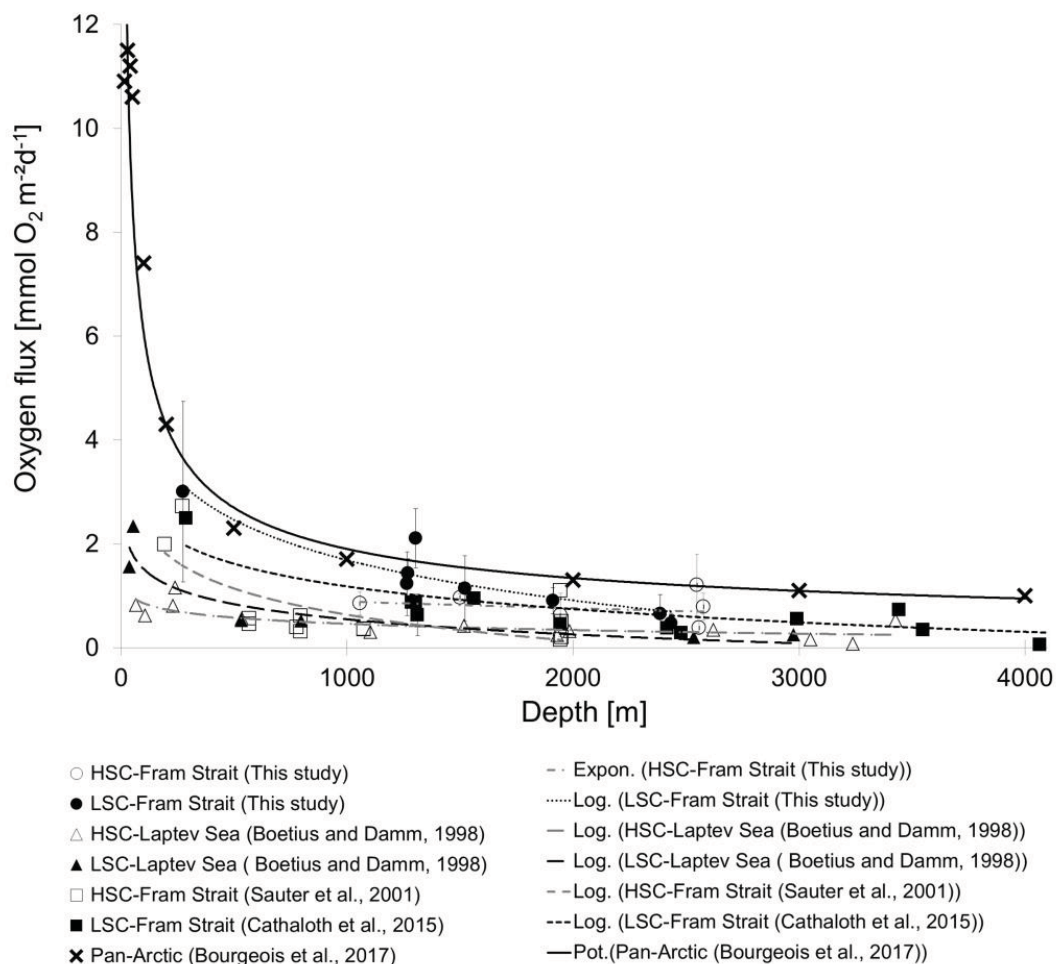


**Figure 5.6.** Sediment oxygen uptakes in different water depths (15–4000 m) for HSC and LSC sea-ice categories from this study and from literature data for the Laptev Sea, Fram Strait, and Pan-Arctic region and related regressions. HSC regression from this study:  $y = -0.124 \ln(x) + 1.7388$  ( $R^2 = 0.0255$ ); LSC regression from this study:  $y = -1.119 \ln(x) + 9.4144$  ( $R^2 = 0.8695$ ); HSC regression from Sauter et al. [2001]:  $y = -0.727 \ln(x) + 5.6587$  ( $R^2 = 0.5026$ ); LSC regression from Cathalot et al. [2015]:  $y = -0.63 \ln(x) + 5.534$  ( $R^2 = 0.7013$ ); HSC regression from Boetius and Damm [1998]:  $y = -0.172 \ln(x) + 1.6496$  ( $R^2 = 0.6074$ ); LSC regression from Boetius and Damm [1998]:  $y = -0.421 \ln(x) + 3.4515$  ( $R^2 = 0.8428$ ); pan-Arctic regression from Bourgeois et al [2017]:  $y = 7.1338e^{-4x}$  ( $R^2 = 0.7288$ ). Regression types were chosen based on best fit ( $R^2$ ). The model of Bourgeois et al. [2017] included DOU and TOU values, while all other references refer only to DOU values.

### 5.5.3 A future deep-sea benthic Arctic Ocean scenario

Our results indicate that a development from a permanently sea-ice covered to a seasonally sea-ice covered Arctic Ocean will change the benthic-pelagic relationship from a sea-ice dependent towards a water depth dependent environment (Figure 5.4). This may go along with a predicted compositional shift in the spring phytoplankton bloom from diatom-dominated to coccolithophorid [Bauerfeind et al., 2009] or *Phaeocystis* sp. and nanoflagellates dominated bloom [Soltwedel et al., 2015]. An altered algal composition will affect zooplankton communities [Caron and Hutchins, 2013] and partly organic particle fluxes [Wohlers et al., 2009]. An additional predicted effect is an increasing annual matter flux towards the seafloor [Wassmann, 2011; Boetius et al., 2013, this study], while the labile detritus flux is predicted to decrease [Hop et al., 2006; van Oevelen et al., 2011]. Therefore, the change in sea-ice cover in the Arctic Ocean may alter the quality and quantity of the organic matter flux to the seafloor, where it maybe affects benthic deep-sea communities [Jones et al., 2014; Harada, 2015]. However, the comparable DOU of the EG and HG site at water depth >1500 m (Figure 5.4) indicates that the remineralization by the deep-sea benthos will possibly remain stable in the Arctic Ocean.

Our scenario is only suitable if sea-ice disappears and nutrient supply increases, which will result in enhanced primary production. The development of future Arctic Ocean primary production patterns and changes is still under debate [Wassmann, 2011; Arrigo et al., 2012; Nicolaus et al., 2012, Boetius et al., 2013]. However, it is likely that the described scenario becomes true in the Chukchi Sea and the Beaufort Sea, owing to the predicted strengthening of the nutrient-rich Pacific inflow [Harada, 2015]. Furthermore, owing to an increased atlantification, an increased nutrient supply is also likely for the continental margin at the Barents Sea [Neukermans et al., 2018]. In addition, nutrient inflow by glacial and permafrost soil melt is also predicted to increase [Vonk et al., 2015]. However, this riverine load might only enhance primary production at the shelf areas and therefore is not relevant for the deep sea. An enhanced primary production in the western Fram Strait is unlikely, even if the light availability will increase as the required nutrient supply increase is not expected for this region [Mauritzen et al., 2011].

Additionally, the sea ice in the Fram Strait is already thinning [Krumpen et al., 2016]. This may be led to more light in the upper water column and an already higher primary production in the EG area, which consequently may have resulted in a higher food supply to the deep-sea benthos in this area and thereby biases our former-Arctic-Ocean perspective. However, fast sinking algae patches as reported by Boetius et al [2013] in the central Arctic, which would lead to increased benthic remineralization, were not observed during a video transect at EG IV in 2014 (pers. comm. James Taylor, Alfred-Wegener-Institut, Helmholtz-Zentrum für Polar- und Meeresforschung, Bremerhaven, Germany (AWI)). A further limitation of our scenario might be, that in contrast to the HG stations, there are no long-term data available about the benthic environment at the EG stations. Thus, an assessment of ongoing changes in the EG area, similar to the HG stations [Soltwedel et al., 2015], and insights into the natural variability of benthic changes remains difficult at the moment. Nevertheless, the general sea-ice concentration pattern in Fram Strait was stable over the last 14 years (Figure 5.2) was stable. This indicates that at least the production period and therefore, the low food supply at the EG stations was also stable within the last 14 years. In addition, the scenario is only valid for areas changing from permanent to very low sea-ice cover as our data does not allow to estimate a scenario for an intermediate (20–60%) sea-ice cover.

Despite its uncertainties, observations are currently still the best method to create such a scenario of future developments as consistent time series data from the entire Arctic Ocean, required to model reliable future predictions, are yet missing [Wassmann et al., 2011]. Thus, our comparative study provides new insights into the relationship between sea-ice cover at the surface and benthic oxygen fluxes in Fram Strait via surface primary production, benthic food supply, benthic community and their functions. We hypothesize that if surface primary and secondary production will increase due to the retreating sea-ice cover, the deep-sea benthos of the Arctic Ocean may shift from a sea-ice dependent towards a water depth dependent environment. There might be a slightly increased food supply and an altered macrofauna community, but remineralization at water depths greater than 1500 m seems to be hardly affected by these changes because it remains food limited.

## 5.6 Supplements

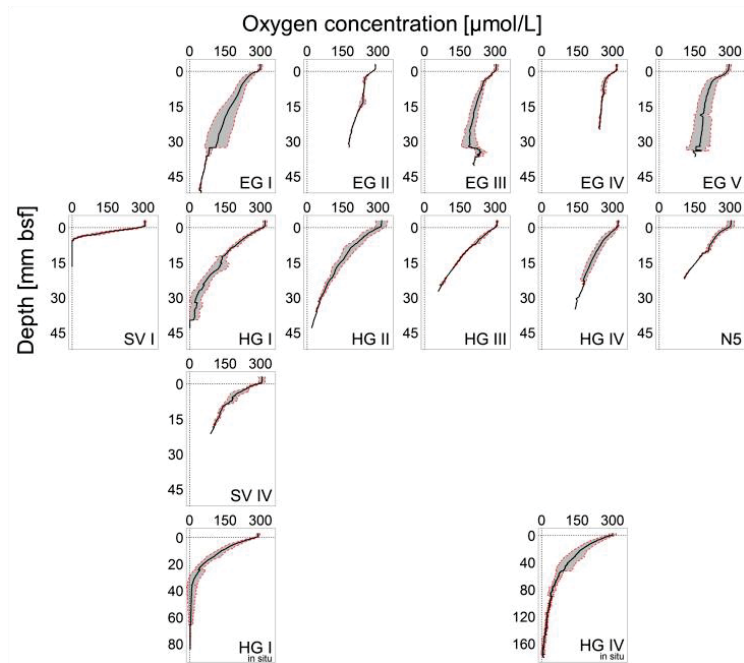


**Figure S5.1.** Oxygen profiles at each station. The first row shows the profiles from the EG area, while the second to fourth rows show the profiles from the WS area. Columns are in order of water depth, with the shallow stations on the left-hand site. The black line in each profile represents the mean oxygen concentration; the grey area represents the standard deviation. Strong breaks in the profile, like in EG I, are explained by merging profiles of different lengths. For a better inter-comparison of the profiles, the depth scale in the unit millimeter below surface (bsf) is equal, with the exception of the *in situ* stations at HG I and HG IV.

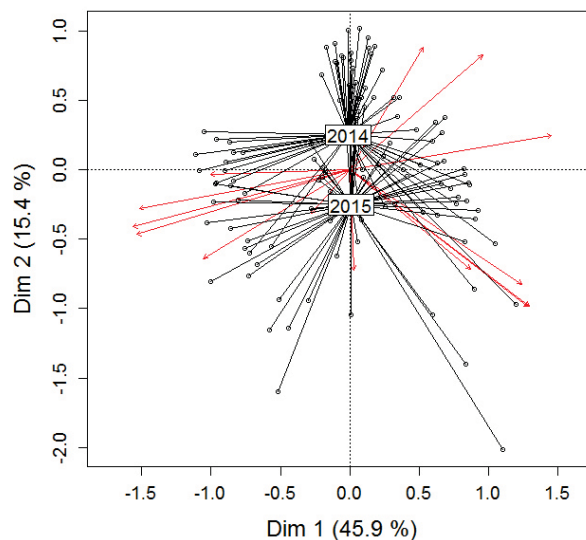


**Figure S5.2.** Visualization of the comparison between the sampling years 2014 and 2015 using a PCA. Each dot refers to a sediment horizon at a certain station while red arrows indicate used parameters. The labels of the parameters were omitted, as they are not needed for the interpretation of the figure.

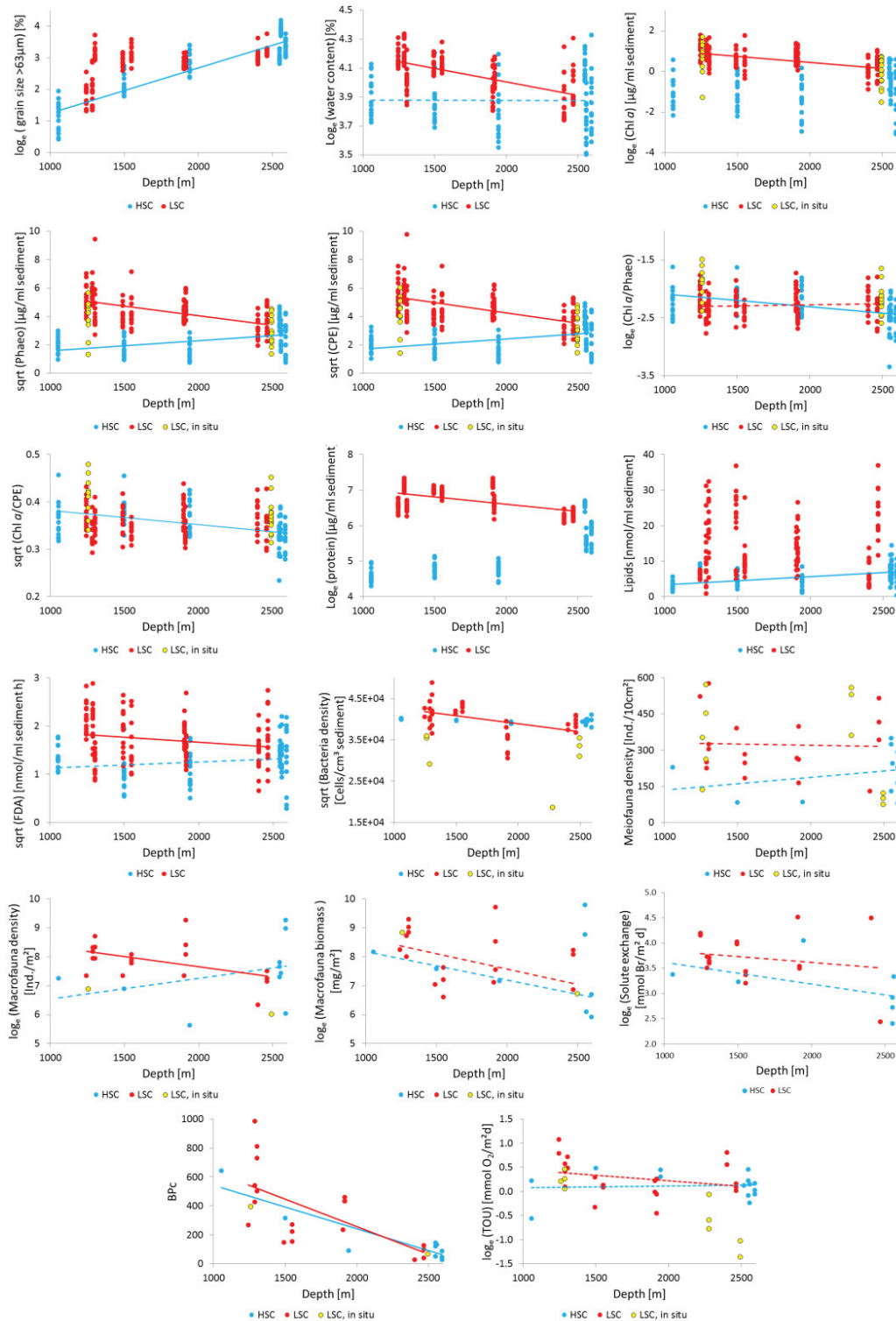


**Figure S5.3.** Parameters used in PCA (Figure 5.5) displayed as a function of water depth in the HSC and LSC categories. A continuous line indicates a significant correlation; a dashed line indicates that the residuals of the regression follow a Gaussian distribution, but the correlation is not significant. No regression line means that no regression could be calculated because assumptions for regression were violated, even with transformed data (for p-values of statistical analyzes see Table S5.9).

**Table S5.1.** Number of samples for analyzes of different parameters.

Station name	Year	Number of available sediment cores	Number of DOU profiles	Number of sediment cores for bacterial subsampling	Number of sediment cores for meiofauna subsampling	Number of sediment cores for macrofauna sampling	Number of sediment cores for solute exchange determination
EG I	2014	2	4	1	1	1	2
EG II	2014	1	2	1	1	1	1
EG III	2014	2	4	1	1	1	2
EG IV	2015	3	6	3	3	3	3
	2015	1	4	3	3	3	3
EG V	2014	2	4	1	1	1	2
SV I	2015	3	6	-	-	-	-
HG I	2014	2	4	1	1	1	2
	2015	3	8	3	3	3	3
HG I Lander	2014	1	1	2	2	2	-
	2015	3	15	1	3	3	-
SV IV	2015	3	8	3	3	3	3
HG II	2014	2	3	1	1	1	2
	2015	3	6	3	3	3	3
HG III	2014	2	3	1	1	1	2
	2015	3	4	3	3	3	3
HG IV	2014	2	4	1	1	1	2
	2015	3	4	3	3	3	3
HG IV Lander	2014	2	11	3	3	3	-
	2015	3	7	1	3	3	-
N5	2015	3	8	3	3	3	3



**Table S5.2.** Results of Pearson correlation (Pearson R).

	Water depth	Sea ice coverage	Days with sea ice coverage	Grain size fraction >63µm	Median grain size	Water content	Chl <i>a</i>	Phaeo	CPE	Chl <i>a</i> /CPE	Chl <i>a</i> /Phaeo	TOC	Organic matter	Protein	Lipids	FDA	DOU	TOU	Bacteria density	Meio-fauna density	Macro-fauna biomass	Macro-fauna density	Solute exchange	BPC
Water depth	1.000																							
Sea ice coverage	0.264	1.000																						
% of days with sea ice coverage	0.403	0.977	1.000																					
Grainsize fraction >63µm	0.614	0.036	0.122	1.000																				
Median grainsize	0.485	0.253	0.284	0.891	1.000																			
Water content	-0.301	-0.632	-0.610	-0.515	-0.589	1.000																		
Chl <i>a</i>	-0.680	-0.474	-0.498	-0.120	-0.238	0.132	1.000																	
Phaeo	-0.662	-0.621	-0.635	-0.120	-0.279	0.293	0.963	1.000																
CPE	-0.666	-0.610	-0.623	-0.119	-0.280	0.282	0.968	0.999	1.000															
Chl <i>a</i> /CPE	-0.711	-0.271	-0.366	-0.274	-0.218	-0.016	0.770	0.630	0.635	1.000														
Chl <i>a</i> /Phaeo	-0.691	-0.303	-0.386	-0.288	-0.236	0.047	0.743	0.607	0.613	0.989	1.000													
TOC	-0.405	-0.757	-0.735	-0.128	-0.319	0.437	0.689	0.788	0.780	0.331	0.354	1.000												
Organic matter	-0.115	-0.698	-0.640	-0.152	-0.324	0.579	0.246	0.406	0.395	-0.110	-0.103	0.679	1.000											

**Table S5.2** (continued)

Protein	-0.543	-0.598	-0.757	-0.681	0.385	-0.606	-0.693	-0.417	-0.200	-0.869
Lipids	-0.604	-0.345	-0.453	-0.281	0.291	-0.535	-0.396	-0.282	-0.532	-0.341
FDA	-0.620	-0.361	-0.492	-0.325	0.286	-0.542	-0.414	-0.292	-0.611	-0.430
DOU	-0.637	-0.062	-0.254	-0.128	0.008	-0.019	-0.158	0.083	-0.176	-0.274
TOU	-0.075	-0.168	-0.406	-0.225	0.121	-0.166	-0.276	-0.099	-0.200	-0.287
Bacteria density	-0.259	-0.028	-0.106	-0.010	0.116	0.114	0.131	-0.021	0.234	0.106
Meiofauna density	0.193	0.137	0.269	0.939	-0.806	0.970	0.979	0.771	0.116	0.849
Macrofauna biomass	0.953	0.947	0.857	0.889	-0.669	0.942	0.951	0.784	0.158	0.844
Macrofauna density	0.950	0.935	0.893	0.896	-0.675	0.948	0.955	0.785	0.140	0.849
Solute exchange	0.640	0.768	0.580	0.736	-0.821	0.724	0.722	0.390	0.334	0.686
BPc	0.624	0.736	0.572	0.695	-0.820	0.700	0.698	0.315	0.329	0.653
	0.831	0.651	0.620	0.509	-0.519	0.700	0.656	0.469	0.302	0.543
	0.459	0.165	0.260	-0.024	-0.094	0.284	0.196	0.343	0.192	0.184
	1.000	0.938	0.796	0.829	-0.791	0.935	0.911	0.751	0.146	0.736
		0.902	0.839	0.872	-0.756	0.963	0.892	0.720	0.193	0.795
		1.000	0.774	0.920	-0.866	0.949	0.951	0.740	0.058	0.786
			1.000	0.842	-0.542	0.836	0.882	0.733	-0.035	0.907
				1.000	-0.689	0.887	0.950	0.726	0.045	0.840
					1.000	-0.800	-0.767	-0.524	-0.162	-0.562
						1.000	0.946	0.747	0.095	0.834
							1.000	0.760	0.044	0.881
								1.000	-0.179	0.697
									1.000	0.059
										1.000

**Table S5.3.** Annual sea-ice cover values, standard deviation and the annual percentages of days with sea-ice cover from 01/09/2001 until 31/08/2015. The sampling year of the stations is given in brackets. It refers to the location of the station, as this differs slightly between the sampling years.

EG I	Station		Year														
	% of days with sea-ice cover	Sea-ice cover [%] SD	Parameter														
					01/09-3 1/12/200 1	2002	2003	2004	2005	2006	2007	2008	2009	2010	2011	2012	2013
93.4	27	80		67	78	72	82	80	83	77	89	81	83	87	83	81	81
84.9	36	67															
95.6	26	78															
85.2	34	72															
99.5	21	82															
98.6	23	80															
99.2	17	83															
97.8	26	77															
99.7	13	89															
95.9	24	81															
99.5	15	83															
100.0	13	87															
98.9	21	83															
100.0	16	81															
98.0	21	81															

Table S5.3. (continued)

SV I		EG V		EG IV		EG III		EG II					
% of days with sea-ice cover	Sea-ice cover [%]	% of days with sea-ice cover	Sea-ice cover [%]	% of days with sea-ice cover	Sea-ice cover [%]	% of days with sea-ice cover	Sea-ice cover [%]	% of days with sea-ice cover	Sea-ice cover [%]				
	SD		Mean		SD		Mean		SD	Mean	SD	Mean	
15	14	5	37	41	75	40	52.1	85.2	35	62.4	90.2	30	77.2
19	15	6	33	38	84	34	50.9	84.7	35	61.3	85.8	36	66.1
35	24	15	31	44	90	31	59.8	94.2	26	71.8	95.6	26	76.2
31	32	19	31	28	77	36	49.2	82.0	35	58.8	84.2	34	68.8
25	16	8	32	44	92	32	59.9	97.3	26	71.9	99.5	22	80.0
10	10	3	31	33	91	33	53.7	96.7	27	69.7	98.4	24	77.7
8	8	2	28	53	99	24	71.5	99.5	17	81.8	99.5	15	83.4
14	12	4	29	59	98	24	74.3	99.7	17	79.6	98.9	23	77.3
14	13	5	33	60	99	26	71.4	99.7	17	83.4	99.7	12	88.8
7	7	2	31	40	93	31	61.6	94.0	27	73.7	95.1	24	78.9
25	20	9	29	41	95	27	63.7	98.6	20	77.0	99.7	16	81.0
5	4	1	31	52	99	26	70.2	99.2	20	79.5	100.0	13	86.2
3	5	0	34	55	87	31	68.3	92.9	27	74.1	98.4	21	81.9
4	6	1	22	71	100	16	80.9	100	10	85.7	100.0	13	85.7
7	5	1	32	38	89	32	37.9	94	26	74.5	98.8	20	81.6

Table S5.3. (continued)

SV IV		HG I Lander (2015)		HG I Lander (2014)		HG I (2015)		HG I (2014)	
		% of days with sea-ice cover	Sea-ice cover [%] SD	% of days with sea-ice cover	Sea-ice cover [%] SD	% of days with sea-ice cover	Sea-ice cover [%] SD	% of days with sea-ice cover	Sea-ice cover [%] SD
0	0	0	0	0.0	0	0.0	0	0	0.0
1	3	0	3	1.1	3	0.2	3	0	1.1
2	2	0	9	9.6	9	2.4	9	2	9.6
11	13	4	8	8.5	9	2.0	8	2	8.5
1	2	0	0	0.0	0	0.0	0	0	0.0
0	0	0	0	0.0	0	0.0	0	0	0.0
0	0	0	2	0.5	2	0.1	2	0	0.5
3	4	1	12	13.1	12	3.9	13	4	13.1
0	0	0	2	1.9	2	0.3	2	0	1.9
0	1	0	2	0.8	2	0.1	1	0	0.8
2	5	1	4	1.9	4	0.5	2	0	1.9
1	1	0	5	3.6	5	0.7	4	1	3.6
0	0	0	7	3.3	7	1.0	3	1	3.3
0	1	0	10	8.8	10	2.5	9	2	8.8
0	3	0	3	0.4	3	0.2	0	0	0.4

Table S5.3. (continued)

HG IV (2014)			HG III (2015)			HG III (2014)			HG II (2015)			HG II (2014)		
% of days with sea-ice cover	Sea-ice cover [%]		% of days with sea-ice cover	Sea-ice cover [%]		% of days with sea-ice cover	Sea-ice cover [%]		% of days with sea-ice cover	Sea-ice cover [%]		% of days with sea-ice cover	Sea-ice cover [%]	
	SD	Mean		SD	Mean		SD	Mean		SD	Mean		SD	Mean
5.7	6	1.1	2	1	0	1.6	1	0.2	0	0	0	0.0	0	0.0
11.0	12	3.5	7	9	2	3.0	6	0.9	3	5	1	3.0	5	0.7
30.7	24	12.5	25	18	9	15.1	15	5.0	14	13	4	14.2	13	4.3
8.7	12	3.3	10	9	2	7.4	8	1.6	8	7	2	7.9	7	1.6
11.2	12	3.5	5	6	1	1.1	3	0.3	1	2	0	0.8	2	0.1
1.1	3	0.3	0	2	0	0.3	2	0.1	0	2	0	0.3	2	0.1
17.5	13	4.7	12	10	3	3.3	5	0.8	3	3	0	3.3	3	0.4
42.1	27	19.2	33	22	13	25.4	16	7.4	23	14	6	22.7	15	6.4
23.6	19	8.4	17	12	4	7.1	9	1.8	6	8	1	6.3	8	1.5
4.4	10	1.7	2	6	1	1.1	5	0.5	1	3	0	0.8	3	0.3
13.4	13	3.8	10	12	3	5.2	10	1.9	4	6	1	3.8	6	1.0
21.9	24	10.6	16	19	7	12.0	17	5.3	10	13	4	9.8	14	3.9
17.3	19	7.3	12	14	4	8.5	14	3.9	8	12	3	7.9	12	2.9
50.1	26	19.8	44	21	15	28.8	18	9.5	26	17	8	26.0	17	7.8
3.3	5	0.6	2	4	0	0.8	3	0.2	1	4	0	1.2	4	0.3

Table S5.3. (continued)

N5		HG IV Lander (2015)		HG IV Lander (2014)		HG IV (2015)	
% of days with sea-ice cover	Sea-ice cover [%]	% of days with sea-ice cover	Sea-ice cover [%]	% of days with sea-ice cover	Sea-ice cover [%]	% of days with sea-ice cover	Sea-ice cover [%]
	SD		Mean		SD		Mean
50	29	4	2	0	5.8	5.7	6
	21		1.1				1
56	30	8	10	3	11.9	11.0	11
	24		3.5				3
85	35	28	21	10	23.6	30.7	31
	47		12.5				12
46	27	10	10	2	12.4	8.7	9
	19		3.3				3
65	24	7	8	2	12.2	11.2	11
	21		3.5				4
40	29	0	3	0	3.1	1.1	1
	18		0.3				0
78	33	15	12	4	12.8	17.5	18
	44		4.7				5
71	39	37	24	15	27.3	42.1	42
	47		19.2				19
87	34	20	15	6	18.6	23.6	24
	53		8.4				8
64	25	2	7	1	9.7	4.4	4
	21		1.7				2
54	25	12	13	4	13.2	13.4	13
	19		3.8				4
63	34	18	22	9	23.8	21.9	22
	31		10.6				11
58	31	14	17	6	19.0	17.3	17
	27		7.3				7
91	31	47	23	17	25.5	50.1	50
	58		19.8				20
67	24	2	5	1	5.1	2.9	3
	23		0.6				1

**Table S5.4.** P-values of the Shapiro-Wilk test, Levene's test, Students t-test, Welch t-test and Wilcoxon signed rank sum test to identify differences between the EG and WS area.

	Area	Shapiro test	Levene's test	Students t-test	Welch t-test	Wilcoxon
Grain size fraction >63µm [%]	EG	1.3 <sup>-05</sup>	-	-	-	0.92
	WS	2.6 <sup>-05</sup>				
Median grain size [µm]	EG	2.1 <sup>-11</sup>	-	-	-	3.2 <sup>-04</sup>
	WS	3.0 <sup>-02</sup>				
Water content [%]	EG	3.6 <sup>-03</sup>	0.65	<2.2 <sup>-16</sup>	-	-
	WS	1.9 <sup>-01</sup>				
Porosity	EG	8.4 <sup>-02</sup>	0.01	-	7.9 <sup>-15</sup>	-
	WS	4.6 <sup>-02</sup>				
Chl a [µg/ml sediment]	EG	3.0 <sup>-06</sup>	-	-	-	<2.2 <sup>-16</sup>
	WS	6.5 <sup>-09</sup>				
Phaeo [µg/ml sediment]	EG	2.6 <sup>-06</sup>	-	-	-	<2.2 <sup>-16</sup>
	WS	7.6 <sup>-11</sup>				
CPE [µg/ml sediment]	EG	3.0 <sup>-06</sup>	-	-	-	<2.2 <sup>-16</sup>
	WS	1.3 <sup>-10</sup>				
Chl a/CPE [%]	EG	1.7 <sup>-02</sup>	-	-	-	0.58
	WS	1.1 <sup>-06</sup>				
Chl a/Phaeo	EG	1.0 <sup>-03</sup>	-	-	-	0.49
	WS	2.4 <sup>-08</sup>				
TOC [%]	EG	1.9 <sup>-03</sup>	-	-	-	<2.2 <sup>-16</sup>
	WS	6.4 <sup>-05</sup>				
Organic matter [%]	EG	1.1 <sup>-02</sup>	-	-	-	<2.2 <sup>-16</sup>
	WS	1.8 <sup>-07</sup>				
Protein [µg/ml sediment]	EG	6.0 <sup>-07</sup>	-	-	-	<2.2 <sup>-16</sup>
	WS	8.0 <sup>-06</sup>				
Lipids [nmol/ml sediment]	EG	9.7 <sup>-03</sup>	-	-	-	<2.2 <sup>-16</sup>
	WS	3.4 <sup>-11</sup>				
FDA [nmol/ml sediment h]	EG	2.2 <sup>-06</sup>	-	-	-	3.58 <sup>-10</sup>
	WS	2.5 <sup>-07</sup>				
Bacteria density [Cells x10 <sup>9</sup> /ml sediment]	EG	2.8 <sup>-01</sup>	0.13	-	0.23	-
	WS	4.5 <sup>-01</sup>				
Meiofauna density [Ind./10cm <sup>2</sup> ]	EG	1.5 <sup>-01</sup>	0.13	0.01	-	-
	WS	1.8 <sup>-01</sup>				
Macrofauna density [Ind/m <sup>2</sup> ]	EG	7.3 <sup>-01</sup>	0.09	0.03	-	-
	WS	5.7 <sup>-03</sup>				
Macrofauna biomass [mg/m <sup>2</sup> ]	EG	1.8 <sup>-01</sup>	0.16	0.11	-	-
	WS	7.0 <sup>-06</sup>				
Solute exchnage [mmol Br/m <sup>2</sup> d]	EG	1.1 <sup>-01</sup>	0.30	0.39	-	-
	WS	1.1 <sup>-01</sup>				
BPc	EG	1.7 <sup>-02</sup>	-	-	-	0.86
	WS	1.4 <sup>-07</sup>				
DOU [mmol O <sub>2</sub> /m <sup>2</sup> d]	EG	3.2 <sup>-01</sup>	0.02	-	3.0 <sup>-04</sup>	-
	WS	6.8 <sup>-05</sup>				
TOU [mmol O <sub>2</sub> /m <sup>2</sup> d]	EG	9.4 <sup>-01</sup>	0.16	0.51	-	-
	WS	1.7 <sup>-02</sup>				
DOU/TOU	EG	6.6 <sup>-01</sup>	0.71	0.09	-	-
	WS	5.0 <sup>-01</sup>				

**Table S5.5.** Macrofauna density in individuals m<sup>-2</sup>, values base on sediment core replicates.

SV I	HG I Lander	HG I	HG I	HG I	HG I	EG V	EG IV	EG IV	EG IV	EG III	EG II	EG I	Station
2015	2014	2015	2015	2015	2015	2014	2015	2015	2015	2014	2014	2014	Year
-	12.5	-	-	-	141.8	-	-	-	-	-	-	-	Amphipoda
-	-	-	-	-	-	-	-	-	-	-	-	-	Anthozoa sp
-	-	-	-	-	-	-	-	-	-	141.8	-	-	Aplacophora
-	487.5	564.3	282.2	564.3	141.8	846.5	141.8	-	-	141.8	141.8	141.8	Bivalvia
79.7	-	493.8	846.5	1551.9	-	-	116.9	656.4	-	-	141.8	-	Copepoda
-	37.5	-	-	141.8	141.8	-	-	141.8	-	141.8	-	-	Cumacea
-	-	-	-	-	-	-	-	-	-	-	-	-	Echinodermata
-	-	141.8	-	-	-	-	-	-	-	-	-	-	Gastropoda
-	12.5	141.8	-	-	-	141.8	-	-	-	-	282.2	141.8	Isopoda
395.3	162.5	987.6	564.3	282.2	141.8	-	282.2	141.8	-	-	-	-	Nematoda
-	-	-	-	-	-	-	-	-	-	-	141.8	423.2	Nemertea
-	-	-	141.8	-	-	-	-	-	-	-	-	-	Oligochaeta
-	-	-	-	-	-	-	-	-	-	-	-	-	Ostracoda
313.8	212.5	987.6	846.5	1269.8	75.4	75.4	141.8	1128.7	423.3	141.8	-	141.8	Polychaeta
-	12.5	141.8	-	-	-	-	-	-	-	-	-	-	Scaphopoda
-	-	-	-	141.8	-	-	-	-	-	-	141.8	423.2	Sipunculidae
-	5	141.8	141.8	141.8	282.2	-	-	-	-	-	-	141.8	Tanaidacea
788.9	942.5	3600.6	2823.2	4093.7	924.7	1063.7	682.8	2068.7	423.3	283.6	991.1	1413.6	Total density



Table S5.5. (continued)

HG IV Lander	HG IV	HG IV	HG IV	HG IV	HG III	HG III	HG III	HG III	HG II	HG II	HG II	HG II	HG II	SV I	SV I
2014	2015	2015	2015	2014	2015	2015	2015	2015	2015	2015	2015	2015	2014	2015	2015
16.7	-	141.8	-	-	141.8	-	-	-	-	-	141.8	-	-	-	-
8.3	-	-	-	-	-	-	-	-	-	-	-	-	-	-	-
-	-	-	-	-	-	-	-	-	-	-	-	-	-	-	-
41.7	-	-	-	141.8	282.2	282.2	-	141.8	282.2	141.8	141.8	141.8	-	-	564.3
-	423.3	282.2	423.3	-	7759.6	2539.5	-	-	423.3	-	-	-	-	-	2116.3
41.7	-	-	-	-	-	-	141.8	141.8	141.8	-	141.8	-	-	-	-
-	-	-	-	-	-	-	-	-	-	-	-	-	-	-	141.8
8.3	-	141.8	-	-	141.8	-	-	-	-	-	-	-	-	-	-
16.7	-	141.8	-	-	-	-	282.2	-	141.8	141.8	-	-	-	-	-
58.3	423.3	282.2	282.2	141.8	141.8	282.2	-	141.8	423.3	141.8	564.3	423.2	-	-	2116.3
25	-	-	-	-	-	-	-	141.8	-	-	-	-	-	-	-
-	-	-	-	-	141.8	141.8	423.3	-	-	-	-	-	-	141.8	141.8
8.3	-	-	-	-	-	-	-	-	-	-	-	-	-	-	-
191.7	423.3	846.5	75.4	282.2	75.4	987.6	2398.4	75.4	1551.9	1975.2	1551.9	846.5	75.4	8747.2	
-	-	-	-	-	-	141.8	-	141.8	-	-	-	-	-	-	-
-	-	-	-	-	141.8	-	-	-	-	-	-	-	-	-	-
-	-	-	-	-	-	-	-	141.8	282.2	-	141.8	282.2	282.2	-	-
416.7	1269.8	1836.4	780.8	565.7	8684.5	4517	3245.7	926.1	3246.4	2400.7	2683.6	1551.9	217.3	13827.7	

Portion on entire community [%]	N5		N5		SV IV		SV IV	
	2015	2015	2015	2015	2015	2015	2015	2015
1.0	-	-	-	-	-	141.8	141.8	141.8
0.01	-	-	-	-	-	-	-	-
0.2	-	-	-	-	-	-	-	-
8.6	564.3	423.3	-	564.3	141.8	141.8	282.2	
26	282.2	634.9	211.6	2962.8	-	-	352.8	
2.1	-	141.8	-	282.2	-	-	141.8	
0.2	-	-	-	-	-	-	-	
0.5	-	-	-	-	-	-	-	
2.0	-	-	-	-	-	282.2	-	
12	564.3	423.3	141.8	141.8	141.8	846.5	75.4	
1.0	-	-	-	141.8	-	-	-	
1.3	-	-	-	-	-	-	-	
0.2	-	-	-	-	-	-	141.8	
40	564.3	846.5	1128.7	1834.9	1128.7	1128.7	2257.3	
0.5	-	-	-	-	-	-	-	
1.3	-	-	-	141.8	-	141.8	-	
2.5	141.8	-	-	-	-	141.8	141.8	
	2117	2469.7	1482.1	6069.6	2824.7	3535.1		

**Table S5.6.** Macrofauna biomass in mg blotted wet weight m<sup>-2</sup>, values base on sediment core replicates.

Station	Year	EG I	EG II	EG III	EG IV	EG IV	EG IV	Total biomass
Amphipoda	2014	-	-	-	-	-	-	
Anthozoa sp	2014	-	-	-	-	-	-	
Aplacophora	2014	-	141.1	-	-	-	-	
Bivalvia	2014	29.6	29.6	-	-	-	-	
Cumacea	2014	-	-	1207.6	-	-	-	
Echinodermata	2014	-	-	-	-	-	-	
Gastropoda	2014	-	-	-	-	-	-	
Isopoda	2014	95.9	976.3	-	-	-	-	
Nematoda	2014	-	-	-	-	-	-	
Nemertea	2014	2662.2	752	-	-	-	-	
Oligochaeta	2014	-	-	-	-	-	-	
Ophiuroidea	2014	-	-	-	-	-	-	
Ostracoda	2014	-	-	-	-	-	-	
Polychaeta	2014	173.5	-	93.1	117.1	38.1	117.1	
Porifera	2014	-	-	-	-	-	-	
Scaphopoda	2014	-	-	-	-	-	-	
Sipunculidae	2014	561.5	69.1	-	-	-	-	
Tanaidacea	2014	1.4	-	-	-	-	-	
Total biomass	2014	3524.2	1968.1	1300.7	117.1	811.2	117.1	

Table S5.6. (continued)

HG II	HG II	HG II	HG II	SVIV	SVIV	SVIV	HG I	HG I	HG I	HG I	HG I	HG I	SV I	SV I	SV I	SV I	EG V
2015	2015	2014	2015	2015	2015	2015	2015	2015	2015	2015	2015	2014	2015	2015	2015	2015	2014
-	510.7	-	141.1	1090.6	1.6	-	-	-	1.4	-	-	-	-	-	-	-	-
-	-	-	-	-	-	-	-	-	-	-	-	-	-	-	-	-	-
-	-	-	-	-	-	-	-	-	-	-	-	-	-	-	-	-	-
-	28.2	-	2497.2	2320.8	3792.1	1540.6	25204.6	681.4	1207.6	-	-	7234.8	-	-	-	-	134
-	57.8	-	983.4	1134.3	40.5	-	-	-	2198	-	-	-	-	-	-	-	-
-	-	-	-	-	-	-	-	-	-	-	-	-	-	-	5949.5	-	-
-	-	-	-	-	-	112.9	-	-	-	-	-	-	-	-	-	-	-
135.4	-	-	117.1	-	1.3	747.7	-	-	-	-	-	-	-	-	-	-	24
-	-	26.8	-	94.5	146.1	-	-	-	2.8	-	-	-	-	-	-	-	-
-	-	-	-	40.9	-	-	-	-	-	-	-	-	-	-	-	-	-
-	-	-	-	-	-	-	626.4	-	-	-	-	-	1324.8	-	-	-	-
-	-	-	-	-	-	-	-	-	-	-	-	225.7	-	-	-	-	-
-	-	-	-	-	-	-	-	-	-	-	-	-	-	-	-	-	-
1213.3	1467.3	1084.9	2608.6	6271.2	2576.5	3252	9923.8	1453.2	237	73561	36098	11717	292	-	-	-	-
-	-	-	-	-	-	-	-	-	-	-	-	-	-	-	-	-	-
-	-	-	-	-	344.1	550.2	-	-	-	-	-	-	-	-	-	-	-
-	-	-	829.6	214.4	-	-	-	842.3	-	-	-	-	-	-	-	-	-
-	-	38.1	-	-	26.8	-	-	29.6	173.5	-	-	-	-	-	-	-	-
1348.8	2064.1	1149.8	6918.7	10952.3	6929	6203.4	35754.8	3006.5	3820.4	73787	50608	11717	45	-	-	-	-

Table S5.6. (continued)

Portion on entire community [%]	N5	N5	N5	HG IV	HG IV	HG IV	HG IV	HG IV	HG IV	HG III	HG III	HG III	HG III	HG III	HG II
	2015	2015	2015	2015	2015	2015	2015	2015	2015	2015	2015	2015	2015	2015	2015
0.9	-	-	-	426.6	-	-	-	-	-	409.1	-	-	-	-	-
0.04	-	-	-	107.2	-	-	-	-	-	-	-	-	-	-	-
0.05	-	-	-	-	-	-	-	-	-	-	-	-	-	-	-
16	40.9	46.6	-	4.3	-	-	-	22.6	77.6	-	-	-	32.4	-	-
2.7	-	1100.5	-	87.8	-	-	-	-	-	36.7	323.1	-	-	-	-
2.1	-	-	-	-	-	-	-	-	-	-	-	-	-	-	-
0.4	-	-	-	48.3	-	719.5	-	-	273.7	-	-	-	-	-	-
0.9	-	-	-	1.3	-	-	-	-	-	536.1	-	-	-	16.9	-
0.2	-	-	-	1.7	-	-	-	-	180.6	-	-	-	1.4	-	-
1.4	-	-	-	80.3	-	-	-	-	-	-	-	-	397.8	-	-
1.2	-	-	-	-	-	-	-	-	-	409.1	-	-	-	-	-
0.1	-	-	-	-	-	-	-	-	-	-	-	-	-	-	-
0.001	-	-	-	1.8	-	-	-	-	-	-	-	-	-	-	-
57	56.4	134	812.6	76.9	244.1	114.3	1410.8	77.6	380.9	846.5	931.2	419	667.3	-	-
14	-	5220.1	17089.4	-	2991	126.3	2327.9	-	12191	-	-	-	-	-	-
1.2	-	-	-	-	-	-	-	-	-	2497.2	-	-	40.9	-	-
2.1	-	-	-	-	-	-	-	-	3493.2	-	-	-	-	-	-
0.1	-	-	-	-	-	-	-	-	-	-	-	-	32.4	56.4	-
	97.3	6501.1	17902.1	836	3235	960.1	3738.7	100.2	16519.5	5066.3	1913.1	1247.1	740.7	-	-

**Table S5.7.** Meiofauna density in individuals 10 cm<sup>-2</sup>, values base on sediment core replicates.

HG I	HG I	HG I	SV I	SV I	SV I	EG V	EG IV	EG IV	EG IV	EG IV	EG III	EG II	EG I	Station
2015	2015	2015	2015	2015	2015	2014	2015	2015	2015	2015	2014	2014	2014	Year
-	-	-	-	-	-	-	-	-	-	-	-	-	-	Cladocera
-	-	-	3.2	3.2	3.2	-	-	-	-	-	-	-	-	Cnidaria
20	3.2	5.9	111.4	11.9	28.6	9.5	15.9	-	3.2	3.2	3.2	9.5	6.4	Copepoda
-	-	-	3.2	-	-	-	-	-	-	-	-	-	-	Halacaroidea
-	-	9.5	22.3	6.4	9.5	-	-	-	-	-	-	-	9.5	Kinorhyncha
22.3	20	44.6	82.8	73.2	85.9	15.9	3.2	15.9	3.2	-	-	-	9.5	Nauplii
20	2.5	391.5	786.2	671.7	1142.8	21.8	7.3	248.3	159.2	226.7	82.8	63.7	197.4	Nematoda
3.2	-	-	12.7	20	12.7	-	3.2	3.2	-	-	-	-	-	Oligochaeta
6.4	-	6.4	57.3	20	47.7	3.2	-	6.4	-	-	-	9.5	3.2	Ostracoda
9.5	3.2	16	31.8	35.2	20	3.2	3.2	3.2	-	-	-	-	3.2	Polychaeta
-	-	-	-	-	-	3.2	-	-	-	-	-	-	-	Porifera
-	-	-	-	-	-	-	-	-	-	-	-	-	-	Priapulida
-	-	-	6.4	-	6.4	-	-	-	-	-	-	-	-	Rotifera
-	-	3.2	3.2	3.2	-	-	-	-	-	-	-	-	-	Sipuncula
-	-	-	-	-	-	-	-	-	3.2	-	-	-	-	Tanaidacea
-	-	-	12.7	31.8	-	-	-	-	-	-	-	-	-	Tardigrada
-	-	-	3.2	-	-	-	-	-	-	-	-	-	-	Unidentified
81.4	28.9	477.1	1133.2	876.4	1353.7	56.9	16.9	292.9	165.5	229.9	85.9	82.8	229.2	Total density

**Table S5.7.** (continued)

HGIV	HGIV	HGIV	HGIV	HGIV	HGIII	HGIII	HGIII	HGIII	HGIII	HGII	HGII	HGII	HGII	HGII	HG I Lander	HG I Lander	HG I Lander	HG I Lander	HG I Lander		
2015	2015	2015	2015	2015	2015	2015	2015	2015	2015	2015	2015	2015	2015	2015	2015	2015	2015	2015	2015	2014	
-	-	-	-	-	-	-	-	-	-	-	-	-	-	-	-	-	-	-	-	-	
-	-	-	-	-	-	-	-	-	-	-	-	-	-	-	-	-	-	-	-	-	
3.2	6.4	6.4	12.7	12.7	12.7	6.4	6.4	6.4	6.4	3.2	3.2	3.2	6.4	25.5	6.4	6.4	-	-	-	9.5	
-	3.2	-	-	-	-	-	-	-	-	-	-	-	-	-	-	-	-	-	-	-	-
-	-	-	6.4	3.2	3.2	3.2	6.4	6.4	6.4	-	-	-	-	-	-	-	-	-	-	-	-
9.5	-	-	3.2	6.4	6.4	6.4	6.4	6.4	6.4	3.2	3.2	3.2	12.7	15.9	6.4	6.4	3.2	3.2	3.2	3.2	3.2
493.4	44.3	334.2	353.3	235.6	165.5	235.5	257.8	168.8	226.7	366.6	241.9	515.7	437	13.6	13.6	437	13.6	13.6	13.6	331.4	331.4
-	-	-	9.5	-	-	-	3.2	-	-	-	-	-	-	-	-	-	-	-	-	-	-
-	-	-	3.2	-	-	6.4	6.4	-	3.2	3.2	-	3.2	-	3.2	-	-	-	-	-	-	3.2
3.2	-	-	9.5	3.2	-	-	9.5	3.2	3.2	-	3.2	6.4	3.2	6.4	3.2	3.2	3.2	3.2	3.2	6.4	6.4
-	-	3.2	-	-	-	-	-	-	-	-	-	-	-	-	-	-	-	-	-	-	-
-	-	-	-	-	-	-	-	-	-	-	-	-	-	-	-	-	-	-	-	-	-
-	-	-	-	-	-	-	-	-	-	-	-	-	-	-	-	-	-	-	-	-	-
6.4	-	-	-	-	-	-	-	6.4	-	-	-	-	-	-	-	-	-	-	-	-	-
-	-	-	-	-	-	-	-	-	-	-	-	-	-	-	-	-	-	-	-	-	-
-	3.2	-	-	-	-	-	-	-	-	-	-	-	-	-	-	-	-	-	-	-	-
515.7	57	343.8	397.9	261	165.5	268.3	283.3	184.7	249	392	264.2	573	456.1	19.9	456.1	19.9	19.9	19.9	19.9	353.7	353.7

Table S5.7. (continued)

Portion on entire community [%]	N5		N5		SV IV		SV IV		HG IV Lander		HG IV Lander	
	2015	2015	2015	2015	2015	2015	2015	2015	2015	2015	2014	2014
0.02	-	-	3.2	-	-	-	-	-	-	-	-	-
0.05	-	-	-	-	-	-	-	-	3.2	-	-	-
3.4	-	-	6.4	15.9	22.3	-	9.5	28.6	3.2	-	-	-
0.1	-	-	-	-	-	3.2	-	-	-	-	-	-
0.6	-	-	-	3.2	-	3.2	-	-	-	-	-	-
4.5	9.5	3.2	3.2	20	22.3	6.4	6.4	22.3	-	-	-	-
86	324.7	299.2	114.6	276.9	518.9	261.2	34.6	52.9	114.6	11.9	76.4	76.4
0.9	9.5	12.7	9.5	-	-	3.2	6.4	-	-	-	-	-
1.7	-	3.2	-	6.4	3.2	6.4	-	-	3.2	-	-	-
1.8	6.4	3.2	3.2	9.5	6.4	3.2	3.2	-	3.2	-	-	-
0.05	-	-	-	-	-	-	-	-	-	-	-	-
0.02	-	-	-	-	-	-	-	-	-	-	-	-
0.2	-	3.2	3.2	-	3.2	-	-	-	-	-	-	-
0.1	-	-	-	-	-	-	-	-	-	-	-	-
0.1	-	-	-	-	-	-	-	-	-	-	-	-
0.3	-	-	-	-	-	-	-	-	-	-	-	-
0.2	-	-	-	-	-	-	-	9.5	9.5	-	-	-
	350.2	324.7	130.5	305.6	577.1	324.9	56.9	78.4	124.1	11.9	76.4	76.4

**Table S5.8.** Eigenvalue, explained proportion and species score of the PCA to explore if data from 2014 and 2015 differ. In dimension two, the species score of Year of Sampling is high and goes along with high Phaeo, CPE, and Organic matter values. This means, that on the second dimension, which explains only 15.4% of the total variability in the dataset, the differences between the years are mostly explained by differences in the food supply, which in turn can be explained by the different sampling periods in 2014 and 2015 (see Table 5.1).

		Dim. 1	Dim. 2
Importance of components	Eigenvalue	6.4	2.2
	Proportion explained	45.9	15.4
Species scores	Year of sampling	0.03	-0.72
	Water depth	-1.56	<0.01
	Sea-ice cover	-1.54	0.11
	% of days with sea ice	-1.52	0.21
	Grain size >63 $\mu$ m	-1.06	-0.45
	Median grain size	-1	1
	TOC	1.46	0.42
	Organic matter	0.53	0.88
	Chl <i>a</i>	1.24	-0.82
	Phaeo	1.29	-0.99
	CPE	1.3	-0.98
	FDA	0.87	-0.71
	Protein	0.96	0.83
Lipids	-0.28	-0.31	

**Table S5.9.** P-values of Shapiro-Wilk test and p-values of the slope of the linear regression between water depth and a determined parameter within the HSC and LSC categories. If the p-value of the Shapiro-Wilk test is < 0.05, the residuals over the slope of the linear regression did not follow the Gaussian distribution, linear regression analyzes were not allowed. Therefore, a significance test of the slope could not be performed (cases marked with an X). A p-value <0.05 of the linear regression between water depth and the parameter indicates a significant correlation with water depth. The table only shows parameters, for which at least in one sea-ice category the p-value of the Shapiro-Wilk test was >0.05. The abbreviation "Log<sub>e</sub>" refers to a natural logarithmic transformation of the data and "Sqrt" refers to a square root transformation.

Parameter	Sea-ice category	Transformation	P-value of Shapiro-Wilk test	P-value of correlation water depth vs parameter
Grainsize fraction >63 $\mu$ m	HSC	Log <sub>e</sub>	0.1335	<2.2 <sup>-16</sup>
	LSC	Log <sub>e</sub>	6.08 <sup>-5</sup>	X
Median grain size	–	–	–	–
Water content	HSC	Log <sub>e</sub>	0.2555	0.982
	LSC	Log <sub>e</sub>	0.5499	8.03 <sup>-16</sup>
TOC	–	–	–	–
Organic matter	–	–	–	–
Chl <i>a</i>	HSC	Log <sub>e</sub>	0.02738	X
	LSC	Log <sub>e</sub>	0.8455	6.27 <sup>-10</sup>
Phaeo	HSC	Sqrt	0.4688	3.64 <sup>-05</sup>
	LSC	Sqrt	0.2599	4.53 <sup>-11</sup>
CPE	HSC	Sqrt	0.436	5.88 <sup>-05</sup>
	LSC	Sqrt	0.2966	4.16 <sup>-11</sup>
Chl <i>a</i> /Phaeo	HSC	Log <sub>e</sub>	0.1722	6.99 <sup>-06</sup>
	LSC	Log <sub>e</sub>	0.1711	0.393



**Table S5.9.** (continued)

Chl <i>a</i> /CPE	HSC	Sqrt	0.2957	5.01 <sup>-06</sup>
	LSC	Sqrt	5.681 <sup>-3</sup>	X
Lipid	HSC	–	0.2131	1.71 <sup>-07</sup>
	LSC	–	5.06 <sup>-6</sup>	X
Protein	HSC	Log <sub>e</sub>	2.981 <sup>-3</sup>	X
	LSC	Log <sub>e</sub>	0.1535	1.49 <sup>-10</sup>
FDA	HSC	Sqrt	0.273	0.09921
	LSC	Sqrt	0.1974	0.02761
Bacteria density	HSC	Sqrt	0.02426	X
	LSC	Sqrt	0.1301	4.695 <sup>-03</sup>
Meiofauna density	HSC	–	0.4126	0.3965
	LSC	–	0.4029	0.8904
Macrofauna density	HSC	Log <sub>e</sub>	0.5036	0.3176
	LSC	Log <sub>e</sub>	0.3221	0.03781
Macrofauna biomass	HSC	Log <sub>e</sub>	0.2181	0.358
	LSC	Log <sub>e</sub>	0.9267	0.0916
Bioirrigation	HSC	Log <sub>e</sub>	0.2556	0.1884
	LSC	Log <sub>e</sub>	0.4628	0.4846
BPc	HSC	–	0.8313	3.97 <sup>-04</sup>
	LSC	–	0.7673	2.60 <sup>-3</sup>
DOU	HSC	Log <sub>e</sub>	0.3479	0.7941
	LSC	Log <sub>e</sub>	0.219	3.45 <sup>-5</sup>
TOU	HSC	Log <sub>e</sub>	0.6604	0.8043
	LSC	Log <sub>e</sub>	0.5351	0.1999

**Table S5.10.** Results of SIMPER analysis regarding the sea-ice categories HSC and LSC. The table shows the three most contributing taxa to the within-group similarity and to the dissimilarity between the groups.

Meiofauna density				Macrofauna density				Macrofauna biomass			
HSC		LSC		HSC		LSC		HSC		LSC	
In-group similarity		In-group similarity		In-group similarity		In-group similarity		In-group similarity		In-group similarity	
Taxa	Contribution [%]	Taxa	Contribution [%]	Taxa	Contribution [%]	Taxa	Contribution [%]	Taxa	Contribution [%]	Taxa	Contribution [%]
Nematoda	81	Nematoda	77	Polychaeta	53	Polychaeta	45	Polychaeta	63	Polychaeta	76
Nauplii	5	Copepoda	9	Copepoda	17	Nematoda	23	Bivalvia	16	Bivalvia	9
Copepoda	5	Nauplii	7	Bivalvia	14	Bivalvia	10	Cumacea	12	Porifera	3
Dissimilarity between groups				Dissimilarity between groups				Dissimilarity between groups			
Taxa		Contribution [%]		Taxa		Contribution [%]		Taxa		Contribution [%]	
Nematoda		33		Copepoda		25		Polychaeta		22	
Nauplii		14		Polychaeta		15		Porifera		18	
Copepoda		13		Nematoda		14		Bivalvia		13	

**Table S5.11.** ANOSIM and SIMPER results of the meio- and macrofauna community within water depth categories. The table shows that significant differences in the meiofauna community are only found between the shallow station SV I (275 m) and all other stations. Within the macrofauna community differences are found between 1000 m and 2000 m, additionally. The most contributing taxa regarding the within-group similarity within the water depth categories and the dissimilarity between the water depth categories are given in Table S5.10.

Meiofauna density												
ANOSIM	Global R		0.219									
	p-value		0.01									
	Pairwise test	Depth category pairs	275-1000 m	275-1500 m	275-2000 m	275-2500 m	1000-1500 m	1000-2000 m	1000-2500 m	1500-2000 m	1500-2500 m	2000-2500 m
		R	0.92	1	0.86	0.91	0.13	0.11	0.15	-0.14	-0.06	-0.06
p-value		0.01	0.02	0.02	<0.01	0.15	0.18	0.07	0.87	0.63	0.69	
SIMPER	Depth category		275 m		1000 m		1500 m		2000 m		2500 m	
	In-group similarity [%]		67		78		70		67		68	
	Depth category pairs		275-1000 m	275-1500 m	275-2000 m	275-2500 m	1000-1500 m	1000-2000 m	1000-2500 m	1500-2000 m	1500-2500 m	2000-2500 m
	Dissimilarity [%]		41	55	56	56	28	30	33	29	31	31
Macrofauna density												
ANOSIM	Global R		0.2									
	p-value		0.008									
	pairwise test	Depth category pairs	275-1000 m	275-1500 m	275-2000 m	275-2500 m	1000-1500 m	1000-2000 m	1000-2500 m	1500-2000 m	1500-2500 m	2000-2500 m
		R	0.57	0.19	-0.10	0.33	-0.01	0.25	0.16	-0.04	0.16	0.24
p-value		0.01	0.2	0.61	0.06	0.44	0.06	0.02	0.62	0.19	0.06	
SIMPER	Depth category		275 m		1000 m		1500 m		2000 m		2500 m	
	In-group similarity [%]		39		56		48		35		51	
	Depth category pairs		275-1000 m	275-1500 m	275-2000 m	275-2500 m	1000-1500 m	1000-2000 m	1000-2500 m	1500-2000 m	1500-2500 m	2000-2500 m
	Dissimilarity [%]		61	67	60	60	46	56	52	59	56	59
Macrofauna biomass												
ANOSIM	Global R		0.35									
	p-value		0.01									
	pairwise test	Depth category pairs	275-1000 m	275-1500 m	275-2000 m	275-2500 m	1000-1500 m	1000-2000 m	1000-2500 m	1500-2000 m	1500-2500 m	2000-2500 m
		R	0.39	0.56	0.49	0.78	0.27	0.38	0.50	-0.09	0.16	0.12
p-value		0.04	0.03	0.04	0.20	0.07	0.01	<0.01	0.76	0.18	0.14	
SIMPER	Depth category		275 m		1000 m		1500 m		2000 m		2500 m	
	In-group similarity [%]		52		41		35		23		33	
	Depth category pairs		275-1000 m	275-1500 m	275-2000 m	275-2500 m	1000-1500 m	1000-2000 m	1000-2500 m	1500-2000 m	1500-2500 m	2000-2500 m
	Dissimilarity		68	81	85	89	68	73	79	71	74	74

**Table S5.12.** Results of the two-way crossed PERMANOVA on standardized and fourth roots transformed macrofauna density and macrofauna biomass data based on a Bray Curtis similarity. The term “sp” includes the sea-ice categories HSC and LSC and the term “de” the water depth category levels 1000 m, 1500 m, 2000 m, and 2500 m.

	Source	df	SS	MS	Pseudo-F	P(perm)	perms
Macrofauna density	sp	1	113.59	113.59	3.219	0.0075	9948
	de	3	168.28	56.093	1.590	0.0568	9917
	sp x de	3	157.13	52.376	1.480	0.0857	9903
	Res	21	741.09	35.29	-	-	-
	Total	28	1132.2	-	-	-	-
Macrofauna biomass	sp	1	3116.9	3116.9	3.701	0.0511	4512
	de	3	7114.5	2371.5	2.816	0.0584	9558
	sp x de	3	6421.1	2140.4	2.542	0.0342	9905
	Res	3	2526.4	842.13	-	-	-
	Total	10	19235	-	-	-	-

**Table S5.13.** Results of the PERMANOVA pairwise test on standardized and fourth roots transformed macrofauna density and macrofauna biomass data based on a Bray Curtis similarity.

	Groups	p-value	P(perm)	P(MC)	t
Macrofauna density	1000 m-1500 m	0.4546	8260	-	0.989
	1000 m-2000 m	0.0116	9427	-	1.836
	1000 m-2500 m	0.0004	9952	-	2.446
	1500 m-2000 m	0.0192	2470	-	1.841
	1500 m-2500 m	0.0072	9924	-	2.139
	2000 m-2500 m	0.0424	9938	-	1.651
	LSC-HSC	0.0048	9949	-	2.055
Macrofauna biomass	1000 m-1500 m	0.3311	15	0.4804	1.0314
	1000 m-2000 m	0.1196	15	0.2451	1.7717
	1000 m-2500 m	0.0187	420	0.0464	2.2335
	1500 m-2000 m	No test			
	1500 m-2500 m	0.115	38	0.1266	1.9021
	2000 m-2500 m	0.1619	38	0.2902	1.291
	LSC-HSC	0.0515	4488	0.0787	1.9239

## Acknowledgment

We thank the officers and crew members of RV Polarstern for their help during our expeditions to the Fram Strait. Furthermore, we like to thank Volker Asendorf and Axel Nordhausen for preparing the Lander and executing the deployment and recovery during the expeditions, Cäcilia Wiegand and Ines Schröder for the production of the Clark-typ oxygen sensors, Bart Beuselinck for granulometric analyzes, Anja Pappert, Svenja Schütte and Meike Spill for biogenic compound and bacterial density analyzes, Naomi De Roeck, Thomas Luypaert, Emiel Platjouw, Ellen Pape and Katja Guilini for processing of macro- and meiofauna samples, Thomas Krumpfen for providing the additional sea-ice concentrations at station EG V and Pier Buttigieg and Christiane Hassenrück for support regarding statistical analyzes in R. This research was funded by the European Union FP7 Project SenseOCEAN Marine Sensors for the 21st century (Grant Agreement Number 614141), by the Flemish Research Fund, by institutional funds of the Alfred-Wegener-Institut, Helmholtz-Zentrum für Polar-und Meeresforschung, and by the infrastructure framework of the FRAM project (Frontiers in Arctic Marine Monitoring).

## 6 Authors contribution to manuscripts I–III

---

### 6.1 Contribution to manuscript I

I developed the study idea, provided resources, performed sediment sampling, *in situ* PAR measurement at the location 'Creek', oxygen flux measurements and calculations, calculation of diatom biomasses, statistical analyzes, elaborated the figures and wrote the draft of the manuscript.

The co-authors of the manuscript are Adil Yousif Al-Handal, Angela Wulff, Dolores Deregibus, Ulrike Braeckman, María Liliana Quartino, and Frank Wenzhöfer. AYA and AW analyzed the sediment samples regarding present diatom taxa and measured the diatom cell sizes. DD and MLQ provided *in situ* PAR data from the locations 'Faro' and 'Isla D'. UB supervised oxygen flux measurements and decisions regarding statistical analyzes. FW was responsible for funding acquisition. At the current state, AYA, AW and UB reviewed the draft version and contributed to the discussion. Before submission to the journal 'Frontiers in Marine Science', the remaining co-authors will be invited to contribute to the discussion.

### 6.2 Contribution to manuscript II

I calculate diffusive oxygen fluxes from *in situ* microprofiles. Furthermore, I calculated total and diffusive nutrient and dissolved inorganic carbon fluxes from pore water profiles, analyzes prokaryotic biomasses and was responsible for sediment analyzes regarding total carbon, total organic carbon, and total nitrogen. In addition, I performed the statistical analyzes, elaborated the figures and wrote the draft of the manuscript.

The co-authors of the manuscript are Francesca Pasotti, Susana Vázquez, Nene Lefaible, Anders Torstensson, Walter MacCormack, Frank Wenzhöfer, and Ulrike Braeckman. UB and FW developed the study idea. The work at the study site (*in situ* dive work, sediment sampling, and storage, determination of oxygen concentrations by Winkler titration) was performed by FP, SV, AT, UB and me. UB calculate total oxygen fluxes, performed grain size analyzes and was responsible for pigment and macrofauna analyzes. For the latter task, UB was supported by NL, which also calculated the BPc. Meiofauna analysis was performed by FP and NL, while prokaryotic densities were determined by SV. FW, WMC, and UB were responsible for funding acquisition, while resources were provided by FW, UB and me. FW and UB were also responsible for supervision during the field campaign and during the laboratory analyzes, data analyzes and the writing process.

All co-authors contribute to the final manuscript, which was submitted to the 'PLoS One' journal and is currently under review (first reviewer round). The manuscript presented in this thesis was edited in accordance with the formatting style of this thesis, but no changes were conducted regarding the content.

### 6.3 Contribution to manuscript III

I calculate diffusive oxygen fluxes, total bromide fluxes, analyzed microbial densities, and was responsible for sediment analyzes regarding total carbon, total organic carbon, and total nitrogen. In addition, I elaborated the figures and wrote the draft of the manuscript.

The co-authors of the manuscript are Ulrike Braeckman, Christiane Hasemann, and Frank Wenzhöfer. FW and UB developed the study idea. During the field campaigns *in situ* and *ex situ* oxygen flux measurements (total and diffusive oxygen fluxes) were performed by UB and me, while CH analyzed pigments and FDA. UB calculate total oxygen fluxes, performed grain size analyzes, and was responsible for pigment, bromide concentration and macrofauna analyzes and calculated the BPc. CH was responsible for analyzes regarding proteins and lipids. UB and FW provided resources and supervised my during the field campaign and during the laboratory analyzes, data analyzes and the

writing process. Statistical analyzes were performed by CH and me. FW was responsible for funding acquisition.

All co-authors contribute to the final manuscript, which was submitted to the 'Biogeosciences' journal and is currently under review (invited to second reviewer round). The manuscript presented in this thesis was edited in accordance with the formatting style of this thesis, but no changes were conducted regarding the content.





## 7 Discussion

---

### 7.1 The impact of particle release on the biological carbon cycle in shallow coastal polar regions

#### 7.1.1 Effects of particle release on primary production in shallow coastal polar regions

The general temperature increase in the Southern and Arctic Ocean led to an increased glacial and permafrost soil melt in coastal areas of the Southern and Arctic Ocean [Turner et al., 2005; Vaughn et al., 2013; Vonk et al., 2015]. As a result, more particles, freshwater, and nutrients are transported into the marine habitats of the Southern and Arctic Ocean [Monien et al., 2014; Sahade et al., 2015; Vonk et al., 2015; Wassmann, 2015]. Secondary effects of an increased particle release are higher turbidity in the water column and an enhanced sediment accumulation. These secondary effects reduce the light availability and thus, might influence primary productivity. The investigated Potter Cove (Southern Ocean) is heavily influenced by the melting Fourcade glacier [Rückamp et al., 2011; Sahade et al., 2015; Monien et al., 2017] and thus, an ideal area for studying the impact of sediment accumulation on primary production.

The MPB in Potter Cove is dominated by diatoms [Al-Handal and Wulff, 2008a], which showed a reduced primary production when exposed to high turbidities and a high sedimentation rates [section 3]. Directly at the glacial front, net primary production was even completely suppressed. Therefore, the results presented in section 3 confirmed the

first hypothesis of this thesis, that glacial melt-related particle release affects MPB primary productivity in the studied location in the Southern Ocean. An impact on the diatom community structure, however, was not found.

Southern Ocean diatoms have been reported to be well adapted to low light conditions. Light saturation can already be reached at  $11 \mu\text{mol photons m}^{-2} \text{s}^{-1}$  [Palmisano et al., 1985; Rivkin and Putt, 1987; Gómez et al., 2009]. In Potter Cove, the light saturation was not investigated, but the light compensation point (net primary production and mineralization are balanced) of  $26 \mu\text{mol photons m}^{-2} \text{s}^{-1}$  was frequently exceeded on annual and daily scales (Figure 3.2). Therefore, it is unlikely that the light-suppressing impact of the increased turbidity was responsible for the reduced primary production. It is more likely that the enhanced sedimentation was responsible for the lower primary productivity [Wulff et al., 1997]. If covered with sediment, the light availability for MPB drops drastically towards zero. As benthic diatoms are able to migrate through the sediment, they may move vertically upwards with speeds between  $0.6\text{--}1.0 \text{ mm h}^{-1}$  to again reach ideal light conditions [Hopkins, 1963; Harper, 1977; Hay et al., 1993; Consalvey et al., 2004]. Nevertheless, full recovery in terms of MPB primary productivity would have taken longer than two weeks [Wulff et al., 1997], and only be possible if sedimentation would cease.

The degree of the reduction of MPB primary production depends on the volume and rate of sedimentation. A linear regression between the median sediment accumulation rates from Pasotti et al. [2015] and measured carbon fluxes at  $70 \mu\text{mol photons m}^{-2} \text{s}^{-1}$  [section 3], reveals a reduction of MPB primary productivity of  $4.6 \text{ mmol C m}^{-2} \text{d}^{-1}$  (= 10% of MPB primary production) per  $0.1 \text{ g sediment cm}^{-2} \text{yr}^{-1}$  of sediment accumulation. The sedimentation rates in Potter Cove ranged between  $0.06\text{--}1.17 \text{ g sediment cm}^{-2} \text{yr}^{-1}$  [Pasotti et al., 2015]. At the shelf regions of the Arctic Ocean, sedimentation rates ranged between  $0.03\text{--}2.20 \text{ g sediment cm}^{-2} \text{yr}^{-1}$  [Kuzyk et al., 2017]. As MPB primary production seems to be affected by sediment accumulation in shallow coastal regions of both polar Oceans [Woelfel et al., 2008; section 3], increased sedimentation rates could lead to a significant reduction or even a complete suppression of MPB primary productivity in the Southern and Arctic Ocean.

Within this thesis, the impact of secondary effects on MPB primary production was investigated. However, above-mentioned secondary effects may also affect macroalgae and pelagic primary production, which needs to be considered to understand the effects particle release on polar primary production in shallow coastal polar regions on ecosystem level. Polar macroalgae, as well important primary producers in shallow coastal polar regions [section 1], have also been reported to be well adapted to low light conditions [Gómez et al., 2009]. Therefore, again it is unlikely that an increased turbidity is responsible for a reduced macroalgae primary production. Particles may occasionally cover the blades of macroalgae, but hydrodynamic processes and the associated induced movements of the blades frequently shake free the majority of accumulated sediment [Roleda et al., 2008] with only long-term sediment coverage (>16 days) known to damage the photosynthetically apparatus of macroalgae [Roleda and Dethleff, 2011]. Therefore, a direct effect on the macroalgae primary production due to increased particle exposure at polar coasts is unlikely. However, sedimentation affected the depth distribution and diversity of macroalgae and prohibited the recruitment and early development stages of macroalgae [Spurkland and Iken, 2011; Bartsch et al., 2016; Zacher et al., 2016; Traiger and Konar, 2018]. This impact on early development stages likely reduces the contribution of macroalgae primary production to the total polar primary production. On the other hand, sedimentation may increase the areas where MPB communities are able to establish [section 4]. Hence, the contribution of the MPB primary production to the total primary production may increase, in case sedimentation rates stay moderate [section 3].

Phytoplankton primary production in polar regions may not be impacted by an increased particle release, contrasting to the benthic primary producers. Again, most species have been reported to be generally adapted to low light conditions [Kirst and Wiencke, 1995; Lacour et al., 2017]. Aside from particle release, melting glaciers and permafrost soils release also large amounts of nutrients and iron into the marine environment [Monien et al., 2014; Vonk et al., 2015; Monien et al., 2017]. This may enhance phytoplankton primary production in shallow coastal polar regions [Schloss, 2017; Kim et al., in press]. Such a hypothesis is supported by findings of Pabi et al. [2008], which determined the highest primary production values at arctic estuaries, and

by Klöser et al. [1994], which observed higher primary production in the sedimentation plume at a glacial river runoff. A boost in MPB or macroalgae primary production due to the increased availability of nutrient is, however, unlikely. Their reduction in primary production is a result of a light suppression [section 3] and a prohibited settling success, respectively [Spurkland and Iken, 2011; Bartsch et al., 2016; Zacher et al., 2016; Traiger and Konar, 2018], both caused by particle cover.

The described impact on polar primary production is limited to the summer season, as glacial and permafrost soils melt intensity undergo seasonal changes accompanied by a seasonal change in intensity of the particle and nutrient release [Schloss et al., 1999; Fisher et al., 2012; Deregibus et al., 2016; Monien et al., 2017]. Other factors influencing the distribution of particles in the polar shallow coastal areas may vary on daily scales and are influenced by the local current system, current speeds, wind speeds and wind directions [Klöser et al., 1994]. As a result, the spatial and seasonal limitations of glacial and permafrost soil melt impact on polar primary production is difficult to assess from observations and perhaps local models potentially illuminate the processes more succinctly.

### 7.1.2 Effects of particle release on benthic mineralization in shallow coastal polar regions

The release of particles effects primary production in shallow coastal polar regions and thus, a main process in the biological carbon cycle. The second main process in the biological carbon cycle is the mineralization of organic carbon. Owing to the relationship between primary production and benthic mineralization [section 4; section 7.3] and due to the direct impact of released particles on benthic fauna biomass, density and structure [Pasotti et al., 2015; Sahade et al., 2015; Lager et al., 2017], it was investigated whether particle release by glacial and permafrost soil melt also affects benthic mineralization.

In Potter Cove (Antarctic), shallow coastal benthic mineralization was affected by glacial melt-related particle release and the effects of the associated sedimentation [section 4]. Compared to a location impacted by low sediment accumulation rates, a 30% enhanced benthic mineralization was observed at a location impacted by

intermediate sediment accumulation rates; whereas a 40% reduced benthic mineralization was observed at a location impacted by high sediment accumulation rates. Thereby, the second hypothesis of this thesis, that glacial melt-related particle release affects the benthic mineralization in the shallow coastal Southern Ocean, was confirmed. This pattern was explained by the physiological reactions of the dominating macrofauna [section 4]. As manuscript II was the first that addressed the topic of the impact of particle release on shallow, coastal benthic community mineralization in the Southern Ocean, the results can only be compared with studies from other shallow coastal locations.

In the Norwegian Fanafjorden, benthic mineralization in 60–90 m water depths seemed to be not impacted by increased particle fluxes but was positively correlated with the particulate organic carbon content [Wassmann, 1984]. This may explain the increased mineralization at Creek in Potter Cove, besides the physiological reaction of the present macrofauna on sedimentation [section 4]. The close-by river runoff at Creek supplied nutrients and iron to Potter Cove [Monien et al., 2014; Monien et al., 2017] which enhanced primary production in the turbidity plume at Creek [Klöser et al., 1994] and led to an increased organic carbon supply (indicated by highest CPE values at location Creek) [section 4]. Hence, benthic mineralization can increase under moderate sedimentation rates and if more organic particles are provided [Wassmann, 1984; section 4 (mineralization at location Creek)].

At the Faroe Islands, the lowest total oxygen uptake was measured in months with the highest total particulate material flux (water depths: 20–60 m). However, the diffusive oxygen uptake did not show particularly marked variations throughout a year [Norði et al., 2018]. The diffusive to total oxygen flux ratio expresses the microbial contribution to the total mineralization [Glud, 2008]. As the microbial mineralization was stable during the investigated time period, the variation in the total mineralization was caused by the benthic fauna. Thus, the study of Norði et al. [2018] confirmed that the benthic fauna can react with suppressed respiration rates (and the associated reduced mineralization rates) in periods when a high particle flux is present. Therefore, benthic mineralization can decrease under high sedimentation rates [Norði et al., 2018; section 4 (mineralization at location Isla D)].

Particles released by glacial melt were >90% inorganic [Khim et al., 2007] and thus 'dilute' the organic material in the water column and at the sea floor. An addition of organic particles, resulting from boosted primary production in the water column [Schloss, 2017; Kim et al., in press], might balance out the 'dilution' and could even result in higher food availability for the benthic macrofauna. This would result in increased mineralization rates [section 4 (at location Creek)]. At high sedimentation rates, however, suspension feeders and deposit feeders, which are the dominating benthic feeding modes in the area [Levinton, 2009], had to ingest more particles to cover their organic carbon demand [Lopez and Levinton, 1987]. This may lead to a reduction of macrofauna densities [Ellis et al., 2017]. In addition, the high inorganic 'dilution' takes place at the glacial front, where macrofauna mortality by ice scouring further lowers macrofauna densities and biomass [Pasotti et al., 2015] and thereby benthic mineralization [section 4]. Therefore, the inorganic carbon proportion of glacial melt-related particle release can lead to decreasing benthic mineralization, if not balanced out by organic input from pelagic primary production.

Particles released by permafrost soil melt are 65–93% inorganic and therefore can contain a higher percentage of organic material compared to glacial melt-related particles [Rachold et al., 2004; Khim et al., 2007]. When the proportion of organic material in the water column and at the sea floor increases, then benthic mineralization by suspension and deposit feeders is likely enhanced as well [Wassmann, 1984; section 4]. However, the proportion of organic particles released by permafrost soil depends on several factors, such as permafrost region, river discharge and rivers current speed [Vonk et al., 2015] and thus shows great spatial variation. For example, the organic proportion of particles in the river discharge to the Barents Sea and the Kara Sea have been reported to be ~30%, whereas discharges to the Chukchi Sea were 18% [Rachold et al., 2004]. The organic proportion of particles in the river discharge to the East Siberian Sea was only 7% and thus, comparable to the organic proportion of particle released by glacial melt [Rachold et al., 2004; Khim et al., 2007]. Thus, permafrost soil melt-related particle release can lead to both, increasing or decreasing benthic mineralization, depending on location, sedimentation rates, and proportion of organic content.

Suspension and deposit feeders dominate the macrofauna community in Southern and Arctic Ocean ecosystems [Saiz-Salinas et al., 1998; Starmans et al., 1999; Jørgensen et al., 2017; Kokarev et al., 2017; Jansen et al., 2018] and thus are mainly responsible for the mediated benthic mineralization community [Blackburn, 1987; Glud et al., 2016; Norði et al., 2018; section 4]. The bivalve *L. elliptica* was the dominant suspension feeder in Potter Cove (Antarctic) [Momo et al., 2002, section 4] and showed a reduced respiration under high sedimentation rates [Philipp et al., 2011]. This response is similar to those observed in other suspension-feeding bivalve, ascidian, porifera and bryozoan species [Summers et al., 1996; Kowalke et al., 2001; Philipp et al., 2011; Torre et al., 2012; Bell et al., 2015]. In addition, deposit-feeding bivalves and polychaetes [Levinton, 2009] are also affected by increasing particle release [Wlodarska-Kowalczyk et al., 2005]. Furthermore, increasing sediment loads in the water column have been reported to lead to an enhanced production of pseudofaeces in suspension and deposit feeders [Bayne et al., 1993; Navarro and Widdows, 1997]. Pseudofaeces production is associated with mucus production, which is a carbon-rich polysaccharide [Jørgensen, 1990]. Therefore, increased sedimentation rates may also lead to an enhanced release of dissolved organic carbon, which is able to stimulate the microbial loop and growth of primary producers [Pomeroy, 1974; Cognie and Barille, 1990]. In conclusion, the observed changes in the benthic mineralization due to an increased discharge of particles to the marine environment is likely to impact shallow coastal benthic mineralization in both the Southern and the Arctic Ocean.

## 7.2 The impact of sea ice on polar benthic mineralization

Many studies investigated, whether changing sea-ice conditions, such as sea-ice thinning, longer sea-ice free periods, an increased occurrence of melt ponds, a decreased sea-ice concentration over time, and a retreated summer sea-ice extent may influence primary production in polar ecosystems [Comiso, 2002, 2012; Rösel and Kaleschke, 2012; Arrigo, 2013; Fernández-Méndez et al., 2015; DeJong et al., 2018; Leeuwe et al., 2018; Lowry et al., 2018]. As primary production and benthic mineralization, both important processes within the biological carbon cycle, are connected with each other [Graf, 1989; Boetius and Damm, 1998; Wenzhöfer and Glud,

2002; section 5; section 7.3], it is likely that benthic mineralization is also impacted by the occurrence of sea-ice.

In Fram Strait (Arctic deep sea), the parameter 'sea ice' was used as a proxy for a reduced light availability and nutrient supply [section 5]. The resulting suppressed primary production led to a suppressed benthic mineralization in water depths between 1000 m and <2000 m. In water depths  $\geq 2000$  m, the influence of sea ice is progressively reduced and water depth, as a proxy for the loss of organic carbon by pelagic mineralization, became dominant [section 5]. The benthic mineralization values presented in section 5 are the first results of a simultaneous assessment of deep-sea region of the western and eastern Fram Strait. The determined benthic mineralization rates are comparable to results of other studies, which conducted their measurements either in the western or the eastern Fram Strait [Piepenburg et al., 1997; Sauter et al., 2001; Cathalot et al., 2015]. This confirms the reliability of the performed measurements. The results presented in section 5 thereby supported the third hypothesis of this thesis, that the presence of sea ice impacts polar deep-sea benthic mineralization patterns.

In section 5, benthic mineralization between a low and highly sea-ice covered area could only be compared in water depths between 1000–2500 m. Results from the Laptev Sea indicate that sea-ice cover also suppresses benthic mineralization in shallower water depths of <1000 m [Boetius and Damm, 1998]. The impact of sea ice on benthic mineralization at the Arctic shelves (<200 m), however, seems to be low, as similar benthic mineralization values were found at the shelf of the eastern Fram Strait (permanently sea-ice covered) and the Barents Sea shelf region (frequently sea-ice free) [Bourgeois et al., 2017]. As primary production is contrasting in the shelf areas of the eastern Fram Strait and the Barents Sea [Pabi et al., 2008], the similarity in benthic mineralization might be a result of advective food transport processes, which is supported by the complex Fram Strait current system [Hartmann et al., 2016]. Nevertheless, the impact of sea ice on the benthic mineralization seems to be restricted to water depths of >200 m to <2000 m.

Benthic mineralization rates, however, do not solely depend on primary production and water depth but also on the benthic organisms. The microbial community contributed ~80% to the total mineralization (DOU/TOU), which is even more than in the



Atlantic Ocean [Wenzhöfer and Glud, 2002; section 5]. Hence, the observed pattern in benthic mineralization probably reflects effects of sea-ice cover on the microbial community. However, the prokaryotic densities did not show differences between the western and the eastern Fram Strait, such as the benthic mineralization. Benthic microbial biomasses and benthic prokaryotic community structures, factors which may explain the differences in the benthic mineralization patterns of high and low sea-ice covered areas, have been to date only investigated in the eastern Fram Strait [Jacob et al., 2013] but not in the western Fram Strait. The macrofauna community structure may also influence benthic mineralization [Brey, 2010]. And, indeed, the macrofauna community differed considerably across water depths of 1000–2500 m between the highly sea-ice covered western and the low sea-ice covered eastern Fram Strait [section 5]. However, the faunal community only contributed ~20% to the total benthic mineralization [section 5] and thus can only explain a small proportion of the differences between the benthic mineralization in the western and eastern Fram Strait. An additional factor, which influences benthic mineralization, is bioturbation [Mermillod-Blondin et al., 2004; Braeckman et al., 2010; Quintana et al., 2015], represented by BPC [section 5]. BPC was well correlated with benthic mineralization rates, which indicated its likely impact on the process. The influence of bioturbation on benthic processes was also found at continental margins in the Greenland Sea [Graf et al., 1995], where food was transported to up to 9 cm sediment depth within a few weeks [Graf, 1989]. However, deep-sea sediments in polar regions are well oxygenated due to the higher oxygen concentrations often found in the bottom water, when compared to other Oceans [Seiter et al., 2005]. Furthermore, the high oxygen penetration depths of >5 mm reported in water depths of >1000 m [Boetius and Damm, 1998; Donis et al., 2016; section 5] also indicate a profound oxygenation of the sedimentary sea floor. Therefore, the impact of bioturbation on the benthic mineralization rates might be lower compared to less oxygenated regions such as the North Sea [Braeckman et al., 2010] or the Brazilian coast [Quintana et al., 2015]. Nevertheless, the presence of sea ice impacts deep-sea benthic mineralization patterns in the Arctic Ocean. Whether the suppressed primary production is solely responsible for the reduced benthic mineralization in sea-ice covered areas or if also differences in the microbial community were responsible, could not be identified by this thesis and would need further investigations.

As highlighted above, the impact of the presence of sea ice on deep-sea benthic mineralization is restricted to water depths of >200 m to <2000 m and thus to the continental margins. In the Arctic Ocean, the continental margins encompass 30% of entire Ocean [Smith, 2010]. In contrast, the Southern Ocean is dominated by water depths >2000 m [Arndt et al., 2013] and the continental margin only encompasses 2% of the entire Southern Ocean [Smith, 2010]. Thus, the effect of sea-ice cover on deep-sea benthic mineralization might substantially impact organic carbon cycling in the Arctic Ocean, whereas the impact on the organic carbon cycle in the Southern Ocean might be low. However, further investigations are needed to verify the found pattern of a suppressed benthic mineralization in water depths of >200 m to <2000 m in further regions of the Arctic Ocean and in the Southern Ocean.

### 7.3 Relationships of inter-dependent abiotic and biotic factors with benthic mineralization

Holistic ecological studies require the linking of structural and functional ecosystem components [Odum, 1962, 1968]. The former refers to the quantity and distribution of present biota and abiotic factors, while the latter refers to the energy and material flow and the regulation of both by the physical environment and organisms [Odum, 1968]. As a consequence, high sampling and measurement effort is necessary to obtain a holistic snapshot of an ecosystem. Holistic snapshots were rarely taken in remote regions such as the shallow coastal Southern Ocean, where strong winds might prohibit the necessary dives to deploy measurement devices or the Arctic deep sea, where sea-ice cover might prevent sampling. The studies presented in section 4 and 5 belong to this type of study and addressed the second objective of this thesis, the identification of key parameters influencing benthic mineralization in polar ecosystems.

The holistic benthic ecosystem summer snapshot of the Fram Strait (Arctic deep sea, 1000–2500 m water depth) revealed that sea-ice cover and water depth were independent abiotic factors influencing benthic mineralization [section 5]. However, both parameters were considered as proxies. Sea-ice cover represented a suppressed light availability and, owing to the current conditions in the Fram Strait (nutrient-rich Atlantic

water in the east, compared to nutrient-poorer polar waters in the west), also a reduced nutrient supply [Menlay, 1995]. As a result, sea-ice cover mirrored the primary production pattern in the Fram Strait [Pabi et al., 2008] and thus, was used as a proxy for primary production. Water depth represented the loss of organic carbon in the pelagial. During sedimentation, organic particles might be ingested by zooplankton species and might be mineralized in the water column [Chisholm, 2000; Christensen, 2000; Sakshaug, 2004]. Both ingestion and mineralization go along with the reduction of organic carbon. Therefore, water depth was considered as a proxy for the amount of food and the food quality that reached the sea floor. Thus, both factors combined, sea-ice cover and water depth, had a major impact on the benthic ecosystem in the Fram Strait and thereby on the benthic mineralization [section 5].

Similar to the found relationships in the Fram Strait [section 5], the independence of sea-ice cover and water depth was also reported in late summer for the Laptev Sea (37–3427 m water depth) [Boetius and Damm, 1998]. In addition, Piepenburg et al. [1997] also revealed correlations of inter-dependent abiotic and biotic factors with benthic mineralization in the western Fram Strait (40–515 m water depth), but primary production was not considered. Assuming sediment pigments content as another proxy for surface primary production, a strong correlation between benthic mineralization with primary production was revealed by Piepenburg et al. [1997], with water depth as a less important determining factor. This supports the finding presented in section 5 that water depth is of less importance for the benthic mineralization in highly sea-ice covered areas, such as the western Fram Strait.

The holistic benthic ecosystem summer snapshot of Potter Cove (6–9 m water depth) [section 4] revealed that benthic mineralization was positively and well correlated with sediment-bound chlorophyll *a* concentration and macrofauna biomass (excluding *L. elliptica*) and negatively with turbidity in the water column. There is no other Antarctic study available using a similar approach to link inter-dependent abiotic and biotic factors with benthic mineralization [section 4]. Therefore, a comparison of the results with other Antarctic locations is not possible. However, the single link of the positive correlation of benthic mineralization with organic matter (equivalent to Chl *a* or CPE) was also identified by Nedwell et al. [1993] for Antarctic Signy Island (South Orkney Islands).

Benthic mineralization is globally also positively correlated with benthic biomass and bioturbation [Glud et al., 1994; Boetius and Damm, 1998; Wenzhöfer and Glud, 2004; Braeckman et al., 2010; Ruhl et al., 2014; Quintana et al., 2015]. Therefore, it can be assumed that the observed correlations are reliable.

Key parameters and inter-dependent relations, which impact on benthic mineralization, however, differ strongly on large spatial scales. Organic matter supply and sediment composition were identified as main factors influencing the benthic ecosystem in the Arctic Laptev Sea [Boetius and Damm, 1998], which partly contrasts with findings from Fram Strait [section 5]. Furthermore, CPE and TOC were independent of each other in the Laptev Sea, whereas benthic mineralization was negatively correlated with sea-ice cover [Boetius and Damm, 1998]. In the Fram Strait, however, CPE and TOC were highly positively correlated, food supply (Chl *a*, TOC, and organic carbon) were negatively correlated with sea-ice cover, and benthic mineralization was negatively correlated with water depth [section 5]. In the southeastern Beaufort Sea (47–577 m water depth), benthic mineralization was positively correlated with water depth, while chlorophyll *a* was negatively correlated with benthic mineralization [Link et al., 2013b]. At the Saanich Inlet and its opening to the Pacific at the temperate west coast of Canada (97–301 m water depth), benthic mineralization was positively correlated with temperature and bio-irrigation, but negatively with prokaryotic abundances [Belley et al., 2016; Belley and Snelgrove, 2016]. Surprisingly, benthic mineralization was found to be independent of water depth and food quality [Belley et al., 2016; Belley and Snelgrove, 2016]. In Potter Cove [section 4], benthic mineralization was positively and well correlated with chlorophyll *a* and macrofauna biomass (excluding *L. elliptica*) and negatively with the turbidity in the water column. It should be highlighted, that in Potter Cove sea-ice cover only occurs during autumn and winter [Schloss et al., 2012] and that water depth was similar at each of the investigated locations. Therefore, these parameters were not considered, which makes this study less immediately comparable with the Arctic studies. Nevertheless, the parameter that correlated best with benthic mineralization changed at each of the studied locations. Consequently, a generalized assumption on the relationships between inter-dependent ecosystem

components and processes influencing benthic mineralization may bias global benthic mineralization models.

To create a holistic snapshot of an ecosystem, the parameters controlling the key processes within the ecosystem carbon cycle should be considered. Based on the results of this thesis, an appropriate set of parameters including carbon fluxes, carbon pools, and inter-dependent carbon cycle controlling parameters can be recommended to create such a holistic ecosystem snapshot (Table 7.1). These snapshots can either explain changes on spatial [Boetius and Damm, 1998; Link et al., 2013b] or temporal scales [Belley et al., 2016; Belley and Snelgrove, 2016]. To model an ecosystem, which is a major aim in ecology [Bick, 1999], both temporal and spatial changes need to be included. A frequent repetition of holistic ecosystem snapshots at one location might produce data suitable for integration into a simple but realistic ecosystem model. Such a model would indicate whether the controlling parameters undergo seasonal changes and would give a very detailed insight in pelagic-benthic and benthic-pelagic coupled relations, which is of great value for understanding ecosystems and can be used to predict future ecosystem developments.

**Table 7.1.** Recommended list of ecosystem carbon cycle components and processes, its controlling factors and proxies or measurable parameters, to create a holistic ecosystem snapshot.

Carbon cycle component	Controlling factor	Proxy or measurable parameter
Primary production	Light availability	Sea-ice cover, turbidity, sedimentation, <i>in situ</i> PAR
	Nutrient availability	Nutrient concentration in the water column and river runoffs
	-	Oxygen flux, carbon flux, change of Chl <i>a</i> concentrations or other pigment concentrations over time, depletion of nutrients over time
Primary producer	Light availability, nutrient supply	Chl <i>a</i> concentration, algae cell density, algae biomass
Pelagic carbon mineralization	Primary production, time for vertical carbon flux	Water depth, currents
	-	Oxygen uptake or DIC release of sinking particles
Available benthic food	Primary productivity, pelagic mineralization	Chl <i>a</i> , CPE, DIC, TOC, DOC
Carbon flux mediating biota	Available food	Biomass or density of prokaryotes, meiofauna, and macrofauna
Benthic carbon mineralization	Available benthic food, carbon flux mediating biota	Oxygen flux, carbon flux, nutrient fluxes
Seasonality	Time, food quantity and quality	Temperature, Chl <i>a</i> , CPE, TOC, organic matter, biomass

Tools to identify inter-dependent abiotic and biotic factors within the organic carbon cycle within this thesis and by other studies were a principal component analysis (PCA) and a redundancy analysis (RDA) [Boetius and Damm, 1998; Link et al., 2013b; Belley et al., 2016; Belley and Snelgrove, 2016]. The data acquisition and data preparation prior to the PCA or RDA differed among the studies. In contrast to Boetius and Damm [1998], well-correlated parameters were merged prior to the PCA in section 4 and 5 to strengthen the final output. Furthermore, satellite-based mean sea-ice coverage data were used, averaged over the period before sampling, while Boetius and Damm [1998] used visual estimates on arrival. The RDA of Link et al. [2013b] did not include parameters such as sea-ice cover, sediment grain size or benthic biomass. Therefore, an adjustment of the PCA procedures of Boetius and Damm [1998] to the approach presented in section 4 and 5 and the incorporation of more parameters into the RDA of Link et al. [2013b] might have changed their output substantially. Furthermore, the parameter ordination in a PCA or an RDA is based on linear correlations [Buttigieg and Ramette, 2014]. However, whether there is a causal relationship between two correlated parameters, whether this relationship is actually linear, exponential or power law and whether the relationship between two correlated parameters is significant, cannot be elucidated by a PCA. In summary, PCA and RDA are suitable tools, by which linkages of inter-dependent abiotic and biotic factors within the biological carbon cycle can be identified. Though, further investigations are necessary to prove the reliability of these linkages [Belley et al., 2016] and a direct comparison of results of different studies is difficult and has to be interpreted with caution.

## 7.4 Potential future developments in polar carbon cycles due to changing ice conditions and related secondary effects

### 7.4.1 A two-step scenario for the Southern Ocean

As highlighted in the introduction of this thesis, processes and components of the biological carbon cycle in the Southern Ocean are impacted by climate change-induced alterations. A year-round data acquisition in the Southern Ocean is restricted to a limited amount of locations [Takahashi et al., 2009; Sabine et al., 2013] and thus, modeled

predictions of future carbon flux dynamics need to be assessed carefully. Therefore, I will outline a future scenario of potential changes regarding the biological carbon cycle in the Southern Ocean based on current knowledge from modeled and observational studies.

In a first step, the sea-ice concentration in the Southern Ocean further decrease and shelf ice further loose volume and thickness [Paolo et al., 2015; Gutt et al., 2015]. These changes likely lead to an increased light availability in the upper Southern Ocean. As the continental margin and the shelf regions are well supplied by nutrients and iron due to upwelling processes and sediment resuspension associated with ice scouring, an increase in pelagic primary productivity is likely [Arrigo et al., 2008a]. As a follow-up consequence, benthic biomass is likely to increase [Fillinger et al., 2013; Barnes et al., 2016], which is related to an enhanced benthic mineralization. This first step may be accompanied by an increase in the ice scour frequency by icebergs [Barnes et al., 2009]. The latter might counteract the biomass increase but favor resuspension of nutrients and might result in a locally impoverished benthic macrofauna community and higher carbon export fluxes from the pelagic primary production.

As a second step, shelf ice will turn into tidal glaciers and permafrost soil will start to melt [Barnes et al., 2009; Lee et al., 2017]. This will result in an increasing particle discharge. The related additional iron supply may further enhance pelagic primary production on larger spatial scales [Monien et al., 2017]. In addition, newly ice-free areas will be inhabited by primary producers and heterotrophic consumers [Deregibus et al., 2016; Lager et al., 2017; Seefeldt et al., 2017]. MPB and macroalgae primary production, however, will be suppressed due to increased sedimentation rates [section 3; section 7.1]. Whether enhanced pelagic primary production is sufficient to counterbalance the reduced MPB and macroalgae primary production, as well as to cover the increased benthic carbon demand is debatable. Nevertheless, under the assumption that the results from manuscript II of this thesis are transferable to other coastal regions in the Southern Ocean, benthic mineralization might drop directly at glacial fronts by ~40% but increase at some distance (hundreds of meters) to the glacial front by ~30% [section 4]. With time, glaciers might redraw completely onto land and thus secondary effects of glacial melting will cease. A re-establishment of a more

diverse and less patchy macrofauna community, as assumed by Pasotti et al. [2015], is unlikely, as the disturbance by secondary effects of permafrost melting remains. Benthic mineralization at the Southern Ocean shelf and in the deep sea is likely to remain constant at this development step for two reasons. First, an enhanced pelagic primary production does not necessarily lead to an increased vertical carbon flux, as the pelagic food web may take up a much of the enhanced primary production [Kim et al., 2016]. Second, Southern Ocean benthic fauna does not react on increased food supply with increased metabolism or increased benthic biomass [Mincks et al., 2005; Smith et al., 2006]. Therefore, only a reduction in food supply would affect benthic remineralization in shelf regions.

The described potential future Southern Ocean scenario may take place within the next 100 years but with significant uncertainties in the details. Alterations in primary production and benthic mineralization patterns will mainly occur in the summer seasons when melting discharge is highest and sea-ice extent lowest. The retreat of shelf ice and glaciers is spatially limited to the Antarctic Peninsula [Lee et al., 2017]. Large-scale investigations on permafrost soil melt are largely missing from the literature and only reported for Casey Bay (70.5°S, 12°E), the McMurdo Sound (74–78°S, 165°E) and the Antarctic Peninsula (55–72°S, 45–70°W) [Barnes et al., 2009; Pablo et al., 2018]. In general, extensive large-scale variations in primary production are likely given to the heterogeneity of controlling factors [Priddle et al., 1992]. In addition, there are further existing or upcoming threats such as increasing water temperature and ocean acidification, which will likely also impact on primary production patterns and biodiversity [Gutt et al., 2015] and thereby change benthic mineralization rates.

### 7.4.2 The sea-ice free Arctic Ocean in summer

Similar to the Southern Ocean, a year-round data acquisition in the Arctic Ocean is also restricted to a limited amount of locations [Wassmann et al., 2011; Bourgeois et al., 2017]. Based on the results of section 5 and on results of other modeled and observational studies, I will outline a future scenario of potential changes regarding the biological carbon cycle in a sea-ice free Arctic Ocean.



The Arctic Ocean is predicted to become sea-ice free in summer months [Arzel et al., 2006; Wang and Overland, 2012; Vaughan et al., 2013]. In addition, air temperature may increase by 8°C [Wassmann, 2011]. With this development, the habitat currently utilized by sea-ice algae will disappear [section 7.1]. With the abolition of the sea-ice algae primary production, the available nutrients could be used for pelagic primary production. Photoinhibition, owing to the increased light intensity, is unlikely, as pelagic Arctic primary producers can cope with light intensities of  $>400 \mu\text{mol photons m}^{-2} \text{s}^{-1}$  [Fernández-Méndez et al., 2015]. Further, the increased primary production along the MIZ will be temporally limited. In parallel, more particles and nutrients will be transported into the Arctic Ocean by glacial and permafrost soil melt [AMAP, 2012]. This may reduce the primary production of MPB and macroalgae at the shallow coasts, but favor pelagic primary production across the Arctic shelf within a few kilometers [section 7.1]. If pelagic primary production is finally substantially higher compared to present conditions is debatable, as pelagic primary production in these areas is already among the highest in the Arctic Ocean [Pabi et al., 2008]. Nevertheless, more nutrients will enter the Arctic Ocean through the Bering and Barents Sea [Neukermans et al., 2018; Woodgate, 2018], which will lead to an increased primary production in the Chukchi and Beaufort Sea, across the Barents Sea shelf and maybe at its continental margins [Arrigo and Dijken, 2015; Harada, 2015; Hunt et al., 2016]. An increase in the stratification of the surface layers is predicted for the central Arctic Ocean, owing to sea-ice melt and increased precipitation [McLaughlin and Carmack, 2010; Bintanja and Selten, 2014; Bracegirdle et al., 2015]. This would hamper nutrient supply to the ocean's surface. However, increasing wind speeds are also predicted for the central Arctic Ocean [Sprenn et al., 2011], which would frequently disturb the stratification development and may promote the upwelling of nutrients, which in turn would enhance primary production. In addition, the predicted increase in air temperature and advective transport from the Arctic shelves may supply further nutrients to the central Arctic Ocean [Wassmann, 2011; Popova et al., 2013]. Therefore, an at least moderate increase of primary productivity is likely for the central Arctic Ocean.

Benthic mineralization at the coast might drop due to the high sedimentation rates within a spatial scale of hundreds of meters [section 4]. Beyond the immediate coastal

area, enhanced particulate organic carbon availability is likely to be available for the benthos, owing to the discussed increase in primary production [section 7.1]. This and the physiological reaction of suspension and deposit feeders on intermediate sedimentation [section 4] might lead to an increase in benthic mineralization at the Arctic shelves. The Arctic deep-sea benthic mineralization will be water depth dependent [section 5]. If the deep-sea benthic mineralization will increase, owing to the described enhanced primary production, is debatable. On the one hand, the phytoplankton community may adapt by favoring smaller species (nanoplankton) which are more efficient in low nutrient conditions [Ardyna et al., 2013]. Such a change would be accompanied by a slower particle sinking speed and in turn, more carbon would be mineralized in the pelagial. On the other hand, the retreat and loss of sea ice are accompanied by a volumetric increase of eddies [Watanabe et al., 2014], which would result in an increased vertical carbon flux [Harada, 2015]. The results in section 5 however, suggest that an increase in primary production would not impact benthic mineralization in water depths deeper than 2000 m.

The described scenario for the sea-ice free Arctic Ocean may develop by the mid of the 21<sup>st</sup> century [Arzel et al., 2006; Wang and Overland, 2012; Vaughan et al., 2013], and be limited to summer months. This scenario is accompanied by an early start of sea-ice retreat and therefore higher light intensities will reach the Arctic Ocean earlier in each year, which will likely result in an earlier spring bloom onset. If under-ice fauna and zooplankton life-cycles are not able to adapt to the new conditions, a mismatch between primary producers and grazers will appear [Ji et al., 2013]. This would lead to an increasing vertical carbon export in spring, which may favor an enhanced benthic deep-sea mineralization during that season [Graf, 1989]. However, there are further existing or upcoming threats, e.g. increasing atmospheric and water temperatures, changing wind patterns and wind speeds, and ocean acidification [IPCC, 2013]. These threats likely impact on primary production patterns and thus, on benthic mineralization rates.

## 8 Conclusion and outlook

---

### 8.1 Conclusion

Within this thesis, it was investigated whether polar carbon fluxes are impacted by secondary effects of changes in the polar ice conditions. In terms of carbon fluxes, the focus was set on a) primary production and b) benthic mineralization. The studied secondary effects included a) the reduced light availability due to an increased turbidity and related increased particle sedimentation caused by particle release of glacial and permafrost soil melt and b) the increased light availability owing to diminishing and retreating sea ice. The secondary effect of particle sedimentation impacts shallow coastal regions in the western Southern Ocean and the Arctic Ocean, while turbidity is assessed as a less important secondary effect. In addition, increased light availability mainly impacts the open ocean in the western Southern Ocean, the Beaufort Sea, the Chukchi Sea and the central Arctic Ocean.

The increased turbidity reduces the light availability but does not impact primary production itself, owing to the strong low light adaption potential of polar primary producers. Nevertheless, MBP primary production can be totally suppressed when particles frequently cover the MPB community as more energy is needed for migration. Benthic mineralization is also impacted by sedimentation. However, whether sedimentation leads to an enhanced or reduced benthic mineralization depends on the quantity of particle sedimentation and the benthic supply with organic carbon by pelagic primary production.

With diminishing sea ice, the habitat for ice algae also diminishes and reduces the primary production contribution of ice algae to the total primary production in polar ecosystems. Increased light availability, owing to the diminishing and retreating sea ice, only results in an increased pelagic primary production, when also the nutrient supply increases. If the latter comes true, deep-sea benthic mineralization is expectable to increase only in water depth between 200 m and 2000 m.

To summarize, the investigated secondary effect 'sedimentation' has a direct impact on primary production and mineralization in shallow coastal polar regions, while the impact of the associated increased turbidity is assessed to be low. Diminishing sea-ice and associated secondary effects affect primary production and mineralization in deep-sea polar regions only, if it is accompanied by an increase in nutrient supply.

The uniqueness of this thesis lays in the holistic ecosystem approach. Most studies investigating climate change-related secondary effects focus on primary production, community structure, and faunal biomasses. The presented results in the manuscripts II and III [sections 4, section 5] go beyond that and are one of a few that also include benthic mineralization. In addition, the complex linkages of primary production, benthic biomass, benthic mineralization and controlling factors were also investigated. Therefore, this thesis gives a holistic ecological insight on carbon fluxes in polar ecosystems.

In conclusion, this thesis closed the identified knowledge gaps of a) to which degree glacial melt-related particle release affects Southern Ocean MPB primary production in shallow, coastal areas, b) to which degree glacial melt-related particle release affects Southern Ocean benthic mineralization in shallow, coastal areas, and c) the impact of sea ice on polar deep-sea benthic mineralization patterns. Thereby, results of this thesis contribute to the development of future scenarios regarding the polar organic carbon flux, in case climate change-induced alterations in the cryosphere and related secondary effects continue.

## 8.2 Outlook

The thesis, however, also left some questions unanswered or gained some new. In manuscript III [section 5], the revealed mineralization patterns in the Fram Strait could not be fully explained so far, as studies regarding the benthic microbial community are missing so far. In addition, knowledge on current velocities and current directions below 300 m water depths would help to trace back vertical carbon fluxes in order to locate and estimate the catchment area of Fram Strait's food supply.

Potter Cove is located in the area of the fastest temperature increase in the Southern Ocean [Turner et al., 2005], which makes it an ideal field laboratory. In order to make reliable predictions for Southern Ocean coastal areas in case of continuing temperature increase and relate changes in the cryosphere and associated secondary effects, a model of Potter Coves ecosystem in terms of carbon fluxes should be developed. This will be a quite challenging task, but a basis is already given by Potter Coves food web model [Marina et al., 2017] and by primary production and benthic mineralization studies [Schloss et al., 1998, 2012; section 3; section 4]. As a next step, it should be determined, whether and when Potter Cove is an autotrophic or heterotrophic ecosystem. This includes the determination of a) the temporal changes in the MPB community structure and biomass, b) the in situ MBP primary production on spatial and temporal scales combined with sediment accumulation rates, c) the determination of area-specific macroalgae primary production, and d) the pelagic and benthic mineralization on temporal scales [Braeckman et al., in preparation]. Manuscript II [section 4] does not answer, whether sedimentation is the most influential factor shaping the small-scale spatial variability of biogeochemical fluxes in Potter Cove. To make a reliable statistical analysis on that question, a sufficient number of at least five locations in Potter Cove should be investigated regarding benthic mineralization, benthic community, and food availability. Thereby, each location has to be located along the sedimentation gradient. Additionally, this approach might allow the quantification of thresholds at which sedimentation rates benthic mineralization starts to increase and when it starts to drop. In addition, sediment trap data in a high spatial resolution are required to better understand the carbon sources and sinks and to better characterize the inorganic sedimentation. In that perspective, also carbon burial rates are missing. Furthermore,

the unimodal regression of benthic mineralization with increasing disturbance [section 4] is similar to the unimodal regression of biodiversity with increased disturbance [Grime, 1973; Horn, 1975; Connell, 1978]. This raises the question, whether there is a general triangular relationship between biodiversity, mineralization, and disturbance.

To model future developments of primary production and pelagic and benthic mineralization in polar regions as well as globally, especially under climate change-related threats and associated secondary effects, long-term datasets with an appropriate temporal and spatial resolution are required. In polar regions, for example, such data are provided by the long-term observatory HAUSGARTEN (operated by AWI) and by stations run by the Ocean Networks Canada (<http://www.oceannetworks.ca>). Primary production data might be calculated from satellite data. However, due to technical limitations, primary production in and under sea ice, which contributes substantially to the total primary production in the Polar Oceans, cannot be calculated from satellite data. Therefore, a combination of remote and on-site measurements of primary production is mandatory. In addition, also microbial, meiofaunal and macrofaunal community data are required. This implies choosing a sampling approach which covers all relevant species in one sampling event and an appropriate number of replicates to allow smoother data analyses. Regarding benthic mineralization, Bourgeois et al. [2017] provide a first reliable spatial model of the Arctic. Interestingly, the Arctic deep sea seems to be better investigated than the coastal shallow sites. Nevertheless, the study of Bourgeois et al. [2017] mainly provides a baseline of benthic mineralization and seasonal changes were only observable in few Arctic Ocean areas. The data coverage regarding benthic mineralization in the Southern Ocean is even worse. Only four studies (including manuscript II of this thesis [section 4]) are available regarding shallow coastal benthic mineralization and only one of the four includes a temporal resolution [Nedwell et al., 1993]. There are a few more studies available and upcoming on benthic mineralization at the Southern Ocean shelf [section 1; Holtappels et al., 2017; Link et al., 2017]. However, the spatial and temporal resolution on benthic mineralization in the Southern Ocean is still too sparse to repeat the modeling approach of Bourgeois et al. [2017] for the Southern Ocean. Christensen [2000] modeled benthic deep-sea mineralization on a global scale in water depths >1000 m and included the Southern

Ocean. However, ground truthing measurements are missing. An appropriate tool to measure *in situ* total benthic mineralization, besides the described methods [section 2], is the Eddy covariance approach [Berg et al., 2003]. Owing to a better sensitivity to oxygen concentrations in currents [Donis et al., 2015], optodes instead of microelectrodes should be used [Chipman et al., 2012]. The great advantage of this method is its non-destructive use on soft, hard and heterogeneous sea floors in shallow and deep-sea regions [Berg et al., 2003; Berg et al., 2009; Attard et al., 2016] and its great catchment area of 10–100 m<sup>2</sup> [Berg et al., 2007]. Especially in shallow coastal areas of polar regions, which are easier accessible in terms of logistical effort, the usage of the Eddy covariance approach is likely to lead to a fast increase of our knowledge about benthic mineralization on spatial scales with a good spatial resolution [Holtappels et al., 2017]. The reason, why the Eddy covariance approach is not used more frequently for ecological studies on all kinds of sea floors (soft sediment, rocks, corals, mixture of all three) might be the initial costs of ~60 k€, the additional required knowledge on hydrodynamics and transport processes in turbulent currents and an extensive data processing procedure (pers. comm. Moritz Holtappels, AWI). However, the costs are still 40% lower, compared to an autonomous benthic lander system (with a similar setup used in section 5). Furthermore, deployment and recovery can be made by hand and does not necessarily need great technical support, and with the latest technological improvements [Chipman et al., 2012] the obtained data are reliable and are in the same range as other and by now more established methods [Donis et al., 2015, Glud et al., 2016].

In addition, the separated investigation of carbon cycle processes and components, e.g. only primary production or only benthic mineralization or only benthic biomass and structure, biases its understanding and hampers a holistic ecosystem snapshot of the carbon cycle. The project FRAM (<https://www.awi.de/en/expedition/observatories/ocean-fram.html>) is a good example, how to overcome this bias. Satellites, ice-tethered platforms, AUVs and upwards profiling mooring devices observe surface processes. Moored particle traps, zooplankton observing devices, e.g. LOKI, and conductivity, temperature, velocity and water depth sensors observe water column process. Autonomous benthic landers, benthic crawlers such as the AWI TRAMPER and towed

video-sleds obtain benthic data. Most of these systems can work year round and therefore allow the identification of temporal variabilities. Especially the rarely observed winter season, when barely any food supply takes place, is of great ecological interest. As also spatial scales are covered within FRAM, the final outcome will push forward our knowledge about the carbon cycle in the Arctic Fram Strait. A similar project in the Southern Ocean would even be of greater value. Climate change related implications, e.g. sea surface temperature increase, diminishing sea-ice cover, and glacial melt, were by now only observed in a restricted area of the Southern Ocean, but are predicted to extend [Barnes et al., 2009; Gutt et al., 2015]. Already existing long-term observatories such as LTER Palmer and McMurdo station (USA) or the IT17 (Italy) should be improved and extended regarding their used measurement technologies. The HAFOS project (Hybrid Antarctic Float Observation System) in the Weddel Sea combined with the usage of the non-destructive Eddy correlation approach for the determination of benthic mineralization would also be a suitable approach to get a deeper and (partly) holistic insight into the Southern Ocean carbon cycle. Indeed, a huge financial, technological and logistical effort is necessary to install and regularly maintain such infrastructures. The resulting data from the suggested projects however, would mark an important step towards a reliable holistic Southern Ocean ecosystem carbon cycle model and can be used as a baseline to compare with future data.

Primary production and mineralization are processes based on cell internal reactions [section 1]. Therefore, it would be worth to investigate correlations of both processes with genetic activities e.g. via meta-proteomic and meta-transcriptomic analyzes. In combination with known correlations, such an approach would give a more detailed holistic ecosystem snapshot and connect the biological disciplines of genetics with ecology.



## Acknowledgment

---

During my time in the German Navy, the beauty and the myth of the sea caught me. I decided that my future work should be related to the sea and located at or on the sea. Therefore, during the four years as a Ph.D. student at the AWI, I was living my dream and it further fueled my sea-addiction. This was made possible by my daily and first main supervisor Dr. Frank Wenzhöfer, whom I want to offer my sincerest gratitude. You did not like my idea for a Ph.D. topic (oxygen fluxes on the rocky seafloor), but you made me an offer I could not refuse. I am proud that you took me as your student. Besides your knowledge, your relaxed way dealing with stressful situations was always very impressive for me. In addition, I would like to thank Prof. Dr. Antje Boetius, my second main supervisor and reviewer of my thesis. Your dedication to science and awareness that science is done by people makes you a role model for me. Dr. Ulrike Braeckman, my unofficial third supervisor, also deserves my gratitude. Your kindness, your criticism and your ability to motivate me brought me here — and how can I ever forget our shared expeditions. I feel honored that the three of you trusted me, allowed me to visit such remote places, and shared your wisdom and thoughts with me. In addition to these three people, I would like to thank Dr. Stefan Forster for reviewing my thesis. I really enjoyed your lectures during my studies in Rostock and I hope you enjoyed to read my thesis (at least a bit).

Besides supervisors and reviewers, a lot more people were involved in my research, influenced my decisions, discussed scientific and non-scientific issues with me, accompanied me and made a few things just possible for me. For this support, I would like to thank the entire HGF-MPG Joint Research Group for Deep Sea Ecology and Technology. I hope to be able to give you something back at some point in my future

career. Special thanks go out to the laboratory and tech-hall technicians. You are the basis of the science that I conducted and without you, there would not have been any sensors, landers, profilers, or reliable results. Particular thanks go to my expedition partners. Elisa, Chris, and Moritz: you made my life as dive-, station- and expedition leader an easy one. Fran, Anders, Angela, and Katharina: With you, the Potter Cove challenge was a piece of cake. In addition to these influencing people, I would like to thank Dr. Matthias Zabel. I really appreciate your support as the 'external' member during my thesis committee meetings.

Furthermore, I would like to acknowledge the essential work of the logistics department and the scientific diving division at the AWI and of the crew and staff members on the RV Polarstern and at the Carlini Station. In addition, a big 'thank you' go to all co-authors for the valuable contributions given to our manuscripts. Most of the funding for my doctoral studies was provided by the EU-Project SenseOCEAN, with additional funding being provided by the AWI. I was further supported by offered courses and by financing short stays in Gothenburg by the graduate school POLMAR.

But there happened more within four years than just science. James, we really shared a lot: our look, ship cabin, office, your flat and a really good Ph.D. time. Kim, I miss your garden. Pitty, I hope we will drink a Jever from time to time in Port Piet. And a huge hug goes to Josi. We started it together and we finished it together. I may not call you twice a week, but I consider you as my friends for the rest of my life and if you need help, support or just want to share a beer, just call (and will bother you, whenever I am around).

My greatest thanks are dedicated to my family. Mam and Paps, you support my way since 1983 – what a long-term investment. I hope you like the preliminary result. To my beloved brother and his wife: let's keep climbing up mountains, literally and in our research fields. Ilvy, you made me take breaks, which helped to sort my thoughts.

With my final words, I would like to thank Nadine. I left you several months (and several times) and lived my sea-addicted dream. By standing this out, you became mine. I love you.

## References

---

- Adams, B., Arthern, R., Atkinson, A., Barbante, C., Bargagli, R., Bergstrom, D., Bertler, N., Bindschadler, R., Bockheim, J., Boutron, C., Bromwich, D., Chown, S., Comiso, J., Convey, P., Cook, A., di Prisco, G., Fahrbach, E., Fasrook, J., Forcada, J., Gili, J.-M., Gugliemin, M., Gutt, J., Hellmer, H., Hennion, F., Heywood, K., Hodgson, D., Holland, D., Hong, S., Huiskes, A., Isla, E., Jacobs, S., Jones, A., Lenton, A., Marshall, G., Mayewski, P., Meredith, M., Metzl, N., Monaghan, A., Naveira-Garabato, A., Newsham, K., Orejas, C., Peck, L., Pörtner, H.-O., Rintoul, S., Robinson, S., Roscoe, H., Rossi, S., Scambos, T., Shanklin, J., Smetacek, V., Speer, K., Stevens, M., Summerhayes, C., Trathan, P., Turner, J., van der Veen, K., Vaughan, D., Verde, C., Webb, D., Wiencke, C., Woodworth, P., Worby, T., Worland, R., and Yamanouchi, T.: *The Instrumental Period*, in: Antarctic climate change and the environment: A contribution to the International Polar Year 2007–2008, Bindschadler, R., Convey, P., di Prisco, G., Fahrbach, E., Gutt, J., Hodgson, D., Mayewski, P., Summerhayes, C., and Turner, J. (Eds.), Scientific Committee on Antarctic Research, Cambridge, 183–298, 2009.
- Ainley, D., Barret, P., Bindschadler, R., Clarke, A., Convey, P., Fahrbach, E., Gutt, J., Hodgson, D., Meredith, M., Murray, A., Pörtner, H.-O., di Prisco, G., Schiel, S., Speer, K., Summerhayes, C., Turner, J., Verde, C., and Willems, A.: *The Antarctic Environment in the Global System*, in: Antarctic climate change and the environment: A contribution to the International Polar Year 2007–2008, Bindschadler, R., Convey, P., di Prisco, G., Fahrbach, E., Gutt, J., Hodgson, D., Mayewski, P., Summerhayes, C., and Turner, J. (Eds.), Scientific Committee on Antarctic Research, Cambridge, 1–32, 2009.
- Al-Handal, A. Y. and Wulff, A.: *Marine benthic diatoms from Potter Cove, King George Island, Antarctica*, Bot. Mar., 51, 51–68, doi:10.1515/BOT.2008.007, 2008a.
- Al-Handal, A. Y. and Wulff, A.: *Marine epiphytic diatoms from the shallow sublittoral zone in Potter Cove, King George Island, Antarctica*, Bot. Mar., 51, 411–435, doi:10.1515/BOT.2008.053, 2008b.
- AMAP: *Arctic climate issues 2011: Changes in Arctic snow, water, ice and permafrost*, Arctic monitoring and assessment programm, Oslo, Norway, 2012.
- Ambrose, W. G. and Renaud, P. E.: *Benthic response to water column productivity patterns: Evidence for benthic-pelagic coupling in the Northeast Water Polynya*, J. Geophys. Res., 100, 4411–4421, doi:10.1029/94JC01982, 1995.
- Amsler, C. D., Rowley, R. J., Laur, D. R., Quetin, L. B., and Ross, R. M.: *Vertical distribution of Antarctic peninsular macroalgae: cover, biomass and species composition*, Phycologia, 34, 424–430, doi:10.2216/i0031-8884-34-5-424.1, 1995.
- Anderson, L. A. and Sarmiento, J. L.: *Redfield ratios of remineralization determined by nutrient data analysis*, Global Biogeochem. Cy., 8, 65–80, doi:10.1029/93GB03318, 1994.
- Anderson, L. G. and Kaltin, S.: *Carbon fluxes in the Arctic Ocean – potential impact by climate change*, Polar Res., 20, 225–235, doi:10.3402/polar.v20i2.6521, 2001.
- Anderson, M. J.: *PERMANOVA: a FORTRAN computer program for permutational multivariate analysis of variance*, Department of Statistics, University of Auckland, New Zealand, 2005.
- Anderson, M. J., Gorley, R. N., and Clarke, K. R.: *PERMANOVA+ for PRIMER: guide to software and statistical methods*, PRIMER-E, Plymouth, 2007.

## References

---

- Apollonio, S.: *Primary production in Dumbell Bay in the Arctic Ocean*, Mar. Biol., 61, 41–51, doi:10.1007/BF00410340, 1980.
- Ardyna, M., Babin, M., Gosselin, M., Devred, E., Bélanger, S., Matsuoka, A., and Tremblay, J.-É.: *Parameterization of vertical chlorophyll a in the Arctic Ocean: impact of the subsurface chlorophyll maximum on regional, seasonal and annual primary production estimates*, Biogeosciences, 10, 4383–4404, doi:10.5194/bg-10-4383-2013, 2013.
- Armand, L. K. and Leventer, A.: *Palaeo sea ice distribution and reconstruction derived from the geological record*, in: Sea Ice, Thomas, D. N., and Dieckmann, G. S. (Eds.), Wiley-Blackwell, Oxford, UK, 469–529, 2009.
- Arndt, J. E., Schenke, H. W., Jakobsson, M., Nitsche, F. O., Buys, G., Goleby, B., Rebesco, M., Bohoyo, F., Hong, J., Black, J., Greku, R., Udintsev, G., Barrios, F., Reynoso-Peralta, W., Taisei, M., and Wigley, R.: *The International Bathymetric Chart of the Southern Ocean (IBCSO) Version 1.0 - A new bathymetric compilation covering circum-Antarctic waters*, Geophys. Res. Lett., 40, 3111–3117, doi:10.1002/grl.50413, 2013.
- Arrigo, K. R.: *The changing Arctic Ocean*, Elem. Sci. Anth., 1, 10, doi:10.12952/journal.elementa.000010, 2013.
- Arrigo, K. R. and Dijken, G. L. van: *Continued increases in Arctic Ocean primary production*, Prog. Oceanogr., 136, 60–70, doi:10.1016/j.pocean.2015.05.002, 2015.
- Arrigo, K. R. and Dijken, G. I. van: *Secular trends in Arctic Ocean net primary production*, J. Geophys. Res., 116, L19603, doi:10.1029/2011JC007151, 2011.
- Arrigo, K. R. and Thomas, D. N.: *Large scale importance of sea ice biology in the Southern Ocean*, Antarct. Sci., 16, 471–486, doi:10.1017/S0954102004002263, 2004.
- Arrigo, K. R., Perovich, D. K., Pickart, R. S., Brown, Z. W., van Dijken, G. L., Lowry, K. E., Mills, M. M., Palmer, M. A., Balch, W. M., Bahr, F., Bates, N. R., Benitez-Nelson, C., Bowler, B., Brownlee, E., Ehn, J. K., Frey, K. E., Garley, R., Laney, S. R., Lubelczyk, L., Mathis, J., Matsuoka, A., Mitchell, B. G., Moore, G. W. K., Ortega-Retuerta, E., Pal, S., Polashenski, C. M., Reynolds, R. A., Schieber, B., Sosik, H. M., Stephens, M., and Swift, J. H.: *Massive phytoplankton blooms under Arctic sea ice*, Science, 336, 1408, doi:10.1126/science.1215065, 2012.
- Arrigo, K. R., van Dijken, G. L., and Bushinsky, S.: *Primary production in the Southern Ocean, 1997–2006*, J. Geophys. Res., 113, 609, doi:10.1029/2007JC004551, 2008a.
- Arrigo, K. R., van Dijken, G., and Pabi, S.: *Impact of a shrinking Arctic ice cover on marine primary production*, Geophys. Res. Lett., 35, doi:10.1029/2008GL035028, 2008b.
- Arrigo, K. R., Worthen, D., Schnell, A., and Lizotte, M. P.: *Primary production in Southern Ocean waters*, J. Geophys. Res., 103, 15587–15600, doi:10.1029/98JC00930, 1998.
- Arzel, O., Fichefet, T., and Goosse, H.: *Sea ice evolution over the 20th and 21st centuries as simulated by current AOGCMs*, Ocean Model., 12, 401–415, doi:10.1016/j.ocemod.2005.08.002, 2006.
- Atkinson, A., Siegel, V., Pakhomov, E. A., Rothery, P., Loeb, V., Ross, R. M., Quetin, L. B., Schmidt, K., Fretwell, P., Murphy, E. J., Tarling, G. A., and Fleming, A. H.: *Oceanic circumpolar habitats of Antarctic krill*, Mar. Ecol. Prog. Ser., 362, 1–23, doi:10.3354/meps07498, 2008.
- Atkinson, A., Siegel, V., Pakhomov, E., and Rothery, P.: *Long-term decline in krill stock and increase in salps within the Southern Ocean*, Nature, 432, 100–103, doi:10.1038/nature02996, 2004.
- Attard, K. M., Glud, R. N., McGinnis, D. F., and Rysgaard, S.: *Seasonal rates of benthic primary production in a Greenland fjord measured by aquatic eddy correlation*, Limnol. Oceanogr., 59, 1555–1569, doi:10.4319/lo.2014.59.5.1555, 2014.
- Attard, K. M., Hancke, K., Sejr, M. K., and Glud, R. N.: *Benthic primary production and mineralization in a High Arctic fjord: in situ assessments by aquatic eddy covariance*, Mar. Ecol. Prog. Ser., 554, 35–50, doi:10.3354/meps11780, 2016.
- Azam, F., Fenchel, T., Field, J. G., Gray, J. S., La Meyer-Reil, and Thingstad, F.: *The ecological role of water-column microbes in the sea*, Mar. Ecol. Prog. Ser., 10, 257–263, doi:10.3354/meps010257, 1983.

- Baldwin, R. and Smith, K.: *Temporal dynamics of particulate matter fluxes and sediment community response in Port Foster, Deception Island, Antarctica*, Deep-Sea Res. Pt. II, 50, 1707–1725, doi:10.1016/S0967-0645(03)00089-4, 2003.
- Banse, K.: *Low seasonality of low concentrations of surface chlorophyll in the Subantarctic water ring: underwater irradiance, iron, or grazing?*, Prog. Oceanogr., 37, 241–291, doi:10.1016/S0079-6611(96)00006-7, 1996.
- Barnes, D. K. A.: *The influence of ice on polar nearshore benthos*, J. Mar. Biol. Assoc. UK, 79, 401–407, 1999.
- Barnes, D. K. A. and Souster, T.: *Reduced survival of Antarctic benthos linked to climate-induced iceberg scouring*, Nat. Clim. change, 1, 365–368, doi: 10.1038/nclimate1232, 2011.
- Barnes, D. K. A., Ireland, L., Hogg, O. T., Morley, S., Enderlein, P., and Sands, C. J.: *Why is the South Orkney Island shelf (the world's first high seas marine protected area) a carbon immobilization hotspot?*, Glob. Change Biol., 22, 1110–1120, doi:10.1111/gcb.13157, 2016.
- Barnes, D. K. A., Bergstrom, D., Bindschadler, R., Bockheim, J., Bodeker, G., Bopp, L., Bracegirdle, T., Chown, S., Convey, P., di Prisco, G., Fahrbach, E., Forcada, J., Frenot, Y., Goose, H., Gutt, J., Hodgson, D., Huiskes, A., Jones, A., Leaper, R., Lefebvre, W., Lenton, A., Lynch, A., Metzl, N., Murray, A., O'Farrell, S., Peck, L., Pörtner, H.-O., Roscoe, H., Smale, D., Smetacek, V., Summerhayes, C., Turner, J., Vanreusel, A., Vaughan, D., Verde, C., and Wang, Z.: *The next 100 years*, in: Antarctic climate change and the environment: A contribution to the International Polar Year 2007–2008, Bindschadler, R., Convey, P., di Prisco, G., Fahrbach, E., Gutt, J., Hodgson, D., Mayewski, P., Summerhayes, C., and Turner, J. (Eds.), Scientific Committee on Antarctic Research, Cambridge, 2009.
- Bartsch, I., Paar, M., Fredriksen, S., Schwanitz, M., Daniel, C., Hop, H., and Wiencke, C.: *Changes in kelp forest biomass and depth distribution in Kongsfjorden, Svalbard, between 1996–1998 and 2012–2014 reflect Arctic warming*, Polar Biol., 39, 2021–2036, doi:10.1007/s00300-015-1870-1, 2016.
- Barry, F.: *The influence of temperature on chemical reaction in general*, Am. J. Bot., 1, 203–225, doi:10.2307/2435254, 1914.
- Bauerfeind, E., Nöthig, E.-M., Beszczynska, A., Fahl, K., Kaleschke, L., Kreker, K., Klages, M., Soltwedel, T., Lorenzen, C., and Wegner, J.: *Particle sedimentation patterns in the eastern Fram Strait during 2000–2005: Results from the Arctic long-term observatory HAUSGARTEN*, Deep-Sea Res. Pt. I, 56, 1471–1487, doi:10.1016/j.dsr.2009.04.011, 2009.
- Bauerfeind, E., Leipe, T., and Ramseier, R. O.: *Sedimentation at the permanently ice-covered Greenland continental shelf (74°57.7'N/12°58.7'W): significance of biogenic and lithogenic particles in particulate matter flux*, J. Marine Syst., 56, 151–166, doi:10.1016/j.jmarsys.2004.09.007, 2005.
- Bauerfeind, E., Garrity, C., Krumbholz, M., Ramseier, R. O., and Voß, M.: *Seasonal variability of sediment trap collections in the Northeast Water Polynya. Part 2. Biochemical and microscopic composition of sedimenting matter*, J. Marine Syst., 10, 371–389, doi:10.1016/S0924-7963(96)00069-3, 1997.
- Bauerfeind, E., Bodungen, B. V., Arndt, K., and Koeve, W.: *Particle flux, and composition of sedimenting matter, in the Greenland Sea*, J. Marine Syst., 5, 411–423, doi:10.1016/0924-7963(94)90005-1, 1994.
- Beer, D. de, Sauter, E., Niemann, H., Kaul, N., Foucher, J., Witte, U., Schlüter, M., and Boetius, A.: *In situ fluxes and zonation of microbial activity in surface sediments of the Håkon Mosby Mud Volcano*, Limnol. Oceanogr., 51, 1315–1331, doi: 10.4319/lo.2006.51.3.1315, 2006.
- Belcher, A., Iversen, M., Manno, C., Henson, S. A., Tarling, G. A., and Sanders, R.: *The role of particle associated microbes in remineralization of fecal pellets in the upper mesopelagic of the Scotia Sea, Antarctica*, Limnol. Oceanogr., 61, 1049–1064, doi:10.1002/lno.10269, 2016.
- Bell, J. J., McGrath, E., Biggerstaff, A., Bates, T., Bennett, H., Marlow, J., and Shaffer, M.: *Sediment impacts on marine sponges*, Mar. Pollut. Bull., 94, 5–13, doi:10.1016/j.marpolbul.2015.03.030, 2015.
- Belley, R. and Snelgrove, P. V.: *Relative contributions of biodiversity and environment to benthic ecosystem functioning*, Front. Mar. Sci., 3, 53, doi:10.3389/fmars.2016.00242, 2016.
- Belley, R., Snelgrove, P. V., Archambault, P., Juniper, S. K., and Vopel, K. C.: *Environmental drivers of benthic flux variation and ecosystem functioning in Salish Sea and Northeast Pacific sediments*, PLoS ONE, 11, e0151110, doi:10.1371/journal.pone.0151110, 2016.

## References

---

- Berg, P., Røy, H., and Wiberg, P. L.: *Eddy correlation flux measurements: The sediment surface area that contributes to the flux*, *Limnol. Oceanogr.*, 52, 1672–1684, doi:10.4319/lo.2007.52.4.1672, 2007.
- Berg, P., Glud, R. N., Hume, A., Stahl, H., Oguri, K., Meyer, V., and Kitazato, H.: *Eddy correlation measurements of oxygen uptake in deep ocean sediments*, *Limnol. Oceanogr.-Meth.*, 7, 576–584, doi:10.4319/lom.2009.7.576, 2009.
- Berg, P., Røy, H., Janssen, F., Meyer, V., Jørgensen, B. B., Huettel, M., and Beer, D. de: *Oxygen uptake by aquatic sediments measured with a novel non-invasive eddy-correlation technique*, *Mar. Ecol. Prog. Ser.*, 261, 75–83, doi:10.3354/meps261075, 2003.
- Bergtrom, G.: *Cell and molecular biology: What we know & how we found out (Basic iText)*, Cell and molecular biology i-text, Book2, 2015.
- Bick, H.: *Grundzüge der Ökologie*, 3., überarb. und erg. Aufl, Spektrum, Akad. Verl., Heidelberg, 1999.
- Bintanja, R. and Selten, F. M.: *Future increases in Arctic precipitation linked to local evaporation and sea-ice retreat*, *Nature*, 509, 479–482, doi:10.1038/nature13259, 2014.
- Bischof, K., Hanelt, D., Tüg, H., Karsten, U., Brouwer, Patty E. M., and Wiencke, C.: *Acclimation of brown algal photosynthesis to ultraviolet radiation in Arctic coastal waters (Spitsbergen, Norway)*, *Polar Biol.*, 20, 388–395, doi:10.1007/s003000050319, 1998.
- Blackburn, T. H.: *Microbial food webs in sediments*, in: *Microbes in the sea*, Sleigh, M. A. (Ed.), Ellis Horwood series in marine science, Ellis Horwood, Halsted Press, Chichester, New York, 39–58, 1987.
- Boetius, A. and Damm, E.: *Benthic oxygen uptake, hydrolytic potentials and microbial biomass at the Arctic continental slope*, *Deep-Sea Res. Pt. I*, 45, 239–275, doi:10.1016/S0967-0637(97)00052-6, 1998.
- Boetius, A. and Lochte, K.: *Regulation of microbial enzymatic degradation of organic matter in deep-sea sediments*, *Mar. Ecol. Prog. Ser.*, 104, 299–307, 1994.
- Boetius, A., Albrecht, S., Bakker, K., Bienhold, C., Felden, J., Fernandez-Mendez, M., Hendricks, S., Katlein, C., Lalande, C., Krumpfen, T., Nicolaus, M., Peeken, I., Rabe, B., Rogacheva, A., Rybakova, E., Somavilla, R., and Wenzhöfer, F.: *Export of algal biomass from the melting Arctic sea ice*, *Science*, 339, 1430–1432, doi:10.1126/science.1231346, 2013.
- Booth, B. C. and Horner, R. A.: *Microalgae on the arctic ocean section, 1994: species abundance and biomass*, *Deep-Sea Res. Pt. II*, 44, 1607–1622, doi:10.1016/S0967-0645(97)00057-X, 1997.
- Børsheim, K. Y., Bratbak, G., and Heldal, M.: *Enumeration and biomass estimation of planktonic bacteria and viruses by transmission electron microscopy*, *Appl. Environ. Microb.*, 56, 352–356, 1990.
- Boudreau B. P.: *Diagenetic models and their implementation*, Springer Berlin Heidelberg, Berlin, Heidelberg, doi:10.1007/978-3-642-60421-8, 1997.
- Bourgeois, S., Archambault, P., and Witte, U.: *Organic matter remineralization in marine sediments: A Pan-Arctic synthesis*, *Global Biogeochem. Cy.*, 31, 190–213, doi:10.1002/2016GB005378, 2017.
- Bracegirdle, T. J., Stephenson, D. B., Turner, J., and Phillips, T.: *The importance of sea ice area biases in 21st century multimodel projections of Antarctic temperature and precipitation*, *Geophys. Res. Lett.*, 42, 832–839, doi:10.1002/2015GL067055, 2015.
- Braeckman, U., Hoffmann, R., Pasotti, F., Vazquez, S., Torstensson, A., Vanreusel, A., and Wenzhöfer, F.: *Spatio-temporal variability in biogeochemistry in Antarctic benthic communities influenced by glacier retreat*, in preparation.
- Braeckman, U., Provoost, P., Gribsholt, B., van Gansbeke, D., Middelburg, J. J., Soetaert, K., Vincx, M., and Vanaverbeke, J.: *Role of macrofauna functional traits and density in biogeochemical fluxes and bioturbation*, *Mar. Ecol. Prog. Ser.*, 399, 173–186, doi:10.3354/meps08336, 2010.
- Brandt, R. E., Warren, S. G., Worby, A. P., and Grenfell, T. C.: *Surface albedo of the Antarctic sea ice zone*, *J. Climate*, 18, 3606–3622, doi:10.1175/JCLI3489.1, 2005.
- Brey, T.: *An empirical model for estimating aquatic invertebrate respiration*, *Methods Ecol. Evol.*, 1, 92–101, doi:10.1111/j.2041-210X.2009.00008.x, 2010.
- Brown, K. M., Fraser, K. P. P., Barnes, D. K. A., and Peck, L. S.: *Links between the structure of an Antarctic shallow-water community and ice-scour frequency*, *Oecologia*, 141, 121–129, doi:10.1007/s00442-004-1648-6, 2004.

- Burdige, D. J.: *Geochemistry of Marine Sediments*, Princeton University Press, Princeton, NJ, 2006.
- Buttigieg, P. L. and Ramette, A.: *A guide to statistical analysis in microbial ecology: a community-focused, living review of multivariate data analyses*, FEMS Microbiol. Ecol., 90, 543–550, doi:10.1111/1574-6941.12437, 2014.
- Bayne, B. L., Iglesias, J. I. P., Hawkins, A. J. S., Navarro, E., Heral, M., and Deslous-Paoli, J. M.: *Feeding behaviour of the mussel, Mytilus edulis: responses to variations in quantity and organic content of the seston*, J. Mar. Biol. Ass., 73, 813–829, doi:10.1017/S0025315400034743, 1993.
- Canfield, D. E., Kristensen, E., and Thamdrup, B.: *Aquatic geomicrobiology*, Adv. Mar. Biol., 48, Academic Press, Amsterdam, London, 2005.
- Caron, D. A. and Hutchins, D. A.: *The effects of changing climate on microzooplankton grazing and community structure: drivers, predictions and knowledge gaps*, J. Plankton Res., 35, 235–252, doi:10.1093/plankt/fbs091, 2013.
- Catalano, G., Budillon, G., La feria, R., Povero, P., Ravaioli, M., Saggiomo, V., Accornero, A., Azzaro, M., Carrada, G. C., Giglio, F., Langone, L., Mangoni, O., Mistic, C., and Modigh, M.: *The Ross Sea*, in: Carbon and nutrient fluxes in continental margins, Liu, K.-K., Atkinson, L., Quiñones, R., and Talaue-McManus, L. (Eds.), Springer Berlin Heidelberg, Berlin, Heidelberg, 303–318, 2010.
- Cathalot, C., Rabouille, C., Sauter, E., Schewe, I., Soltwedel, T., and Vopel, K. C.: *Benthic oxygen uptake in the Arctic ocean margins - A case study at the deep-Sea observatory HAUSGARTEN (Fram Strait)*, PLoS ONE, 10, doi:10.1371/journal.pone.0138339, 2015.
- Chapman, W. L. and Walsh, J. E.: *A synthesis of Antarctic temperatures*, J. Climate, 20, 4096–4117, doi:10.1175/JCLI4236.1, 2007.
- Cherkasheva, A., Bracher, A., Melsheimer, C., Köberle, C., Gerdes, R., Nöthig, E.-M., Bauerfeind, E., and Boetius, A.: *Influence of the physical environment on polar phytoplankton blooms: A case study in the Fram Strait*, J. Marine Syst., 132, 196–207, doi:10.1016/j.jmarsys.2013.11.008, 2014.
- Chester, R.: *Marine geochemistry*, Chapman and Hall, New York, 1990.
- Chipman, L., Huettel, M., Berg, P., Meyer, V., Klimant, I., Glud, R., and Wenzhöfer, F.: *Oxygen optodes as fast sensors for eddy correlation measurements in aquatic systems*, Limnol. Oceanogr. Meth., 10, 304–316, doi:10.4319/lom.2012.10.304, 2012.
- Chisholm, S. W.: *Stirring times in the Southern Ocean*, Nature, 407, 685–686, doi:10.1038/35037696, 2000.
- Christensen, J. P.: *A relationship between deep-sea benthic oxygen demand and oceanic primary productivity*, Oceanol. Acta, 23, 65–82, doi:10.1016/S0399-1784(00)00101-8, 2000.
- Clarke, K. R. and Gorley, R. N.: *Primer v6: User Manual/Tutorial*, PRIMER-E, Plymouth, 2006.
- Clarke, K. R. and Warwick, R. M.: *Similarity-based testing for community pattern: the two-way layout with no replication*, Mar. Biol., 118, 167–176, doi:10.1007/BF00699231, 1994.
- Clem, K. R. and Fogt, R. L.: *Varying roles of ENSO and SAM on the Antarctic Peninsula climate in austral spring*, J. Geophys. Res. Atmos., 118, 11481–11492, doi:10.1002/jgrd.50860, 2013.
- Clough, L. M., Renaud, P. E., and William, G. A.: *Impacts of water depth, sediment pigment concentration, and benthic macrofaunal biomass on sediment oxygen demand in the western Arctic Ocean*, Can. J. Fish. Aquat. Sci., 62, 1756–1765, doi:10.1139/F05-102, 2005.
- Coachman, L. K. and Aagaard, K.: *Transports through Bering Strait: Annual and interannual variability*, J. Geophys. Res., 93, doi:10.1029/JC093iC12p15535, 1988.
- Codispoti, L. A., Kelly, V., Thessen, A., Matrai, P., Suttles, S., Hill, V., Steele, M., and Light, B.: *Synthesis of primary production in the Arctic Ocean: III. Nitrate and phosphate based estimates of net community production*, Prog. Oceanogr., 110, 126–150, doi:10.1016/j.pocean.2012.11.006, 2013.
- Cognie, B. and Barille, L.: *Does bivalve mucus favour the growth of their main food source, microalgae?*, Oceanol. Acta, 22, 441–450, doi:10.1016/S0399-1784(00)88727-7, 1999.
- Comiso, J. C.: *Large decadal decline of the Arctic multiyear ice cover*, J. Climate, 25, 1176–1193, doi:10.1175/JCLI-D-11-00113.1, 2012.
- Comiso, J. C.: *A rapidly declining perennial sea ice cover in the Arctic*, Geophys. Res. Lett., 29, doi:10.1029/2002GL015650, 2002.

## References

---

- Comiso, J. C., Parkinson, C. L., Gersten, R., and Stock, L.: *Accelerated decline in the Arctic sea ice cover*, *Geophys. Res. Lett.*, 35, doi:10.1029/2007GL031972, 2008.
- Conlan, K. E., Lenihan, H. S., Kvitek, R. G., and Oliver, J. S.: *Ice scour disturbance to benthic communities in the Canadian High Arctic*, *Mar. Ecol. Prog. Ser.*, 166, 1–16, doi: 10.3354/meps166001, 1998.
- Connell, J. H.: *Diversity in tropical rain forests and coral reefs*, *Science*, 199, 1302–1310. doi:10.1126/science.199.4335.1302, 1978.
- Consalvey, M., Paterson, D. M., and Underwood, Graham J. C.: *The ups and downs of life in a benthic biofilm: Migration of benthic diatoms*, *Diatom Res.*, 19, 181–202, doi:10.1080/0269249X.2004.9705870, 2004.
- Cook, A. J., Holland, P. R., Meredith, M. P., Murray, T., Luckman, A., and Vaughan, D. G.: *Ocean forcing of glacier retreat in the western Antarctic Peninsula*, *Science*, 353, 283–286, doi:10.1126/science.aae0017, 2016.
- Cranston, R. E.: *Organic carbon burial rates across the Arctic Ocean from the 1994 Arctic Ocean Section expedition*, *Deep-Sea Res. Pt. II*, 44, 1705–1723, doi:10.1016/S0967-0645(97)00065-9, 1997.
- Dalokken, R., Sandvik, R., Sakshaug, E., and Jaffe, J. S.: *Variations in bio-optical properties in the Greenland/Iceland/Norwegian seas*, in: *Ocean Optics XII*, Bergen, Norway, SPIE Proceedings, SPIE, 266–276, 1994.
- Dayton, P. K., Watson, D., Palmisano, A., Barry, J. P., Oliver, J. S., and Rivera, D.: *Distribution patterns of benthic microalgal standing stock at McMurdo Sound, Antarctica*, *Polar Biol.*, 6, 207–213, doi:10.1007/BF00443397, 1986.
- DeJong, H. B., Dunbar, R. B., and Lyons, E. A.: *Late summer frazil ice-associated algal blooms around Antarctica*, *Geophys. Res. Lett.*, 45, 826–833, doi:10.1002/2017GL075472, 2018.
- Demidov, A. B., Sheberstov, S. V., Gagarin, V. I., and Khlebopashev, P. V.: *Seasonal variation of the satellite-derived phytoplankton primary production in the Kara Sea*, *Oceanology*, 57, 91–104, doi:10.1134/S0001437017010027, 2017.
- Deregibus, D., Quartino, M. L., Campana, G. L., Momo, F. R., Wiencke, C., and Zacher, K.: *Photosynthetic light requirements and vertical distribution of macroalgae in newly ice-free areas in Potter Cove, South Shetland Islands, Antarctica*, *Polar Biol.*, 39, 153–166, doi:10.1007/s00300-015-1679-y, 2016.
- Devol, A. H., Codispoti, L. A., and Christensen, J. P.: *Summer and winter denitrification rates in western Arctic shelf sediments*, *Cont. Shelf Res.*, 17, 1029–1050, doi:10.1016/S0278-4343(97)00003-4, 1997.
- Dierssen, H. M., Smith, R. C., and Vernet, M.: *Glacial meltwater dynamics in coastal waters west of the Antarctic Peninsula*, *P. Nat. Acad. Sci. USA*, 99, 1790–1795, 2002.
- Ding, Q., Steig, E. J., Battisti, D. S., and Küttel, M.: *Winter warming in West Antarctica caused by central tropical Pacific warming*, *Nature Geosci.*, 4, 398–403, doi:10.1038/ngeo1129, 2011.
- Donis, D., McGinnis, D. F., Holtappels, M., Felden, J., and Wenzhöfer, F.: *Assessing benthic oxygen fluxes in oligotrophic deep sea sediments (HAUSGARTEN observatory)*, *Deep-Sea Res. Pt. I*, 111, 1–10, doi:10.1016/j.dsr.2015.11.007, 2016.
- Donis, D., Holtappels, M., Noss, C., Cathalot, C., Hancke, K., Polsenaere, P., Wenzhöfer, F., Lorke, A., Meysman, Filip J. R., Glud, R. N., and McGinnis, D. F.: *An assessment of the precision and confidence of aquatic eddy correlation measurements*, *J. Atmos. Oceanic Technol.*, 32, 642–655, doi:10.1175/JTECH-D-14-00089.1, 2015.
- Ducklow, H. W., Baker, K., Martinson, D. G., Quetin, L. B., Ross, R. M., Smith, R. C., Stammerjohn, S. E., Vernet, M., and Fraser, W.: *Marine pelagic ecosystems: the West Antarctic Peninsula*, *Philos. T. Roy. Soc. B*, 362, 67–94, doi:10.1098/rstb.2006.1955, 2007.
- Dunn, O. J.: *Multiple comparisons using rank sums*. In: *Technometrics*, 6, doi: 10.2307/1266041, 1964.
- Edler, L.: *Recommendations on methods for marine biological studies in the Baltic Sea. Phytoplankton and chlorophyll*, *Balt. Mar. Biol. Publ.*, 1–38, 1979.
- Ellis, J. I., Clark, D., Atalah, J., Jiang, W., Taiapa, C., Patterson, M., Sinner, J., and Hewitt, J.: *Multiple stressor effects on marine infauna: responses of estuarine taxa and functional traits to sedimentation, nutrient and metal loading*, *Sci. Rep.*, 7, doi:10.1038/s41598-017-12323-5, 2017.



- Emmerton, C. A., Lesack, L. F., and Vincent, W. F.: *Nutrient and organic matter patterns across the Mackenzie River, estuary and shelf during the seasonal recession of sea-ice*, J. Marine Syst., 74, 741–755, doi:10.1016/j.jmarsys.2007.10.001, 2008.
- English, T. S.: *Some biological observations in the central North Polar Sea. Drift Station Alpha. 1957–1958*, Arctic Inst. N. Am. Res. Pap., 13, 1961.
- Esper, O., Gersonde, R., and Kadagies, N.: *Diatom distribution in southeastern Pacific surface sediments and their relationship to modern environmental variables*, Palaeogeogr. Palaeoclimatol., 287, 1–27, doi:10.1016/j.palaeo.2009.12.006, 2010.
- Ezraty, R., Girard-Ardhuin, F., Piollé, J.-F., Kaleschke, L., and Heygster, G.: *Arctic and Antarctic Sea Ice concentration and Arctic Sea Ice drift estimated from Special Sensor Microwave Data: User's Manual, Version 2.1*, Département d'Océanographie Physique et Spatiale, IFREMER (Brest, France) and Institute of Environmental Physics, University of Bremen, 2007.
- Fahrbach, E., Meincke, J., Østerhus, S., Rohardt, G., Schauer, U., Tverberg, V., and Verduin, J.: *Direct measurements of volume transports through Fram Strait*, Polar Res., 20, 217–224, doi:10.1111/j.1751-8369.2001.tb00059.x, 2001.
- Falkowski, P. G. and Raven, J. A.: *Aquatic photosynthesis*, Second edition, Princeton University Press, Woodstock, 2007.
- Fennel, K.: *The role of continental shelves in nitrogen and carbon cycling: Northwestern North Atlantic case study*, Ocean Sci., 6, 539–48. doi:10.5194/os-6-539-2010, 2010.
- Fernández-Méndez, M., Katlein, C., Rabe, B., Nicolaus, M., Peeken, I., Bakker, K., Flores, H., and Boetius, A.: *Photosynthetic production in the central Arctic Ocean during the record sea-ice minimum in 2012*, Biogeosciences, 12, 3525–3549, doi:10.5194/bg-12-3525-2015, 2015.
- Field, C. B., Behrenfeld, M. J., Randerson, J. T., and Falkowski, P.: *Primary production of the biosphere: integrating terrestrial and oceanic components*, Science, 281, 237–240, doi:10.1126/science.281.5374.237, 1998.
- Fillinger, L., Janussen, D., Lundälv, T., and Richter, C.: *Rapid glass sponge expansion after climate-induced Antarctic ice shelf collapse*, Curr. Biol., 23, 1330–1334, doi:10.1016/j.cub.2013.05.051, 2013.
- Findlay, H. S., Gibson, G., Kędra, M., Morata, N., Orchowska, M., Pavlov, A. K., Reigstad, M., Silyakova, A., Tremblay, J.-É., Walczowski, W., Weydmann, A., and Logvinova, C.: *Responses in Arctic marine carbon cycle processes: conceptual scenarios and implications for ecosystem function*, Polar Res., 34, 24252, doi:10.3402/polar.v34.24252, 2015.
- Findlay, R. H., King, G. M., and Watling, L.: *Efficacy of phospholipid analysis in determining microbial biomass in sediments*, Appl. Environ. Microb., 55, 2888–2893, 1989.
- Fisher, J. A., Jacob, D. J., Soerensen, A. L., Amos, H. M., Steffen, A., and Sunderland, E. M.: *Riverine source of Arctic Ocean mercury inferred from atmospheric observations*, Nature Geosci., 5, 499–504, doi:10.1038/ngeo1478, 2012.
- Flach, E., Muthumbi, A., and Heip, C.: *Meiofauna and macrofauna community structure in relation to sediment composition at the Iberian margin compared to the Goban Spur (NE Atlantic)*, Prog. Oceanogr., 52, 433–457, doi:10.1016/S0079-6611(02)00018-6, 2002.
- Forest, A., Wassmann, P., Slagstad, D., Bauerfeind, E., Nöthig, E.-M., and Klages, M.: *Relationships between primary production and vertical particle export at the Atlantic-Arctic boundary (Fram Strait, HAUSGARTEN)*, Polar Biol., 33, 1733–1746, doi:10.1007/s00300-010-0855-3, 2010.
- Fox, J., Weisberg, S.: *An {R} Companion to Applied Regression*, Second Edition, Thousand Oaks CA, URL: <http://socserv.socsci.mcmaster.ca/jfox/Books/Companion>, 2011.
- Fritzsche, E., Gruber, P., Schutting, S., Fischer, J. P., Strobl, M., Müller, J. D., Borisov, S. M., and Klimant, I.: *Highly sensitive poisoning-resistant optical carbon dioxide sensors for environmental monitoring*, Anal. Methods, 9, 55–65, doi:10.1039/c6ay02949c, 2017.
- Galley, R. J., Key, E., Barber, D. G., Hwang, B. J., and Ehn, J. K.: *Spatial and temporal variability of sea ice in the southern Beaufort Sea and Amundsen Gulf: 1980–2004*, J. Geophys. Res., 113, doi:10.1029/2007JC004553, 2008.

## References

---

- Games, P. A. and Howell, J. F.: *Pairwise multiple comparison procedures with unequal N's and/or variances: A Monte Carlo study*, *J. Educ. Behav. Stat.*, 1, 113–125, doi:10.3102/10769986001002113, 1976.
- Gibbs, J. W.: *A method of geometrical representation of the thermodynamic properties of substances by means of surfaces*, *T. Connecticut Acad. Arts S.*, 382–404, 1873.
- Giblin, A. E., Hopkinson, C. S., and Tucker, J.: *Benthic Metabolism and Nutrient Cycling in Boston Harbor, Massachusetts*, *Estuaries*, 20, 346–364, doi: 10.2307/1352349, 1997.
- Gilbert, N. S.: *Microphytobenthic seasonality in near-shore marine sediments at Signy Island, South Orkney Islands, Antarctica*, *Estuar. Coast. Shelf S.*, 33, 89–104, doi:10.1016/0272-7714(91)90072-J, 1991a.
- Gilbert, N. S.: *Primary production by benthic microalgae in nearshore marine sediments of Signy Island, Antarctica*, *Polar Biol.*, 11, 339–346, doi:10.1007/BF00239026, 1991b.
- Gleiber, M. R., Steinberg, D. K., and Ducklow, H. W.: *Time series of vertical flux of zooplankton fecal pellets on the continental shelf of the western Antarctic Peninsula*, *Mar. Ecol. Prog. Ser.*, 471, 23–36, doi:10.3354/meps10021, 2012.
- Glover, A. G., Smith, C. R., Mincks, S. L., Sumida, P. Y., and Thurber, A. R.: *Macrofaunal abundance and composition on the West Antarctic Peninsula continental shelf: Evidence for a sediment 'food bank' and similarities to deep-sea habitats*, *Deep-Sea Res. Pt. II*, 55, 2491–2501, doi:10.1016/j.dsr2.2008.06.008, 2008.
- Glud, R. N.: *Oxygen dynamics of marine sediments*, *Mar. Biol. Res.*, 4, 243–289, doi:10.1080/17451000801888726, 2008.
- Glud, R. N., Berg, P., Stahl, H., Hume, A., Larsen, M., Eyre, B. D., and Cook, P. L. M.: *Benthic carbon mineralization and nutrient turnover in a Scottish Sea Loch: An integrative in situ study*, *Aquat. Geochem.*, 22, 443–467, doi:10.1007/s10498-016-9300-8, 2016.
- Glud, R. N., Woelfel, J., Karsten, U., Kühl, M., and Rysgaard, S.: *Benthic microalgal production in the Arctic: applied methods and status of the current database*, *Bot. Mar.*, 52, 559–571, doi:10.1515/BOT.2009.074, 2009.
- Glud, R. N., Kühl, M., Wenzhöfer, F., and Rysgaard, S.: *Benthic diatoms of a high Arctic fjord (Young Sound, NE Greenland): importance for ecosystem primary production*, *Mar. Ecol. Prog. Ser.*, 238, 15–29, doi:10.3354/meps238015, 2002.
- Glud, R. N., Holby, O., Hoffmann, F., and Canfield, D. E.: *Benthic mineralization and exchange in Arctic sediments (Svalbard, Norway)*, *Mar. Ecol. Prog. Ser.*, 173, 237–251, doi:10.3354/meps173237, 1998.
- Glud, R. N., Gundersen, J. K., Jørgensen, B. B., Revsbech, N. P., and Schulz, H. D.: *Diffusive and total oxygen uptake of deep-sea sediments in the eastern South Atlantic Ocean: in situ and laboratory measurements*, *Deep-Sea Res. Pt. I*, 41, 1767–1788, doi:10.1016/0967-0637(94)90072-8, 1994.
- Gómez, I., Wulff, A., Roleda, M. Y., Huovinen, P., Karsten, U., Quartino, M. L., Dunton, K., and Wiencke, C.: *Light and temperature demands of marine benthic microalgae and seaweeds in polar regions*, *Bot. Mar.*, 52, 593–608, doi:10.1515/BOT.2009.073, 2009.
- Gontikaki, E., van Oevelen, D., Soetaert, K., and Witte, U.: *Food web flows through a sub-arctic deep-sea benthic community*, *Prog. Oceanogr.*, 91, 245–259, doi:10.1016/j.pocean.2010.12.014, 2011.
- Górska, B., Grzelak, K., Kotwicki, L., Hasemann, C., Schewe, I., Soltwedel, T., and Włodarska-Kowalczyk, M.: *Bathymetric variations in vertical distribution patterns of meiofauna in the surface sediments of the deep Arctic ocean (HAUSGARTEN, Fram strait)*, *Deep-Sea Res. Pt. I*, 91, 36–49, doi:10.1016/j.dsr.2014.05.010, 2014.
- Gosselin, M., Levasseur, M., Wheeler, P. A., Horner, R. A., and Booth, B. C.: *New measurements of phytoplankton and ice algal production in the Arctic Ocean*, *Deep-Sea Res. Pt. II*, 44, 1623–1644, doi:10.1016/S0967-0645(97)00054-4, 1997.
- Gradinger, R.: *Sea-ice algae: Major contributors to primary production and algal biomass in the Chukchi and Beaufort Seas during May/June 2002*, *Deep-Sea Res. Pt. II*, 56, 1201–1212, doi:10.1016/j.dsr2.2008.10.016, 2009.
- Graeve, M. and Ludwichowski, K.-U.: *Inorganic nutrients measured on water bottle samples during POLARSTERN cruise PS85 (ARK-XXVIII/2)*, PANGAEA, doi.org/10.1594/PANGAEA.882217, 2017a.

- Graeve, M. and Ludwichowski, K.-U.: *Inorganic nutrients measured on water bottle samples during POLARSTERN cruise PS93.2 (ARK-XXIX/2.2)*, PANGAEA, doi.org/10.1594/PANGAEA.884130, 2017b.
- Graf, G.: *Benthic-pelagic coupling in a deep-sea benthic community*, *Nature*, 341, 437–439, doi:10.1038/341437a0, 1989.
- Graf, G., Gerlach, S., Linke, P., Queisser, W., Ritzrau, W., Scheltz, A., Thomsen, L., and Witte, U.: *Benthic-pelagic coupling in the Greenland-Norwegian Sea and its effect on the geological record*, *Geol. Rundsch.*, 84, doi:10.1007/BF00192241, 1995.
- Grasshoff, K., Kremling, K., and Ehrhardt, M.: *Methods of Seawater Analysis*, Wiley, Weinheim, Germany, doi:10.1002/9783527613984, 1999.
- Grebmeier, J. M. and Barry, J. P.: *Chapter 11 – Benthic processes in polynyas*, in: *Polynyas: Windows to the World*, Elsev. Oceanogr. Serie., Elsevier, 363–390, 2007.
- Grebmeier, J. M. and Cooper, L. W.: *Influence of the St. Lawrence Island Polynya upon the Bering Sea benthos*, *J. Geophys. Res.*, 100, 4439–4460, doi:10.1029/94JC02198, 1995.
- Grebmeier, J. M., Ditullio, G. R., Barry, J. P., and Cooper, L. W.: *Benthic carbon cycling in the Ross Sea polynya, Antarctica: Benthic Cmmunity metabolism and sediment tracers*, in: *Biogeochemistry of the Ross Sea*, Ditullio, G. R., and Dunbar, R. B. (Eds.), American Geophysical Union, 313–326, 2003.
- Grebmeier, J. M., McRoy, P. C., and Feder, H. M.: *Pelagic-benthic coupling on the shelf of the northern Bering and Chukchi Seas. I. Food supply source and benthic biomass*, *Mar. Ecol. Prog. Ser.*, 48, 57–67, 1988.
- Greiser, N. and Faubel, A.: *Biotic factors*, in: *Introduction to the study of meiofauna*, Higgins, R. P., and Thiel, H. (Eds.), Smithsonian Institution Press, Washington, D.C, 79–114, 1988.
- Griffiths, H. J.: *Antarctic marine biodiversity – what do we know about the distribution of life in the Southern Ocean?*, *PLoS ONE*, 5, doi:10.1371/journal.pone.0011683, 2010.
- Grime, J. P.: *Control of species density in herbaceous vegetation*, *J. Environ. Manage.*, 1, 151–167, doi:10.2307/3546874, 1973.
- Grossmann, S. and Reichardt, W.: *Impact of Arenicola marina on bacteria in intertidal sediments*, *Mar. Ecol. Prog. Ser.*, 77, 85–93, doi:10.3354/meps077085, 1991.
- Gundersen, J. K. and Jorgensen, B. B.: *Microstructure of diffusive boundary layers and the oxygen uptake of the sea floor*, *Nature*, 345, 604–607, doi:10.1038/345604a0, 1990.
- Gutt, J., Bertler, N., Bracegirdle, T. J., Buschmann, A., Comiso, J., Hosie, G., Isla, E., Schloss, I. R., Smith, C. R., Tournadre, J., and Xavier, J. C.: *The Southern Ocean ecosystem under multiple climate change stresses—an integrated circumpolar assessment*, *Glob. Change Biol.*, 21, 1434–1453, doi:10.1111/gcb.12794, 2015.
- Haese, R. R.: *The Biogeochemistry of iron*, in: *Marine Geochemistry*, Schulz, H. D. and Zabel, M. (Eds.), Springer Berlin Heidelberg, Berlin, Heidelberg, 241–270, 2006.
- Hall, P.J. and Aller, R.C.: *Rapid, small-volume, flow injection analysis for CO<sub>2</sub>, and NH<sub>4</sub><sup>+</sup> in marine and freshwaters*, *Limnol. Oceanogr.*, 37, 1113–1119, doi:10.4319/lo.1992.37.5.1113, 1992.
- Hansell, D., Carlson, C., Repeta, D., and Schlitzer, R.: *Dissolved organic matter in the ocean: A controversy stimulates new insights*, *Oceanography*, 22, 202–211, doi:10.5670/oceanog.2009.109, 2009.
- Hansen, E., Gerland, S., Granskog, M. A., Pavlova, O., Renner, A. H. H., Haapala, J., Løyning, T. B., and Tschudi, M.: *Thinning of Arctic sea ice observed in Fram Strait: 1990–2011*, *J. Geophys. Res. Oceans*, 118, 5202–5221, doi:10.1002/jgrc.20393, 2013.
- Harada, N.: *Review: Potential catastrophic reduction of sea ice in the western Arctic Ocean: Its impact on biogeochemical cycles and marine ecosystems*, *Global Planet. Change*, 136, 1–17, doi:10.1016/j.gloplacha.2015.11.005, 2015.
- Harper, E. M., Clark, M. S., Hoffman, J. I., Philipp, Eva E. R., Peck, L. S., Morley, S. A., and Briffa, M.: *Iceberg scour and shell damage in the Antarctic bivalve Laternula elliptica*, *PLoS ONE*, 7, doi:10.1371/journal.pone.0046341, 2012.
- Harper, M. A.: *Movements*, in: *The biology of diatoms*, Werner, D. (Ed.), Blackwell, Oxford, 224–249, 1977.

## References

---

- Hart, T. J.: *Phytoplankton periodicity in Antarctic surface waters*, Cambridge University Press, 1942.
- Hartnett, H., Boehme, S., Thomas, C., DeMaster, D., and Smith, C.: *Benthic oxygen fluxes and denitrification rates from high-resolution porewater profiles from the Western Antarctic Peninsula continental shelf*, *Deep-Sea Res. Pt. II*, 55, 2415–2424, doi:10.1016/j.dsr2.2008.06.002, 2008.
- Hassol, S.: *Impacts of a warming Arctic: Arctic climate impact assessment*, Cambridge University Press, Cambridge, U.K, New York, N.Y., 2004.
- Hattermann, T., Isachsen, P. E., von Appen, W.-J., Albretsen, J., and Sundfjord, A.: *Eddy-driven recirculation of Atlantic Water in Fram Strait*, *Geophys. Res. Lett.*, 43, 3406–3414, doi:10.1002/2016GL068323, 2016.
- Haumann, F. A., Notz, D., and Schmidt, H.: *Anthropogenic influence on recent circulation-driven Antarctic sea ice changes*, *Geophys. Res. Lett.*, 41, 8429–8437, doi:10.1002/2014GL061659, 2014.
- Hay, S. I., Maitland, T. C., and Paterson, D. M.: *The speed of diatom migration through natural and artificial substrata*, *Diatom Res.*, 8, 371–384, doi:10.1080/0269249X.1993.9705268, 1993.
- Heinze, C., Meyer, S., Goris, N., Anderson, L., Steinfeldt, R., Chang, N., Le Quéré, C., and Bakker, D. C. E.: *The ocean carbon sink—impacts, vulnerabilities and challenges*, *Earth Syst. Dynam.*, 6, 327–358, doi:10.5194/esd-6-327-2015, 2015.
- Heip, C., Vincx, M., and Vranken, G.: *The Ecology of marine nematodes*, in: *Oceanography and Marine Biology: An Annual Review*, Barnes, M. (Ed.), 23, 399–489, 1985.
- Helland-Hansen, B. and Nansen, F.: *The Norwegian Sea – its physical oceanography based upon the Norwegian researches 1900–1904*, 2, Fiskeridirektoratets havforskningsinstitut, 1909.
- Henson, S. A., Beaulieu, C., and Lampitt, R.: *Observing climate change trends in ocean biogeochemistry: when and where*, *Glob. Change Biol.*, 22, 1561–1571, doi:10.1111/gcb.13152, 2016.
- Hensen, C., Zabel, M., and Schulz, H. N.: *Benthic cycling of oxygen, nitrogen and phosphorus*, in: *Marine Geochemistry*, Schulz, H. D. and Zabel, M. (Eds.), Springer Berlin Heidelberg, Berlin, Heidelberg, 207–240, 2006.
- Hensen, C., Zabel, M., and Schulz, H. D.: *A comparison of benthic nutrient fluxes from deep-sea sediments off Namibia and Argentina*, *Deep-Sea Res. Pt. II*, 47, 2029–2050, doi:10.1016/S0967-0645(00)00015-1, 2000.
- Héquette, A., Desrosiers, M., and Barnes, P. W.: *Sea ice scouring on the inner shelf of the southeastern Canadian Beaufort Sea*, *Mar. Geol.*, 128, 201–219, doi:10.1016/0025-3227(95)00095-G, 1995.
- Herrera, A., Gómez, M., Packard, T. T., and Fernández de Puelles, M.L.: *Reprint of “Zooplankton biomass and electron transport system activity around the Balearic Islands (western Mediterranean)”*, *J. Marine Syst.*, 138, 95–103, doi:10.1016/j.jmarsys.2014.06.006, 2014.
- Hill, V. J., Matrai, P. A., Olson, E., Suttles, S., Steele, M., Codispoti, L. A., and Zimmerman, R. C.: *Synthesis of integrated primary production in the Arctic Ocean: II. In situ and remotely sensed estimates*, *Prog. Oceanogr.*, 110, 107–125, doi:10.1016/j.pocean.2012.11.005, 2013.
- Hillebrand, H., Dürselen, C.-D., Kirschtel, D., Pollinger, U., and Zohary, T.: *Biovolume calculation for pelagic and benthic microalgae*, *J. Phycol.*, 35, 403–424, doi:10.1046/j.1529-8817.1999.3520403.x, 1999.
- Hobbie, J. E., Daley, R. J., and Jasper, S.: *Use of nuclepore filters for counting bacteria by fluorescence microscopy*, *Appl. and Environ. Microb.*, 33, 1225–1228, 1977.
- Hoffmann, R., Braeckman, U., and Wenzhöfer, F.: *In situ measured oxygen profiles in Potter Cove at the stations Faro, Creek and Isla D*, PANGAEA, doi:10.1594/PANGAEA.885472, 2018.
- Holm-Hansen, O., El-Sayed, S. Z., Franceschini, G. A., Cuhel, G. A., and Cuhel, R. L.: *Primary production and the factors controlling phytoplankton growth in the Southern Ocean*, in: *Adaptions within Antarctic ecosystems: Proceedings of the third SCAR symposium on Antarctic biology [held at Washington, D.C., August 26.–30., 1974]*, Llano, G. A. (Ed.), Smithsonian Institution, Washington, D.C., 11–73, 1977.
- Holtappels, M., Hoffmann, R., Nowak, C., Merz, E., Sahade, R., Wenzhöfer, F. and Richter, C.: *Benthic oxygen fluxes in coastal waters at King George Island*, conference talk, XIth SCAR Biology Symposium, Leuven, Belgium, 10/07–14/07/2017.

- Hop, H., Falk-Petersen, S., Svendsen, H., Kwasniewski, S., Pavlov, V., Pavlova, O., and Søreide, J. E.: *Physical and biological characteristics of the pelagic system across Fram Strait to Kongsfjorden*, Prog. Oceanogr., 71, 182–231, doi:10.1016/j.pocean.2006.09.007, 2006.
- Hop, H., Kovaltchouk, N. A., and Wiencke, C.: *Distribution of macroalgae in Kongsfjorden*, Svalbard, Polar Biol., 39, 2037–2051, doi:10.1007/s00300-016-2048-1, 2016.
- Hop, H., Pearson, T., Hegseth, E. N., Kovacs, K. M., Wiencke, C., Kwasniewski, S., Eiane, K., Mehlum, F., Gulliksen, B., Wlodarska-Kowalczyk, M., Lydersen, C., Weslawski, J. M., Cochrane, S., Gabrielsen, G. W., Leakey, Raymond J. G., Lønne, O. J., Zajaczkowski, M., Falk-Petersen, S., Kendall, M., Wängberg, S.-Å., Bischof, K., Voronkov, A. Y., Kovaltchouk, N. A., Wiktor, J., Poltermann, M., Prisco, G., Papucci, C., and Gerland, S.: *The marine ecosystem of Kongsfjorden*, Svalbard, Polar Research, 21, 167–208, doi:10.1111/j.1751-8369.2002.tb00073.x, 2002.
- Hop, H., Wiencke, C., Vögele, B., and Kovaltchouk, N. A.: *Species composition, zonation, and biomass of marine benthic macroalgae in Kongsfjorden*, Svalbard, Bot. Mar., 55, 399–414, doi:10.1515/bot-2012-0097, 2012.
- Hopkins, J. T.: *Some light-induced changes in the behaviour and cytology of an estuarine mudflat diatom*, in: Light as an Ecological Factor, Bainbridge, R. (Ed.), Blackwell, Oxford, 335–358, 1963.
- Horn, H. S.: *Markovian properties of forest succession*, in: Ecology and evolution of communities, Cody, M. L. and Diamond, J. M. (Eds), Belknap Press. Cambridge, MA, 196–211. 1975.
- Horner, R., Ackley, S. F., Dieckmann, G. S., Gulliksen, B., Hoshiai, T., Legendre, L., Melnikov, I. A., Reeburgh, W. S., Spindler, M., and Sullivan, C. W.: *Ecology of sea ice biota*, Polar Biol., 12, 417–427, doi:10.1007/BF00243113, 1992.
- Hügler, M. and Sievert, S. M.: *Beyond the calvin cycle: autotrophic carbon fixation in the ocean*, Annu. Rev. Mar. Sci., 3, 261–289, doi:10.1146/annurev-marine-120709-142712, 2011.
- Hulth, S., Tengberg, A., Landén, A., and Hall, P. O.: *Mineralization and burial of organic carbon in sediments of the southern Weddell Sea (Antarctica)*, Deep-Sea Res. Pt. I, 44, 955–981, doi:10.1016/S0967-0637(96)00114-8, 1997.
- Hunt, G. L., Drinkwater, K. F., Arrigo, K., Berge, J., Daly, K. L., Danielson, S., Daase, M., Hop, H., Isla, E., Karnovsky, N., Laidre, K., Mueter, F. J., Murphy, E. J., Renaud, P. E., Smith, W. O., Trathan, P., Turner, J., and Wolf-Gladrow, D.: *Advection in polar and sub-polar environments: Impacts on high latitude marine ecosystems*, Prog. Oceanogr., 149, 40–81, doi:10.1016/j.pocean.2016.10.004, 2016.
- IPCC, 2.: *Summary for Policymakers*, in: Climate Change 2013: The Physical Science Basis. Contribution of Working Group I to the Fifth Assessment Report of the Intergovernmental Panel on Climate Change, Stocker, T. F., Qin, D., Plattner, G.-K., Tignor, M., Allen, S. K., Boschung, J., Nauels, A., Xia, Y., Bex, V., and Midgley, P. (Eds.), Cambridge University Press, Cambridge, United Kingdom and New York, NY, USA, 1–30, 2013.
- Jacob, M., Soltwedel, T., Boetius, A., Ramette, A., and Gilbert, J. A.: *Biogeography of deep-sea benthic bacteria at regional scale (LTER HAUSGARTEN, Fram Strait, Arctic)*, PLoS ONE, 8, doi:10.1371/journal.pone.0072779, 2013.
- Jahnke, R. A. and Jackson, G. A.: *The spatial distribution of sea floor oxygen consumption in the Atlantic and Pacific Oceans*, in: Deep-Sea Food Chains and the Global Carbon Cycle, Rowe, G. T., and Pariente, V. (Eds.), Springer Netherlands, Dordrecht, 295–307, 1992.
- Jansen, J., Hill, N. A., Dunstan, P. K., McKinlay, J., Sumner, M. D., Post, A. L., Eléaume, M. P., Armand, L. K., Warnock, J. P., Galton-Fenzi, B. K., and Johnson, C. R.: *Abundance and richness of key Antarctic seafloor fauna correlates with modelled food availability*, Nat. Ecol. Evol., 2, 71–80, doi:10.1038/s41559-017-0392-3, 2018.
- Ji, R., Jin, M., and Varpe, Ø.: *Sea ice phenology and timing of primary production pulses in the Arctic Ocean*, Glob. Change Biol., 19, 734–741, doi:10.1111/gcb.12074, 2013.
- Jones, D. O., Yool, A., Wei, C.-L., Henson, S. A., Ruhl, H. A., Watson, R. A., and Gehlen, M.: *Global reductions in seafloor biomass in response to climate change*, Glob. Change Biol., 20, 1861–1872, doi:10.1111/gcb.12480, 2014.
- Jones, E. P., Rudels, B., and Anderson, L. G.: *Deep waters of the Arctic Ocean: origins and circulation*, Deep-Sea Res. Pt. I, 42, 737–760, doi:10.1016/0967-0637(95)00013-V, 1995.

## References

---

- Jørgensen, C. B.: *Bivalve filter feeding: Hydrodynamics, bioenergetics, physiology and ecology*, Olsen and Olsen, Fredensborg, 1990.
- Jørgensen, B. B. and des Marais, D. J.: *The diffusive boundary layer of sediments: Oxygen microgradients over a microbial mat*, *Limnol. Oceanogr.*, 35, 1343–1355, doi:10.4319/lo.1990.35.6.1343, 1990.
- Jørgensen, L. L., Archambault, P., Blicher, M., Denisenko, N., Guðmundsson, G., Iken, K., Roy, V., Sørensen, J., Anisimova, N., Behe, C., Bluhm, B. A., Denisenko, S., Metcalf, V., Olafsdóttir, S., Schiøtte, T., Tendal, O., Ravelo, A. M., Kędra, M., and Piepenburg, D.: *Benthos*, in: CAFF 2017: State of the Arctic Marine Biodiversity Report. Conservation of arctic flora and fauna international secretariat, Barry, T., Price, C., Olsen, M., Christensen, T., and Frederiksen, M. (Eds.), Akureyri, Iceland, 85–104, 2017.
- Kahru, M., Brotas, V., Manzano-Sarabia, M., and Mitchell, B. G.: *Are phytoplankton blooms occurring earlier in the Arctic?*, *Glob. Change Biol.*, 17, 1733–1739, doi:10.1111/j.1365-2486.2010.02312.x, 2011.
- Karsten, U., Schlie, C., Woelfel, J., and Becker, B.: *Benthic diatoms in Arctic Seas - Ecological functions and adaptations*, *Polarforschung*, 81, 77–84, 2012.
- Khim, B. K., Shim, J., Yoon, H. I., Kang, Y. C., and Jang, Y. H.: *Lithogenic and biogenic particle deposition in an Antarctic coastal environment (Marian Cove, King George Island): Seasonal patterns from a sediment trap study*, *Estuar. Coast. Shelf S.*, 73, 111–122, doi:10.1016/j.ecss.2006.12.015, 2007.
- Kim, S.-H., Ducklow, D. H., Abele, D., Ruiz-Bartlett, E., Buma, A. G. J., Meredith, M. P., Rozema, P. D., Schofield, O. M., Venables, H. J., and Schloss, I. R.: *Interdecadal variability of phytoplankton biomass along the coastal West Antarctic Peninsula*; *P. R. Soc. B.*, in press.
- Kim, S.-H., Choi, A., Jin Yang, E., Lee, S., and Hyun, J.-H.: *Low benthic respiration and nutrient flux at the highly productive Amundsen Sea Polynya, Antarctica*, *Deep-Sea Res. Pt. II*, 123, 92–101, doi:10.1016/j.dsr2.2015.10.004, 2016.
- King, G. M.: *Ecophysiology of microbial respiration*, in: *Respiration in aquatic ecosystems*, del Giorgio, P. and Williams, P. (Eds.), Oxford University Press, 18–35, 2005.
- Kirk, J. T.: *Light and photosynthesis in aquatic ecosystems*, Third edition, Cambridge University Press, Cambridge, 2011.
- Kirst, G. O. and Wiencke, C.: *Ecophysiology of polar algae*, *J. Phycol.*, 31, 181–199, doi:10.1111/j.0022-3646.1995.00181.x, 1995.
- Klages, M., Boetius, A., Christensen, J. P., Deubel, H., Piepenburg, D., Schewe, I., and Soltwedel, T.: *The benthos of Arctic seas and its role for the organic carbon cycle at the seafloor*, in: *The organic carbon cycle in the Arctic Ocean*, Stein, R. and MacDonald, R. W. (Eds.), Springer Berlin Heidelberg, Berlin, Heidelberg, 139–167, 2004.
- Klimant, I., Meyer, V., and Kühl, M.: *Fiber-optic oxygen microsensors, a new tool in aquatic biology*, *Limnol. Oceanogr.*, 40, 1159–1165, doi:10.4319/lo.1995.40.6.1159, 1995.
- Klöser, H., Ferreyra, G., Schloss, I., Mercuri, G., Laternus, F., and Curtosi, A.: *Hydrography of Potter Cove, a small fjord-like inlet on King George Island (South Shetlands)*, *Estuar. Coast. Shelf S.*, 38, 523–537, doi:10.1006/ecss.1994.1036, 1994.
- Klöser, H., Ferreyra, G., Schloss, I., Mercuri, G., Laternus, F., and Curtosi, A.: *Seasonal variation of algal growth conditions in sheltered Antarctic bays: the example of Potter Cove (King George Island, South Shetlands)*, *J. Marine Syst.*, 4, 289–301, doi:10.1016/0924-7963(93)90025-H, 1993.
- Knox, G. A.: *Biology of the Southern Ocean*, 2nd ed, Marine biology series, CRC, Taylor & Francis, Boca Raton, 2007.
- Kokarev, V. N., Vedenin, A. A., Basin, A. B., and Azovsky, A. I.: *Taxonomic and functional patterns of macrobenthic communities on a high-Arctic shelf: A case study from the Laptev Sea*, *J. Sea Res.*, 129, 61–69, doi:10.1016/j.seares.2017.08.011, 2017.
- Köster, M., Jensen, P., and Meyer-Reil, L.-A.: *Hydrolytic activities of organisms and biogenic structures in deep-sea sediments*, in: *Microbial Enzymes in Aquatic Environments*, Chróst, R. J. (Ed.), Springer New York, New York, NY, 298–310, 1991.

- Kowalke, J., Tatián, M., Sahade, R., and Arntz, W.: *Production and respiration of Antarctic ascidians*, *Polar Biol.*, 24, 663–669, doi:10.1007/s003000100266, 2001.
- Kristensen, E., Andersen, F. Ø., and Blackburn, T. H.: *Effects of benthic macrofauna and temperature on degradation of macroalgal detritus: The fate of organic carbon*, *Limnol. Oceanogr.*, 37, 1404–1419. doi:10.4319/lo.1992.37.7.1404, 1992.
- Krumpen, T.: *Sea ice and atmospheric conditions at HAUSGARTEN between 2000–2016 (daily resolution), link to model results*, PANGAEA, doi:10.1594/PANGAEA.878244, 2017.
- Krumpen, T., Gerdes, R., Haas, C., Hendricks, S., Herber, A., Selyuzhenok, V., Smedsrud, L., and Spreen, G.: *Recent summer sea ice thickness surveys in the Fram Strait and associated volume fluxes*, *The Cryosphere*, 10, 523–534, doi: 10.5194/tc-10-523-2016, 2016.
- Kruskal, J. B.: *Multidimensional scaling by optimizing goodness of fit to a nonmetric hypothesis*, *Psychometrika*, 29, 1–27, doi:10.1007/BF02289565, 1964.
- Kruss, A., Tęgowski, J., Tatarek, A., Wiktor, J., and Blondel, P.: *Spatial distribution of macroalgae along the shores of Kongsfjorden (West Spitsbergen) using acoustic imaging*, *Pol. Polar Res.*, 38, 133, doi:10.1515/popore-2017-0009, 2017.
- Kuzyk, Z. Z. A., Gobeil, C., Goñi, M. A., and Macdonald, R. W.: *Early diagenesis and trace element accumulation in North American Arctic margin sediments*, *Geochim. Cosmochim. Ac.*, 203, 175–200, doi:10.1016/j.gca.2016.12.015, 2017.
- Kwok, R. and Rothrock, D. A.: *Decline in Arctic sea ice thickness from submarine and ICESat records: 1958–2008*, *Geophys. Res. Lett.*, 36, doi:10.1029/2009GL039035, 2009.
- Lagger, C., Servetto, N., Torre, L., Sahade, R., and Belgrano, A.: *Benthic colonization in newly ice-free soft-bottom areas in an Antarctic fjord*, *PLoS ONE*, 12, doi:10.1371/journal.pone.0186756, 2017.
- Lacour, T., Larivière, J., and Babin, M.: *Growth, Chl a content, photosynthesis, and elemental composition in polar and temperate microalgae*, *Limnol. Oceanogr.*, 62, 43–58, doi:10.1002/lno.10369, 2017.
- Lalande, C., Nöthig, E.-M., Bauerfeind, E., Hardge, K., Beszczynska-Möller, A., and Fahl, K.: *Lateral supply and downward export of particulate matter from upper waters to the seafloor in the deep eastern Fram Strait*, *Deep-Sea Res. Pt. I*, 114, 78–89, doi:10.1016/j.dsr.2016.04.014, 2016.
- Lalande, C., Nöthig, E.-M., Somavilla, R., Bauerfeind, E., Shevchenko, V., and Okolodkov, Y.: *Variability in under-ice export fluxes of biogenic matter in the Arctic Ocean*, *Global Biogeochem. Cy.*, 28, 571–583, doi:10.1002/2013GB004735, 2014.
- Le Quere, C., Rodenbeck, C., Buitenhuis, E. T., Conway, T. J., Langenfelds, R., Gomez, A., Labuschagne, C., Ramonet, M., Nakazawa, T., Metzl, N., Gillett, N., and Heimann, M.: *Saturation of the Southern Ocean CO<sub>2</sub> sink due to recent climate change*, *Science*, 316, 1735–1738, doi:10.1126/science.1136188, 2007.
- Lee, J. R., Raymond, B., Bracegirdle, T. J., Chadès, I., Fuller, R. A., Shaw, J. D., and Terauds, A.: *Climate change drives expansion of Antarctic ice-free habitat*, *Nature*, 547, 49–54, doi:10.1038/nature22996, 2017.
- Lee, Z., Weidemann, A., Kindle, J., Arnone, R., Carder, K. L., and Davis, C.: *Euphotic zone depth: Its derivation and implication to ocean-color remote sensing*, *J. Geophys. Res.*, 112, doi:10.1029/2006JC003802, 2007.
- Leeuwe, M. A. van, Tedesco, L., Arrigo, K. R., Assmy, P., Campbell, K., Meiners, K. M., Rintala, J.-M., Selz, V., Thomas, D. N., Stefels, J., and Deming, J. W.: *Microalgal community structure and primary production in Arctic and Antarctic sea ice: a synthesis*, *Elem. Sci. Anth.*, 6, doi:10.1525/elementa.267, 2018.
- Lefèvre, N. and Watson, A. J.: *Modeling the geochemical cycle of iron in the oceans and its impact on atmospheric CO<sub>2</sub> concentrations*, *Global Biogeochem. Cy.*, 13, 727–736, doi:10.1029/1999GB900034, 1999.
- Legendre, L., Ackley, S. F., Dieckmann, G. S., Gulliksen, B., Horner, R., Hoshiai, T., Melnikov, I. A., Reeburgh, W. S., Spindler, M., and Sullivan, C. W.: *Ecology of sea ice biota*, *Polar Biol.*, 12, doi:10.1007/BF00243114, 1992.
- Levinton, J. S.: *Marine biology: Function, biodiversity, ecology*, Third edition, Oxford University Press, New York, 2009.

## References

---

- Li, Y.-H. and Gregory, S.: *Diffusion of ions in sea water and in deep-sea sediments*, *Geochim. Cosmochim. Ac.*, 38, 703–714, doi:10.1016/0016-7037(74)90145-8, 1974.
- Li, W. K., McLaughlin, F. A., Lovejoy, C., and Carmack, E. C.: *Smallest algae thrive as the Arctic Ocean freshens*, *Science*, 326, 539, doi:10.1126/science.1179798, 2009.
- Lichtschlag, A., Felden, J., Brüchert, V., Boetius, A., and Beer, D. de: *Geochemical processes and chemosynthetic primary production in different thiotrophic mats of the Håkon Mosby Mud Volcano (Barents Sea)*, *Limnol. Oceanogr.*, 55, 931–949, doi:10.4319/lo.2010.55.2.0931, 2010.
- Lim, C. H., Lettmann, K., and Wolff, J.-O.: *Numerical study on wave dynamics and wave-induced bed erosion characteristics in Potter Cove, Antarctica*, *Ocean Dynamics*, 63, 1151–1174, doi:10.1007/s10236-013-0651-z, 2013.
- Link, H., Bodur, Y., Hauquier, F., Piepenburg, D., Seifert, D., and Veit-Köhler, G.: *Role of the biotic habitat for benthic biogeochemical fluxes and function in the Weddell Sea*, conference talk, XIth SCAR Biology Symposium, Leuven, Belgium, 10/07–14/07/2017.
- Link, H., Piepenburg, D., Archambault, P., and Lin, S.: *Are hotspots always hotspots? The relationship between diversity, resource and ecosystem functions in the Arctic*, *PLoS ONE*, 8, doi:10.1371/journal.pone.0074077, 2013a.
- Link, H., Chaillou, G., Forest, A., Piepenburg, D., and Archambault, P.: *Multivariate benthic ecosystem functioning in the Arctic – benthic fluxes explained by environmental parameters in the southeastern Beaufort Sea*, *Biogeosciences*, 10, 5911–5929, doi:10.5194/bg-10-5911-2013, 2013b.
- Lintern, D. G., Macdonald, R. W., Solomon, S. M., and Jakes, H.: *Beaufort Sea storm and resuspension modeling*, *J. Marine Syst.*, 127, 14–25, doi:10.1016/j.jmarsys.2011.11.015, 2013.
- Lizotte, M. P.: *The contributions of sea ice algae to Antarctic marine primary production*, *Am. Zool.*, 41, 57–73, doi:10.1668/0003-1569(2001)041[0057:TCOSIA]2.0.CO;2, 2001.
- Lochman, L., Zimcik, P., Klimant, I., Novakova, V., and Borisov, S. M.: *Red-emitting CO<sub>2</sub> sensors with tunable dynamic range based on pH-sensitive azaphthalocyanine indicators*, *Sensors and Actuators B: Chemical*, 246, 1100–1107, doi:10.1016/j.snb.2016.10.135, 2017.
- Lohrer, A. M., Cummings, V. J., and Thrush, S. F.: *Altered sea ice thickness and permanence affects benthic ecosystem functioning in coastal Antarctica*, *Ecosystems*, 16, 224–236, doi:10.1007/s10021-012-9610-7, 2013.
- Longhi, M. L., Schloss, I. R., and Wiencke, C.: *Effect of irradiance and temperature on photosynthesis and growth of two Antarctic benthic diatoms, Gyrosigma subsalinum and Odontella litigiosa*, *Bot. Mar.*, 46, 276–284, doi:10.1515/BOT.2003.025, 2003.
- Lopez, G. R. and Levinton, J. S.: *Ecology of deposit-feeding animals in marine sediments*, *Quart. Rev. Biol.*, 62, 235–260, doi:10.1086/415511, 1987.
- Lowry, K. E., Pickart, R. S., Selz, V., Mills, M. M., Pacini, A., Lewis, K. M., Joy-Warren, H. L., Nobre, C., van Dijken, Gert L., Grondin, P.-L., Ferland, J., and Arrigo, K. R.: *Under-ice phytoplankton blooms inhibited by spring convective mixing in refreezing leads*, *J. Geophys. Res. Oceans*, 123, 90–109, doi:10.1002/2016JC012575, 2018.
- Lustwerk, R. L. and Burdige, D. J.: *Elimination of dissolved sulfide interference in the flow injection determination of CO<sub>2</sub>, by addition of molybdate*, *Limnol. Oceanogr.*, 40, 1011–1012, doi:10.4319/lo.1995.40.5.1011, 1995.
- Maccario, L., Sanguino, L., Vogel, T. M., and Larose, C.: *Snow and ice ecosystems: not so extreme*, *Research in Microbiology*, 166, 782–795, doi:10.1016/j.resmic.2015.09.002, 2015.
- Macdonald, R. W., Anderson, L. G., Christensen, J. P., Miller, L. A., Semiletov, I. P., and Stein, R.: *The Arctic Ocean*, in: *Carbon and nutrient fluxes in continental margins*, Liu, K.-K., Atkinson, L., Quiñones, R., and Talaue-McManus, L. (Eds.), Springer Berlin Heidelberg, Berlin, Heidelberg, 291–302, 2010.
- Mahadevan, A.: *The impact of submesoscale physics on primary productivity of plankton*, *Annu. Rev. Mar. Sci.*, 8, 161–184, doi:10.1146/annurev-marine-010814-015912, 2016.
- Manabe, S. and Stouffer, R. J.: *Sensitivity of a global climate model to an increase of CO<sub>2</sub> concentration in the atmosphere*, *J. Geophys. Res.*, 85, 5529–5554, doi:10.1029/JC085iC10p05529, 1980.
- Manley, T. O.: *Branching of atlantic water within the Greenland-Spitsbergen passage: An estimate of recirculation*, *J. Geophys. Res.*, 100, 20627–20634, doi:10.1029/95JC01251, 1995.



- Marina, T. I., Salinas, V., Cordone, G., Campana, G., Moreira, E., Deregibus, D., Torre, L., Sahade, R., Tatián, M., Barrera Oro, E., Troch, M. de, Doyle, S., Quartino, M. L., Saravia, L. A., and Momo, F. R.: *The food web of Potter Cove (Antarctica): complexity, structure and function*, Estuar. Coast. Shelf S., 200, 141–151, doi:10.1016/j.ecss.2017.10.015, 2018.
- Marshall, G. J., Orr, A., van Lipzig, Nicole P. M., and King, J. C.: *The impact of a changing Southern Hemisphere annular mode on Antarctic Peninsula summer temperatures*, J. Climate, 19, 5388–5404, doi:10.1175/JCLI3844.1, 2006.
- Mauritzen, C., Hansen, E., Andersson, M., Berx, B., Beszczynska-Möller, A., Burud, I., Christensen, K. H., Debernard, J., Steur, L. de, Dodd, P., Gerland, S., Godøy, Ø., Hansen, B., Hudson, S., Høydalsvik, F., Ingvaldsen, R., Isachsen, P. E., Kasajima, Y., Koszalka, I., Kovacs, K. M., Køltzow, M., LaCasce, J., Lee, C. M., Lavergne, T., Lydersen, C., Nicolaus, M., Nilsen, F., Nøst, O. A., Orvik, K. A., Reigstad, M., Schyberg, H., Seuthe, L., Skagseth, Ø., Skarðhamar, J., Skogseth, R., Sperrevik, A., Svensen, C., Søiland, H., Teigen, S. H., Tverberg, V., and Wexels Riser, C.: *Closing the loop – Approaches to monitoring the state of the Arctic Mediterranean during the International Polar Year 2007–2008*, Prog. Oceanogr., 90, 62–89, doi:10.1016/j.pocean.2011.02.010, 2011.
- McClintic, M. A., DeMaster, D. J., Thomas, C. J., and Smith, C. R.: *Testing the FOODBANCS hypothesis: Seasonal variations in near-bottom particle flux, bioturbation intensity, and deposit feeding based on <sup>234</sup>Th measurements*, Deep-Sea Res. Pt. II, 55, 2425–2437, doi:10.1016/j.dsr2.2008.06.003, 2008.
- McGlathery, K. J., Anderson, I. C., and Tyler, A. C.: *Magnitude and variability of benthic and pelagic metabolism in a temperate coastal lagoon*, Mar. Ecol. Prog. Ser., 216, 1–15, doi:10.3354/meps216001, 2001.
- McLaughlin, F. A. and Carmack, E. C.: *Deepening of the nutricline and chlorophyll maximum in the Canada Basin interior, 2003–2009*, Geophys. Res. Lett., 37, doi:10.1029/2010gl045459, 2010.
- McMinn, A., Ashworth, C., Bhagooli, R., Martin, A., Salleh, S., Ralph, P., and Ryan, K.: *Antarctic coastal microalgal primary production and photosynthesis*, Mar. Biol., 159, 2827–2837, doi:10.1007/s00227-012-2044-0, 2012.
- McMinn, A. and Hegseth, E. N.: *Quantum yield and photosynthetic parameters of marine microalgae from the southern Arctic Ocean, Svalbard*, J. Mar. Biol. Assoc. UK, 84, 865–871, doi:10.1017/S0025315404010112h, 2004.
- McMinn, A., Pankowskii, A., Ashworth, C., Bhagooli, R., Ralph, P., and Ryan, K.: *In situ net primary productivity and photosynthesis of Antarctic sea ice algal, phytoplankton and benthic algal communities*, Mar. Biol., 157, 1345–1356, doi:10.1007/s00227-010-1414-8, 2010.
- Meehl, G. A., Arblaster, J. M., Bitz, C. M., Chung, Christine T. Y., and Teng, H.: *Antarctic sea-ice expansion between 2000 and 2014 driven by tropical Pacific decadal climate variability*, Nature Geosci., 9, 590–595, doi:10.1038/ngeo2751, 2016.
- Meehl, G. A., Collins, W. D., Boville, B. A., Kiehl, J. T., Wigley, T. M., and Arblaster, J. M.: *Response of the NCAR Climate System Model to increased CO<sub>2</sub> and the role of physical processes*, J. Climate, 13, 1879–1898, doi:10.1175/1520-0442(2000)013<1879:ROTNCS>2.0.CO;2, 2000.
- Mermillod-Blondin, F., Rosenberg, R., François-Carcaillet, F., Norling, K., and Mauclair, L.: *Influence of bioturbation by three benthic infaunal species on microbial communities and biogeochemical processes in marine sediment*, Aquat. Microb. Ecol., 36, 271–284, doi: 10.3354/ame036271, 2004.
- Middelburg, J. J., Soetaert, K., and Herman, P.M.: *Empirical relationships for use in global diagenetic models*, Deep-Sea Res. Pt I, 44, 327–344, doi:10.1016/S0967-0637(96)00101-X, 1997.
- Miller, K. A. and Pearse, J. S.: *Ecological Studies of Seaweeds in McMurdo Sound, Antarctica*, Am. Zool., 31, 35–48, doi:10.1093/icb/31.1.35, 1991.
- Mincks, S. L., Smith, C. R., and DeMaster, D. J.: *Persistence of labile organic matter and microbial biomass in Antarctic shelf sediments: evidence of a sediment ‘food bank’*, Mar. Ecol. Prog. Ser., 300, 3–19, doi:10.3354/meps300003, 2005.
- Momo, F., Kowalke, J., Schloss, I., Mercuri, G., and Ferreyra, G.: *The role of Laternula elliptica in the energy budget of Potter Cove (King George Island, Antarctica)*, Ecol. Model., 155, 43–51, doi:10.1016/S0304-3800(02)00081-9, 2002.

## References

---

- Monien, D., Monien, P., Brünjes, R., Widmer, T., Kappenberg, A., Silva Busso, A. A., Schnetger, B., and Brumsack, H.-J.: *Meltwater as a source of potentially bioavailable iron to Antarctica waters*, *Antarct. Sci.*, 29, 277–291, doi:10.1017/S095410201600064X, 2017.
- Monien, P., Lettmann, K. A., Monien, D., Asendorf, S., Wöfl, A.-C., Lim, C. H., Thal, J., Schnetger, B., and Brumsack, H.-J.: *Redox conditions and trace metal cycling in coastal sediments from the maritime Antarctic*, *Geochim. Cosmochim. Ac.*, 141, 26–44, doi:10.1016/j.gca.2014.06.003, 2014.
- Monien, D., Monien, P., Schnetger, B., and Brumsack, H.-J.: *Suspended particulate matter in melt water streams on Potter Peninsula, King George Island, maritime Antarctica*, *PANGAEA*, doi:10.1594/PANGAEA.810312, 2013.
- Moodley, L., Steyaert, M., Epping, E., Middelburg, J. J., Vincx, M., van Avesaath, P., Moens, T., and Soetaert, K.: *Biomass-specific respiration rates of benthic meiofauna: Demonstrating a novel oxygen micro-respiration system*, *J. Exp. Mar. Biol. Ecol.*, 357, 41–47, doi:10.1016/j.jembe.2007.12.025, 2008.
- Morrison, A. K., Frölicher, T. L., and Sarmiento, J. L.: *Upwelling in the Southern Ocean*, *Phys. Today*, 68, 27–32, doi:10.1063/PT.3.2654, 2015.
- Murray, J. W.: *Ocean carbonate chemistry: The aquatic chemistry fundamentals*, in: *The Ocean Carbon Cycle and Climate*, Follows, M., and Oguz, T. (Eds.), Springer Netherlands, Dordrecht, 1–29, 2004.
- Navarro, J. M. and Widdows, J.: *Feeding physiology of Cerastoderma edule in response to a wide range of seston concentrations*, *Mar. Ecol. Prog. Ser.*, 152, 175–186, doi:10.3354/meps152175, 1997.
- Nedwell, D. B., Walker, T. R., Ellis-Evans, J. C., and Clarke, A.: *Measurements of seasonal rates and annual budgets of organic carbon fluxes in an Antarctic coastal environment at Signy Island, South Orkney Islands, suggest a broad balance between production and decomposition*, *Appl. and Environ. Microb.*, 59, 3989–3995, 1993.
- Nelson, D. M., DeMaster, D. J., Dunbar, R. B., and Smith, W. O.: *Cycling of organic carbon and biogenic silica in the Southern Ocean: Estimates of water-column and sedimentary fluxes on the Ross Sea continental shelf*, *J. Geophys. Res.*, 101, 18519–18532, doi:10.1029/96JC01573, 1996.
- Neukermans, G., Oziel, L., and Babin, M.: *Increased intrusion of warming Atlantic water leads to rapid expansion of temperate phytoplankton in the Arctic*, *Glob. Change Biol.*, doi:10.1111/gcb.14075, 2018.
- Nicolaus, M., Katlein, C., Maslanik, J., and Hendricks, S.: *Changes in Arctic sea ice result in increasing light transmittance and absorption*, *Geophys. Res. Lett.*, 39, doi:10.1029/2012GL053738, 2012.
- Nicolaus, M., Gerland, S., Hudson, S. R., Hanson, S., Haapala, J., and Perovich, D. K.: *Seasonality of spectral albedo and transmittance as observed in the Arctic Transpolar Drift in 2007*, *J. Geophys. Res.*, 115, doi:10.1029/2009JC006074, 2010.
- Niebauer, H. J.: *Bio-physical oceanographic interactions at the edge of the Arctic ice pack*, *J. Marine Syst.*, 2, 209–232, doi:10.1016/0924-7963(91)90025-P, 1991.
- Nilsen, F., Skogseth, R., Vaardal-Lunde, J., and Inall, M.: *A simple shelf circulation model: Intrusion of Atlantic water on the West Spitsbergen shelf*, *J. Phys. Oceanogr.*, 46, 1209–1230, doi:10.1175/JPO-D-15-0058.1, 2016.
- NOAA. <https://www.pmel.noaa.gov/arctic-zone/detect/ice-seaice.shtml>, visited 08.02.2018.
- Norði, G. á, Glud, R. N., Simonsen, K., and Gaard, E.: *Deposition and benthic mineralization of organic carbon: A seasonal study from Faroe Islands*, *J. Marine Syst.*, 177, 53–61, doi:10.1016/j.jmarsys.2016.09.005, 2018.
- Nöthig, E.-M., Bracher, A., Engel, A., Metfies, K., Niehoff, B., Peeken, I., Bauerfeind, E., Cherkasheva, A., Gäbler-Schwarz, S., Hardge, K., Kiliyas, E., Kraft, A., Mebrahtom Kidane, Y., Lalande, C., Piontek, J., Thomisch, K., and Wurst, M.: *Summertime plankton ecology in Fram Strait – a compilation of long- and short-term observations*, *Polar Res.*, 34, 23349, doi:10.3402/polar.v34.23349, 2015.
- O'Brien, M. C., Macdonald, R. W., Melling, H., and Iseki, K.: *Particle fluxes and geochemistry on the Canadian Beaufort Shelf: Implications for sediment transport and deposition*, *Cont. Shelf Res.*, 26, 41–81, doi:10.1016/j.csr.2005.09.007, 2006.
- Odum, E. P.: *Energy flow in ecosystems: a historical review*, *Am. Zool.*, 8, 11–18, doi:10.1093/icb/8.1.11, 1968.
- Odum, E. P.: *Relationships between structure and function in the ecosystem*, *Jpn. J. Ecol.*, 12, 108–118, doi:10.18960/seitai.12.3\_108, 1962.

- Oksanen, J., Blanchet, F. G., Friendly, M., Kindt, R., Legendre, P., McGlinn, D., Minchin, P. R., O'Hara, R. B., Simpson, G. L., Solymos, P., Stevens, M. H. H., Szoecs, E., and Wagner, H.: *Vegan: Community Ecology Package 2017*, R package version 2.4-4, <https://CRAN.R-project.org/package=vegan>. 2018.
- Overland, J. E., Wood, K. R., and Wang, M.: *Warm Arctic—cold continents: climate impacts of the newly open Arctic Sea*, *Polar Res.*, 30, 15787, doi:10.3402/polar.v30i0.15787, 2011.
- Pabi, S., Dijken, G. L. van, and Arrigo, K. R.: *Primary production in the Arctic Ocean, 1998–2006*, *J. Geophys. Res.*, 113, 225, doi:10.1029/2007JC004578, 2008.
- Pablo, M. A. de, Ramos, M., Molina, A., and Prieto, M.: *Thaw depth spatial and temporal variability at the Limnopolar Lake CALM-S site, Byers Peninsula, Livingston Island, Antarctica*, *Sci. Total Environ.*, 615, 814–827, doi:10.1016/j.scitotenv.2017.09.284, 2018.
- Pakhomov, E. A., Froneman, P. W., and Perissinotto, R.: *Salp/krill interactions in the Southern Ocean: spatial segregation and implications for the carbon flux*, *Deep-Sea Res. Pt. II*, 49, 1881–1907, doi:10.1016/S0967-0645(02)00017-6, 2002.
- Palmisano, A. C., SooHoo, J. B., White, D. C., Smith, G. A., Stanton, G. R., and Burckle, L. H.: *Shade adapted benthic diatoms beneath Antarctic sea ice*, *J. Phycol.*, 21, 664–667, doi:10.1111/j.0022-3646.1985.00664.x, 1985.
- Paolo, F. S., Fricker, H. A., and Padman, L.: *Volume loss from Antarctic ice shelves is accelerating*, *Science*, 348, 327–331, doi:10.1126/science.aaa0940, 2015.
- Paquette, R. G., Bourke, R. H., Newton, J. F., and Perdue, W. F.: *The East Greenland Polar Front in autumn*, *J. Geophys. Res.*, 90, 4866–4882, doi:10.1029/JC090iC03p04866, 1985.
- Park, J., Kuzminov, F. I., Bailleul, B., Yang, E. J., Lee, S., Falkowski, P. G., and Gorbunov, M. Y.: *Light availability rather than Fe controls the magnitude of massive phytoplankton bloom in the Amundsen Sea polynyas, Antarctica*, *Limnol. Oceanogr.*, 62, 2260–2276, doi:10.1002/lno.10565, 2017.
- Parkinson, C. L.: *Global sea ice coverage from satellite data: Annual cycle and 35-yr trends*, *J. Climate*, 27, 9377–9382, doi:10.1175/JCLI-D-14-00605.1, 2014.
- Pasotti, F., Manini, E., Giovannelli, D., Wöfl, A.-C., Monien, D., Verleyen, E., Braeckman, U., Abele, D., and Vanreusel, A.: *Antarctic shallow water benthos in an area of recent rapid glacier retreat*, *Mar. Ecol.*, 36, 716–733, doi:10.1111/maec.12179, 2015.
- Peck, L. S., Barnes, D. K., Cook, A. J., Fleming, A. H., and Clarke, A.: *Negative feedback in the cold: ice retreat produces new carbon sinks in Antarctica*, *Global Change Biology*, 16, 2614–2623, doi:10.1111/j.1365-2486.2009.02071.x, 2010.
- Perovich, D. K., Grenfell, T. C., Light, B., and Hobbs, P. V.: *Seasonal evolution of the albedo of multiyear Arctic sea ice*, *J. Geophys. Res.*, 107, 20-1–20-13, doi:10.1029/2000JC000438, 2002.
- Perovich, D. K. and Polashenski, C.: *Albedo evolution of seasonal Arctic sea ice*, *Geophys. Res. Lett.*, 39, doi:10.1029/2012GL051432, 2012.
- Pesant, S., Legendre, L., Gosselin, M., Smith, Ralph E. H., Kattner, G., and Ramseier, R. O.: *Size-differential regimes of phytoplankton production in the Northeast Water Polynya (77°–81° N)*, *Mar. Ecol. Prog. Ser.*, 142, 75–86, doi:10.3354/meps142075, 1996.
- Peters, G.: *Userfriendlyscience: Quantitative analysis made accessible*, R package version 0.7.0, doi:10.17605/OSF.IO/TX EQU, 2017.
- Peterson, B. J.: *Increasing river discharge to the Arctic Ocean*, *Science*, 298, 2171–2173, doi:10.1126/science.1077445, 2002.
- Philipp, E. E., Husmann, G., and Abele, D.: *The impact of sediment deposition and iceberg scour on the Antarctic soft shell clam *Laternula elliptica* at King George Island, Antarctica*, *Antarct. Sci.*, 23, 127–138, doi:10.1017/S0954102010000970, 2011.
- Piatt, T., Harrison, W. G., Lewis, M. R., Li, W. K.W., Sathyendranath, S., Smith, R. E., and Venzina, A. F.: *Biological production of the oceans: the case of a consensus*, *Mar. Ecol. Prog. Ser.*, 52, 77–88, 1989.
- Piepenburg, D., Ambrose, W. G., Brandt, A., Renaud, P. E., Ahrens, M. J., and Jensen, P.: *Benthic community patterns reflect water column processes in the Northeast Water polynya (Greenland)*, *J. Marine Syst.*, 10, 467–482, doi:10.1016/S0924-7963(96)00050-4, 1997.

## References

---

- Piepenburg, D., Blackburn, T. H., Dorrien, C. F. von, Gutt, J., Hall, P. O., Hulth, S., Kendall, M. A., Opalinski, K. W., Rachor, E., and Schmid, M. K.: *Partitioning of benthic community respiration in the Arctic (northwestern Barents Sea)*, Mar. Ecol. Prog. Ser., 118, 199–213, doi:10.3354/meps118199, 1995.
- Pimm, S. L.: *Food webs*, New edition, University of Chicago Press, Chicago, London, 2002.
- Pohlert T.: *The pairwise multiple comparison of mean ranks package (PMCMR)*, R package version 4.2, <https://cran.r-project.org/web/packages/PMCMR/index.html>, 2018.
- Pollard, R., Tréguer, P., and Read, J.: *Quantifying nutrient supply to the Southern Ocean*, J. Geophys. Res., 111, 563, doi:10.1029/2005JC003076, 2006.
- Pomeroy, L. R.: *The ocean's food web, a changing paradigm*, Bioscience, 24, 499–504, doi:10.2307/1296885, 1974.
- Popova, E. E., Yool, A., Aksenov, Y., and Coward, A. C.: *Role of advection in Arctic Ocean lower trophic dynamics: A modeling perspective*, J. Geophys. Res. Oceans, 118, 1571–1586, doi:10.1002/jgrc.20126, 2013.
- Popova, E. E., Yool, A., Coward, A. C., Aksenov, Y. K., Alderson, S. G., Cuevas, B. A. de, and Anderson, T. R.: *Control of primary production in the Arctic by nutrients and light: insights from a high resolution ocean general circulation model*, Biogeosciences, 7, 3569–3591, doi:10.5194/bg-7-3569-2010, 2010.
- Priddle, J., Smetacek, V., Bathmann, U., Stromberg, J.-O., and Croxall, J. P.: *Antarctic marine primary production, biogeochemical carbon cycles and climatic change*, Philos. T. Roy. Soc. B, 338, 289–297, doi:10.1098/rstb.1992.0149, 1992.
- Puigcorbé, V., Roca-Martí, M., Masqué, P., Benitez-Nelson, C. R., Rutgers v. d. Loeff, Michiel, Laglera, L. M., Bracher, A., Cheah, W., Strass, V. H., Hoppema, M., Santos-Echeandía, J., Hunt, B. P., Pakhomov, E. A., and Klaas, C.: *Particulate organic carbon export across the Antarctic Circumpolar Current at 10°E: Differences between north and south of the Antarctic Polar Front*, Deep-Sea Res. Pt. II, 138, 86–101, doi:10.1016/j.dsr2.2016.05.016, 2017.
- Quartino, M. L. and Zaixso, A. B. de: *Summer macroalgal biomass in Potter Cove, South Shetland Islands, Antarctica: its production and flux to the ecosystem*, Polar Biol., 31, 281–294, doi:10.1007/s00300-007-0356-1, 2008.
- Quartino, M. L., Klöser, H., Zaixso, A. B. de, and Zaixso, H.: *Communities of benthic marine algae at the sheltered site in Potter Cove, King George Island, South Shetlands, Antarctica*, in: The Potter Cove coastal ecosystem, Antarctica: Synopsis of research performed within the frame of the Argentinean - German Cooperation at the Dallmann Laboratory and Jubany Station (King George Island, Antarctica, 1991–1997), Wiencke, C., Ferreyra, G. A., Arntz, W., and Rinaldi, C. (Eds.), Rep. Polar Res., 299, 74–81, 1998.
- Queirós, A. M., Stephens, N., Cook, R., Ravaglioli, C., Nunes, J., Dashfield, S., Harris, C., Tilstone, G. H., Fishwick, J., Braeckman, U., Somerfield, P. J., and Widdicombe, S.: *Can benthic community structure be used to predict the process of bioturbation in real ecosystems?*, Prog. Oceanogr., 137, 559–569, doi:10.1016/j.pocean.2015.04.027, 2015.
- Queirós, A. M., Birchenough, Silvana N. R., Bremner, J., Godbold, J. A., Parker, R. E., Romero-Ramirez, A., Reiss, H., Solan, M., Somerfield, P. J., van Colen, C., van Hoey, G., and Widdicombe, S.: *A bioturbation classification of European marine infaunal invertebrates*, Ecol. Evol., 3, 3958–3985, doi:10.1002/ece3.769, 2013.
- Quéric, N.-V., Soltwedel, T., and Arntz, W. E.: *Application of a rapid direct viable count method to deep-sea sediment bacteria*, J. Microbiol. Meth., 57, 351–367, doi:10.1016/j.mimet.2004.02.005, 2004.
- Quintana, C. O., Shimabukuro, M., Pereira, C. O., Alves, Betina G. R., Moraes, P. C., Valdemarsen, T., Kristensen, E., and Sumida, Paulo Y. G.: *Carbon mineralization pathways and bioturbation in coastal Brazilian sediments*, Sci. Rep., 5, 1, doi:10.1038/srep16122, 2015.
- Rabouille, C., Gaillard, J.-F., Relexans, J.-C., Tréguer, P., and Vincendeau, M.-A.: *Recycling of organic matter in Antarctic sediments: A transect through the polar front in the Southern Ocean (Indian Sector)*, Limnol. Oceanogr., 43, 420–432, doi:10.4319/lo.1998.43.3.0420, 1998.

- Rachold, V., Eicken, H., Gordeev, V. V., Grigoriev, M. N., Hubberten, H.-W., Lisitzin, A. P., Shevchenko, V. P., and Schirrmeister, L.: *Modern terrigenous organic carbon input to the Arctic Ocean*, in: The organic carbon cycle in the Arctic Ocean, Stein, R. and Macdonald, R. W. (Eds.), Springer Berlin Heidelberg, Berlin, Heidelberg, 33–55, 2004.
- Rasmussen, H. and Jørgensen, B. B.: *Microelectrode studies of seasonal oxygen uptake in a coastal sediment: role of molecular diffusion*, Mar. Ecol. Prog. Ser., 81, 289–303, 1992.
- Raven, J. A.: *Contributions of anoxygenic and oxygenic phototrophy and chemolithotrophy to carbon and oxygen fluxes in aquatic environments*, Aquat. Microb. Ecol., 56, 177–192, doi:10.3354/ame01315, 2009.
- Redfield, A. C.: *On the proportions of organic derivatives in sea water and their relation to the Composition of plankton*, University Press of Liverpool, 1934.
- Redfield, A. C.: *The influence of organisms on the composition of seawater*, in: The Sea, Hill, M. N. (Ed.), 3, Wiley, New York, N.Y., 26–77, 1963.
- Reimers, C. E.: *An in situ microprofiling instrument for measuring interfacial pore water gradients: methods and oxygen profiles from the North Pacific Ocean*, Deep-Sea Res. Pt. I, 34, 2019–2035, doi:10.1016/0198-0149(87)90096-3, 1987.
- Renaud, P. E., Løkken, T. S., Jørgensen, L. L., Berge, J., and Johnson, B. J.: *Macroalgal detritus and food-web subsidies along an Arctic fjord depth-gradient*, Front. Mar. Sci., 2, doi:10.3389/fmars.2015.00031, 2015.
- Renaud, P. E., Morata, N., Ambrose, W. G., Bowie, J. J., and Chiuchiolo, A.: *Carbon cycling by seafloor communities on the eastern Beaufort Sea shelf*, J. Exp. Mar. Biol. Ecol., 349, 248–260, doi:10.1016/j.jembe.2007.05.021, 2007.
- Renaud, P. E., Morata, N., Carroll, M. L., Denisenko, S. G., and Reigstad, M.: *Pelagic–benthic coupling in the western Barents Sea: Processes and time scales*, Deep-Sea Res. Pt. II, 55, 2372–2380, doi:10.1016/j.dsr2.2008.05.017, 2008.
- Renner, A. H., Gerland, S., Haas, C., Spreen, G., Beckers, J. F., Hansen, E., Nicolaus, M., and Goodwin, H.: *Evidence of Arctic sea ice thinning from direct observations*, Geophys. Res. Lett., 41, 5029–5036, doi:10.1002/2014GL060369, 2014.
- Repeta, D. J.: *Chemical characterization and cycling of dissolved organic matter*, in: Biogeochemistry of marine dissolved organic matter, Hansell, D. A., and Carlson, C. A. (Eds.), Elsevier, 21–63, 2015.
- Revsbech, N. P.: *An oxygen microsensor with a guard cathode*, Limnol. Oceanogr., 34, 474–478, doi:10.4319/lo.1989.34.2.0474, 1989.
- Rey, F., Noji, T. T., and Miller, L. A.: *Seasonal phytoplankton development and new production in the central Greenland Sea*, Sarsia, 85, 329–344, doi:10.1080/00364827.2000.10414584, 2011.
- Richardson, K., Markager, S., Buch, E., Lassen, M. F., and Kristensen, A. S.: *Seasonal distribution of primary production, phytoplankton biomass and size distribution in the Greenland Sea*, Deep-Sea Res. Pt. I, 52, 979–999, doi:10.1016/j.dsr.2004.12.005, 2005.
- Rigual-Hernández, A. S., Trull, T. W., Bray, S. G., Closset, I., and Armand, L. K.: *Seasonal dynamics in diatom and particulate export fluxes to the deep sea in the Australian sector of the southern Antarctic Zone*, J. Marine Syst., 142, 62–74, doi:10.1016/j.jmarsys.2014.10.002, 2015.
- Rivkin, R. B. and Putt, M.: *Photosynthesis and cell division by Antarctic microalgae: Comparison of benthic, planktonic and ice algae*, J. Phycol., 23, 223–229, doi:10.1111/j.1529-8817.1987.tb04129.x, 1987.
- Roach, A. T., Aagaard, K., Pease, C. H., Salo, S. A., Weingartner, T., Pavlov, V., and Kulakov, M.: *Direct measurements of transport and water properties through the Bering Strait*, J. Geophys. Res., 100, 18443, doi:10.1029/95JC01673, 1995.
- Roberts, R. D., Kuhl, M., Glud, R. N., and Rysgaard, S.: *Primary production of crustose coralline red algae in high Arctic fjords*, J. Phycol., 38, 273–283, doi:10.1046/j.1529-8817.2002.01104.x, 2002.
- Roleda, M. Y. and Dethleff, D.: *Storm-generated sediment deposition on rocky shores: Simulating burial effects on the physiology and morphology of *Saccharina latissima* sporophytes*, Mar. Biol. Res., 7, 213–223, doi:10.1080/17451000.2010.497189, 2011.

## References

---

- Roleda, M. Y., Dethleff, D., and Wiencke, C.: *Transient sediment load on blades of Arctic Saccharina latissima can mitigate UV radiation effect on photosynthesis*, Polar Biol., 31, 765–769, doi:10.1007/s00300-008-0434-z, 2008.
- Rösel, A. and Kaleschke, L.: *Exceptional melt pond occurrence in the years 2007 and 2011 on the Arctic sea ice revealed from MODIS satellite data*, J. Geophys. Res., 117, doi:10.1029/2011JC007869, 2012.
- Round, F. E.: *A diatom assemblage living below the surface of intertidal sand flats*, Mar. Biol., 54, 219–223, doi:10.1007/BF00395784, 1979.
- Rowe, G. T., Boland, G. S., Phoel, W. C., Anderson, R. F., and Biscaye, P. E.: *Deep-sea floor respiration as an indication of lateral input of biogenic detritus from continental margins*, Deep-Sea Res. Pt. II, 41, 657–668, doi:10.1016/0967-0645(94)90039-6, 1994.
- Rubin, S. I.: *Carbon and nutrient cycling in the upper water column across the Polar Frontal Zone and Antarctic Circumpolar Current along 170°W*, Global Biogeochem. Cy., 17, doi:10.1029/2002GB001900, 2003.
- Rückamp, M., Braun, M., Suckro, S., and Blindow, N.: *Observed glacial changes on the King George Island ice cap, Antarctica, in the last decade*, Global Planet. Change, 79, 99–109, doi:10.1016/j.gloplacha.2011.06.009, 2011.
- Ruhl, H. A., Bett, B. J., Hughes, Sarah J. M., Alt, Claudia H. S., Ross, E. J., Lampitt, R. S., Pebody, C. A., Smith, K. L., and Billett, David S. M.: *Links between deep-sea respiration and community dynamics*, Ecology, 95, 1651–1662, doi:10.1890/13-0675.1, 2014.
- Rullkötter, J.: *Organic Matter: The driving force for early diagenesis*, in: Marine Geochemistry, Schulz, H. D. and Zabel, M. (Eds.), Springer Berlin Heidelberg, Berlin, Heidelberg, 125–168, 2006.
- Russell, J. L., Dixon, K. W., Gnanadesikan, A., Stouffer, R. J., and Toggweiler, J. R.: *The southern hemisphere westerlies in a harming world: propping open the door to the deep ocean*, J. Climate, 19, 6382–6390, doi:10.1175/JCLI3984.1, 2006.
- Rysgaard, S. and Nielsen, T. G.: *Carbon cycling in a high-arctic marine ecosystem – Young Sound, NE Greenland*, Prog. Oceanogr., 71, 426–445, doi:10.1016/j.pocean.2006.09.004, 2006.
- Sabine, C. L., Hankin, S., Koyuk, H., Bakker, D. C., Pfeil, B., Olsen, A., Metzl, N., Kozyr, A., Fassbender, A., Manke, A., Malczyk, J., Akl, J., Alin, S. R., Bellerby, R. G., Borges, A., Boutin, J., Brown, P. J., Cai, W.-J., Chavez, F. P., Chen, A., Cosca, C., Feely, R. A., González-Dávila, M., Goyet, C., Hardman-Mountford, N., Heinze, C., Hoppema, M., Hunt, C. W., Hydes, D., Ishii, M., Johannessen, T., Key, R. M., Körtzinger, A., Landschützer, P., Lauvset, S. K., Lefèvre, N., Lenton, A., Lourantou, A., Merlivat, L., Midorikawa, T., Mintrop, L., Miyazaki, C., Murata, A., Nakadate, A., Nakano, Y., Nakaoka, S., Nojiri, Y., Omar, A. M., Padin, X. A., Park, G.-H., Paterson, K., Perez, F. F., Pierrot, D., Poisson, A., Ríos, A. F., Salisbury, J., Santana-Casiano, J. M., Sarma, V. V., Schlitzer, R., Schneider, B., Schuster, U., Sieger, R., Skjelvan, I., Steinhoff, T., Suzuki, T., Takahashi, T., Tedesco, K., Telszewski, M., Thomas, H., Tilbrook, B., Vandemark, D., Veness, T., Watson, A. J., Weiss, R., Wong, C. S., and Yoshikawa-Inoue, H.: *Surface Ocean CO<sub>2</sub> Atlas (SOCAT) gridded data products*, Earth Syst. Sci. Data, 5, 145–153, doi:10.5194/essd-5-145-2013, 2013.
- Sachs, O., Sauter, E. J., Schlüter, M., Rutgers van der Loeff, Michiel M., Jerosch, K., and Holby, O.: *Benthic organic carbon flux and oxygen penetration reflect different plankton provinces in the Southern Ocean*, Deep-Sea Res. Pt. I, 56, 1319–1335, doi:10.1016/j.dsr.2009.02.003, 2009.
- Sahade, R., Lagger, C., Torre, L., Momo, F., Monien, P., Schloss, I., Barnes, D. K. A., Servetto, N., Tarantelli, S., Tatian, M., Zamboni, N., and Abele, D.: *Climate change and glacier retreat drive shifts in an Antarctic benthic ecosystem*, Sci. Adv., 1, doi:10.1126/sciadv.1500050, 2015.
- Saiz-Salinas, J. I., Ramos, A., Munilla, T., and Rauschert, M.: *Changes in the biomass and dominant feeding mode of benthic assemblages with depth off Livingston Island (Antarctica)*, Polar Biol., 19, 424–428, doi:10.1007/s0030000050269, 1998.
- Sakshaug, E.: *Primary and secondary production in the Arctic Seas*, in: The organic carbon cycle in the Arctic Ocean, Stein, R. and Macdonald, R. W. (Eds.), Springer Berlin Heidelberg, Berlin, Heidelberg, 57–81, 2004.
- Sakshaug, E., Andresen, K., Myklesstad, S., and Olsen, Y.: *Nutrient status of phytoplankton communities in Norwegian waters (marine, brackish, and fresh) as revealed by their chemical composition*, J. Plankton Res., 5, 175–196, doi:10.1093/plankt/5.2.175, 1983.

- Sauter, E. J., Schlüter, M., and Suess, E.: *Organic carbon flux and remineralization in surface sediments from the northern North Atlantic derived from pore-water oxygen microprofiles*, Deep-Sea Res. Pt. I, 48, 529–553, doi:10.1016/S0967-0637(00)00061-3, 2001.
- Sayles, F. L., Martin, W. R., Chase, Z., and Anderson, R. F.: *Benthic remineralization and burial of biogenic SiO<sub>2</sub>, CaCO<sub>3</sub>, organic carbon, and detrital material in the Southern Ocean along a transect at 170° West*, Deep-Sea Res. Pt. II, 48, 4323–4383, doi:10.1016/S0967-0645(01)00091-1, 2001.
- Schauer, U.: *Arctic warming through the Fram Strait: Oceanic heat transport from 3 years of measurements*, J. Geophys. Res., 109, doi:10.1029/2003JC001823, 2004.
- Schewe, I. and Soltwedel, T.: *Benthic response to ice-edge-induced particle flux in the Arctic Ocean*, Polar Biol., 26, 610–620, doi:10.1007/s00300-003-0526-8, 2003.
- Schlitzer, R.: *Carbon export fluxes in the Southern Ocean: results from inverse modeling and comparison with satellite-based estimates*, Deep-Sea Res. Pt. II, 49, 1623–1644, doi:10.1016/S0967-0645(02)00004-8, 2002.
- Schloss, I.R.: *What does phytoplankton tell us about global change?*, conference talk, XIIth SCAR Biology Symposium, Leuven, Belgium, 10/07–14/07/2017.
- Schloss, I. R., Abele, D., Moreau, S., Demers, S., Bers, A., González, O., and Ferreyra, G. A.: *Response of phytoplankton dynamics to 19-year (1991–2009) climate trends in Potter Cove (Antarctica)*, J. Marine Syst., 92, 53–66, doi:10.1016/j.jmarsys.2011.10.006, 2012.
- Schloss, I. G., Ferreyra, G. A., Mercuri, G., and Kowalke, J.: *Particle flux in an Antarctic shallow coastal environment: a sediment trap study*, Sci. Mar., 63, 99–111, doi:10.3989/scimar.1999.63s199, 1999.
- Schloss, I. R., Ferreyra, G. A., and Curtosi, A.: *Phytoplankton primary production in Potter Cove, King George Island*, in: The Potter Cove coastal ecosystem, Antarctica: Synopsis of research performed within the frame of the Argentinean - German Cooperation at the Dallmann Laboratory and Jubany Station (King George Island, Antarctica, 1991–1997), Wiencke, C., Ferreyra, G. A., Arntz, W., and Rinaldi, C. (Eds.), Rep. Polar Res., 299, 67–73, 1998.
- Schlüter, M., Sauter, E. J., Schulz-Bull, D., Balzer, W., and Suess, E.: *Fluxes of organic carbon and biogenic silica reaching the seafloor: A comparison of high northern and southern latitudes of the Atlantic Ocean*, in: The Northern North Atlantic: A Changing Environment, Schäfer, P., Ritzrau, W., Schlüter, M., and Thiede, J. (Eds.), Springer Berlin Heidelberg, Berlin, Heidelberg, 225–240, 2001.
- Schulz, H. D.: *Quantification of early diagenesis: Dissolved constituents in pore water and signals in the solid phase*, in: Marine Geochemistry, Schulz, H. D. and Zabel, M. (Eds.), Springer Berlin Heidelberg, Berlin, Heidelberg, 73–124, 2006.
- Schwarz, A. M., Hawes, I., Andrew, N., Mercer, S., Cummings, V., and Thrush, S.: *Primary production potential of non-geniculate coralline algae at Cape Evans, Ross Sea, Antarctica*, Mar. Ecol. Prog. Ser., 294, 131–140, doi:10.3354/meps294131, 2005.
- Scott, F. J. and Thomas, D. P.: *Diatoms*, in: Antarctic marine protists, Scott, F. J., and Marchant, H. J. (Eds.), Australian biological resources study, Australian antarctic division, Canberra, Hobart, 13–201, 2005.
- Seefeldt, M. A., Campana, G. L., Deregiibus, D., Quartino, M. L., Abele, D., Tollrian, R., and Held, C.: *Different feeding strategies in Antarctic scavenging amphipods and their implications for colonisation success in times of retreating glaciers*, Front. Zool., 14, doi:10.1186/s12983-017-0248-3, 2017.
- Seiter, K., Hensen, C., and Zabel, M.: *Benthic carbon mineralization on a global scale*, Global Biogeochem. Cy., 19, 65, doi:10.1029/2004GB002225, 2005.
- Serreze, M. C. and Barry, R. G.: *Physical characteristics and basic climatic features*, in: The Arctic Climate System, Serreze, M. C. and Barry, R. G. (Eds.), Cambridge University Press, Cambridge, 23–64, 2014.
- Serreze, M. C. and Barry, R. G.: *Processes and impacts of Arctic amplification: A research synthesis*, Global Planet. Change, 77, 85–96, doi:10.1016/j.gloplacha.2011.03.004, 2011.
- Shao, Z.-D. and Ke, C.-Q.: *Spring–summer albedo variations of Antarctic sea ice from 1982 to 2009*, Environ. Res. Lett., 10, 64001, 2015.
- Shim, J., Kang, Y. C., Kang, D.-J., and Han, M. W.: *Fluxes and budgets of biogenic elements at the sediment-water interface of Marian Cove, King George Island, Antarct. Sci.*, 23, 358–368, doi:10.1017/S0954102011000137, 2011.

## References

---

- Shuman, F. R. and Lorenzen, C. J.: *Quantitative degradation of chlorophyll by a marine herbivore*, *Limnol. Oceanogr.*, 20, 580–586, doi:10.4319/lo.1975.20.4.0580, 1975.
- Skowronski, R. S. de, Gheller, P. F., Bromberg, S., David, C. J., Petti, M. A., and Corbisier, T. N.: *Distribution of microphytobenthic biomass in Martel Inlet, King George Island (Antarctica)*, *Polar Biol.*, 32, 839–851, doi:10.1007/s00300-009-0584-7, 2009.
- Smith, C. R., DeMaster, D., Thomas, C., Srsen, P., Grange, L., Evrard, V., and DeLeo, F.: *Pelagic-benthic coupling, food banks, and climate change on the west Antarctic peninsula shelf*, *Oceanography*, 25, 188–201, doi:10.5670/oceanog.2012.94, 2012.
- Smith, C. R., De Leo, F. C., Bernardino, A. F., Sweetman, A. K., and Arbizu, P. M.: *Abyssal food limitation, ecosystem structure and climate change*, *Trends Ecol. Evol.*, 23, 518–528, doi:10.1016/j.tree.2008.05.002, 2008.
- Smith, C. R., Mincks, S., and DeMaster, D. J.: *A synthesis of benthic-pelagic coupling on the Antarctic shelf: Food banks, ecosystem inertia and global climate change*, *Deep-Sea Res. Pt. II: Topical Studies in Oceanography*, 53, 875–894, doi:10.1016/j.dsr2.2006.02.001, 2006.
- Smith, K. L.: *Benthic community respiration in the N.W. Atlantic Ocean: in situ measurements from 40 to 5200 m*, *Mar. Biol.*, 47, 337–347, doi:10.1007/BF00388925, 1978.
- Smith, K. L., Ruhl, H. A., Kahru, M., Huffard, C. L., and Sherman, A. D.: *Deep ocean communities impacted by changing climate over 24 y in the abyssal northeast Pacific Ocean*, *P. Natl. Acad. Sci. USA*, 110, 19838–19841, doi:10.1073/pnas.1315447110, 2013.
- Smith, W. O.: *Polar Margins*, in: Carbon and nutrient fluxes in continental margins, Liu, K.-K., Atkinson, L., Quiñones, R., and Talaue-McManus, L. (Eds.), Springer Berlin Heidelberg, Berlin, Heidelberg, 289–330, 2010.
- Smith, W. O.: *Primary productivity and new production in the Northeast Water (Greenland) Polynya during summer 1992*, *J. Geophys. Res.*, 100, 4357, doi:10.1029/94JC02764, 1995.
- Smith, W. O., Peloquin, J. A., and Karl, D. M.: *Antarctic Continental Margins*, in: Carbon and nutrient fluxes in continental margins, Liu, K.-K., Atkinson, L., Quiñones, R., and Talaue-McManus, L. (Eds.), Springer Berlin Heidelberg, Berlin, Heidelberg, 318–330, 2010.
- Smith, W. O., Baumann, Marcus E. M., Wilson, D. L., and Aletsee, L.: *Phytoplankton biomass and productivity in the marginal ice zone of the Fram Strait during summer 1984*, *J. Geophys. Res.*, 92, 6777, doi:10.1029/JC092iC07p06777, 1987.
- Soltwedel, T., Bauerfeind, E., Bergmann, M., Bracher, A., Budaeva, N., Busch, K., Cherkasheva, A., Fahl, K., Grzelak, K., Hasemann, C., Jacob, M., Kraft, A., Lalande, C., Metfies, K., Nöthig, E.-M., Meyer, K., Quéric, N.-V., Schewe, I., Włodarska-Kowalczyk, M., and Klages, M.: *Natural variability or anthropogenically-induced variation? Insights from 15 years of multidisciplinary observations at the arctic marine LTER site HAUSGARTEN*, *Ecol. Indic.*, doi:10.1016/j.ecolind.2015.10.001, 2015.
- Soltwedel, T., Bauerfeind, E., Bergmann, M., Budaeva, N., Hoste, E., Jaeckisch, N., Juterzenka, K. von, Matthiesson, J., Moekievsky, V., Nöthig, E.-M., Quéric, N.-V., Sablotny, B., Sauter, E., Schewe, I., Urban-Malinga, B., Wegner, J., Maria Włodarska-Kowalczyk, M., and Klages, M.: *HAUSGARTEN: Multidisciplinary investigations at a deep-sea, long-term observatory in the Arctic Ocean*, *Oceanography*, 18, 46–61, doi:10.5670/oceanog.2005.24, 2005.
- Sørensen, H. L., Meire, L., Juul-Pedersen, T., Stigter, H. C. de, Meysman, F. J., Rysgaard, S., Thamdrup, B., and Glud, R. N.: *Seasonal carbon cycling in a Greenlandic fjord: an integrated pelagic and benthic study*, *Mar. Ecol. Prog. Ser.*, 539, 1–17, doi:10.3354/meps11503, 2015.
- Spielhagen, R. F., Müller, J., Wagner, A., Werner, K., Lohmann, G., Prange, M., and Stein, R.: *Holocene environmental variability in the Arctic gateway*, in: Integrated analysis of interglacial climate dynamics (INTERDYNAMIC), Schulz, M. and Paul, A. (Eds.), Springer Briefs in Earth System Sciences, Springer International Publishing, Cham, 37–42, 2015.
- Spies, A.: *Phytoplankton in the marginal ice zone of the Greenland Sea during summer, 1984*, *Polar Biol.*, 7, 195–205, doi:10.1007/BF00287416, 1987.
- Spreen, G., Kwok, R., and Menemenlis, D.: *Trends in Arctic sea ice drift and role of wind forcing: 1992–2009*, *Geophys. Res. Lett.*, 38, doi:10.1029/2011GL048970, 2011.
- Spreen, G., Kaleschke, L., and Heygster, G.: *Sea ice remote sensing using AMSR-E 89-GHz channels*, *J. Geophys. Res.*, 113, doi:10.1029/2005JC003384, 2008.



- Spurkland, T. and Iken, K.: *Kelp bed dynamics in estuarine environments in subarctic Alaska*, J. Coastal Res., 275, 133–143, doi:10.2112/JCOASTRES-D-10-00194.1, 2011.
- Stammerjohn, S. E., Maksym, T., Massom, R. A., Lowry, K. E., Arrigo, K. R., Yuan, X., Raphael, M., Randall-Goodwin, E., Sherrell, R. M., and Yager, P. L.: *Seasonal sea ice changes in the Amundsen Sea, Antarctica, over the period of 1979–2014*, Elem. Sci. Anth., 3, 55, doi:10.12952/journal.elementa.000055, 2015.
- Stammerjohn, S., Massom, R., Rind, D., and Martinson, D.: *Regions of rapid sea ice change: An inter-hemispheric seasonal comparison*, Geophys. Res. Lett., 39, doi:10.1029/2012GL050874, 2012.
- Starmans, A., Gutt, J., and Arntz, W. E.: *Mega-epibenthic communities in Arctic and Antarctic shelf areas*, Mar. Biol., 135, 269–280, doi:10.1007/s002270050624, 1999.
- Steig, E. J., Schneider, D. P., Rutherford, S. D., Mann, M. E., Comiso, J. C., and Shindell, D. T.: *Warming of the Antarctic ice-sheet surface since the 1957 International Geophysical Year*, Nature, 457, 459–462, doi:10.1038/nature07669, 2009.
- Stevens, P. M.: *Response of excised gill tissue from the New Zealand scallop Pecten novaezelandiae to suspended silt*, New Zeal. J. Mar. Fresh, 21, 605–614, doi:10.1080/00288330.1987.9516265, 1987.
- Summers, R. B., Thorp, J. H., Alexander, Jr., James E., and Fell, R. D.: *Respiratory adjustment of dreissenid mussels (Dreissena polymorpha and Dreissena bugensis) in response to chronic turbidity*, Can. J. Fish. Aquat. Sci., 53, 1626–1631, doi:10.1139/f96-096, 1996.
- Sun, J. and Liu, D.: *Geometric models for calculating cell biovolume and surface area for phytoplankton*, J. Plankton Res., 25, 1331–1346, doi:10.1093/plankt/fbg096, 2003.
- Sundbäck, K., Nilsson, P., Nilsson, C., and Jönsson, B.: *Balance between autotrophic and heterotrophic components and processes in microbenthic communities of sandy sediments: A field study*, Estuar. Coast. Shelf S., 43, 689–706, doi:10.1006/ecss.1996.0097, 1996.
- Takahashi, T., Broecker, W. S., and Langer, S.: *Redfield ratio based on chemical data from isopycnal surfaces*, J. Geophys. Res., 90, 6907, doi:10.1029/JC090iC04p06907, 1985.
- Takahashi, T., Sutherland, S. C., Wanninkhof, R., Sweeney, C., Feely, R. A., Chipman, D. W., Hales, B., Friederich, G., Chavez, F., Sabine, C., Watson, A., Bakker, D. C., Schuster, U., Metzl, N., Yoshikawa-Inoue, H., Ishii, M., Midorikawa, T., Nojiri, Y., Körtzinger, A., Steinhoff, T., Hoppema, M., Olafsson, J., Arnarson, T. S., Tilbrook, B., Johannessen, T., Olsen, A., Bellerby, R., Wong, C. S., Delille, B., Bates, N. R., and de Baar, H. J.: *Climatological mean and decadal change in surface ocean pCO<sub>2</sub>, and net sea-air CO<sub>2</sub> flux over the global oceans*, Deep-Sea Res. Pt. II, 56, 554–577, doi:10.1016/j.dsr2.2008.12.009, 2009.
- Thamdrup, B. and Canfield, D. E.: *Benthic respiration in aquatic sediments*, in: Methods in Ecosystem Science, Sala, O. E., Jackson, R. B., Mooney, H. A., and Howarth, R. W. (Eds.), Springer New York, New York, NY, 86–103, 2000.
- Thiel, H.: *Benthos in upwelling regions*, in: Upwelling Ecosystems, Boje, R. and Tomczak, M. (Eds.), Springer Berlin Heidelberg, Berlin, Heidelberg, 124–138, 1978.
- Thompson, D. W.: *Interpretation of recent southern hemisphere climate change*, Science, 296, 895–899, doi:10.1126/science.1069270, 2002.
- Thrush, S. F., Hewitt, J. E., Cummings, V. J., Ellis, J. I., Hatton, C., Lohrer, A., and Norkko, A.: *Muddy waters: elevating sediment input to coastal and estuarine habitats*, Front. Ecol. Environ., 2, 299–306, doi:10.1890/1540-9295(2004)002[0299:MWESIT]2.0.CO;2, 2004.
- Tjiputra, J. F., Roelandt, C., Bentsen, M., Lawrence, D. M., Lorentzen, T., Schwinger, J., Seland, Ø., and Heinze, C.: *Evaluation of the carbon cycle components in the Norwegian Earth System Model (NorESM)*, Geosci. Model Dev., 6, 301–325, doi:10.5194/gmd-6-301-2013, 2013.
- Torre, L., Tabares, Paulo C. Carmona, Momo, F., Meyer, João F. C. A., and Sahade, R.: *Climate change effects on Antarctic benthos: a spatially explicit model approach*, Climatic Change, 141, 733–746, doi:10.1007/s10584-017-1915-2, 2017.
- Torre, L., Servetto, N., Eöry, M. L., Momo, F., Tatián, M., Abele, D., and Sahade, R.: *Respiratory responses of three Antarctic ascidians and a sea pen to increased sediment concentrations*, Polar Biol., 35, 1743–1748, doi:10.1007/s00300-012-1208-1, 2012.

## References

---

- Traiger, S. B. and Konar, B.: *Mature and developing kelp bed community composition in a glacial estuary*, J. Exp. Mar. Biol. Ecol., 501, 26–35, doi:10.1016/j.jembe.2017.12.016, 2018.
- Tremblay, J.-É., Anderson, L. G., Matrai, P., Coupel, P., Bélanger, S., Michel, C., and Reigstad, M.: *Global and regional drivers of nutrient supply, primary production and CO<sub>2</sub> drawdown in the changing Arctic Ocean*, Prog. Oceanogr., 139, 171–196, doi:10.1016/j.pocean.2015.08.009, 2015.
- Tremblay, J.-É., Simpson, K., Martin, J., Miller, L., Gratton, Y., Barber, D., and Price, N. M.: *Vertical stability and the annual dynamics of nutrients and chlorophyll fluorescence in the coastal, southeast Beaufort Sea*, J. Geophys. Res., 113, doi:10.1029/2007JC004547, 2008.
- Trener, L. J., McMinn, A., and Ryan, K. G.: *In situ oxygen microelectrode measurements of bottom-ice algal production in McMurdo Sound, Antarctica*, Polar Biol., 25, 72–80, doi:10.1007/s003000100314, 2002.
- Turner, J., Phillips, T., Marshall, G. J., Hosking, J. S., Pope, J. O., Bracegirdle, T. J., and Deb, P.: *Unprecedented springtime retreat of Antarctic sea ice in 2016*, Geophys. Res. Lett., 44, 6868–6875, doi:10.1002/2017GL073656, 2017.
- Turner, J., Lu, H., White, I., King, J. C., Phillips, T., Hosking, J. S., Bracegirdle, T. J., Marshall, G. J., Mulvaney, R., and Deb, P.: *Absence of 21st century warming on Antarctic Peninsula consistent with natural variability*, Nature, 535, 411–415, doi:10.1038/nature18645, 2016.
- Turner, J., Maksym, T., Phillips, T., Marshall, G. J., and Meredith, M. P.: *The impact of changes in sea ice advance on the large winter warming on the western Antarctic Peninsula*, Int. J. Climatol., 33, 852–861, doi:10.1002/joc.3474, 2013.
- Turner, J., Colwell, S. R., Marshall, G. J., Lachlan-Cope, T. A., Carleton, A. M., Jones, P. D., Lagun, V., Reid, P. A., and Iagovkina, S.: *Antarctic climate change during the last 50 years*, Int. J. Climatol., 25, 279–294, doi:10.1002/joc.1130, 2005.
- Urban, H.-J. and Mercuri, G.: *Population dynamics of the bivalve Laternula elliptica from Potter Cove, King George Island, South Shetland Islands*, Antarct. Sci., 10, doi:10.1017/S0954102098000200, 1998.
- Vanreusel, A., Vincx, M., Schram, D., and van Gansbeke, D.: *On the vertical distribution of the metazoan meiofauna in shelf break and upper slope habitats of the NE Atlantic*, Int. Rev. Hydrobiol., 80, 313–326, doi:10.1002/iroh.19950800218, 1995.
- van Oevelen, D., Bergmann, M., Soetaert, K., Bauerfeind, E., Hasemann, C., Klages, M., Schewe, I., Soltwedel, T., and Budaeva, N. E.: *Carbon flows in the benthic food web at the deep-sea observatory HAUSGARTEN (Fram Strait)*, Deep-Sea Res. Pt. I, 58, 1069–1083, doi:10.1016/j.dsr.2011.08.002, 2011.
- Vaughan, D. G.: *Implications of the break-up of Wordie Ice Shelf, Antarctica for sea level*, Antarct. Sci., 5, doi:10.1017/S0954102093000537, 1993.
- Vaughan, D. G., Comiso, J. C., Allison, I., Carrasco, J., Kaser, G., Kwok, R., Mote, P., Murray, T., Paul, F., Ren, J., Rignot, E., Solomina, O., Steffen, K., and Zhang, T.: *Observations: Cryosphere: 4*, in: Climate Change 2013: The Physical Science Basis. Contribution of Working Group I to the Fifth Assessment Report of the Intergovernmental Panel on Climate Change, Stocker, T. F., Qin, D., Plattner, G.-K., Tignor, M., Allen, S. K., Boschung, J., Nauels, A., Xia, Y., Bex, V., and Midgley, P. (Eds.), Cambridge University Press, Cambridge, United Kingdom and New York, NY, USA, 317–382, 2013.
- Vaughan, D. G., Marshall, G. J., Connolley, W. M., King, J. C., and Mulvaney, R.: *Climate change: devil in the detail*, Science, 293, 1777–1779, doi:10.1126/science.1065116, 2001.
- Voet, D., Voet, J. G., and Pratt, C. W.: *Fundamentals of biochemistry: Life at the molecular level*, Fifth edition, John Wiley & Sons, Hoboken, NJ, 2016.
- Vonk, J. E., Tank, S. E., Bowden, W. B., Laurion, I., Vincent, W. F., Alekseychik, P., Amyot, M., Billet, M. F., Canário, J., Cory, R. M., Deshpande, B. N., Helbig, M., Jammet, M., Karlsson, J., Larouche, J., MacMillan, G., Rautio, M., Walter Anthony, K. M., and Wickland, K. P.: *Reviews and syntheses: Effects of permafrost thaw on Arctic aquatic ecosystems*, Biogeosciences, 12, 7129–7167, doi:10.5194/bg-12-7129-2015, 2015.
- Walsh, J.J.: *Importance of continental margins in the marine biogeochemical cycling of carbon and nitrogen*. Nature, 350, 53–55. doi:10.1038/350053a0, 1991.

- Walter, H., Hegner, E., Diekmann, B., Kuhn, G., and Rutgers van der loeff, M.M: *Provenance and transport of terrigenous sediment in the south Atlantic Ocean and their relations to glacial and interglacial cycles: Nd and Sr isotopic evidence*, *Geochim. Cosmochim. Ac.*, 64, 3813–3827, doi:10.1016/S0016-7037(00)00476-2, 2000.
- Wang, M. and Overland, J. E.: *A sea ice free summer Arctic within 30 years: An update from CMIP5 models*, *Geophys. Res. Lett.*, 39, doi:10.1029/2012GL052868, 2012.
- Waniek, J., Koeve, W., and Prien, R. D.: *Trajectories of sinking particles and the catchment areas above sediment traps in the northeast Atlantic*, *J. Mar. Res.*, 58, 983–1006, doi:10.1357/002224000763485773, 2000.
- Wassmann, P.: *Overarching perspectives of contemporary and future ecosystems in the Arctic Ocean*, *Prog. Oceanogr.*, 139, 1–12, doi:10.1016/j.pocean.2015.08.004, 2015.
- Wassmann, P.: *Arctic marine ecosystems in an era of rapid climate change*, *Prog. Oceanogr.*, 90, 1–17, doi:10.1016/j.pocean.2011.02.002, 2011.
- Wassmann, P.: *Sedimentation and benthic mineralization of organic detritus in a Norwegian fjord*, *Mar. Biol.*, 83, 83–94, doi:10.1007/BF00393088, 1984.
- Wassmann, P., Duarte, C. M., Agustí, S., and Sejr, M. K.: *Footprints of climate change in the Arctic marine ecosystem*, *Glob. Change Biol.*, 17, 1235–1249, doi:10.1111/j.1365-2486.2010.02311.x, 2011.
- Wassmann, P., Slagstad, D., Riser, C. W., and Reigstad, M.: *Modelling the ecosystem dynamics of the Barents Sea including the marginal ice zone*, *J. Marine Syst.*, 59, 1–24, doi:10.1016/j.jmarsys.2005.05.006, 2006.
- Wassmann, P., Bauerfeind, E., Fortier, M., Fukuchi, M., Hargrave, B., Moran, B., Noji, T., Nöthig, E.-M., Olli, K., Peinert, R., Sasaki, H., and Shevchenko, V.: *Particulate organic carbon flux to the Arctic Ocean sea floor*, in: *The organic carbon cycle in the Arctic Ocean*, Stein, R. and Macdonald, R. W. (Eds.), Springer Berlin Heidelberg, Berlin, Heidelberg, 101–138, 2004.
- Watanabe, E., Onodera, J., Harada, N., Honda, M. C., Kimoto, K., Kikuchi, T., Nishino, S., Matsuno, K., Yamaguchi, A., Ishida, A., and Kishi, M. J.: *Enhanced role of eddies in the Arctic marine biological pump*, *Nat. Comms.*, 5, 39, doi:10.1038/ncomms4950, 2014.
- Welch, H. E., Siferd, T. D., and Bruecker, P.: *Marine zooplanktonic and benthic community respiration rates at Resolute, Canadian high Arctic*, *Can. J. Fish. Aquat. Sci.*, 54, 995–1005, doi:10.1139/f97-006, 1997.
- Wenzhöfer, F. and Glud, R. N.: *Small-scale spatial and temporal variability in coastal benthic O<sub>2</sub> dynamics: Effects of fauna activity*, *Limnol. Oceanogr.*, 49, 1471–1481, doi:10.4319/lo.2004.49.5.1471, 2004.
- Wenzhöfer, F. and Glud, R. N.: *Benthic carbon mineralization in the Atlantic: a synthesis based on in situ data from the last decade*, *Deep-Sea Res. Pt. I*, 49, 1255–1279, doi:10.1016/S0967-0637(02)00025-0, 2002.
- Wenzhöfer, F., Oguri, K., Middelboe, M., Turnewitsch, R., Toyofuku, T., Kitazato, H., and Glud, R. N.: *Benthic carbon mineralization in hadal trenches: Assessment by in situ O<sub>2</sub> microprofile measurements*, *Deep-Sea Res. Pt. I*, 116, 276–286, doi:10.1016/j.dsr.2016.08.013, 2016.
- Wenzhöfer, F., Holby, O., and Kohls, O.: *Deep penetrating benthic oxygen profiles measured in situ by oxygen optodes*, *Deep-Sea Res. Pt. I*, 48, 1741–1755, doi:10.1016/S0967-0637(00)00108-4, 2001.
- Wenzhöfer, F., Holby, O., Glud, R. N., Nielsen, H. K., and Gundersen, J. K.: *In situ microsensor studies of a shallow water hydrothermal vent at Milos, Greece*, *Mar. Chem.*, 69, 43–54, doi:10.1016/S0304-4203(99)00091-2, 2000.
- Wheatcroft, R. A.: *Experimental tests for particle size-dependent bioturbation in the deep ocean*, *Limnol. Oceanogr.*, 37, 90–104, doi:10.4319/lo.1992.37.1.0090, 1992.
- Wijsman, J. W. M., Herman, P. M. J., and Gomoiu, M.-T.: *Spatial distribution in sediment characteristics and benthic activity on the northwestern Black Sea shelf*, *Mar. Ecol. Prog. Ser.*, 181, 25–39, doi:10.3354/meps181025, 1999.
- Williams, P. J. I. B.: *A review of measurements of respiration rates of marine plankton populations*, in: *Heterotrophic Activity in the Sea*, Hobbie, J. E. and Williams, Peter J. IeB (Eds.), Springer US, Boston, MA, 357–389, 1984.

## References

---

- Williams, P. J. I. B. and del Giorgio, P. A.: *Respiration in aquatic ecosystems: history and background*, in: *Respiration in Aquatic Ecosystems*, del Giorgio, P. and Williams, P. (Eds.), Oxford University Press, 1–17, 2005.
- Winkler, L. W.: *Die Bestimmung des im Wasser gelösten Sauerstoffes*, Ber. Dtsch. Chem. Ges., 21, 2843–2854, doi:10.1002/cber.188802102122, 1888.
- Wit, R. de, Relexans, J.-C., Bouvier, T., and Moriarty, D. J.: *Microbial respiration and diffusive oxygen uptake of deep-sea sediments in the Southern Ocean (ANTARES-I cruise)*, Deep-Sea Res. Pt. II, 44, 1053–1068, doi:10.1016/S0967-0645(97)00002-7, 1997.
- Witkowski, A., Lange-Bertalot, H., and Metzeltin, D.: *Diatom flora of marine coasts I*, Iconographia diatomologica, 7, A.R.G. Gantner, Königstein, 2000.
- Włodarska-Kowalczyk, M., Górska, B., Deja, K., and Morata, N.: *Do benthic meiofaunal and macrofaunal communities respond to seasonality in pelagial processes in an Arctic fjord (Kongsfjorden, Spitsbergen)?*, Polar Biol., 39, 2115–2129, doi:10.1007/s00300-016-1982-2, 2016.
- Włodarska-Kowalczyk, M., Pearson, T. H., and Kendall, M. A.: *Benthic response to chronic natural physical disturbance by glacial sedimentation in an Arctic fjord*, Mar. Ecol. Prog. Ser., 303, 31–41, doi:10.3354/meps303031, 2005.
- Woelfel, J., Schumann, R., Peine, F., Flohr, A., Kruss, A., Tegowski, J., Blondel, P., Wiencke, C., and Karsten, U.: *Microphytobenthos of Arctic Kongsfjorden (Svalbard, Norway): biomass and potential primary production along the shore line*, Polar Biol., 33, 1239–1253, doi:10.1007/s00300-010-0813-0, 2010.
- Wölfel, A.-C., Lim, C. H., Hass, H. C., Lindhorst, S., Tosonotto, G., Lettmann, K. A., Kuhn, G., Wolff, J.-O., and Abele, D.: *Distribution and characteristics of marine habitats in a subpolar bay based on hydroacoustics and bed shear stress estimates—Potter Cove, King George Island, Antarctica*, Geo-Mar. Lett., 34, 435–446, doi:10.1007/s00367-014-0375-1, 2014.
- Wohlers, J., Engel, A., Zollner, E., Breithaupt, P., Jurgens, K., Hoppe, H.-G., Sommer, U., and Riebesell, U.: *Changes in biogenic carbon flow in response to sea surface warming*, P. Natl. Acad. Sci. USA, 106, 7067–7072, doi:10.1073/pnas.0812743106, 2009.
- Woodgate, R. A.: *Increases in the Pacific inflow to the Arctic from 1990 to 2015, and insights into seasonal trends and driving mechanisms from year-round Bering Strait mooring data*, Prog. Oceanogr., 160, 124–154, doi:10.1016/j.pocean.2017.12.007, 2018.
- Woodworth-Lynas, C., Josenhans, H. W., Barrie, J. V., Lewis, C., and Parrott, D. R.: *The physical processes of seabed disturbance during iceberg grounding and scouring*, Cont. Shelf Res., 11, 939–961. doi:10.1016/0278-4343(91)90086-L, 1991.
- Wright, S. W. and Jeffrey, S. W.: *High-resolution HPLC system for chlorophylls and carotenoids of marine phytoplankton*, in: *Phytoplankton pigments in oceanography: Guidelines to modern methods*, 2nd ed, Jeffrey, S. W., Mantoura, R. F. C., and Wright, S. W. (Eds.), Monographs on oceanographic methodology, 10, UNESCO, Paris, 327–341, 1997.
- Wulff, A., Iken, K., Quartino, M. L., Al-Handal, A., Wiencke, C., and Clayton, M. N.: *Biodiversity, biogeography and zonation of marine benthic micro- and macroalgae in the Arctic and Antarctic*, Bot. Mar., 52, 491–507, doi:10.1515/BOT.2009.072, 2009.
- Wulff, A., Zacher, K., Hanelt, D., Al-Handal, A., and Wiencke, C.: *UV radiation - a threat to Antarctic benthic marine diatoms?*, Antarct. Sci., 20, 207, doi:10.1017/S0954102007000739, 2008.
- Wulff, A., Sundbäck, K., Nilsson, C., Carlson, L., and Jönsson, B.: *Effect of sediment load on the microbenthic community of a shallow-water sandy sediment*, Estuaries, 20, 547–558, doi:10.2307/1352613, 1997.
- Zacher, K., Bernard, M., Bartsch, I., and Wiencke, C.: *Survival of early life history stages of Arctic kelps (Kongsfjorden, Svalbard) under multifactorial global change scenarios*, Polar Biol., 39, 2009–2020, doi:10.1007/s00300-016-1906-1, 2016.
- Zaklan, S. D. and Ydenberg, R.: *The body size–burial depth relationship in the infaunal clam Mya arenaria*, J. Exp. Mar. Biol. Ecol., 215, 1–17. doi:10.1016/S0022-0981(97)00021-X, 1997.
- Zhang, J.: *Increasing Antarctic sea ice under warming atmospheric and oceanic conditions*, J. Climate, 20, 2515–2529, doi:10.1175/JCLI4136.1, 2007.

## Appendix

---

### Appendix A: List of abbreviations

AB	Amundsen Basin
AFDW	Ash-Free Dry Weight
ANOSIM	Analysis Of Similarity
ANOVA	Analysis Of Variance
AODC	Acredine Orange Direct Count method
AWI	Alfred-Wegener-Institut, Helmholtz-Zentrum für Polar- und Meeresforschung
BPc	Bioturbation Potential of the benthic Community
BS	Barents Sea
bsf	below surface
C <sub>org</sub>	Organic carbon
Chl <i>a</i>	Chlorophyll a concentration
CPE	Chloroplastic Pigment Equivalents
C-DOU	Carbon flux estimated from Diffusive Oxygen Uptake
C-TOU	Carbon flux estimated from Total Oxygen Uptake
DBL	Diffusive Boundary Layer
DIC	Dissolved Inorganic Carbon
DOC	Dissolved Organic Carbon
DOU	Diffusive Oxygen Uptake
EG	East Greenland area
EGC	East Greenland Current
Fuco	Fucoxanthin concentration
FDA	Fluorescein-Di-Acetate
FRAM	Frontiers in Arctic marine Monitoring
GS	Greenland Sea
HAFOS	Hybrid Antarctic Float Observing System
HG	HAUSGARTEN area
HSC	Highly Sea-ice Covered area

KGI	King George Island
LOKI	Lightframe On-sight Key-species Investigation
LSC	Low Sea-ice Covered area
LTER	Long-Term Ecological Research
MDS	Multidimensional Scaling
MIZ	Marginal Ice Zone
MPB	Microphytobenthos
MPB-C	Carbon content from
MUC	Multiple Corer
NB	Nansen Basin
PAR	Photosynthetically Active Radiation
PCA	Principal Component Analyzes
Phaeo	Phaeophytin concentration
POM	Particulate organic matter
RAC	Return Atlantic Current
RDA	ReDundancy Analyzes
RQ	Respiration Quotient
RuBisCo	Ribulose-1,5-Bisphosphate-Co-enzyme
SB	Svalbard Branch
SCUBA	Self-Containing Underwater Breathing Apparatus
SF	Storfjorden
SIMPER	SIMilarity PERcentage
SPC	Spitsbergen Polar Current
SV	Svalbard
SWI	Sediment-Water Interface
TC	Total Carbon
TOC	Total Organic Carbon
TIC	Total Inorganic Carbon
TN	Total Nitrogen
TOU	Total Oxygen Uptake
YB	Yermak Branch
WS	West Spitsbergen
WSC	West Spitsbergen Current

## Appendix B: Data availability

The data of manuscript II and manuscript III are stored at the PANGAEA<sup>®</sup> data publisher and are online available:

Hoffmann, R., Braeckman, U., Wenzhöfer, F.: *In situ and ex situ oxygen profiles and resulting diffusive oxygen uptake; in situ and ex situ total oxygen flux; benthic community density and biomass, bioturbation potential and solute exchange in the Hausgarten area, Arctic Fram Strait (2014/2015)*, PANGAEA, doi:10.1594/PANGAEA.883410, 2017.

Hoffmann, R., Braeckman, U., Wenzhöfer, F.: *In situ measured oxygen profiles in Potter Cove at the stations Faro, Creek and Isla D*, PANGAEA, doi:10.1594/PANGAEA.885472, 2018.

Hoffmann, R., Pasotti, F., Vázquez, S., Lefaible, N., Wenzhöfer, F., Braeckman, U.: *Sediment properties, benthic biogenic compounds, benthic fauna density and biomasses, and benthic diffusive and total fluxes from three stations (Faro, Creek, Isla D) in Potter Cove, Antarctic*. PANGAEA, doi:10.1594/PANGAEA.886232, 2018.

The data of manuscript I will also be made available via the PANGAEA<sup>®</sup> data publisher as soon as the manuscript is submitted to the journal 'Frontiers in Marine Science'.

## Appendix C: Oral and poster presentations

### Oral presentations

Braeckman, U., Pasotti, F., Hoffmann, R., Vázquez, S., Torstensson, A., Vanreusel, A., and Wenzhöfer, F.: *Carbon cycling in shallow Antarctic benthic communities subject to glacier retreat*, EGU Conference, 08.–13.04.2018, Vienna, Austria.

Braeckman, U., Pasotti, F., Hoffmann, R., Vázquez, S., Torstensson, A., Vanreusel, A., and Wenzhöfer, F.: *Carbon and nutrient cycling in shallow Antarctic communities subject to glacier retreat*, 5th Nereis Park Conference, 08.–11.08.2017, Southampton, USA.

Braeckman, U., Pasotti, F., Hoffmann, R., Vázquez, S., Torstensson, A., Vanreusel, A., and Wenzhöfer, F.: *Unravelling the responses of shallow soft sediment assemblages to rapid glacier retreat in an Antarctic fjord: Carbon and nutrient cycling*, XIIth SCAR Biology Symposium, 10.–14.07.2017, Leuven, Belgium.

Holtappels, M., Hoffmann, R., Novak, C., Merz, E., Sahade, R., Wenzhöfer, F., and Richter, C.: *Benthic oxygen fluxes in coastal waters at King George Island*, XIIth SCAR Biology Symposium, 10.–14.07.2017, Leuven, Belgium.

Hoffmann, R., Braeckman, U., Schewe, I., Krumpfen, T., and Wenzhöfer, F.: *Benthic remineralisation rates under contrasting sea-ice conditions in the deep Arctic Ocean*, Goldschmidt Conference, 26.06.–01.07.2016, Yokohama, Japan.

Hoffmann, R., Braeckman, U., Vázquez, S., Pasotti, F., Torstensson, A., and Wenzhöfer, F.: *Antarctic biogeochemical fluxes influenced by melting glacier*, 2nd European Conference on Scientific Diving, 08.–11.05.2016, Kristineberg, Sweden.



---

## Poster presentations

Hoffmann, R., Al-Handal, A.Y., Wulff, A., Deregibus, D., Braeckman, U., Quartino, M.L., and Wenzhöfer, F.: *Potential primary production of microphytobenthos in the changing Potter Cove*, confirmed for the Polar2018 Conference, 19.–23.06.2018, Davos, Switzerland.

Hoffmann, R., Braeckman, U., and Wenzhöfer, F.: *Implications of changing ice conditions on the benthic carbon remineralization in polar ecosystems*, Helmholtz evaluation of the AWI by external reviewers, 22.03.2018, Bremerhaven, Germany.

Merz, E., Hoffmann, R., Marchant, H.K., Lavik, G., Forster, S., and Wenzhöfer, F.: *N-pathways in coastal sediments of Potter Cove, Antarctica*, KFT Symposium, 02.–03.11.2017, Bremerhaven, Germany.

Pasotti, F., Braeckman, U., Abele, D., Hoffmann, R., De Troch, M., Giovannelli, D., Manini, E., Monien, D., Sahade, R., Saravia, L.A., Tarantelli, M.S., Torstensson, A., Vázquez, S., Verleyen, E., Wenzhöfer, F., Wölfl, A.C., and Vanreusel, A.: *Snapshots of soft sediment benthos influenced by glacier retreat in an Antarctic fjord: assemblage structure, functioning and biogeochemical cycling*, XIIth SCAR Biology Symposium, 10.–14.07.2017, Leuven, Belgium.

Hoffmann, R., Braeckman, U., and Wenzhöfer, F.: *Effects of changing polar conditions on benthic oxygen consumption assessed by in situ measurements*, Evaluation of the Max Planck Institute for Marine Microbiology by the Fachbeirat, 18.04.2018, Bremen, Germany.

Braeckman, U., Pasotti, F., Hoffmann, R., Vázquez, S., Torstensson, A., Vanreusel, A., and Wenzhöfer, F.: *Carbon cycling in Antarctic benthic communities subject to glacier retreat*. VLIZ marine scientist day, 03.03.2017, Bruges, Belgium.

Hoffmann, R., Braeckman, U., and Wenzhöfer, F.: *Benthic oxygen fluxes at East Greenland and West Spitsbergen continental slopes*, AWI PhD-Days, 01.–04.06.2015, List, Germany.

Hoffmann, R., Braeckman, U., and Wenzhöfer, F.: *Oxygen dynamics and exchange rates in polar ecosystems*, AWI PhD-Days, 05.–08.05.2014, Helgoland, Germany.

## Appendix D: Expeditions, courses, teaching, outreach and further activities

### Expeditions:

- KGI 16/17, Potter Cove, 14/10–31/12/2016, Expedition, station and dive leader, scientist, scientific diver
- PS93.2, Fram Strait, 22/07–15/08/2015, Scientist
- KGI 14/15, Potter Cove, 15/01–15/03/2015, Scientist and scientific diver
- PS85, Fram Strait, 06/06–03/07/2014, Scientist

### Attended courses:

#### Courses provided by POLMAR (graduate school):

- Marine Biogeochemistry
- Team Management
- How to cope with the challenges of a Ph.D.
- How to publish in peer-reviewed journals
- Electronics and interfaces
- Leadership skills
- Introduction to ArcGIS
- How to present on international conferences
- Third party funding

#### Additionally attended courses:

- Oral presentation course during the Goldschmidt conference 2016
- Introduction to Ocean data view (ODV)
- Research Funding Information Day at the Leibnitz Centre for tropical marine research
- First aid courses

### Teaching

Unofficial supervisor for the masterthesis of Elisa Merz entitled 'Benthic nitrogen pathways influenced by a melting Antarctic glacier', submitted 18.09.2017 at the Institute for Biological Sciences, University of Rostock, Germany

## Outreach

Article contributions, photos and short movies, e.g.:

- <https://www.awi.de/expedition/stationen/dallmann-labor/artikel/feldlabor-mit-poleposition.html>
- <https://www.awi.de/en/science/special-groups/scientific-diving/news-from-the-csd.html>
- <https://www.fotau.uni-rostock.de/berichte/forschungsreisen/antarktis-expedition-kgi-20162017/>
- <https://www.youtube.com/watch?v=tqLlmmkLa-s>
- <http://www.senseocean.eu/firelogger-optodes-successfully-used-shallow-coastal-antarctic-waters>

Planet e, ZDF documentation 'Planet Antarktis', released: 12/03/2017, <https://www.youtube.com/watch?v=G-5WrIOuOAw>

## Further activities

- Ph.D. representative at the AWI Doc-Team 2014/2015
- Host for the session 'Cold water research –from high latitudes to coasts to deep sea trenches' at the 5<sup>th</sup> YOUMARES Conference, 10–12.09.2014 in Stralsund, Germany
- Contributions to the SenseOCEAN project (reports, meetings, sensor tests)
  - Scientific diving during first underwater tests of AWI TRAMPER at the maritime exploration pool at Deutsches Forschungszentrum für Künstliche Intelligenz GmbH in Bremen
- Scientific diving as holiday replacement on Helgoland in August 2014 and Mai 2015



With my very last words I would like to quote respectfully the dolphins from epilog of the movie

'The Hitchhiker's Guide to the Galaxy':

"So long, and thanks for all the fish."